NORTH ATLANTIC TREATY ORGANISATION

RESEARCH AND TECHNOLOGY ORGANISATION

AC/323(SET-063)TP/49

www.rta.nato.int

RTO EDUCATIONAL NOTES **EN-SET-063**

Knowledge-Based Radar Signal and Data Processing

(Le traitement du signal et des données radar basé sur les connaissances)

The material in this publication was assembled to support a Lecture Series under the sponsorship of the Sensors and Electronics Technology Panel (SET) presented on 3-4 November 2003 in Stockholm, Sweden; 6-7 November 2003 in Rome, Italy; 10-11 November 2003 in Budapest, Hungary; 28-29 October 2004 in Madrid, Spain and 4-5 November 2004 in Gdansk, Poland.

Published August 2005

NORTH ATLANTIC TREATY ORGANISATION

RESEARCH AND TECHNOLOGY ORGANISATION

AC/323(SET-063)TP/49

www.rta.nato.int

RTO EDUCATIONAL NOTES **EN-SET-063**

Knowledge-Based Radar Signal and Data Processing

(Le traitement du signal et des données radar basé sur les connaissances)

The material in this publication was assembled to support a Lecture Series under the sponsorship of the Sensors and Electronics Technology Panel (SET) presented on 3-4 November 2003 in Stockholm, Sweden; 6-7 November 2003 in Rome, Italy; 10-11 November 2003 in Budapest, Hungary; 28-29 October 2004 in Madrid, Spain and 4-5 November 2004 in Gdansk, Poland.

The Research and Technology Organisation (RTO) of NATO

RTO is the single focus in NATO for Defence Research and Technology activities. Its mission is to conduct and promote co-operative research and information exchange. The objective is to support the development and effective use of national defence research and technology and to meet the military needs of the Alliance, to maintain a technological lead, and to provide advice to NATO and national decision makers. The RTO performs its mission with the support of an extensive network of national experts. It also ensures effective co-ordination with other NATO bodies involved in R&T activities.

RTO reports both to the Military Committee of NATO and to the Conference of National Armament Directors. It comprises a Research and Technology Board (RTB) as the highest level of national representation and the Research and Technology Agency (RTA), a dedicated staff with its headquarters in Neuilly, near Paris, France. In order to facilitate contacts with the military users and other NATO activities, a small part of the RTA staff is located in NATO Headquarters in Brussels. The Brussels staff also co-ordinates RTO's co-operation with nations in Middle and Eastern Europe, to which RTO attaches particular importance especially as working together in the field of research is one of the more promising areas of co-operation.

The total spectrum of R&T activities is covered by the following 7 bodies:

- AVT Applied Vehicle Technology Panel
- HFM Human Factors and Medicine Panel
- IST Information Systems Technology Panel
- NMSG NATO Modelling and Simulation Group
- SAS Studies, Analysis and Simulation Panel
- SCI Systems Concepts and Integration Panel
- SET Sensors and Electronics Technology Panel

These bodies are made up of national representatives as well as generally recognised 'world class' scientists. They also provide a communication link to military users and other NATO bodies. RTO's scientific and technological work is carried out by Technical Teams, created for specific activities and with a specific duration. Such Technical Teams can organise workshops, symposia, field trials, lecture series and training courses. An important function of these Technical Teams is to ensure the continuity of the expert networks.

RTO builds upon earlier co-operation in defence research and technology as set-up under the Advisory Group for Aerospace Research and Development (AGARD) and the Defence Research Group (DRG). AGARD and the DRG share common roots in that they were both established at the initiative of Dr Theodore von Kármán, a leading aerospace scientist, who early on recognised the importance of scientific support for the Allied Armed Forces. RTO is capitalising on these common roots in order to provide the Alliance and the NATO nations with a strong scientific and technological basis that will guarantee a solid base for the future.

Published August 2005

ISBN 92-837-1139-4

Knowledge-Based Radar Signal and Data Processing

(RTO-EN-SET-063)

Executive Summary

Radar systems are an important component of NATO military operations. In response to increasingly severe threats from military targets with reduced radar cross sections, slow moving and low flying targets, targets hidden in foliage and under trees, and in environments with large numbers of targets, knowledge-based (KB) signal and data processing techniques offer promise of significantly improved performance of NATO operated radar systems. In addition, radar systems under knowledge-based control can be deployed to better utilize valuable resources such as air space and runways and aid human operators in carrying out their missions. As battlefield scenarios become more complex with ever growing numbers of sensors and weapon systems, the challenge will be to effectively use already available information to enhance radar performance. Knowledge-based processing fills this need and helps meet the challenge.

This Lecture Series presents a state-of-the-art assessment of knowledge-based radar signal and data processing techniques, and thereby increase awareness of their value to the NATO scientific community. It reviews current developments in the area, and presents examples of improved radar performance for augmented and upgraded systems. In addition, the impact of KB technology on future systems is discussed.

This Lecture Series will present all relevant aspects of knowledge-based techniques as they apply to modern radar signal and data processing. The lectures cover:

- Introduction to Radar Signal & Data Processing – the Opportunity.
- Fundamentals of relevant knowledge-based techniques.
- Detailed characterization of the general radar problem in terms amenable to KB solution applications.
- Expert system application to constant false alarm rate processor.
- Knowledge-based control for space time adaptive processing.
- KB techniques applied to performance improvement of existing radar systems.
- Impact of KB techniques for emerging technologies (multi-phased arrays, electronically agile beam forming, waveform diversity).
- Integrated end-to-end radar signal & data processing with overarching KB control.

Le traitement du signal et des données radar basé sur les connaissances

(RTO-EN-SET-063)

Synthèse

Les systèmes radar constituent un élément important des opérations militaires de l'OTAN. Les techniques de traitement du signal et des données radar basées sur les connaissances (KB) permettront d'améliorer considérablement les performances des systèmes radar de l'OTAN, afin de répondre aux menaces de plus en plus sérieuses présentées par des objectifs militaires à surface équivalente radar réduite, des objectifs évoluant à basse vitesse et à basse altitude, des objectifs masqués par le feuillage et les arbres, ainsi que par des environnements contenant un grand nombre d'objectifs. En outre, des systèmes radar contrôlés par des systèmes basés sur les connaissances peuvent être déployés afin de mieux utiliser les moyens précieux que sont l'espace aérien et les pistes d'envol, ainsi que pour aider les opérateurs dans l'exécution de leurs missions. Avec la complexité croissante des scénarios de champ de bataille, intégrant de plus en plus de capteurs et de systèmes d'armes, l'accent sera mis sur l'exploitation efficace des informations déjà disponibles pour améliorer les performances des systèmes radar. Le traitement basé sur les connaissances répond à ces critères et permet de relever le défi qui est posé.

Ce cycle de conférences a pour objectif de présenter une évaluation de l'état actuel des connaissances dans le domaine des techniques de traitement des données et du signal radar basées sur les connaissances, afin de mieux sensibiliser les scientifiques de l'OTAN aux possibilités offertes par ces techniques. On y examinera les développements actuels dans ce domaine, et on y présentera des exemples d'amélioration de performances dans des systèmes augmentés et améliorés. Les conférences couvriront en outre l'impact des technologies KB sur les systèmes futurs.

Ce cycle de conférences présentera tous les aspects des techniques basées sur les connaissances dans la mesure où elles sont applicables au traitement du signal et des données d'aujourd'hui. Les conférences couvrent :

- Une introduction au traitement du signal et des données radar – les possibilités.
- L'essentiel des techniques basées sur les connaissances appropriées.
- La caractérisation détaillée du problème général du radar présentée dans des termes se prêtant à des applications KB.
- L'application des systèmes experts aux processeurs de taux de fausse alarme constant.
- Le contrôle basé sur les connaissances pour le traitement spatiotemporel adaptatif.
- Les techniques KB appliquées à l'amélioration des performances des systèmes radar existants.
- L'impact des techniques KB sur les technologies émergentes (antennes réseaux multiphases, formation de faisceaux agiles, diversité des formes d'ondes).
- Le traitement intégré du signal et des données radar de bout en bout avec contrôle global KB.

Table of Contents

Sensors and Electronics Technology Panel

CHAIRMAN

Professor M. TACKE
FGAN-FOM
Gutleuthausstr. 1
76275 Ettlingen
GERMANY

DEPUTY CHAIRMAN

Dr. Y. JONES KING
Technical Advisor, Spacecraft Technology Division
AFRL/VSS
Kirtland AFB, NM 87117-5776
USA

LECTURE SERIES DIRECTOR

J.F. SPINA
AFRL/SNRT
26 Electronic Parkway
Rome, NY 13341-4514
UNITED STATES
Email: John.F.Spina@rl.af.mil

AUTHORS/LECTURERS

Dr. A. FARINA
ALENIA MARCONI SYSTEMS
AMS Chief Technical Office
Via Tiburtina Km. 12.400
00131 Rome
ITALY
Email: afarina@amsjv.it

Mr. G. CAPRARO
Capraro Technologies, Inc.
311 Turner Street
Utica, NY 13501
UNITED STATES
Email: gcapraro@caprarotechnologies.com

Mr. H.D. GRIFFITHS
Head, Dept. of Electronic & Electrical Eng.
University College London
Torrington Place
London WC1E 7JE
UNITED KINGDOM
Email: h.griffiths@ee.ucl.ac.uk

Mr. M.C. WICKS
AFRT/SNRT
26 Electronic Parkway
Rome, NY 13341-4514
UNITED STATES
Email: Michael.Wicks@rl.af.mil

PANEL EXECUTIVE

Lt. Colonel G. FIAMINGO (ITAF)
Email: fiamingog@rta.nato.int

From Europe:

RTA-OTAN
Attn: SET Executive
BP 25, F-92201 Neuilly-sur-Seine Cedex
FRANCE

From the USA or Canada:

RTA-NATO
Attn: SET Executive
PSC 116
APO AE 09777

Introduction

John F. Spina
AFRL/SNRT
26 Electronic Parkway
Rome, NY 13341-4514
UNITED STATES

Email: John.F.Spina@rl.af.mil

A very good morning to all. It is my great pleasure to welcome you to the Sensors and Electronic Technology Panel Lecture Series 233 on "Knowledge-Based Radar Signal & Data Processing". To all those who have traveled great distances and taken time from their busy schedules, I would like to extend a special welcome. I am particularly pleased to be here in this beautiful city. This is my first visit and I am very impressed with the friendliness and courtesy shown by everyone I've met.

NATO, the Research & Technology Organization (RTO), and the Sensors and Electronic Technology (SET) Panel are proud to sponsor this significant event.

The RTO is a NATO organization and its mission is:

- to conduct and promote co-operative research and information exchange to support the development and effective use of national defense research and technology to meet the military needs of the Alliance;
- to maintain a technological lead;
- and to provide advice to NATO decision makers.

The full range of Research and Technology activities is covered by 6 Panels and a Group, dealing with different subjects. Each of these is made up of national representatives including highly qualified scientific experts. The Panels maintain links with military users and other NATO bodies. The scientific and technological work of the RTO is carried out by Technical Teams created for specific activities and with a specific duration. The Technical Teams organize Workshops, Symposia, Field Trials, Lecture Series and Training Courses and ensure the continuity of the experts' networks. The 6 Panels and one Group are:

- Studies, Analysis and Simulation; (SAS)
- Systems Concepts and Integration; (SCI)
- Sensors and Electronics Technology; (SET)
- Information Systems Technology; (IST)
- Applied Vehicle Technology; (AVT)
- Human Factors and Medicine; (HFM)
- NATO Modeling and Simulation Group. (NMSG)

Paper presented at the RTO SET Lecture Series on "Knowledge-Based Radar Signal and Data Processing", held in Stockholm, Sweden, 3-4 November 2003; Rome, Italy, 6-7 November 2003; Budapest, Hungary, 10-11 November 2003; Madrid, Spain, 28-29 October 2004; Gdansk, Poland, 4-5 November 2004, and published in RTO-EN-SET-063.

The Mission of the Sensors & Electronics Technology (SET) Panel is: to advance technology in electronics and passive/active sensors as they pertain to reconnaissance, surveillance and target acquisition, electronic warfare, communications and navigation; and to enhance sensor capabilities through multi-sensor integration/fusion. This concerns the phenomenology related to target signature, propagation and battlespace environment, EO, RF, acoustic and magnetic sensors, antenna, signal and image processing, components, sensor hardening and electromagnetic compatibility.

The objective of this Lecture Series is to present a state-of-the-art assessment of knowledge-based (expert systems, artificial neural networks) radar signal and data processing techniques, and thereby increase awareness of their value to the NATO scientific community. We will review the current developments in the area and present examples of improved radar performance for augmented and upgraded systems, and project the impact of KB technology on future systems.

The LS team will present all relevant aspects of knowledge-based techniques as they apply to modern radar signal and data processing. The lectures will cover:

- Introduction to Radar Signal & Data Processing;
- Fundamentals of relevant knowledge-based techniques;
- Detailed characterization of the general radar problem in terms amenable to KB solution applications;
- Expert system application to constant false alarm rate processor;
- Knowledge-based control for space time adaptive processing;
- KB techniques applied to performance improvement of existing radar systems;
- Impact of KB techniques for emerging technologies (multi-phased arrays, electronically agile beam forming, waveform diversity); and
- Integrated end-to-end radar signal & data processing with overarching KB control.

I am excited that this lecture Series provides a great opportunity for researchers in this field to exchange ideas and share their discoveries.

We hope to foster synergy between research and industry in order to fine-tune research to the needs of the NATO alliance. This will result in flourishing research and will also generate tangible results for the alliance.

On behalf of the Lecture Series team, I would like to commend Lt. Col. Giuseppe Fiamingo and his predecessor, Lt. Col Arturo Salzano and their colleagues, particularly Jane Brooks and Stephanie Branch, for their energetic efforts in making this Lecture Series possible. A big thank you as well to all local coordinators for their outstanding efforts to make this event a special one. The logistics support and accommodations have been exceptional. I would also like to express my appreciation to all the support personnel participating in the arrangements and operation of the Lecture Series, and to all speakers for coming here to share their ideas with the international community.

We are fortunate to have as speakers for the next two days, men with outstanding reputations and world-class contributors to our area of interest. I believe that the interactions over the next two days will lead to a better understanding and new perspectives, which are critical to the generation of new knowledge and ideas in this field.

I wish one and all a stimulating and rewarding two days. Thank you.

Let me now introduce our distinguished panel of speakers. We are indeed fortunate to have with us today, four of the leading authorities in the area of knowledge-based radar signal processing. In addition to their many contributions to the body of knowledge, they are, as you will see, accomplished lecturers. We hope that this superb combination will allow each of you to achieve the maximum benefit over the next two days.

GERARD T. CAPRARO

Gerard T. Capraro, Ph.D. founded Capraro Technologies, Inc. (CTI) in July 1993. He is presently its President and Senior Scientist. Prior to CTI, Dr. Capraro was a Principal Scientist and co-founder of the Utica, New York office of Kaman Sciences. He has more than thirty five years of experience in Electromagnetic Compatibility (EMC), Operations Research, Database Management, Computer Architectures, and Artificial Intelligence. His employment includes nine years as Project Engineer, Division Chief Engineer, Division Manager, and Principal Scientist at Kaman Sciences, eighteen years as a project engineer and task manager for the USAF at the Rome Air Development Center and nine years of university teaching (Adjunct Associate Professor, Adjunct Assistant Professor, Visiting Assistant Professor, and Adjunct Lecturer at Syracuse University-teaching Probability Theory, Statistics, Information Systems, and Database Systems). Dr. Capraro has made contributions in the areas of artificial intelligence (AI), Signal Processing, electromagnetic pulse (EMP), high power microwaves (HPM), Database Management and EMC. He has authored and co-authored over 40 technical publications and is a Fellow of the IEEE.

ALFONSO FARINA

Alfonso Farina received his doctor degree in electronic engineering from the University of Rome “La Sapienza” (I) in 1973.

In 1974 he joined Selenia (now part of Alenia Marcony Systems, a leading European industry implementing complex integrated systems) where he is now a manager in the Radar & Technology Division. Since 1979 until 1985, he has also been Professor of Radar Techniques at the University of Naples; subsequently, He has also given short courses at other Italian as well as foreign Universities.

Working interests span many fields of radar techniques; in particular the following: adaptive array antenna, detection, signal processing, data processing (including multi-target multi-radar and multi-sensor tracking), ECCM and imaging. Radar systems in which he has gained experience are: ground based three-dimensional multi beam, ship borne phased-array, airborne early warning and synthetic aperture.

He has been involved in a number of NATO international working teams and projects, namely: (i) RSG-3 of Panel X on advanced radar techniques including multi-static radar systems; (ii) DART (Demonstration of Advanced Radar Techniques) involving the conception, design, implementation and testing of an LPI radar; (iii) ACCSCO for the analysis and design of the multi-sensor integration study for NADGE upgrade. He has had the technical responsibility of R&D projects in the European Community frame; these projects were devoted to the design of remote sensing SAR based system. He has also had the technical responsibility for several research programs internally funded by the Company. Recently, He is one of the managers that organizes and supervises the R&D programmes at the Company level.

He is the author of more than 200 peer reviewed publications and the author of the following books and monographs: Radar Data Processing (Vol. 1 and 2) (this book is the first written on tracking; it has been translated in Russian and Chinese), 1985-1986; Optimized Radar Processors, 1987; Antenna Based Signal Processing Techniques for Radar Systems, 1992. He is also the only non US author of a chapter of the Radar Handbook (edited by Dr. M. I. Skolnik), Mc Graw Hill, 1990.

He has been session chairman at many international radar conferences; He is invited to give tutorials (on multi-sensor fusion, adaptive signal processing, space-time adaptive processing, and advanced radar detection) and opening lectures at these Conferences. He uses to lecture at universities and research centers in Italy and abroad (UK, France, The Netherlands, Spain, and Portugal). He received the 1987 Radar Systems Panel Award of IEEE-Aerospace and Electronic Systems Society (AESS) for development of radar data processing techniques. Also he is the Italian representative at the International Radar Systems Panel of IEEE-AESS. He is a Fellow of the IEE (UK). Recently He has been nominated Fellow of the IEEE for development and application of adaptive signal processing methods for radar systems. He is in the Board of Directors of the International Society for Information Fusion (ISIF). He serves as reviewer and co-operates with many technical Journals of IEEE, IEE etc.

HUGH GRIFFITHS

Professor Hugh Griffiths is Head of the Department of Electronic and Electrical Engineering at University College London. He graduated from the University of Oxford in 1978, and then worked in industry for three years before joining University College London. He leads a research group working on radar systems and signal processing, with numerous national and international collaborations. He was a recipient of the IEE Mountbatten and Maxwell Premiums, and the IEEE Fred Nathanson Award.

He served for many years on the PG E15 committee, and from 1994 – 1999 as Chairman. He has also been a member of the Radar Systems Panel of the IEEE AESS since 1989, acting as link between IEE and the IEEE on radar matters, and is currently a member of the AESS Board of Governors. He was Chairman of the RADAR 2002 conference held in Edinburgh in October 2002.

MICHAEL C. WICKS

Dr. Michael C. Wicks is currently a Senior Scientist for Sensor Signal Processing in the Sensors Directorate of the Air Force Research Laboratory. He is a Fellow of the IEEE, an AFRL Fellow, a past recipient of the IEEE/AESS Young Engineer of the Year, and the State University of New York Mohawk Valley Community College Alumni of the Year. He has engineering degrees from Mohawk Valley Community College, Rensselaer Polytechnic Institute, and Syracuse University in addition to a Masters of Arts in Public Administration from the Maxwell School. His research interest includes mathematical algorithms, radar systems engineering, remote sensing of the environment, waveform diversity and knowledge base applications to signal and data processing.

INTRODUCTION TO RADAR SIGNAL & DATA PROCESSING: THE OPPORTUNITY

A. Farina
Chief Technical Office, AMS
Via Tiburtina Km. 12.400, 00131 Rome, Italy
e.mail: afarina@amsjv.it

Key words: radar, signal processing, data processing, adaptivity, space-time adaptive processing, knowledge based systems, CFAR.

1. SUMMARY

This paper introduces to the lecture series dedicated to the knowledge-based radar signal and data processing. Knowledge-based expert system (KBS) is in the realm of artificial intelligence. KBS consists of a knowledge base containing information specific to a problem domain and an inference engine that employs reasoning to yield decisions. KBS have been built: some are very complex with thousands rules while others, relatively simple, are designed to tackle very specialised tasks. This lecture series shows that KBS can be successfully applied to radar systems. This paper introduces the Reader to the world of radar and, specifically, to the topics tackled in the subsequent lectures of the series. The paper starts with an introduction (Section 2) to radar (radar evolution from the early days up today, taxonomy of radar and radar equation). Subsequently, Section 3 considers the schematic of a modern radar system. The phased-array radar is the theme of Section 4. Signal processing, one of the main building blocks of modern radar, is introduced in Section 5. The section also introduces to the various forms of adaptivity in time, space and space-time domains for natural and intentional interference mitigation. Data processing, mainly target tracking, (Section 6) is the other relevant building block of radar. An extensive list of references (Section 9) is helpful to the Reader for a deeper insight to the many interesting topics of radar.

2. INTRODUCTION

2.1 RADAR EVOLUTION

RADAR (Radio Detection And Ranging) story dates back to H. Hertz (Ge), 1885-1888. He experimentally verified the prediction of J. Maxwell's theory of e.m. field published in 1864. He used an apparatus operating at 455MHz similar to a pulsed radar. Subsequently C. Hulsmeyer (Ge) in 1904 had a patent for a monostatic pulse radar. He envisioned the detection of ship for preventing collision at sea. In 1920 G. Marconi (It) observed the radio detection of targets in his experiments. He strongly urged its use in a speech delivered in 1922 at the Institute of Radio Engineers (now IEEE). In 1922 A. Hot et al. (NRL, USA) observed a fluctuating signal at the receiver (RX) when a ship passed between the receiver and the transmitter (TX) located on opposite sides of a river; it was a bistatic CW (continuous wave) radar. Noticeable was in 1940 the British invention (University of Birmingham) of high power micro-wave (μw) magnetron for higher frequency for radar. More details on the radar history can be found in [1] from which the previous notes are taken.

During world war II (wwII) the development of radar had a boost. USA (1941). Over one hundred radar (operating at 200MHz) were delivered to US Navy. Over one hundred radar (at 100MHz) were delivered to US Army for long range air search. One of these detected the Japanese attack on Pearl Harbour. Development of μw radar during wwII was done at MIT Radiation Lab and Bell Telephone Labs. During wwII Radiation Lab developed many different radar types. Germany (end 1940). Three major operational radar were developed: 125 MHz Freya air search radar; Wurburg fire control radar at 565 MHz: 4000 units were produced; Seetack (500MHz) ship-borne radar: 100 units were produced. The first operating radar at 30MHz for the Home Chain was developed in UK (1938). USSR (in 1940). RUS-1: bistatic CW at 75MHz with 35Km separation between TX and RX. RUS-2: monostatic pulse system at 75MHz [1], [2]. Italy (end '30, beginning

Paper presented at the RTO SET Lecture Series on "Knowledge-Based Radar Signal and Data Processing", held in Stockholm, Sweden, 3-4 November 2003; Rome, Italy, 6-7 November 2003; Budapest, Hungary, 10-11 November 2003; Madrid, Spain, 28-29 October 2004; Gdansk, Poland, 4-5 November 2004, and published in RTO-EN-SET-063.

'40). Prof. U. Tiberio gave a substantial contribution to the development of the radar equation [3]. The Owl was the name of the radar developed at that time; it was a 200 MHz ship-borne radar; more than 40 units produced. Activities during wwII were also done in Japan, France and The Netherlands [1].

The list of some major accomplishments of radar after wwII are the following (for details see [1] and [4]). Use of Doppler effect in MTI (Moving Target Indication) pulse radar to separate desired target echoes from undesired clutter echo. High power stable amplifiers (klystron, travelling wave tube, solid state transistors) allow better application of Doppler effect, use of sophisticated waveforms, and much higher power. High accurate angle tracking is achieved with monopulse radar. Pulse compression is a technique that uses long waveforms to obtain high energy and, at same time, achieves resolution of a short pulse by internal modulation of the long pulse and suitable processing of the received echoes. SAR (Synthetic Aperture Radar) obtains high resolution map like for imaging of ground scene; ISAR (Inverse SAR) is adopted for imaging of targets and planets. Carl Wiley of Goodyear Aircraft Corporation theoretised SAR in 1951 [5]. The first demonstration was on board an aircraft in '50s; for a comprehensive introduction to SAR, see [6]. Interferometric SAR allows the generation of the digital elevation model (DEM) of sensed scene; remarkable the Shuttle radar imaging topographic mission (1999). Airborne MTI and pulse Doppler radar is able to detect target in the midst of heavy ground clutter. Electronically steered phased-array permits rapid beam steering without mechanical movement of antenna. HF over the horizon radar detects targets up to 2000nmi. Non Cooperative Target Recognition (NCTR) techniques are based on high range resolution radar, ISAR, jet engine modulation, polarimetry and a combination of the above techniques. Radar is also exploited by meteorologist and for aid for safe and efficient air travel (air traffic control). Space based radar is used for surveillance and remote sensing of the globe [7] and for planetary exploration. Rapid advances in digital technology have made many theoretical capabilities practical with digital signal and data processing; few remarkable examples follow. Adaptivity at antenna level for jammer cancellation (1957, P. Howells, GE Syracuse; 1959 patent on Side Lobe Canceller; S. Applebaum: technical report on adaptive arrays). For a story of adaptivity see [8]. STAP (Space Time Adaptive Processing): invented by F. Dickey (GE), F. Staudaher (NRL), M. Labitt (MIT-Lincoln Laboratory) in 1991; they received the IEEE AESS Pioneer award for development, starting in 1950's, of airborne moving target systems particularly as used in the US Navy E2 series of aircraft [9]. A vision of opportunities for modern radar is described in [10]; [11] is a remarkable report on the MIT-LL developments in radar in the last 50 years.

A more recent major advance in modern radar is the application of KBS technology. Knowledge and expert rules may be used to select the radar operation mode, the algorithms and training data thereby significantly improving the performance of modern adaptive array radar in dynamic and non homogeneous environment. Sources of data are: digital terrain model, surface cover, geographic maps, meteorological condition, data from other sensors, etc. It is expected that the knowledge about local radar environment will enhance the ability of radar to maintain multiple tracks through areas of shadowing, clutter and other sources of interference that might be present in the surveillance scene [52].

Here a possible adaptive signal processing application example. KBS addresses the actual environment and performs better than conventional algorithms that hypothesize iid (identical independently distributed) conditions for clutter data. KBS ensures that shadowed range cells are excluded from training data. KBS based processor using information from diverse sources determines the choice of data also to best match the interference scene [52]. Other possible applications of KBS refer to STAP, to tracker (it is based on a number of rules: maneuver/obstacle rule, shadow rule, discrete rule, etc.). Study cases of KBS applied to radar systems, which are discussed during this Lecture Series, are: general radar problems, CFAR (Constant False Alarm Rate), tracking, STAP, and phased-array radar system.

Techniques, technologies, systems and applications of radar are extensively described in many papers, books and conference proceedings. IEEE Trans. on Aerospace and Electronic Systems and IEE Proc. Radar, Sonar and Navigation are some of the key reference journals. Several are the books published on radar; the following is a not exhaustive list: [12] to [15]. Regular international radar conferences are managed on a five year cycle by IEEE and IEE, with an interlace of long standing conferences organized in France, China, Japan, Germany,

India and, more recently, in Australia. Thus a wealth of top quality technical publications are available to radar scientists, engineers, students, practitioners, managers and users.

2.2 TAXONOMY OF RADAR

This may be in terms of:
1. location of radar: ground-based (fixed/transportable/mobile), ship-borne, air-borne, space-borne;
2. function: surveillance, tracking, reconnaissance, imaging, data link;
3. application: air traffic control (terminal area, en route, collision avoidance, apron), monitoring of surface traffic in the airports (taxi radar), air defence, anti theatre ballistic missile defence, vessel traffic surveillance, remote sensing (application to crop evaluation, hydrology, geodesy, archaeology, astronomy, defence), meteorology (hydrology, rain/hail measurement), study of atmosphere (detection of micro-burst and gust, wind profilers), space-borne altimetry for measurement of sea surface height, acquisition and tracking of satellites in the re-entry phase, monitoring of space debris, anti-collision for cars, ground penetrating radar (geology, gas pipe detection, archaeology, detection and location of mines, etc);
4. band (see [16]); criteria for frequency selection for surveillance radar are in [17]; criteria for frequency selection for an advanced sensor suite for US Navy are discussed in [18];
5. beam scanning: fixed beam, mechanical scan (rotating, oscillating), mechanical scan in azimuth, electronic scan (phase control, frequency control and mixed in azimuth/elevation), mixed (electronic-mechanical) scan, multi-beam configuration;
6. number and type of collected data: range (delay time of echo), azimuth (beam pointing of antenna beam, amplitude of echoes), elevation (only for tri-dimensional - 3D - radar, multifunctional, tracking), height (derived by range and elevation), intensity (echo power), radar cross section - RCS - (derived by echo intensity and range), radial speed (measurement of differential phase along the time on target due to the Doppler effect; it requires a coherent radar), polarimetry (phase and amplitude of echo in the polarisation channels: HH - horizontally transmitted, horizontally received - HV, VH, VV), RCS profiles along range and azimuth (high resolution along range, imaging radar);
7. configuration: monostatic (co-located TX & RX - same antenna, mono-radar/multi-radar), bistatic (not co-located TX & RX - two antennas), multistatic (one or more TX & RX spatially dispersed); suitable references for bistatic, multistatic and passive radar are: [2], [19] to [21];
8. waveform: continuous wave, pulsed wave, digital synthesis;
9. processing: coherent (MTI/MTD/Pulse-Doppler/super-resolution/SAR/ISAR…), non coherent (integration of envelope signals, moving window, adaptive threshold (CFAR)) and mixed;
10. technologies: for antenna (reflector plus feed, array (planar, conformal), corporate feed/air - coupled/lens), transmitter (magnetron, klystron, TWT, mini TWT, solid state) and receiver (analogue and digital technologies, base band, intermediate frequency sampling, etc.; relevant parameters of receiver are: noise figure, bandwidth and dynamic range).

At this point it is interesting to quote a book containing the radar terminology in English, German and French [22]; the subject oriented glossaries contain more than 1000 main and sub terms with definitions, synonyms, acronyms, contrast terms and cross-references.

2.3 RADAR EQUATION

The radar equation, a main ingredient for radar design, gives the target echo received power as a function of: radar parameters, target, environment and geometry. It compares the power with the radar sensitivity which is a function of: P_d and P_{fa} (i.e.: the required detection and false alarm probabilities) to determine the maximum range at which the target can be detected. Some of relevant ingredients of the radar equation are: signal-to-noise power ratio (SNR), target radar cross section, target fluctuating models, algorithms and signal processing schemes. The radar equation is widely explained in Ch. 2 of [1]. Different expressions of the radar equation are available for volume search, tracking, presence of clutter and jamming, see chapters 1, 2 and 9 of [12].

3. SCHEMATIC OF A MODERN RADAR SYSTEM

The simplified scheme of a modern radar system is depicted in Figure 1. The major blocks and their corresponding functions are now briefly described. Antenna and scan pattern generator: this determines the shape and direction of TX/RX beam. The antenna can be either a mechanically rotating reflector or a phased array electronically steered in azimuth and elevation. Transmitter: it is generally a tube generating a coherent pulse train with high peak power and possibly a wide band; alternatively, mini TWT or solid state amplifiers can be used in active phased-array radar. Waveform generator: it tailors the waveform to the environment and to the particular operating mode actually used. The waveforms can be wide pulse with frequency or phase code modulation for improved range resolution and clutter discrimination. Duplexer: this is an RF switch which conveys all the energy from the transmitter to the antenna in the transmitting phase while all the energy gathered by the antenna in the receiving phase is sent directly to the receiver chain. The rotary joint, not shown in the figure, allows the electric connection of the antenna to the remaining part of the radar notwithstanding the mechanical rotation of the antenna. Rotary joint with low loss and optical fibres for the transportation of signals are today available. Receiver: It provides frequency conversion, interference rejection and low noise amplification. The noise reduction is an important consideration in radar receiver design and is accomplished by the matched filter technique which maximises the SNR at the output. Signal down conversion in frequency is done in a number of steps up to base band where the signal is transformed in digital format via analogue-to-digital conversion (ADC) devices. Modern radar performs the ADC directly at intermediate frequency (IF); the advantage is to eliminate the unbalance between the I (in phase) and quadrature (Q) channels with corresponding advantages in terms of coherent rejection of clutter & jammer and integration of target echoes [23]. The trend today is towards a so called digital radar where the ADC is done very close to the antenna. Advantages of this approach are reported in [24]. Signal processor: this determines the presence or absence of targets while rejecting unwanted signals due to ground clutter, sea clutter, weather, radio-frequency interference, noise sources and intentional jammers. It is performed by coherent and/or not-coherent processing of time samples of received signals. The coherent processing acts on the I and Q components of signal collected during the time on target, while the non-coherent processing occurs after phase information is suppressed in the envelope detector. Detection is accomplished by comparing the processed video output with a threshold value, the crossing of the threshold being declared detection. The signal processor is implemented in real time special-processor hardware; more recently due to the extraordinary advances of the digital technology the processor makes extensive use of COTS (Commercial Off The Shelf) devices. Basic operations routinely implemented are: pulse compression, moving target indicator (MTI), pulse Doppler processing, moving target detector (MTD) (see Figure 2), CFAR (see Figures 3 and 4 for typical schemes) [1] and [25]. Also some modern phased-array radar have implemented in their signal processors the adaptive spatial filtering of jammers [23]. NCTR is another function that may be implemented in modern radar. Data extractor: this provides the target measurements in range, angles (azimuth, elevation) (via moving window or monopulse), radial speed and possibly target signature for NCTR. In general, target may cause several detections in adjacent cells in range, Doppler and angles; the centroid (referred to as “plot” in the sequel) of the corresponding pattern of detections gives an estimate of the target measurement. The target extractor was implemented in a dedicated microcomputer; today COTS technology is used also here. Data processor: it is essentially where the tracking filtering is implemented; see [26] and [27] for details. User: the output is generally a display to visualise the information contained in the radar echo signal in a form suitable for operator interpretation and action. There could be a link to convey data in a centre or in a computer for further processing. The visualised information on the display is called synthetic video. The plan position indicator (PPI), the usual display employed in radar, indicates the range and azimuth of a detected target. A modern radar display includes alphanumeric characters and symbols for directly conveying additional information; this is useful when target identity and altitude are to be displayed. Also the track is displayed with arrows and symbols. Controller: this decodes commands from the operator and sets up the operation modes, the appropriate system timing and the signal generator together with the processing functions on the received signals according to range, azimuth and elevation sectors. The controller also analyses signals for fault detection. It normally comprises a set of software programs implemented on a digital computer; used technologies are multiprocessor architectures based on COTS (Power PC and the like); programming languages can be Ada and C; real time operative system may be Lynx-OS or similar.

4. PHASED-ARRAY RADAR SYSTEMS

Electronically steered phased-array antenna is composed of a number of individual radiating elements (such as dipoles and open-ended wave guides) suitably distributed on a certain surface. The planar array is the most used in radar applications, alternative configurations being the linear, conformal (non planar surface) and smart skin (especially for aircraft). One way of regarding the phased-array antenna is as the result of the spatial sampling of a conventional reflector antenna. The most distinctive feature is the control of the feed signals to each radiating element. Control of the relative amplitude and phase of these signals allows the desired radiation pattern to be shaped and the beam to be rapidly steered in each direction of the controlled airspace without suffering the mechanical inertia of the classical rotating antenna. To cover 360° in azimuth there are two alternatives: four fixed planar arrays properly oriented or one rotating planar array [28]; back-to-back rotating antennas is also possible. The power generation and its distribution to the antenna elements can be realised by two methods: (a) in the passive solution the power is generated by a single transmitting tube having generally a low duty cycle; the transmitting power is then shared among the different antenna elements by means of a distributing microwave network. In the reception phase the same network gathers the energy which is returned to the receiver. (b) in the active array each antenna element – or group of elements (called sub-array) – is directly connected to a separate transmission amplifier, which can be a solid state device with high duty cycle, and to a separate amplifier for reception (see figure 5). The active solution is the most promising allowing transmission and reception losses to be reduced and signals with a high duty cycle to be generated; in fact, the solid state components have peak power limitation instead of the mean power limitation of traditional components. A further capability of the phased-array antenna is that of generating multiple beams. One application of this techniques occurs in the three-dimensional phased-array antenna which forms multiple stacked beams in elevation to measure the target height. Another arrangement requires multiple beams only in the reception phase: multiple pulses are transmitted by a wide beam covering the whole controlled airspace region, but for the reception of echoes from all the directions, simultaneous multiple narrow beams are needed. Also simultaneous multiple beams in transmission and reception are needed to speed up the search along a cluster of directions [69]. Another feature of the phased-array antenna is the controlled sidelobe level of the receiving pattern; this reduces the deleterious effect of clutter and directional interference; this can be achieved by generating nulls along the directions of the interferences [23]. The last interesting property to consider refers to reliability and maintenance. Redundancy is inherent in the array antenna due to the great number of identical antenna elements. The active array has in particular the graceful degradation feature. Indeed a failure of n amplifiers out of N connected to the antenna leads to a reduction of the SNR by only a factor of (1-n/N). Furthermore the solid-state devices have a meantime between failure higher than that of vacuum tube. The major problem with active phased-array is the high cost mainly related to the design and production of the transmitter/receiver modules; figure 6 depicts a simplified scheme of it. Relevant references concerning phased-array radar are: [1], [23], [24], [28], [29] and [30].

The flexibility in beam steering afforded by the electronic control makes the use of phased-array antennas attractive in radar applications. This is because of the possibility of using variable dwell-time (i.e.: time on target) and variable data rate. The dwell-time can be selected according to specific requirements, whereas mechanically scanning antennas process all targets in the same manner. The possibility of integrating a variable number of pulses, depending on target characteristics and on the environment, allows control of the detection probability - whatever the distance and the RCS of target are. Moreover, the probability of false alarms in the detection of a new target is strongly reduced by the possibility of a second look in those directions where verification is necessary (target confirmation). The variability of dwell-time is exploited to revisit different sectors of the surveillance volume with different rates; low elevation sector is revisited with high rate, while medium elevation and high elevation sectors are refreshed with lower rates. The capability of a phased-array to set the beam in any direction in a very short time allows tracking of many targets simultaneously. The updating of tracks after their initiation is performed by steering the beam in those directions foreseen by the tracking algorithm. This method of processing radar data is different from the classical track while scan (TWS), where the tracking function is subordinate to the requirements of the search function; TWS is typical of a mechanically scanning radar. Moreover, flexibility in beam allocation allows variable processing of different types of targets. The targets can be grouped and tracks can be updated at a rate depending on a specific priority: this organisation allows optimum management of radar information.

In order to take advantage of the management of the beam steering, dwell time and emitted energy in a manner that is adaptive to the environment, it is necessary to have flexible signal and data processing units. Indeed, in contrast to a mechanically scanned radar, the filtering algorithms and the parameters of signal and data processing can be changed on-line, depending on the radar data previously processed. It is clear that the core of such a complex radar is the controller which performs appropriately matching of system resources to the dynamically evolving operational environment.

The working principle of the controller and the functions it performs in a phased-array radar is now briefly presented. The controller shown in figure 1 for a general monostatic radar becomes a key sub-system in the phased-array case. The main tasks performed by the controller are: i. decision on which radar activities have to be accomplished in a certain time-frame; ii. preparation of commands to the different radar units in order to execute the planned radar "looks"; iii. gathering of the information on the status of the radar units (e.g.: digital words indicating the operational mode of the signal and data processors) for performance monitoring and fault detection; iv. interface with the human operator. The controller, comprising a set of programs, is usually implemented in a general purpose computer which interfaces with the radar hardware (signal processor, wave form generator, beam steering computer, etc.) and the other external devices such as keyboard and display. Because of the different speeds of operation, the computer interfaces with the surrounding devices by means of buffers and data buses.

The algorithms of the controller are now briefly considered. Each radar activity (e.g.: search, target confirmation, track initiation and track maintenance) requiring radar and computer resources is tagged with a priority index. The radar resources are the time (dwell time in a certain direction) and the transmitted energy, while the computer resources are the processing time and the memory. Scheduling of the radar activities is made according to their priority; in this way, saturation of radar and computer should be avoided. In other words, the radar activities are scheduled in such a way that the demand on radar and computer resources does not exceed the capabilities of the two systems. Every time a high-priority task is requested, the controller puts aside the partially completed low-priority activity which is resumed when time permits. In the event of saturation arising due to a large number of requests, the controller allows a graceful degradation mode of operation by cancelling the low-priority requests. Operation of the controller in a phased-array can be understood by considering figure 7 showing the functional interaction of the controller, the radar hardware, the data processor and the external peripherals. In the radar controller, the following three subsystems can be recognised: the manger, the scheduler, the real-time controller. The manager receives requests for radar activities (e.g. search, tracking) from the keyboard according to a specific mode of working or operator requirements. Based on the importance of the requests, the manager generates a prioritised list in order to be executed by the radar. This list is passed to the scheduler which should complete all the requests within a prescribed time period. Taking account of the limited resources of radar and computer, the scheduler establishes a specific time table of radar events. From this time table, it constructs a list of commands for the radar hardware which are distributed to the radar units by the real-time controller. The results of radar actions are detections which are used to generate clutter and jammer maps and to yield the co-ordinates of the useful targets. These detections are stored in a buffer and used to modify the specified normal mode of radar by sending requests for new radar activities to the controller through the bus which closes the control loop linking the controller, the radar hardware and the data processor. Examples of requests for new radar activities are *search mode in clutter* for the directions in the controlled airspace which pertains to the clutter map, *target-confirmation* and *track-initiation* modes for the useful target detections, and track updates for the established tracks. The contents of the detection and track buffers are periodically shown on the display.

One of the lecture of the series will study the use of KBS technology in phased-array radar systems.

5. SIGNAL PROCESSING

Radar signal processing can be defined as the manipulation of the received signal, represented in digital format, to extract the desired information whilst rejecting unwanted signals. In particular, a surveillance radar takes a decision about the presence or absence of targets whilst cancelling radar echoes caused by ground

clutter, radio frequency interference and noise source. An airborne radar accomplishes the same job in spite of the strong clutter return and its Doppler spread caused by the platform motion. A tracking radar, in addition to detection, is concerned with an accurate estimation of the target kinematics parameters (resort is made to maximum likelihood estimation procedure and its sub-optimum implementations). The list could be extended to other radar systems as the low probability of intercept, the synthetic aperture radar, the space-based radar and the multistatic radar. Whatever the radar system, the basic operations performed by the signal and data processors are as follows: detection of presence of targets, if any; extraction of information from the received waveform to determine a wealth of relevant parameters of the targets (such as position, velocity, shape, and electromagnetic signature). The first step of the design can be recognised in the formulation of mathematical models more adherent to the real environment in which the radar operates. Several major areas of research and development can be singled out in connection with radar detection: theory of optimum detection, adaptive detection theory, detection of signals having non-Gaussian probability density function (pdf), multidimensional processing and super resolution algorithms. Some of these are extensively described in the literature; see for instance, [23], [25]. Some techniques have been successfully implemented in real radar systems.

5.1 MTI, MTD, PULSE-DOPPLER

MTI, MTD (figure 2) and pulse Doppler radar concepts are successful processing schemes to reject clutter echoes and detect targets. An extensive literature describes these techniques; see for instance, [1], [63] and [32]. Recent research has focussed on an accurate statistical modelling of clutter echoes. A remarkable result is the collection and processing of recorded live data from vegetated ground clutter organised by MIT-LL: probably the most extensive collection of ground clutter data ever done; the details are in reported in the recent book [31]. Some of these data have been processed with modern processing algorithms, the achieved results being described in [33]. Furthermore, under certain conditions (radar operating at low grazing angle and/or with high resolution) the clutter echoes could be described as having a non Gaussian pdf; the exploitation of multidimensional coherent non Gaussian pdf brings to new processing schemes: see [34] and [64] for details.

5.2 CFAR (Constant False Alarm Rate)

Clutter and/or hostile noise jamming can be much larger than receiver internal noise. As a consequence the detection threshold can be exceeded and many false alarms can occur; an automatic detection and tracking system can be overloaded. CFAR automatically raises the threshold level thus avoiding the overload of the automatic tracker with extraneous information [1]. CFAR is achieved at the expense of a lower probability of detection of desired targets. Cell averaging – CA CFAR (Figure 3) - is due to Finn and Johnson; it is the optimum when the statistic of the envelope is Rayleigh. It uses an adaptive threshold whose level is determined by the clutter and/or noise in the vicinity of the radar echo. Two tapped delay-lines sample echo signals from the environment in a number N of reference cells located on both sides of the cell under test (CUT). The spacing between reference cells is equal to the radar range resolution (usually the pulse width) [1]. The CUT signal is compared to the adaptive threshold derived from the sum of the outputs of the tapped delay lines defining the reference cells. It changes as the radar environment changes and as the received pulse travels out in time. When multiplied by a constant K, the sum provides an adaptive threshold to maintain a CFAR. Thus the threshold can adapt to the environment as the pulse travels in time [1]. The greater the number of reference cells in the CA-CFAR the better is the estimate of the background clutter or noise and the less will be the loss in target detectability. There is a limit, however, to the number of reference cells that can be used in practice since the clutter must be relatively homogeneous over the reference cells. A typical CFAR design for an aircraft-surveillance radar might have a total of 20 reference cells that sample the environment a half-mile to either side of the signal in the CUT [1]. In a pulse Doppler radar, the reference cells can be taken from adjacent Doppler filters as well as from adjacent range cells. It can be shown that the CA-CFAR is embedded in the so called adaptive matched filter, one of the most modern and powerful adaptive processing schemes [65].

Limitations of CA-CFAR. (a) False alarms can result when the leading or trailing edges of a clutter patch move along the reference cells. This deleterious effect can be mitigated by summing the leading and lagging

reference cells separately and using the greater of the two to determine the threshold; this is the greater of (GO) CFAR; it introduces however an additional CFAR loss of 0.1-0.3 dB [1]. (b) One or more targets within the reference cells along with a primary target in the CUT raise the threshold, thus the detection of the primary target in the CUT might be lost. One method for reducing the effect of multiple targets is to censor (remove) the outputs of those reference cells that are much larger than the rest. A predetermined number J of reference cells (those with the largest returns) are removed and the adaptive threshold is determined by the remaining (N-J) cells; this is the censored mean-level detector. Loss associated with this CFAR may be in the order of 1 dB. Another approach to handling multiple nearby targets is the ordered statistic (OS) CFAR; the threshold is determined from one single value selected from the OS. The output from the N reference cells are put in order from smallest to largest, and the K-th ordered value when multiplied by a scalar is the threshold [1]. (c) The usual CFAR considerably reduces the range resolution so that two equal-amplitude targets can be resolved only if they are spaced greater than 2.5 pulse widths [1]. One reason for the poor resolution is that the range cells adjacent to the CUT are not used as part of reference cells since the target energy in the sidelobes would affect the threshold. (d) In many cases the form of clutter pdf is not known; in general it is different to the Rayleigh hypothesised in the CA-CFAR. A non parametric or distribution free detector has also been considered for CFAR; it has relatively large loss [1].

A clutter map (figure 4) divides the radar coverage area into cells on a polar or a rectangular grids. The clutter echo stored in each cell of the map can be used to establish a threshold for that range and azimuth. A number proportional to the amplitude of the clutter within the cell is stored at each cell of the clutter map. Since the clutter can change with time, the value of the clutter in each cell is continuously updated by resorting to a recursive loop with a prescribed forgetting memory factor [1], [35]. The larger the number of scans the more accurate will be the estimate of the clutter and the lower the loss (in the order of 0.8dB for averaging time of approximately 2 minutes [1]). On the other hand, the averaging time should be shorter than the limited dwell-time in which moving clutter (rain or chaff) is within the cell. A short averaging time also allows the threshold to recover to its improper state within a few scans after a target has passed through the cell. Self-masking and mutual masking problems are analysed in details in [35]. The response of the clutter map CFAR might be affected when a target of slow speed remains within the cell long enough to modify the threshold. This effect can be reduced by making the map cell greater than the radar resolution cell [35]. The increase of the size of the clutter-map cell should not be excessive since it reduces the interclutter visibility [35]. A clutter map CFAR has an advantage over the CA-CFAR in that it is not affected by non homogeneous clutter (edge effects) [1]. Another attribute of the clutter map is the potential to suppress slowly moving objects such as birds. Each threshold setting is checked against a clutter map before initiating a track. This technique is also referred to as scan-to-scan correlator [26, pp. 139-143].

One of the lecture series will study the use of KBS technology to CFAR.

5.3 ADAPTIVITY

Adaptive signal processing applies to three different types of radars, namely: i. ground based or ship-borne radars for clutter cancellation, ii. ground based or ship-borne radars equipped with a multi-channel phased-array antenna for jamming cancellation, iii. airborne early warning (AEW) radar equipped with a multi-channel phased-array antenna for clutter and jammer cancellation.

In all three cases the received radar echoes are converted to a digital format and the adaptive signal processing performed with digital technology. Common to the three applications is the type of adaptive processing: it takes an appropriate linear combination (assumption is made that radar echoes have Gaussian pdf) of signals received by the radar. The filter output is envelope-detected and compared against a suitable detection threshold set so as to maximize the detection probability (P_d) and to obtain a prescribed probability of false alarm (P_{fa}). Let N be the number of degrees of freedom used in adaptive processing, i.e. the dimension of the vector collecting the snapshot of radar data at a certain sampling instant. In the application area i., N is the number of echoes (T seconds apart, where T is the radar pulse repetition time (PRT)) captured by the radar receiving channel commensurate with a train of N coherent pulses transmitted by the radar. The clutter interference is cancelled by an adaptive filter, operating in the Doppler frequency domain, which obscures the

Doppler frequency interval occupied by the clutter spectrum. The filter sets a peak at the Doppler frequency which is expected from the useful target to be detected (for details see part I of [25]). In the application area ii., N is the number of sub-arrays (in which the radar antenna is decomposed) and associated receiving channels. The directional jamming/radio frequency interferences are cancelled by adaptively shaping the received antenna pattern to get deep nulls in the directions of arrival of interferences (for details see [23] and [40]). In the application area iii., N is the product of the number of received radar echoes, T seconds apart, and the number of sub-arrays in which the array aperture is decomposed. Both the clutter and jammer directional interferences are cancelled by synthesizing a two-dimensional filter that operates in the domains of Doppler frequency and direction of arrival. This type of filtering is also referred to as space-time adaptive processing (STAP); for details see [37] and the next subsection 5.4. The common problem of all the three applications is the online calculation of the weights to be used in the linear combination for the derivation of the adapted filter output. While the desired signal can be assumed to be known a priori, the interference is not known and is changing with time and in space; this means that the interference characteristics (represented by a covariance matrix) have to be estimated on line. A numerically robust and computationally efficient procedure to compute the adaptive filter output is known as QR-decomposition (QR); for details see, for instance, [23], [38] and [39]. A further advantage of the QR method is that it has a high degree of inherent parallelism which can be exploited to speed up the computations which are necessary in the applications considered here. Typical values of the computational requirements are as follows. For the first two application areas N is 10 to 20, the sampling rate is in the order of MHz and the number of operations amounts from Mflops to few Gflops. In application area iii., N is between 50 and 100 and even more, the sampling rate is in the order of MHz and the number of operations is 10 Gflops up. To reduce the considerable computational load especially required for application area iii., the following computational strategy can be devised. Extract the adapted weights at a rate lower (say, an order of magnitude) than the input data rate and apply them to the radar snapshots at their natural rate. This strategy is applicable only if the interferences change not too fast in time and space. An efficient algorithmic procedure to extract the weights is named Inverse QR (IQR) (see [66] for details).

A further point to address is the need to simultaneously focus more than one search beam (either one-dimensional, in Doppler frequency or direction of arrival, or two-dimensional in Doppler frequency and direction of arrival) to speed up the search within a prescribed sector or volume. The minimum variance distortion less response (MVDR) algorithm gives the technical mean to solve this operational problem (see[66] for details) in contrast to the generalized sidelobe canceller (GSLC) approach that focuses one search beam at a time [23]. The implementation of adaptive beam forming algorithms turns out to be a challenging computational problem due to the high data rate requested and to the ill conditioning of the interference covariance matrix in typical radar scenarios. Not surprisingly, the problem motivated the development of systolic algorithms and the investigation of mapping strategies on different parallel computing architectures; remarkable is the MUSE (Matrix Update Systolic Experiment), described in [67], for adaptive nulling with 64 degrees of freedom (DoF).

5.4 SPACE-TIME ADAPTIVE PROCESSING (STAP)

The detection of low flying aircrafts and/or surface moving targets, and the stand-off surveillance of areas of interest require a radar on an elevated platform like an aircraft. The AEW (Airborne Early Warning) radars pose a number of interesting technical problems especially in the signal processing area. The issue is not new: detect target echoes in an environment crowded of natural (clutter), intentional (jammer), and other unintentional radio frequency (especially in the low region of microwaves, e.g. VHF/UHF bands) interference. The challenge is related to the large dynamic range of the received signals, the non-homogeneous and non-stationary nature of the interference, and the need to fulfill the surveillance and detection functions in real time. One technique proposed today to solve the problem is based on STAP [36] to [39], [41] and [66]. Essentially, the radar is required to have an array (for instance, a linear array along the aircraft axis) of N antennas each receiving M echoes from a transmitted train of M coherent pulses. Under the hypothesis of disturbance having a Gaussian pdf and a Swerling target model, the optimum processor is provided by the linear combination of the NM echoes with weights $\mathbf{w}=\mathbf{M}^{-1}\mathbf{s}^*$, envelope detection and comparison with threshold. $\mathbf{M}$ is the space-time interference covariance matrix, i.e. $\mathbf{M}=E\{\mathbf{z}^*\mathbf{z}^T\}$ where $\mathbf{z}$ (dimension NMx1) is the collection of the NM disturbance echoes in a range cell, $\mathbf{s}$ - the space-time steering vector - is the collection

of the NM samples expected by the target, and (*) stands for complex conjugate (see Figure 8). This linear combination permits a two-dimensional filtering of clutter echoes that is more efficient than the one-dimensional filters in Doppler and angle respectively; this is shown in the well known Figure 9 (see also the paper by Klemm in [39, pp.2-1, 2-24]). A side-looking sensor configuration is assumed. The clutter spectrum extends along the diagonal of the (cos Φ- f_D) plot. Note the modulation by the transmit beam. Conventional temporal processing means that the projection of the clutter spectrum onto the f_D axis is cancelled via an inverse filter. Such filter is depicted in the back of the plot. As can be seen the clutter notch is determined by the projected clutter mainlobe which is a Doppler response of the transmit beam. Slow targets are attenuated. Spatial processing used for jammer nulling requires that the clutter spectrum is projected onto the (cos Φ) axis. Applying an inverse spatial clutter filter, however, forms a broad stop band in the look direction so that the radar becomes blind. Both fast and slow targets fall onto the clutter notch. Space-time processing exploits the fact that the clutter spectrum is basically a narrow ridge. A space-time clutter filter, therefore, has a two-dimensional narrow clutter notch so that even slow targets fall into the pass band.

A direct implementation, (via Sample Matrix Inversion, SMI) of the weight equation $\mathbf{w}=\mathbf{M}^{-1}\mathbf{s}^*$ is not recommended. One reason is related to the poor numerical stability in the inversion of the interference covariance matrix especially when large dynamic range signal is expected during the operation; another one is the very high computational cost. There is a need of extremely high arithmetic precision during digital calculation. Note that double precision costs four times as much as single precision. The situation would be different if, instead of operating on the covariance matrix **M**, we would operate directly on the data snapshots **z**(k), k=1,2,...,n, where n is the number of snapshots (i.e. : range cells) used to estimate the weights **w**. It can be shown that the required number of bits to calculate the weights, within a certain accuracy, by inversion of **M** is two times the number of bits to calculate the weights operating directly on the data snapshots **z**(k). This is so because the calculation of power values is avoided thus the required dynamic is halved. The algorithms that operate directly on the data are referred to as “data domain algorithms” in contrast to the “power domain algorithms” requiring the estimation of **M**. Figure 10 depicts both approaches. References [66] and [68] explain the details of power and data domain algorithms; an example of their application to recorded live data is in [41].

Much attention today is put on the so-called reduced-dimension (RD) STAP with the intent to limit the computational burden and the number of secondary data for adaptivity. Figure 11 is an overview of RD-STAP methods. The processor can transform the space-time data via the *data independent* transformation matrix **T** with size PQ<<NM. Common transformations include beam forming and Doppler processing steps. Examples of RD-STAP techniques are reported in the paper by B. Melvin [39, pp. 1-1, 1-19]. The Factored Time-Space (FTS) algorithm is a post-Doppler method suitable for long coherent dwells and high radial velocity targets. The FTS method essentially involves spatial notching of the clutter in a given Doppler filter. Since FTS provides no temporal adaptivity, it is not a true STAP algorithm. To enhance performance with only modest increase in required sample support and computational burden, DiPietro proposed the Extended Factored Algorithm (EFA). The EFA method involves adaptively combining several adjacent Doppler filters (typically three) and all spatial channels. The EFA method often exhibits performance very close to the theoretical joint-domain space-time bound. To provide diversity in spatial and temporal DoF, Wang and Cai developed the Joint Domain Localized (JDL) technique which is a post-Doppler, beam space method. Basically, the processor forms multiple beams, then Doppler processes each beam, and finally selects a collection of adjacent angle-Doppler bins over which to adapt the filter response. JDL provides good performance with very low training data requirements and very modest computational burden (see also A. Farina et al. paper in [38]). Three adjacent beams by three adjacent Doppler bins is a typical localized JDL processing regions.

Reduced-rank STAP methods involve *data-dependent* transformation and selection; details are reported in B. Melvin paper [39, pp. 1-1, 1-19]. The principal components is one of such methods. A benefit of this approach is a reduction in training data support; however, computational burden remains high, since the processor must compute eigenvalues and eigenvectors of the interference covariance matrix.

From a practical point of view, the first (non-adaptive) DPCA (Displaced Phase Center Antenna) experiment involving an array antenna has been carried out by Tsandoulas late ‘50s. More recent experiments conducted

in USA adopt linear side-looking arrays (NRL-AAFTE and MCARM). The Mountaintop program, also in USA, started in 1990 to study advanced processing techniques and technologies to support the requirements of future airborne early warning radar platforms; in particular the effect of terrain scattered jamming has been studied. In Europe the AER II program (Germany), the DO-SAR experiment (Germany) and the DERA experiment (UK) have been conducted. Today there are three operational systems with space-time ground clutter rejection capability: Joint STARS, AN/APG-76, and the AN/APY-6. The first one has a 3-aperture side-looking array antenna. The AN/APG-76 is a forward looking nose radar and the AN/APY-6 has both side-looking and forward looking capability. From the literature it is not clear whether these systems are based on adaptive algorithms (STAP) or use some non-adaptive DPCA-like techniques. References to these systems can also be found in R. Klemm paper in [39, pp.2-1, 2-24].

6. DATA PROCESSING

6.1 TRACKING

The tracking filter processes the target radar measurements (e.g.: range, azimuth, elevation and range rate) in order to achieve the following purposes: reduce the measurement errors by means of a suitable time average, estimate the velocity and acceleration of the target, predict future target position. The tracking filter can be considered as an application of stochastic filtering theory which is an important branch of modern theory of dynamic systems. The latter is characterised by the introduction of the following concepts: dynamic evolution of the system state variables, optimal control under well-defined disturbances and inputs, use of stochastic processes to model noise-corrupted data and uncertain parameters. The concept of a dynamic system is introduced to obtain a mathematical description of the input-output behaviour of a physical object of interest; for instance, the time evolution of the position of an aircraft. Deterministic system theory is not completely sufficient for practical design of operational systems. First, no mathematical model of a system is ever perfect; approximations, uncertain parameters, unmodelled effects are inherent ingredients. Secondly, dynamic systems are driven not only by input commands but also by disturbances from the environment and imperfections in the actuator's ability to deliver commanded controls. These are uncontrollable effects for which there are usually no adequate deterministic models. Finally, sensors that provide data about the system may deliver only partial information about the system state; they introduce their own time lag and other dynamics and are always noise-corrupted. These considerations justify the extension of the dynamic system concepts to the stochastic case where the aforementioned uncertainties and approximations are modelled as randomised input processes. A fundamental problem then arises in that it is necessary to find a method to optimally estimate the dynamic state on the basis of such stochastic mathematical models and incomplete noise-corrupted data from sensors. The solution is given by the optimal filtering theory. Important break troughs in this theory have been the Wiener filtering for stationary processes and the Kalman-Bucy filter (KF) which represents the optimal filter when both the dynamic state and the measurement equations are linear and the forcing and measurement noises are independent and have a Gaussian pdf. Practical implementation of the KF to tracking a flying object has required the following modifications and upgrades: include some form of adaptivity to account for unpredictable target manoeuvres; introduce more complex target models such as a bank of multiple models (MM) to which corresponds the MM and interactive MM (IMM) tracking filters; include a plot-track pairing logic which, in the case of a multi-target scenario, brings to an exponential explosion of the computational complexity if the optimum approach is invoked; successfully implement the multiple hypotheses tracking (MHT) to tackle the plot-track pairing logic at reasonable computational cost; account for the problem of non linearity (e.g.: tracking of ballistic re-entry targets) with some approximated form of non linear filtering (mainly the so-called extended KF); fusion techniques to manage and combine data provided by more than one sensors that look at the same surveillance space.

Text books and monographs are today available that discuss in details the tracking problems; some of them are: [26], [27], [42] to [46] just to mention a few. Recently the need to perform more accurate estimates in non linear, non Gaussian environment has prompted the conception of new approximations of the optimum filtering that effectively go beyond the KF theory. There are two approaches that have progressively acquired the favour of scientist, engineers and practitioners, they are the Unscented KF [47], [48] and the Particle Filtering [49] to [51].

One lecture of the series will study the use of KBS technology in the tracking systems.

7. CONCLUSIONS

This paper is an introduction to the lecture series on the application of KBS to radar signal and data processing. A wide review of the radar system techniques has been provided to facilitate the explanation of the application of KBS to radar that will follow in the next papers of this lecture series. KBS application to radar systems has been envisioned mainly by scientists of Rome Lab (USA) in cooperation with their Colleagues from university and industry; a list of relevant publications on the subjects are: [52] to [62].

8. ACKNOWLEDGEMENTS

This review paper has greatly benefited from papers and books duly referenced in the next section and in the text.

9. REFERENCES

[1] M. I. Skolnik, "Introduction to radar systems", 3rd ed., Mc Graw Hill, pp. 14-19, 2001.
[2] V. S. Chernyak, "Fundamentals of multisite radar systems", Gordon and Breach Science Publishers, 1998.
[3] "L'insegnamento e l'opera di Ugo Tiberio", (in Italian), 24 Ottobre 1998, 50 years after publication of his paper on Proc of IRE.
[4] M.I. Skolnik, "Fifty years of radar", PIEEE, vol. 73, Feb. 1985, pp. 182-197.
[5] IEEE Aerospace and Electronic Systems Magazine, October 2000, no. 10, Jubilee issue, p. 119.
[6] D. Ausherman, A Kozma, J. Walker, H. Jones, E. Poggio, "Developments in radar imaging". IEEE Trans on Aerospace and Electronic Systems, July 1984, pp. 363-400.
[7] L. J. Cantafio (editor), "Space-based radar handbook", Artech House, Inc., Norwood, Ma, 1989.
[8] I. S. Reed, "A brief history of adaptive arrays", Sudbury/Wayland Lecture Series, (Raytheon Div. Education) Notes, 23 October 1985.
[9] IEEE AESS 1991 Pioneer Award to F. R. Dickey, F. M. Staudaher, M. Labitt, IEEE Aerospace and Electronic System Magazine, May 1991, vol. 32, p. 32.
[10] M. I. Skolnik, "Opportunities in radar-2002", Electronic, Communication and Engineering Journal (ECEJ), IEE, December 2002, pp. 263-272.
[11] "Radar development at Lincoln Laboratory: a fifty-year review", MIT-Lincoln Laboratory Journal, vol. 12, no. 2, 2000, pp. 139-444.
[12] M. I. Skolnik, "Radar handbook", 2nd ed., McGraw-Hill, 1990.
[13] D. K. Barton, "Modern radar system analysis", Artech House, Norwood, MA, 1988.
[14] F. E. Nathanson, "Radar design principles", 2nd ed., McGraw Hill, New York, 1991.
[15] E. Brookner (Ed.), "Aspects of modern radars", Artech House, Norwood, MA, 1988.
[16] IEEE Standard (521TM) Letter Designations for Radar-Frequency Bands Sponsored by Letter Band Standard Committee of the IEEE Aerospace and Electronic Systems Society (2002) for the IEEE Standards Activity Department, Piscataway, NJ, USA, 8th January 2003.
[17] R. J. Galejs, "Volume surveillance radar frequency selection", Proc. of IEEE Int. Radar Conference, Alexandria (Va), May 7-12, 2000, pp. 187-192.
[18] W. J. Fontana, R. H. Krueger, "An/SPY-3: the Navy's next generation force protection radar system", Naval Surface Warfare Center, Dahlgreen Division Technology Digest, 2000-2001 Issue: Theater Air Defense, pp. 230-239.
[19] E. Hanle, A. Farina, C. Pell, "Bistatic / Multistatic radar bibliography". Special issue on bistatic and multistatic radar, IEE Communications, Radar and Signal Processing, Pt. F. vol. 133, no. 7, December 1986, pp. 664-668.
[20] N. J. Willis, "Bistatic Radar", TSC, Silver Spring, MD, 1995, 2nd Edition.

[21] P. E. Howland, "Target tracking using television-based bistatic radar", IEE Proc. Radar, Sonar and Navigation, June 1999, vol. 146, no. 3, pp. 166-174.
[22] E. Hanle, "Radar and general radiolocation. Glossary of terms and definition in English, French and German", VDE, Verlag, 2002.
[23] A. Farina, "Antenna based signal processing techniques for radar systems", Artech House, 1992.
[24] R. A. Stapleton, S. R. Horman, H. H. Szu, "DAR technology for volume surveillance radar application", Naval Surface Warfare Center, Dahlgreen Division Technology Digest, 2000-2001 Issue: Theater Air Defense, pp. 240-249.
[25] A. Farina (Editor), "Optimized radar processors". On behalf of IEE, Peter Peregrinus Ltd. London, October 1987.
[26] A. Farina, F.A. Studer, "Radar data processing. Introduction and tracking" (vol. I). Researches Studies Press. England, John Wiley, 1985.
[27] A. Farina, F.A. Studer, "Radar data processing. Advanced topics and applications" (vol. 2). Researches Studies Press, England, John Wiley, 1986.
[28] W. Wirth, "Radar techniques using array antennas", The Institution of Electrical Engineers Editions, London, 2001.
[29] E. Brookner, "Phased-array for the new millennium", Invited paper, Millennium Conference on Antennas and Propagation, AP-2000, Davos, Switzerland.
[30] S. Sabatini, M. Tarantino, "Multifunction Array Radar: System Design and Analysis", Artech House, Inc., Norwood (MA), USA, 1994.
[31] J. B. Billingsley, "Low-angle radar land clutter: measurements and empirical models", Scitech Publishing Inc., William Andrew publishing, IEE, 2002.
[32] A. Farina, E. Protopapa, "New results on linear prediction theory for clutter cancellation", IEEE Trans. on Aerospace and Electronic Systems, vol. AES - 24, no. 3, May 1988, pp. 275-286.
[33] P. Lombardo, M.V. Greco, F. Gini, A. Farina, J.B. Billingsley, "Impact of clutter spectra on radar performance prediction", IEEE Trans. on Aerospace and Electronic Systems, vol. AES-37, no. 3, July 2001, pp. 1022-1038. B. Carlton, best paper award for 2001.
[34] F. Gini, M.V. Greco, A. Farina, "Clairvoyant and adaptive signal detection in non-Gaussian clutter: a data-dependent threshold interpretation". IEEE Trans. on Signal Processing, vol. 47, no. 6, June 1999, pp. 1522-1531.
[35] A. Farina, F.A. Studer, "A review of CFAR detection techniques in radar systems". Microwave Journal, Vol. 29, no. 9, September 1986, pp. 115-128.
[36] J. Ward, "Space-time adaptive processing for airborne radar", MIT Lincoln Laboratory, Technical report TR-1015, December 13, 1994.
[37] R. Klemm, "Space Time Adaptive Processing: Principles and applications", IEE Radar, Sonar, Navigation and Avionics 9, IEE Press, 1998.
[38] "Special issue on STAP", *Electronics & Communication Engineering Journal*, vol. 11, no. 1, pp. 1-63, February 1999.
[39] RTO Lecture Series 228, "Military applications of Space Time Adaptive Processing", September 2002, NATO, Research and Technology Organisation, BP 25, 7 rue Ancelle, F-9221, Neuilly-sur-Seine Cedex France.
[40] A. Farina, "Electronic Counter-Counter Measures". Chapter 9 of Radar Handbook, 2nd Edition (Editor M.I. Skolnik), Mc Graw Hill, 1990.
[41] A. Farina, R. Graziano, F. Lee, L. Timmoneri, "Adaptive space-time processing with systolic algorithm: experimental results using recorded live data". Proc. of Int. Conf. on Radar, Washington D. C. (USA), May 8-11, 1995, pp. 595-602.
[42] Y. Bar-Shalom, T. Fortmann, "Tracking and data association", Academic Press, 1988.
[43] S. Blackman, "Multiple-target tracking with radar applications", Artech House, 1986.
[44] Y. Bar-Shalom, X-Rong Li, "Multitarget-multisensor tracking: principles and techniques", YBS, 1995.
[45] P. Bogler, "Radar principles with applications to tracking systems", John Wiley & Sons, New York, January 1990.
[46] D. Halls, J. Llinas, "Handbook of multisensor data fusion", CRC, 2001.
[47] S. Julier, J. Uhlmann, H. F. Durrant_Whyte, "A new method for the non linear transformation of means and covariances in filters and estimators", IEEE Trans. on Automatic Control, vol. AC-45, no. 3, pp. 477-482, March 2000.

[48] S. Julier, J. Uhlmann, "A new extension of the Kalman filter to nonlinear systems", in The Proceedings of AeroSense: The 11th International Symposium on Aerospace/Defense Sensing, Simulation and Controls, Orlando, Florida, 1997, SPIE, Multi Sensor Fusion, Tracking and Resource Management II, SPIE volume 3068, pp.182-193.

[49] A. Doucet, N. de Freitas, N. J. Gordon, editors, "Sequential Monte Carlo methods in practice", New York: Springer-Verlag, January 2001.

[50] M. S. Arulampalam, S. Maskell, N. Gordon, T. Clapp, "A tutorial on particle filters for on line nonlinear / nonGaussian Bayesian tracking", IEEE Trans. on Signal Processing, vol. 50, no. 2, pp. 174-188.

[51] C. Hue, J.-P. Le Cadre, P. Perez, "Sequential Monte Carlo methods for multiple target tracking and data fusion", IEEE Trans. on Signal Processing, vol. 50, no. 2, pp. 309-325.

[52] R. Adve, P. Antonik, W. Baldygo, C. Capraro, G. Capraro, T. Hale, R. Schneible, "Knowledge-based application to ground moving target detection", AFRL-SN-TR-2001-185, In-House Technical Report, September 2001.

[53] Y. Salama, R. Senne, "Knowledge-based applications to adaptive space-time processing, volume I: Summary ", AFRL-SN-TR-2001-146 vol. I (of vol. VI), Final Technical Report, July 2001.

[54] H. Schuman, "Knowledge-based applications to adaptive space-time processing, volume II: Airborne radar filtering", AFRL-SN-TR-2001-146 vol. II (of vol. VI), Final Technical Report, July 2001.

[55] H. Schuman, "Knowledge-based applications to adaptive space-time processing, volume III: Radar filtering rule book", AFRL-SN-TR-2001-146 vol. III (of vol. VI), Final Technical Report, July 2001.

[56] C. Morgan and L. Moyer, "Knowledge-based applications to adaptive space-time processing, volume IV: Knowledge-based tracking", AFRL-SN-TR-2001-146 vol. IV (of vol. VI), Final Technical Report, July 2001.

[57] C. Morgan and L. Moyer, "Knowledge-based applications to adaptive space-time processing, volume IV: Knowledge-based tracker rule book", AFRL-SN-TR-2001-146 vol. V (of vol. VI), Final Technical Report, July 2001.

[58] Y. Salama, R. Senne, "Knowledge-based applications to adaptive space-time processing. volume VI: Knowledge-based space-time adaptive processing (KBSTAP) user's manual and programmer's manual", AFRL-SN-TR-2001-146 vol. VI (of vol. VI), Final Technical Report, July 2001.

[59] P. Antonik, H. Schuman, P. Li, W. Melvin, M. Wicks, "Knowledge-based space-time adaptive processing", Proc. of the IEEE National Radar Conference, Syracuse, NY, May 1997.

[60] R. Adve, T. Hale, M. Wicks, P. Antonik, "Ground moving target indication using knowledge-based space-time adaptive processing", Proc. of 2000 IEEE Int. Radar Conference, Washington D.C., pp. 735-740, May 2000.

[61] W. Baldygo, et. al., "Artificial intelligence applications to constant false alarm rate (CFAR) processing", Proc. of IEEE 1993 National Radar Conference, 1993, pp. 275-280.

[62] J. R. Guerci, "Knowledge-Aided Sensor Signal Processing and Expert Reasoning", in *Proc. 2002 Knowledge-Aided Sensor Signal Processing and Expert Reasoning (KASSPER)* Workshop, Washington DC, 3 April, 2002, Washington DC, CD ROM.

[63] W. C. Morchin, "Airborne early warning radar", Artech House, 1990.

[64] F. Gini, A. Farina, M. Greco, "Selected list of references on radar signal processing", IEEE Trans. on Aerospace and Electronic Systems, vol. AES-37, no. 1, January 2001, pp. 329-359.

[65] F. Robey, D. Fuhrmann, E. Kelly, R. Nitzberg," A CFAR adaptive matched filter detector", IEEE Trans. on Aerospace and Electronic Systems, vol. AES-28, no. 1, January 1992, pp. 208-216.

[66] P. Bollini, L. Chisci, A. Farina, M. Giannelli, L. Timmoneri, G. Zappa, "QR versus IQR algorithms for adaptive signal processing: performance evaluation for radar applications". Proceedings of IEE on Radar, Sonar and Navigation, October 1996, vol. 143, no. 5, pp.328-340.

[67] C. M. Rader, "Wafer-scale integration of a large systolic array for adaptive nulling", MIT-Lincoln Laboratory Journal, 1991, vol. 4, no. 1, pp. 3-29.

[68] L. Timmoneri, I.K. Proudler, A. Farina, J.G. McWhirter, "QRD-based MVDR algorithm for adaptive multipulse antenna array signal processing", IEE Proc. on Radar, Sonar and Navigation, vol. 141, no. 2, April 1994, pp. 93-102.

[69] M. Cicolani, A. Farina, E. Giaccari, F. Madia, R. Ronconi, S. Sabatini, “Phased array systems and technologies in AMS”, IEEE International Symposium on Phased Array Systems and Technology, 14-17 October 2003, Boston (Ma). Invited Paper.

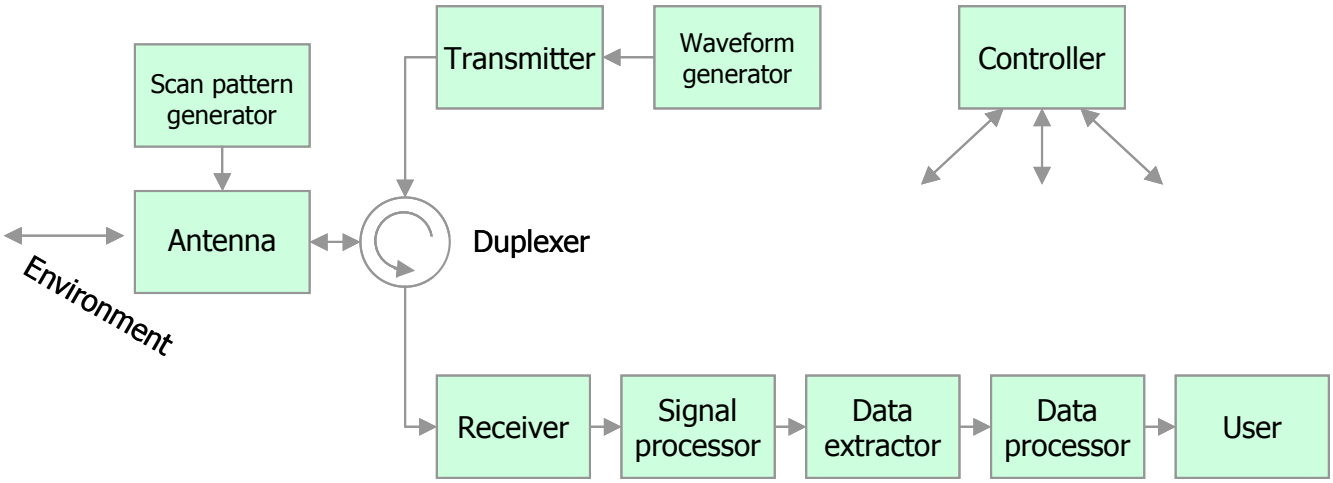

Figure 1: Simplified scheme of a modern radar system. From A. Farina and F. A. Studer [26].

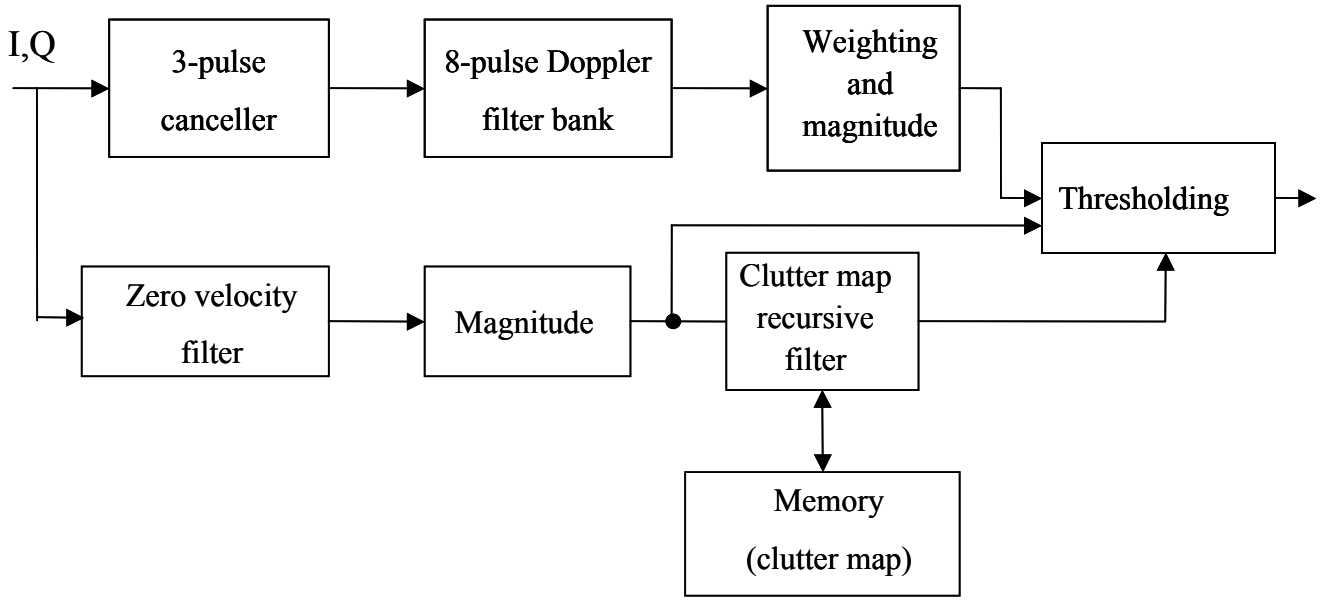

Figure 2: Block diagram of the original Moving Target Detector (MTD) signal processor.

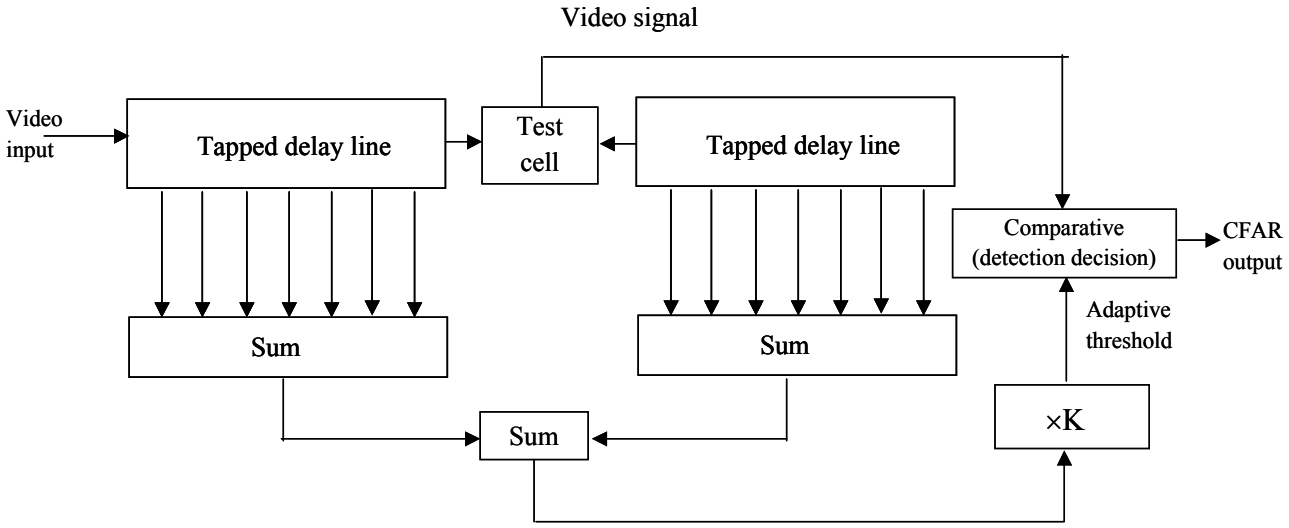

Figure 3: Cell averaging CFAR.

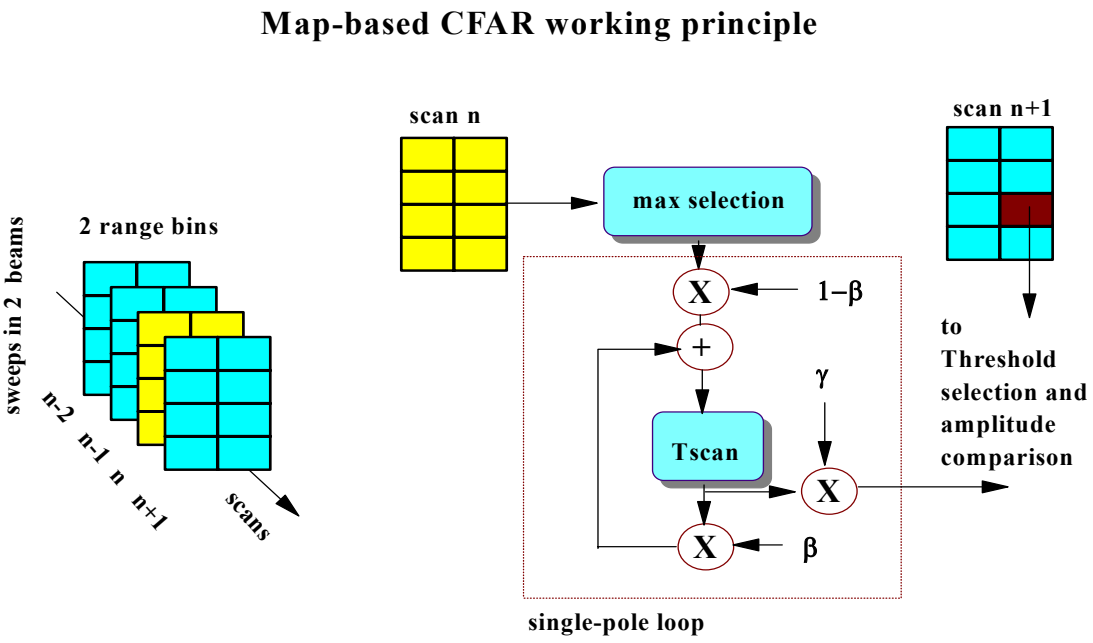

Figure 4: Map-based CFAR. From A. Farina and F. A. Studer [35].

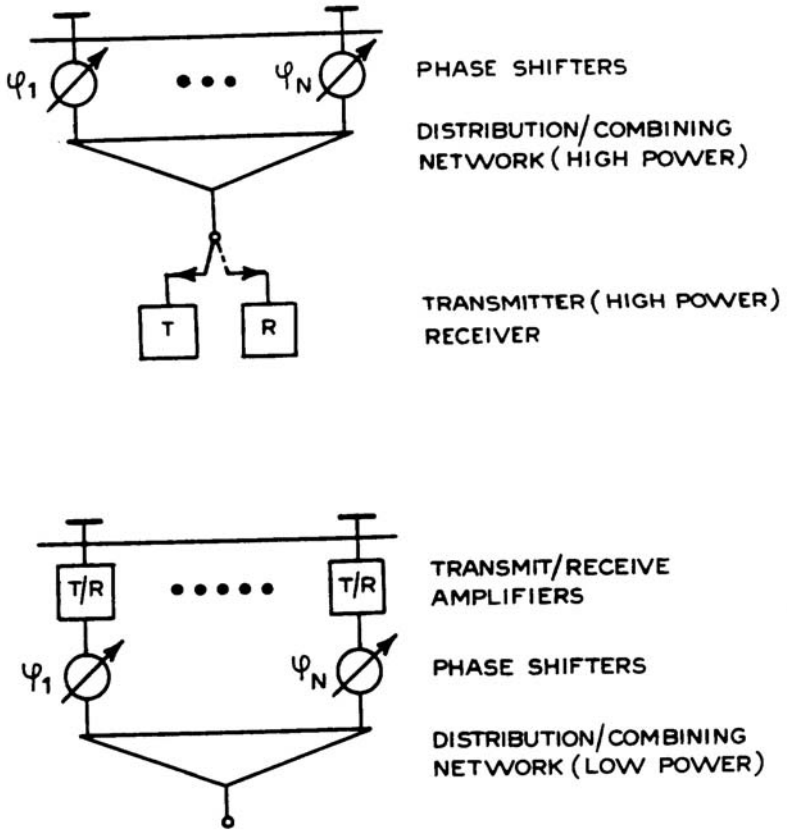

Figure 5: Passive and active phased-array antenna. From W. Wirth [28].

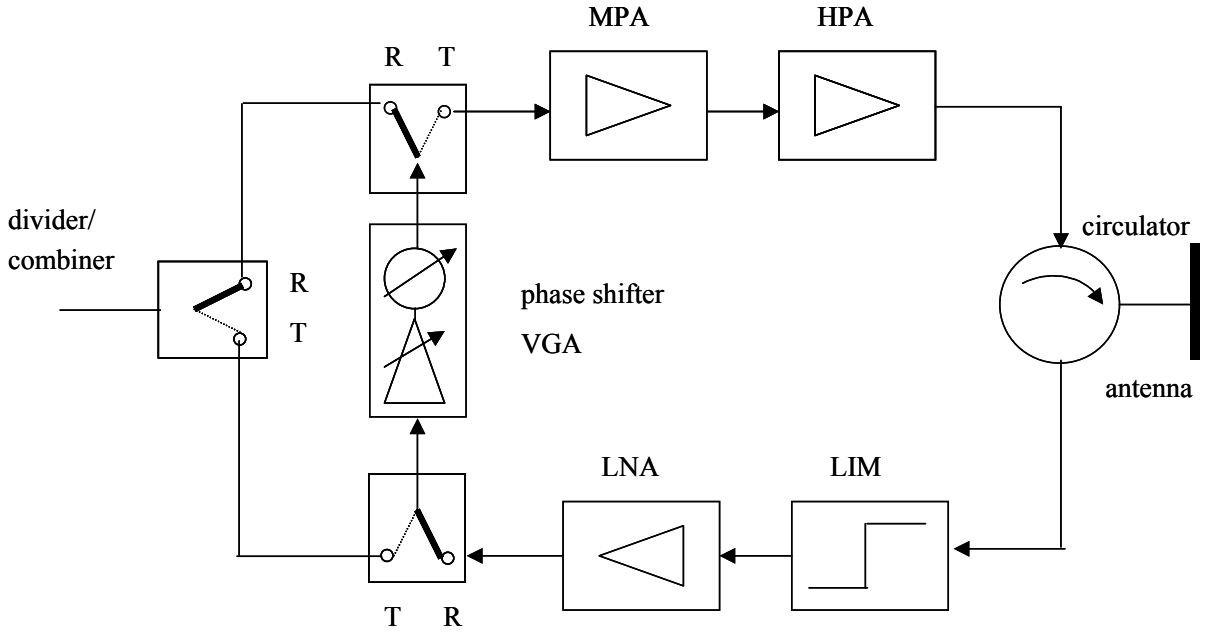

Figure 6: Block diagram of transmit/receive module (TRM). MPA: medium-power driver amplifier, HPA: High Power Amplifier, LNA: Low Noise Amplifier, LIM: Limiter, VGA: Variable Gain Amplifier. From W. Wirth [28].

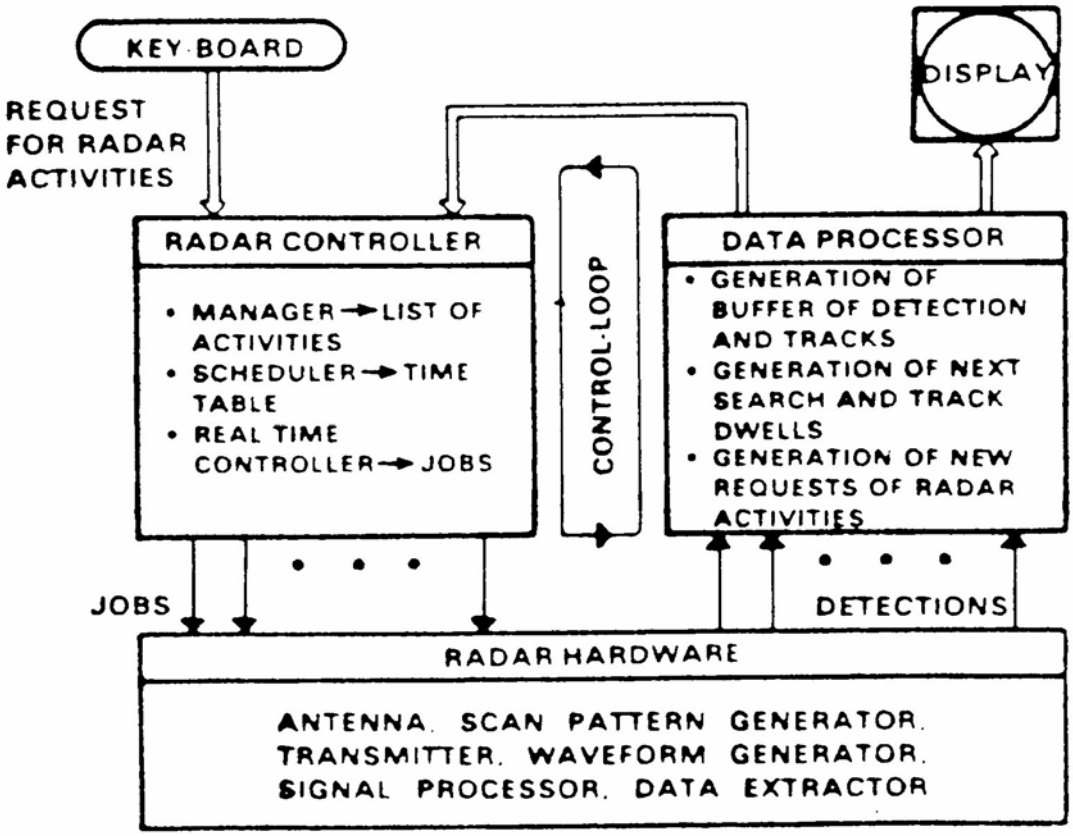

Figure 7. The managing computer in a modern phased array radar. From A. Farina and F.A. Studer [26].

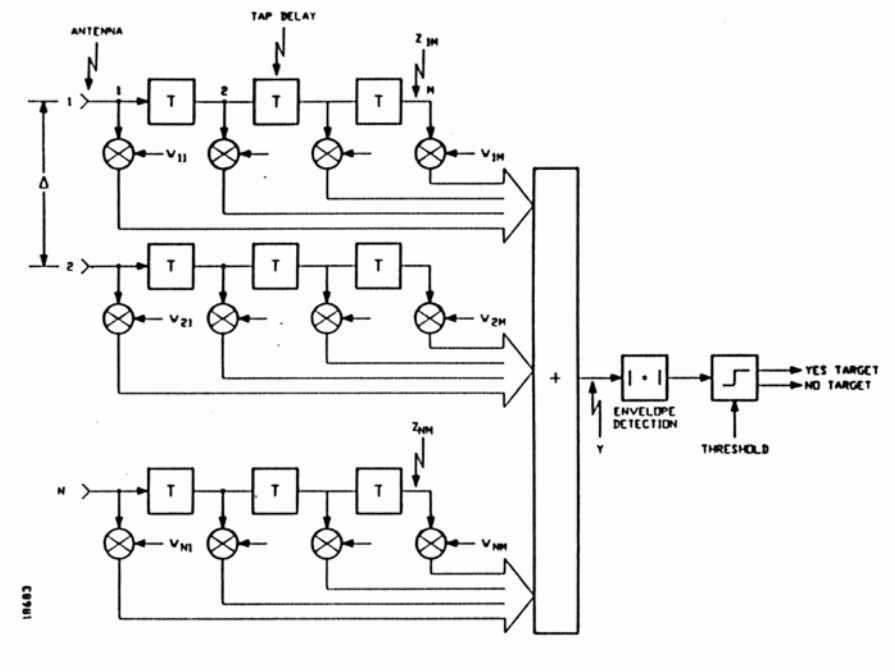

Figure 8: Scheme for STAP.

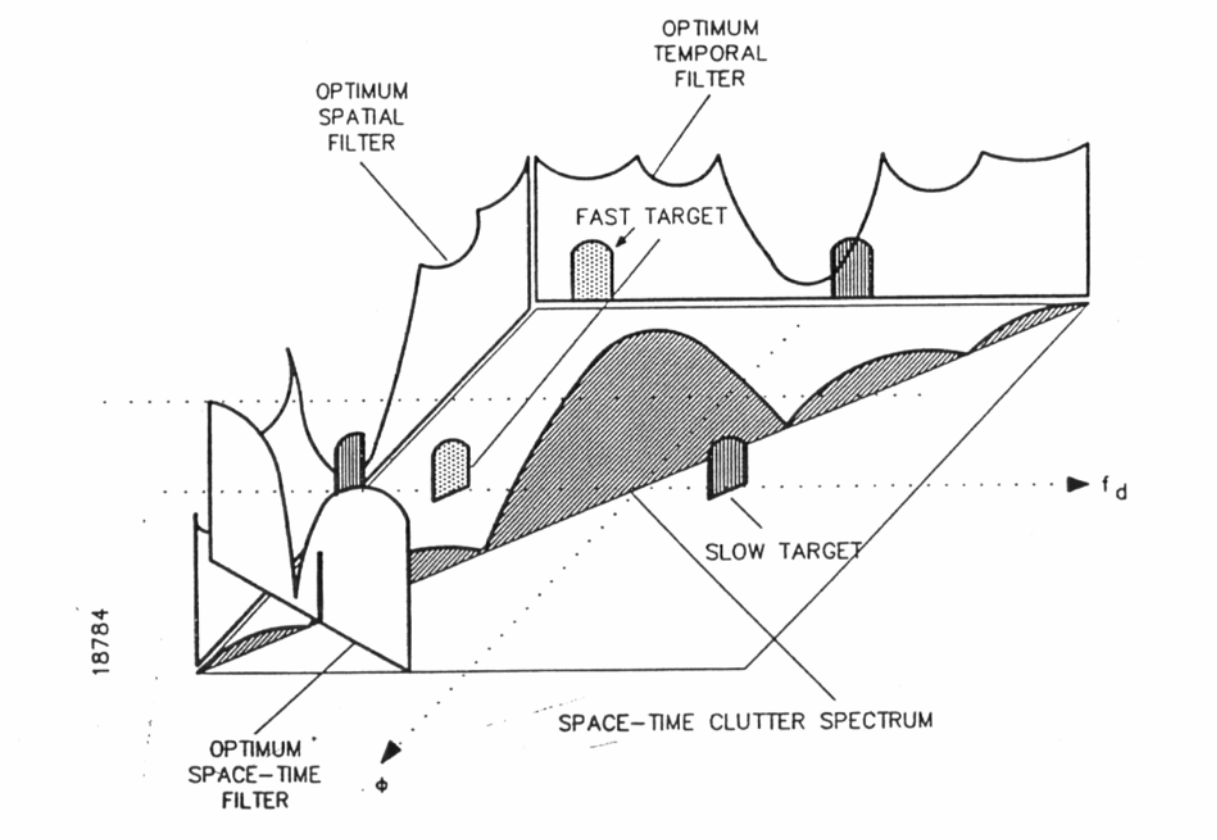

Figure 9: Scheme for STAP. From J. Ender and R. Klemm [37].

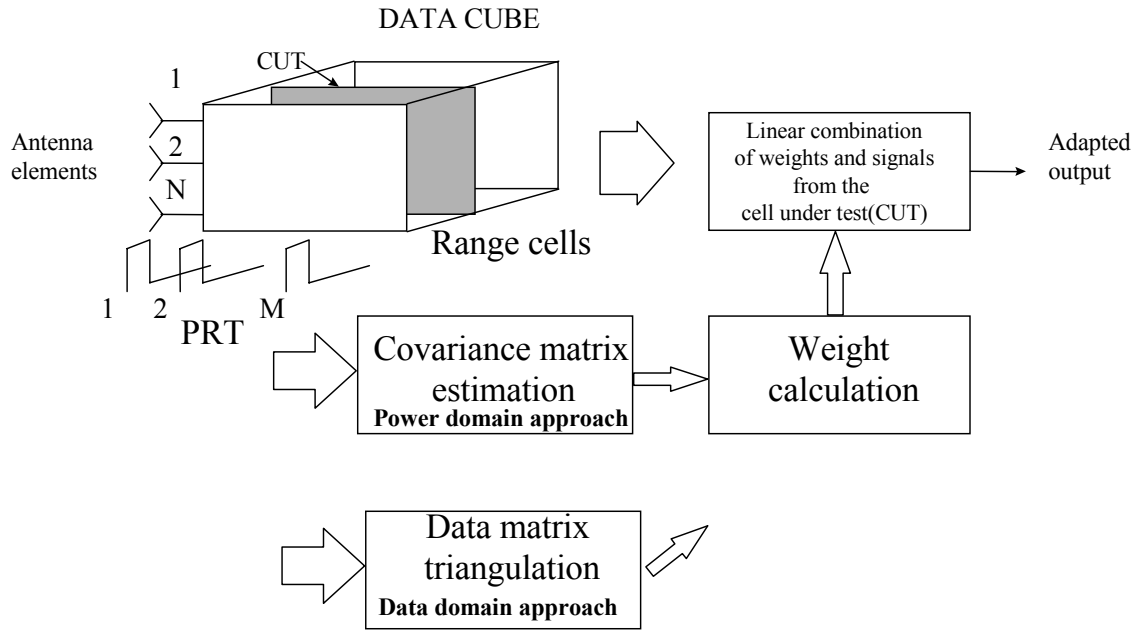

Figure 10: The power and data domain approaches for STAP.

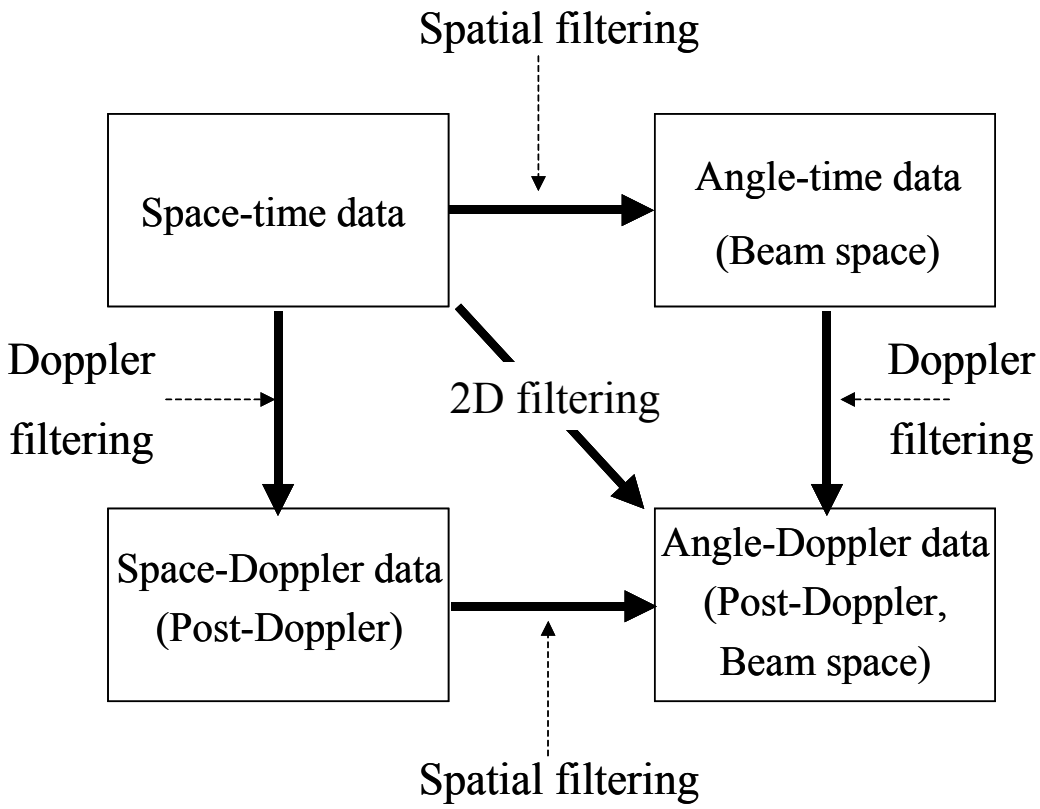

Figure 11: Overview of reduced-dimension STAP methods. From J. Ward [36].

Fundamentals of Knowledge-Based Techniques

Dr. Gerard T. Capraro
Capraro Technologies, Inc.
311 Turner Street – Suite 410
Utica, NY 13501
USA
Email: gcapraro@caprarotechnologies.com

Abstract

This paper provides a brief overview of the fundamentals of Artificial Intelligence (AI) and Knowledge-Based (KB) techniques that we feel are necessary to understand the current research efforts being performed in knowledge base radar signal and data processing. A set of definitions and descriptions of some of the major areas of AI are presented. Examples are provided using radar terminology to illustrate concepts presented. Finally we present a description of those technologies being pursued by the World Wide Web Consortium (W3C) for building the Semantic Web or the next generation Internet. The Semantic Web is perceived by some as being a very large knowledge base.

Introduction

Current signal processing systems are built assuming Gaussian clutter and are optimized for their processing requirements whether the systems are mounted on an aircraft, a missile, a spacecraft, or at a ground based site. The algorithms are "hardwired" into the computer's architecture in order to meet the real-time requirements demanded by the sensor's operating parameters, e.g. scans per second and number of sensor elements. This approach to building radar systems is being assessed today by the radar research and development community because of its rigidity and high costs and will slowly change and evolve. This evolution will manifest itself such that different algorithms and/or their parameters will be modified by the radar's software as the environment changes. For instance if a radar is being jammed by a transmitter from a particular direction, then that radar could place a null in its antenna pattern in the direction of the jammer to reduce its negative affect. This and many more sophisticated algorithms have been studied and numerous research papers written.

Some of the most progressive work in employing artificial intelligence (AI) techniques has been pursued by the US Air Force Research Laboratory's Sensors Directorate. Some of their original efforts have been in the constant false alarm rate (CFAR) portion of a radar's signal processing chain. Work was performed (1, 14) to demonstrate that if the cell under test is near the boundary of two different clutter regions, then blindly applying a CFAR algorithm (like cell averaging) will not perform as well as choosing only those cells with the same type of clutter as the test cell and then performing cell averaging. This approach provides a better probability of detection and lower false alarm rates. However, to apply this approach for a radar looking for targets whose background is the Earth, requires that the registration of each cell on the earth be known and the type of clutter be categorized to determine which cells are the same type. If the radar is resident on a moving platform looking at the Earth then the algorithm must be dynamic in order to register the radar's beam on the Earth for each coherent processing interval (CPI). Laboratory experiments with radar data have shown good results especially when a radar is illuminating heterogeneous clutter such as land sea interface.

This work was extended beyond the detection stage to the rest of a radar's processing chain under a US Air Force (USAF) effort dealing with knowledge based space time adaptive processing (KBSTAP) (2,3). This effort demonstrated the benefits of using outside data sources to affect the filtering, detection, and tracking stages of a surveillance radar sensor. Data from a side looking airborne radar system was used in demonstrating the performance enhancements over a conventional radar. The measurements were obtained

Paper presented at the RTO SET Lecture Series on "Knowledge-Based Radar Signal and Data Processing", held in Stockholm, Sweden, 3-4 November 2003; Rome, Italy, 6-7 November 2003; Budapest, Hungary, 10-11 November 2003; Madrid, Spain, 28-29 October 2004; Gdansk, Poland, 4-5 November 2004, and published in RTO-EN-SET-063.

from the multi-channel airborne radar measurement (MCARM) program (4) conducted by the USAF. Another program showed the benefits of using map data obtained from the US Geological Survey (USGS) to improve the performance of space-time adaptive processing (STAP) on an airborne radar selecting range rings based on computed criteria rather than blindly choosing the range rings surrounding the test range ring. This effort, KBMapSTAP (5,6), along with numerous researchers (e.g. Dr. Michael C. Wicks, Mr. William Baldygo, Mr. Gerard Genello, Dr. William Melvin, and Dr. Joseph Guerci) have laid the ground work for a new DARPA program. The Knowledge-Aided Sensor Signal Processing Expert Reasoning (KASSPER) program is to investigate the use of outside data sources to dynamically change a radar's signal processing chain to enhance a radar's performance.

Can we build new radar systems that can dynamically change its processing given information from other sensors, outside sources, weather data, etc.? We believe that we can. The computing clock rates for computers have been doubling approximately every 18 months. Today's commercial off the shelf computers have clock rates exceeding 3 GHz. We believe that the computing power is available to insert sophisticated "rules/logic" within radar signal and data processing.

This paper provides an overview of knowledge base technologies because we feel that therein lies the methods we will need to design radar systems that can dynamically change their algorithms as required to enhance their performance. The current work described in this lecture series contains examples of this relatively new research field. The knowledge base algorithms are currently only exercising simple rule-based logic. However, in the not too distant future we will be developing KB radar systems that will not only be able to dynamically change their algorithms but be able to explain why they did what they did and be able to learn from their own gathering of data, information, and by measuring their on going performance. The last paper of this series will discuss how KB techniques can be used to build an end-to-end radar signal and data processing system.

The following section will provide an introduction to the field of AI and describe some of the major areas of investigation. The next section will be devoted to knowledge base systems and methods for data representation and processing. The following section will be devoted to some of the basic elements of the Semantic Web and how the W3C technologies along with basic knowledge base processing will allow us to build a knowledge base for radar signal processing. The last section will provide a summary.

Artificial Intelligence

Modern day artificial intelligence has been around since the 1950s. It has been defined by Rich (7) as "the study of how to make computers do things at which, at the moment, people are better." Barr and Feigenbaum (8) define AI as "the part of computer science concerned with designing intelligent computer systems, that is, systems that exhibit the characteristics we associate with intelligence in human behavior." Buchanan and Shortliffe (9) define AI as "that branch of computer science dealing with symbolic, nonalgorithmic methods of problem solving." It is conjectured that there are varied definitions of AI because the field contains many sub-fields or areas of interest within its general domain. Some of these areas are planning, robotics, speech recognition, natural language processing, and expert systems.

Planning is that field where we wish to analyze a significant amount of information in order to develop a methodology to achieve some well defined goal. This area of AI is pursued by business and the military for achieving such goals as maximizing profit and the planning for the delivery of the proper ordinances on targets while conserving life and fuel. These systems are usually interactive and aid decision makers in managing their enterprises.

Robotics is that field that is concerned with developing "thinking" forms of devices that can function within a changing environment. This field is not interested in robotic manufacturing devices where the electromechanical devices only perform a pre-programmed set of actions. This field is interested in developing devices that can achieve its predefined goals by adapting to a dynamic environment, without human intervention.

Speech recognition is concerned about computers understanding human spoken language. The research is part of the general field of natural language understanding whether the communications media is speech or written communications. The goal is to have a computer not only understand a human's language of communications but also to generate responses, usually in the same media.

Expert systems is that field that tries to capture and emulate the actions of an expert within a particular domain of interest. Expert systems are sometimes called knowledge based systems. They are composed of facts about a domain of interest along with heuristics or rules that operate upon these facts.

As can be seen from above the areas of AI that are closest to the radar domain are expert systems and robotics. We chose robotics because we want the radar signal processing to change both on transmit and receive, depending upon its goals and changing environment and operate somewhat autonomously. We chose expert systems and knowledge base systems because we want to change the transmitting and receiving signal processing based upon a changing environment that would be based upon an expert. However, we don't have an "expert", i.e. there is no human that currently modifies the signal processing software chain in real-time based upon the changing environment. We in the radar community are just beginning to develop the rules or heuristics for determining how and when the processing chain should be changed. This is why we emphasize the knowledge base and not the expert system or robotics portions of the AI field. As we become more knowledgeable and have proven techniques we will advance to building our radar sensors as robots. First, we will develop the knowledge base that operates with human intervention. Second, once a knowledge base approach is proven in fielded systems then we may emulate the human intervention portion of the system as an expert system. When this approach is achieved for multiple sensors, possibly operating on an aircraft platform, then our next step will be to have these sensors operate autonomously as a robot.

Knowledge Base Systems (KBS)

As noted above a knowledge base system consists of facts about a particular domain and heuristics or rules that operate upon these facts. A KBS has three main components and can be built in numerous ways. We will highlight some of the main aspects of two out of three of the main components. The main components are the user interface, the knowledge base, and the inference engine. The user interface is that part of the KBS that allows the user to communicate with the computer. This communication can be implemented using voice, keyboard, touch screen, etc. for both input and in some cases output from the computer. This component is not a major concern for the purposes of this paper since the current research in KBS and radar systems is dealing with embedding the KBS within a computer software process. We are not at the point in our research where we are concerned with how a human will operate with the KBS.

The knowledge base and the inference engine are the major components that this paper addresses. The knowledge base representation is a key element in understanding KB systems and how they function. Three methods that have been used are: predicate logic, semantic nets and frames. The following condensed description of knowledge representation was obtained from different sources (7 - 10) and radar examples added to help understand some of the basic concepts.

Predicate Logic

Predicate logic knowledge representation models what are known as facts within a domain and represents these facts so that an inference engine or computer software can operate upon their representation. The basic element is a fact for example "The ANxx is a radar." This can be represented as Radar (ANxx). We can also state that all radar systems have an antenna (i.e. If X is a radar then X has an antenna.) and therefore by using deductive logic we can deduce that ANxx has an antenna, i.e. ANxxHas (antenna). From this we can generate the following fact in English representation that "The ANxx has an antenna." This approach allows us to traverse the different mappings between facts and their representations. See figure 1.

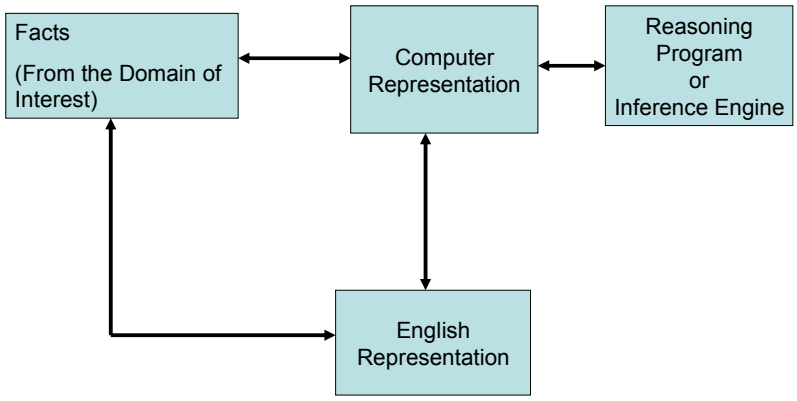

Figure 1. Mappings Between Facts and Their Representations.

Note that these mapping functions or relations may be one to one, many to one, or many to many. For example, "All radars have antennas" and "Every radar has an antenna" could map to the same fact. In predicate logic we can represent domain facts as statements written in well formed formulas. In so doing, this knowledge can be represented in software and inference engines can process them and draw conclusions and learn. Some example facts and clauses are provided in figure 2.

RadarNom(ANxxx)	LocLatTime(ANsss, xxxxN, Time1)
RadarHas(Tx)	LocLonTime(ANsss, xxxxE), Time1)
RadarHas(Rx)	LocLatTime(ANyyy, xxxxN, Time2)
RadarHas(RxAnt)	LocLonTime(ANyyy, xxxxE, Time2)
RadarHas(TxAnt)	
TxHas(RadiatedPowerLevel)	RxNoiseFloor(ANsss, -110dBM)
RxHas(CFARThreasholdLevel)	RxNoiseFloor(Anyyy, -100dBM)
RxHas(NoiseFloor)	
RxHas(Target)	ReflectiveTime(T1, xxxx)
AntHas(Gain)	ReflectiveTIme(T2, xxxx)
AntHas(3dBBeamWidthElv)	
AntHas(3dBBeamWidthAz)	CFARThreasholdLevel(ANsss, xxxx)
RadarHas(LocLon)	CFARThreasholdLevel(ANyyyy, xxxx)
RadarHas(LocLat)	
TargetHas(Range)	Target(ANsss, T1)
TargetHas(RxPowerLevel)	Target(ANyyy, T2)
TargetHas(ReflectiveTime)	
RangeTarget(Units, Meters)	RxPowerLevel(T1, xxxx)
ReflectiveTime(Units, Microsec)	RxPowerLevel(T2, xxxx)
OneSecondHas(10^6 Microsec)	

Figure 2. Some Hypothesized Radar Facts and Clauses

If the knowledge base defined for a particular domain is small relative to a computer's main memory, then all of the facts and clauses can be contained within main memory. This will allow for very fast processing. If however, for large knowledge bases that cannot be contained within main memory, many developers have made use of database management systems (DBMS) to store the facts while the rules were maintained within main memory with the inference engine. DBMS are built to manage large databases with many users

accessing their contents. It has optimized processing functions to manage data stored on secondary storage devices (e.g. hard drives) thereby allowing knowledge base systems to process their rules while maintaining the facts. It should be noted that currently there are some large scale DBMS that contain inference engines within their structure, e.g. Oracle 9i.

For relational DBMS the definition of simple facts such as AntHas (xxx) and RadarHas (xxx) can easily be mapped to an attribute value pair in a relation Has. The attributes are Ant and Radar and their corresponding values are the values in the parenthesis of each of the respective facts. The process of building these facts are similar to the building of entity relationship diagrams for databases. The above facts and clauses can be represented as relations in a DBMS as shown in Figure 3.

Has
Relation [Radar, Tx]
[Radar, Rx]
[Radar, RxAnt]
[Radar, TxAnt]
[Tx, RadiatedPowerLevel]
[Rx, NoiseFloor]
[Rx, Target]
[Rx, CFARThreasholdLevel]
[Ant, Gain]
[Ant, 3dBBeamwidthElv]
[Ant, 3dBBeamwidthAz]
[Radar, LocLon]
[Radar, LocLat]
[Target, RxPowerLevel]
[OneSec, 10^6MicroSec]
[Target, RxPowerLevel]
[Target, Range]
[Target, ReflectiveTime]

IsA
Relation [TxAnt, Ant]
[RxAnt, Ant]
LocLatTime
Relation [ANsss, xxxxN, Time1]
[ANyyy, xxxxN), Time2]

LocLonTime
Relation [ANsss, xxxxE, Time1]
[ANyyy, xxxxE, Time2]
RxNoiseFloor
Relation [ANsss, -110dBM]
[ANyyy, -100dBM]
ReflectiveTime
Relation [T1, xxxx]
[T2, xxxx]
CFARThreasholdLevel
Relation [ANsss, xxxx]
[ANyyy, xxxx]
Target
Relation [ANsss, T1]
[ANyyy, T2]
RxPower
Relation [T1, xxxx]
[T2, xxxx]

Figure 3. Relational DBMS Model of Facts and Causes

Semantic Nets

Originally semantic nets were developed for the purpose of modeling the English language (7), for a computer to understand. A method used by engineers and scientist to understand complex relationships, is to draw pictures. This is true in the DBMS world with regard to designing databases with the use of entity relationship diagrams. It is also true in knowledge representation with the use of similar graphs called semantic nets. Semantic nets are networks composed of nodes and arcs. Nodes represent facts and the arcs or edges represent relationships. For entity relationship diagrams the nodes represent entities and the arcs represent relationships. The nets also help in simplifying the deduction process. Consider the following partial semantic net of our radar example shown in Figure 4.

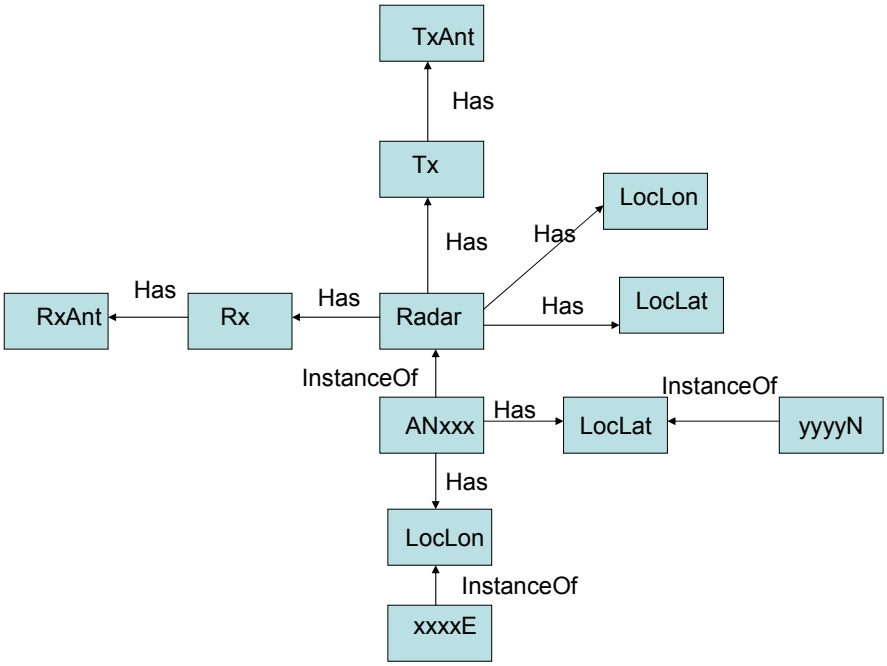

Figure 4. Example Radar Semantic Net

In a semantic net the relations similar to the predicate logic model are seen in our example as the Has relation. To designate an occurrence or instantiation of a fact we used the relation "InstanceOf". One can see from the semantic net that we can deduce facts not explicitly shown or directly connected. For example we can deduce that ANxxx is a radar and since it's a radar, it has both a Rx and a Tx, even though there is no direct nodal connections between ANxxx and Rx or ANxxx and the Tx node. This capability is called by some (10) as the inheritance property. From our simple semantic net a radar entity inherits the property that it has both a Rx and a Tx and that each of these entities has an antenna.

Implementing a semantic net in a computer however, would not be represented as a graphic, but would be broken down into tuples or relations. A tuple is an ordered set of values, e.g. attribute value pair within a DBMS or the attributes that compose a relation in a relational DBMS. For example the Has edge would be a relation and some of the occurrences of the relation would be [Tx, TxAnt], [Rx, RxAnt], [Radar, Tx] and [Radar, Rx]. One can see the similarity between the predicate logic and semantic nets once one tries to implement them in software or within a DBMS. These can also be written in a DBMS format as Has(Tx, TxAnt), Has(Rx, RxAnt) and Has(Radar, Tx) and Has(Radar, Rx) or more directly as TxHas(TxAnt), RxHas(RxAnt), RadarHas(Tx) and RadarHas(Rx). This last representation is identical to those relations shown in figure 2. How we build these relations or knowledge representation is designer dependent and there is no formal science that says there is only one way to represent knowledge whether one uses predicate logic, semantic nets or frames (see below). There are however, better representations than others as there are better ways to write software. The same is true in developing knowledge representations and of course their software instantiations.

Frames

Frames try to capture what is conjured up in one's mind when they think of a particular object such as a radar or transmitter or antenna. When we think of one of these objects we cluster in our minds a set of attributes that describe this object. In frame terminology each of these attributes are called slots and each of these slots contain one or more values. This concept was proposed by Marvin Minsky (10) early in the 1970s. If we try and develop a knowledge representation for our radar example we may come up with frames as shown in Figure 5.

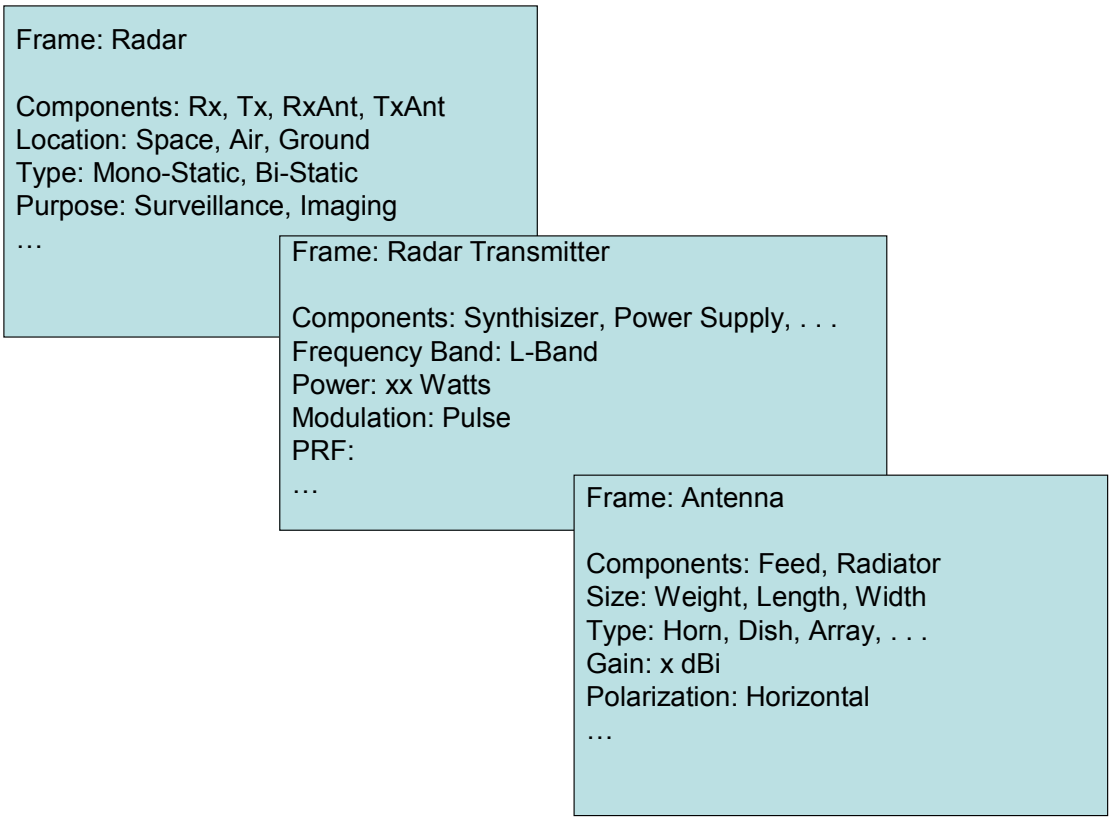

Figure 5. Frame Knowledge Representation Example

Inference Engines

The description and design of the knowledge base is the most important part of building a KB system along with choosing how one is going to describe it, i.e. predicate logic, semantic nets, or frames. This choice is obviously dependent upon the domain of interest, the purpose of the knowledge base, and of course the inference engine or inference engine tool that is best for building the solution. There has been primarily two basic methods used for building KBS. Back in the 1970 to approximately 1985 time frame engineers and scientists either built their solutions using Prolog or Lisp. Since that time people have been purchasing software tools that contain the inference engines and one only needs to define the knowledge base and the tools will help one build a knowledge base or expert system. In this paper we will provide some of the basic elements of both Prolog and Lisp so that the reader will have an appreciation of each.

Prolog

Prolog is an acronym for PROgramming in LOGic. It is (7) "a rule-based language built on top of a predicate-logic theorem prover". It was developed in France during the 1970s and was used heavily in Europe and Japan. It is also used in the USA but not as much in the early years as Lisp. Prolog is a language

but also a theorem prover based upon predicate logic. Some of the information presented here was obtained from (11).

Programming in prolog requires one to describe facts and relationships about objects or entities. One also must describe rules about these objects and their relationships. Once these are defined then questions regarding these objects and relationships can be evaluated.

Facts are described similarly as shown in figure 2's radar facts and clauses. Consider the following hypothetical radar data where their position and their established tracks are presented. Note that we changed are naming convention from upper case to lower case for the first letter of every fact, clause, or occurrences. We did this to be consistent with prolog's identification of variables i.e. any name beginning with a capital letter is taken to be a variable in Prolog.

Radar Nomenclatures	**Locations and Times for Different Objects Based Upon CPI Time Emissions.**	**Established Tracks**
radarNom(aNxxx)	locLatTime(aNsss, xxxxN, time1)	target(aNsss, t1)
radarNom(aNyyy)	locLonTime(aNsss, xxxxE, time1)	target(aNyyy, t2)
radarNom(aNzzz)	locLatTime(aNyyy, xxxxN, time2)	
	locLonTime(aNyyy, xxxxE, time2)	
	locLatTime(t1, xxxxN, time3)	
	locLonTime(t1, xxxxE, time3)	
	locLatTime(t2, xxxxN, time4)	
	locLonTime(t2, xxxxE, time4)	
	locLatTime(aNxxx, xxxxN, time5)	
	locLonTime(aNxxx, xxxxE, time5)	

Table 1. Example Prolog Facts

Once facts are defined within prolog then one may ask questions of the fact base. For example: "Is t2 a target being tracked by aNyyy?" In prolog it would be written as:

```
?-target(aNyyy, t2).
```

If this were typed into prolog with the above facts in its knowledge base then it would respond with "yes". If the following question were asked:

```
?-target(aNyyy, t1).
```

The response from prolog would be "no". This process is very similar to asking a query to a DBMS where you would ask how many records have the values as stated for the relationship "target". The response from the DBMS would be the count of zero if the answer was no or the count of the number of records that contained the values of the attributes as stated in the query.

Prolog allows the use of variables. Suppose we wish to know the locations of all the radars when emitting their CPIs.

```
?- radarNom(X), locLatTime(X, Z, Y), locLonTime(X, W, Y).
```

The variable X is placed in the fact for which we want the system to find a value that will satisfy each part of the conjunctive goal. The commas between the three goals represent the logical AND. First prolog will search the radarNom facts to find the first one with a value, i.e. aNxxx. It will then instantiate the variable X with the value aNxxx. It has satisfied the first goal. It will then search the fact base for locLatTime(aNxxx,

Z, Y). If and when it finds an occurrence then it will have satisfied the second goal. It then will search the fact base for locLonTime(aNxxx, W, time5). If it satisfies this goal it will return with a "yes". If not it will backtrack to the second goal and see if there is another occurrence of locLatTime(aNxxx, Z, Y) with a different value that Y may be instantiated to and begin the process again until either the question is answered with a "yes" or a "no". If the second goal cannot be achieved then it will proceed to the first goal and seek out the next radarNom(X) it can instantiate the X to and begin the process over again. It will answer with a "no" if it exercises all of the relevant facts and no correct response is found.

If we rewrote the question above as the following what would we be asking?

?- locLatTime(X, Z, Y), locLonTime(X, W, Y).

It would be asking for all those objects (i.e. radars or target/tracks) and their locations for all times that are recorded within the knowledge base. If we wanted to know if multiple radars are tracking the same targets then the radar's location of the targets at approximately the same time should be in approximately the same location. For illustrative purposes let's assume that all radars transmit at exactly the same time and their target locations contain no errors (note in reality we can compute the differences based upon radar system errors and build this into our logic). Therefore, two different radars are tracking the same target if two different target tracks are located at the same time and at the same location. Using prolog we can now search for potential common tracks between multiple radars.

Consider the following rule.

commonTracks(X,Y) :- target(A, X), target(E, Y), (E\=A), locLatTime(X, B, C), locLonTime(X, D, C), locLatTime(Y, B, C), locLonTime(Y, D, C).

The ":-" is read "If". The first three rules state that two different radars are tracking two different targets. The next four rules state that the two different targets/tracks should be at the same place at the same time. If these are true then we can say that radars A and E are tracking the same target. (Note E\=A states that A is not equal to E)

Lisp

Lisp is an acronym for LISt Processing. The language is one of the older computer languages and is used by some even today. In many circles, especially in the USA, in 1984 it was considered (12) "the linqua franca of artificial intelligence research". Many AI systems were built using Lisp. However, because of its basic processing of lists conventional computers at the time were not "fast enough" for AI researchers to demonstrate the power of their work. This led to companies like LMI to build special computers designed for processing the Lisp programming language.

The basic element of Lisp is its ability to process lists. Lists are a data structure that is a key element in modeling natural language processing and speech understanding. It is also a key element for creating theorem proving algorithms necessary for knowledge base and expert system reasoning systems which we will need to capitalize upon when we build an end-to-end KB radar system. It would be too cumbersome to discuss Lisp in any great depth, without describing its syntax as we have above with Prolog. Therefore we will provide a brief overview of lists and recursion, two main ingredients in building knowledge base systems, using Prolog for demonstration purposes. A basic understanding of Lisp can be obtained from (12). We will intersperse some of the LISP terms taken from (12) throughout some of the description provided below.

A list (11) "is an ordered sequence of elements that can have any length". The elements of a list can be any acceptable entity, i.e. an element, a variable, even another list. A list can be an empty list i.e. a list with no elements. A list has two elements the head of the list and the tail of the list. (In LISP the head is obtained by using the CAR function and the rest of the list is obtained using the CDR function.) The end of a list is

called the tail and is set to the empty list when the list contains no elements and is written as [ ]. (In LISP it is called NIL.)

In list processing a common operation is to split a list into its head and tail. Prolog represents this as [X|Y]. For example if we had a list of facts about radar nomenclatures denoted as relationship n, then note the following:

n([radarNom(aNxxx), radarNom(aNyyy), radarNom(aNzzz)]).

If we then ask the question to find the value of the head and tail, it would be stated as:

?- n([X|Y])

This will set X = radarNom(aNxxx) and Y = [radarNom(aNyyy), radarNom(aNzzz)]. This type of processing is performed throughout Prolog and LISP programs where one needs to process one element of the list at a time. A method which performs this process is called recursion. To demonstrate this we define the member predicate in Prolog. In any list there is a relationship we can define as membership about any object and whether it appears in any particular list. We can write this as member(X,Y). This relationship is true if X is contained in a list named Y. If X is a member of Y then X is a member of the head or it is a member in the tail.

member(X, [X|_]), where the underscore or anonymous variable is used for the tail of the list to signify that the tail of the list is not used or is not important in this fact. This fact states that X is a member of a list if X is the same as the head of the list.

member(X, [_|Y]) :- member(X,Y). This rule states that if X is a member of a list if X is a member of the tail of the list. These two rules together define the membership predicate and are an example of recursion where the definition of the rule contains the rule.

Stated together the membership rule is:
member(X, [X|_])
member(X, [_|Y]) :- member(X,Y).

Note that if we wanted to know if an element occurs in a list we can state it in Prolog as:

?- member(radarNom(aNxxx), [radarNom(aNxxx), radarNom(aNyyy), radarNom(aNzzz)]).

The first part of the rule would be exercised and the answer would be “yes”. If the question were changed to the following:

?- member(radarNom(aNzzz), [radarNom(aNxxx), radarNom(aNyyy), radarNom(aNzzz)]).

The first part of the rule would come back with “no” and then the second part of the rule would keep X as instantiated with radarNom(aNzzz) and instantiate Y with the tail of the previous list, i.e. [radarNom(aNyyy), radarNom(aNzzz)], thereby re-asking the original question as:

?- member(radarNom(aNzzz), [radarNom(aNyyy), radarNom(aNzzz)]).

Processing this question will result again with the first part of the rule returning ”no” and the second part of the rule would keep X as instantiated with radarNom(aNzzz) and instantiate Y with the tail of the previous list, i.e. [radarNom(aNzzz)], thereby re-asking the original question as:

?- member(radarNom(aNzzz), [radarNom(aNzzz)]).

Processing this question will yield a ”yes” from the first part of the rule. If however, this part failed because the last element in the list was not equal to the head of the list then the second part of the rule would come into play and the following question would be:

?- member(radarNom(aNxxx), [ ]).

If this occurs then the rule fails and a “no” is returned. It should be noted that each time Prolog uses the second clause and the member relation is exercised again that the system keeps a different copy of the member relation. This is necessary so that the processing does not get confused with which variables are used within which instantiation of a clause.

Keeping track of the processing within Prolog and LISP based programs is important within the knowledge base and AI community. Many recursive algorithms are written and are important in solving complex problems. The opportunity of keeping this type of information in knowledge base systems is important for it is needed in explaining how different questions are answered. It can be used in diagnosing errors in programming but more importantly it is used by the system to explain to the user how it derived the solution it provided. In addition, as a system is utilized it also “learns” from its past experiences and can evolve over time.

Now that we spent some time describing how a KBS functions it should be noted that you really don’t need to be an expert at writing Prolog or LISP code in order to build a KBS. You do however need to know how to build a knowledge base and recognize the best methods of representing the knowledge base given the domain of interest and purpose of the KBS. With that in mind there are numerous expert system building shells or tools that one can obtain that will help you in building a KBS. These tools will help one acquire the knowledge and present it to the system. Some are built upon Prolog, some with LISP and others even in C code. One only needs to use a search engine such as Google (http://www.google.com/) and type in “expert system tool” or ‘knowledge base tool”, and numerous sites are presented that will point you to all kinds of tools that can help one build a KBS. These systems are usually easy to use and will allow one to build simple rules that can be used along with the facts provided. Some simple examples are:

If ReceiverTargetLevel(xxx) < ReceiverNoiseFloor(yyy)
Then ~Detect(Target)

If ReceiverTargetLevel(xxx) > RadarThreasholdLevel(yyy)
Then Detect(Target)

TargetRange = (300X10^6 Meters/Sec)X(TargetReflectiveTime(xx)/2

World Wide Web Consortium (W3C)

If one visits the www.w3c.org Internet site they will obtain a definition of who they are:
“The World Wide Web Consortium (W3C) develops interoperable technologies (specifications, guidelines, software, and tools) to lead the Web to its full potential. W3C is a forum for information, commerce, communication, and collective understanding.” They, along with the Defense Advanced Research Project Agency’s (DARPA) Agent Markup Language (DAML) program, are building the next generation Internet or the Semantic Web. The Semantic Web will allow one to develop Web pages that are written such that software can read and understand the contents of Web pages. Our current Web pages are developed for human consumption. They are not built for software to read and understand their contents. This is why when using search engines the responses are numerous. For example if one puts in the words “radar signal processing” then the response pages are those pages that contain one or more of these words in any order and in any place within the page. The next generation Web is being designed in a manner similar to a large knowledge base such that one can define ontologies for different interested domains, like radar or sensors in general. An ontology is best defined for our use by what motivated the development of ontologies for the

Web. The following definition was taken from http://www-ksl.stanford.edu/kst/what-is-an-ontology.html and authored by Dr. Tom Gruber.

"An ontology is a specification of a conceptualization….What is important is what an ontology is *for*. … For pragmatic reasons, we choose to write an ontology as a set of definitions of formal vocabulary. Although this isn't the only way to specify a conceptualization, it has some nice properties for knowledge sharing among AI software (e.g., semantics independent of reader and context). Practically, an ontological commitment is an agreement to use a vocabulary (i.e., ask queries and make assertions) in a way that is consistent (but not complete) with respect to the theory specified by an ontology. We build agents that commit to ontologies. We design ontologies so we can share knowledge with and among these agents."

The concept of an ontology is exactly what we need in our overall pursuit of having sensors operate in cooperation and eventually having sensor platforms operating autonomously as a robot. For them to operate cooperatively they must be able to communicate, share data and information, and understand each other and their environment. If we tried to do this with each sensor system building their own knowledge base with different knowledge base representations it would be difficult for them to communicate and understand each other. Each system would have to build software translators to understand each other. Each sensor system would have N-1 translators for a system with N sensors. This would be expensive to build, it would be processor intensive, and would generate a high maintenance cost over the life of the sensor systems.

Leveraging the approach and technology of the W3C will allow us to develop an ontology for sensors thereby having one knowledge base that can be understood by all new knowledge base sensor systems added to the overall domain including communications, radar, electro-optical, infrared, acoustic, etcetera. This approach will allow multiple sensors on one platform to inference and fuse data and information from all its sensors on board. It will also allow for this platform to share and fuse data and information between sensors on multiple platforms located nearby or miles away within a command center. The building of ontologies is going on today. They can easily be found on the Web and can be used to build and share information within the community and domain of interest. The approach we recommend and used (13) is to not build one's own ontology from scratch but to leverage the object oriented feature of inheritance and reference the resource descriptive framework (RDF) (i.e. an instantiation of an ontology) of those ontologies that already exist and then add those additional facts and rules required for one's own needs. For example if a respective organization has built an RDF describing facts and rules for a transmitter, a receiver, and an antenna then if their facts and rules meet your needs then they should be referenced in the radar ontology that one is building, rather than one building their own. In this manner one needs only to refer to the ontology where they wish to use these rules and facts and they can add additional rules and facts as required.

Summary

This paper has provided a brief discussion of artificial intelligence and why it can play a major role in the next generation of radar systems. The important areas of AI that seem to fit well for radar signal processing are knowledge based processing and robotics. We have provided a brief overview of knowledge bases and the processes of building a knowledge base. Some of the most recent efforts in this field is being pursued in the Internet field for building intelligent agent software that can understand Web pages. We wish to leverage that technology and their success for building knowledge based radar systems. We are currently investigating this technology and have begun building a prototype ontology for radar systems. A lecture on the second day will have more examples of knowledge bases and their uses in building an end-to-end radar signal processing system.

Acknowledgements

The authors would like to recognize the efforts of the following people. We would like to thank Mr. Gerard Genello, Mr. William Baldygo, and Dr. Michael C. Wicks for providing the resources, encouragement, guidance, and the opportunity in the pursuit of our goals. We would also like to thank Mr. John Spina for

chairing this lecture series and Mr. Christopher Capraro and Mr. Gerald Berdan of Capraro Technologies, Inc. for their help throughout. Thank you all.

References

1. W. Baldygo, M. Wicks, R. Brown, P. Antonik, G. Capraro, and L. Hennington, "Artificial intelligence applications to constant false alarm rate (CFAR) processing", Proceedings of the IEEE 1993 National Radar Conference, Boston, MA, April 1993.
2. R. Senn, "Knowledge Base Applications To Adaptive Space-Time Processing", Unpublished Final Report, July 1999.
3. P. Antonik, H. Shuman, P. Li, W. Melvin, and M. Wicks, "Knowledge-Based Space-Time Adaptive Processing", Proceedings of the IEEE 1997 National Radar Conference, Syracuse, NY, May 1997.
4. Multi-Channel Airborne Radar Measurement (MCARM) Final Report, Volume 1 of 4, MCARM Flight Test, Contract F30602-92-C-0161, for Rome Laboratory/USAF, by Westinghouse Electronic Systems.
5. G. T. Capraro, C. T. Capraro, and D. D. Weiner, "Knowledge Based Map Space Time Adaptive Processing (KBMapSTAP)", Unpublished Final Report, March 2000.
6. C. T. Capraro, G. T. Capraro, D. D. Weiner, and M. Wicks, "Knowledge Based Map Space Time Adaptive Processing (KBMapSTAP)," Proceedings of the 2001 International Conference on Imaging Science, Systems, and Technology, June 2001, Las Vegas, Nevada.
7. E. Rich, "Artificial Intelligence", New York, NY, McGraw-Hill, 1983
8. A.Barr and E. A. Feigenbaum, "The Handbook of Artificial Intelligence, 3 vols.", Los Altos, CA: William Kaufman, 1981-1982
9. B. G. Buchanan and E. H. Shortliffe, "Rule-Based Expert Systems", Reading, MA: Addison-Wesley, 1984.
10. H. C. Mishkoff, "Understanding Artificial Intelligence", Dallas, Texas: Texas Instruments Incorporated, 1985.
11. W. F. Clocksin and C. S. Mellish, "Programming in Prolog", Spriner-Verlag Berlin Heidelberg: Beltz, Offsetdruck, Hemsgach, 1981.
12. D. S. Touretzky, "LISP A Gentle Intrduction to Symbolic Computation", New York, NY: Harper & Row, 1984.
13. G. B. Berdan, G. T. Capraro, J. Spina, and R. A. Liuzzi, "Building an Ontology for Computing Devices", Proceedings of the International Conference Information and Knowledge Engineering, June 2003.
14. M. C. Wicks, W. Baldygo, and R. D. Brown, "US Patent 5,499,030 Expert System Constant False Alarm Rate (CFAR) Processor", filed March 18, 1994 issued March 12, 1996

KNOWLEDGE-BASED SOLUTIONS AS THEY APPLY TO THE GENERAL RADAR PROBLEM

H.D. Griffiths
Head, Department of Electronic and Electrical Engineering
University College London
Torrington Place, London WC1E 7JE, UK
Tel: +44 20 7679 7310; fax: +44 20 7388 9325; email: h.griffiths@ee.ucl.ac.uk

Keywords: radar, signal processing, adaptive processing, adaptive arrays, clutter, space-time adaptive processing, knowledge-based systems.

SUMMARY

This tutorial provides an introduction to the application of knowledge-based processing to the general radar problem. We interpret knowledge-based processing as the use of adaptivity and the exploitation of prior knowledge in such a way as to choose the optimum processing method in each case, and we interpret the general radar problem as the detection, classification and tracking of targets against a background of clutter and interference. As such the tutorial attempts to describe the nature of the general radar problem and the basic processing techniques that are used, and to show why knowledge-based signal processing may be advantageous, setting the scene for the subsequent tutorials covering CFAR detection, space-time adaptive processing, tracking, and emerging technologies. The fundamental concepts of matched filtering, superresolution and adaptive filtering are described, emphasizing the equivalence of time/frequency and aperture/angular domains, and introducing the concept of Space-Time Adaptive Processing. A description is given of some of the statistical clutter models in common use (Rayleigh, Ricean, Lognormal, Weibull and Compound-K), with practical examples of sea clutter and of land clutter which demonstrate that clutter is in general non-Gaussian and non-stationary, both in time and space. Two examples are given of the application of adaptive techniques to the suppression on nonhomogeneous clutter, showing that the performance of the adaptive Doppler filtering algorithm is severely compromised at clutter edges, due to incorrect estimation of the clutter covariance matrix, and how in Space-Time Adaptive Processing a non-homogeneity detector can be used in the choice of the most appropriate STAP algorithm, forming the so-called Knowledge-Based STAP (KB-STAP) processor.

1. INTRODUCTION

The concept of adaptivity is central to the operation of modern radar signal and data processing. A single filtering, detection or tracking algorithm is not going to be optimum for all scenarios. Since Brennan and Reed's classic paper in 1973 [12], adaptive algorithms for detection, spatial filtering and Doppler filtering have been extensively studied and different algorithms have been devised to cope with different scenarios of targets, clutter and interference. At the same time, information theory tells us that prior knowledge can (and should) be used to reduce the uncertainty in processing decisions. In the radar context, such prior knowledge may take the form of information about the particular targets being sought, the inhomogeneity and topography of terrain, or meteorological conditions. Knowledge-based systems form part of the subject of artificial intelligence, in which a knowledge base is used to guide an inference engine to make its processing decisions. The concept, then, of knowledge-based signal processing is to make use of prior information in such a way as to choose the optimum processing method in each case.

Paper presented at the RTO SET Lecture Series on "Knowledge-Based Radar Signal and Data Processing", held in Stockholm, Sweden, 3-4 November 2003; Rome, Italy, 6-7 November 2003; Budapest, Hungary, 10-11 November 2003; Madrid, Spain, 28-29 October 2004; Gdansk, Poland, 4-5 November 2004, and published in RTO-EN-SET-063.

We interpret the 'general radar problem' as being the radar detection, classification and tracking of targets against a background of clutter and interference, with acceptable probabilities of detection and of false alarm. The radar may be terrestrial, maritime, airborne or space-based. We will assume in general that the radar will utilise a phased array antenna (linear or planar, or even conformal), allowing electronic control of the radiation pattern on receive and possibly on transmit as well, and we assume that there is explicit control of the radar waveform(s) which will be generated digitally and which may be varied on a pulse-to-pulse basis, and that these waveforms may be of substantial bandwidth, giving high range resolution. As well as the radar waveform, the dwell time and the pulse repetition frequency (PRF) may also be varied.

Thus this tutorial will provide an introduction, successively, to the application of knowledge-based techniques to filtering and detection (including space-time adaptive filtering), the nature of clutter, and tracking, aiming to show why knowledge-based signal processing may be advantageous, and to set the scene for the subsequent tutorials covering CFAR detection, space-time adaptive processing, tracking, and emerging technologies.

2. FILTERING AND DETECTION

2.1 The Matched Filter

We recall here the classical theory of the matched filter [32]. The matched filter maximizes the ratio of peak signal power to mean noise power. Let the transmitted waveform be $u(t)$. Its spectrum $F(\omega)$ is

$$F(\omega) = \int_{-\infty}^{\infty} u(t) \exp(-j\omega t)\, dt \tag{1}$$

If the receiver transfer function is $H(\omega)$ the output signal from the receiver prior to envelope detection is

$$g(t) = \int_{-\infty}^{\infty} F(\omega) G(\omega) \exp(j\omega t)\, df \tag{2}$$

Let $g(t_0)$ be the maximum value of $g(t)$. The power spectrum of the noise at the output of the matched filter is:

$$g(\omega) = \frac{N_0}{2} |H(\omega)|^2 \tag{3}$$

where $N_0/2$ is the noise spectral density at the input. The average noise power is then:

$$N = \frac{N_0}{2} \int_{-\infty}^{\infty} |H(\omega)|^2\, df \tag{4}$$

The energy of the input signal can be written:

$$E = \int_{-\infty}^{\infty} u^2(t)\, dt = \int_{-\infty}^{\infty} |F(\omega)|^2\, d\omega \tag{5}$$

An optimum radar detector must maximize the ratio of peak signal power to mean noise power at its output:

$$\frac{|g(t_0)|^2}{N} = \frac{\left|\int_{-\infty}^{\infty} F(\omega) H(\omega) \exp(j\omega t_0)\, df\right|^2}{\frac{N_0}{2}\int_{-\infty}^{\infty} |H(\omega)|^2\, df} \tag{6}$$

So we seek the receiver transfer function $H(\omega)$ which maximizes this ratio. This can be found using Schwartz's inequality:

$$\frac{|g(t_0)|^2}{N} \leq \frac{2E}{N_0} \tag{7}$$

The maximum output signal-to-noise ratio occurs when the two sides are equal, which is true only if:

$$H(\omega) = K\, F^*(\omega) \exp(-j\omega t_0) \tag{8}$$

where K is a constant (gain) and t_0 is the time delay through the filter.

This says that the frequency response of the matched filter is equal (apart from K and t_0) to the complex conjugate of the signal spectrum $F(\omega)$.

The impulse response of the matched filter is:

$$h(t) = K_2 u^*(t_0 - t) \tag{9}$$

which is a time-delayed inverse of the input waveform, multiplied by a simple gain constant.

The time-domain output is the convolution of the input signal with the impulse response, which is:

$$g_0(t) = \frac{1}{T}\int_{-T/2}^{T/2} f(\tau) f(\tau + t_0 - t)\, d\tau \tag{10}$$

which is the autocorrelation function of the input signal (in the absence of noise).

In summary:

- the matched filter maximizes the ratio of peak signal power to mean noise power;
- its frequency response is the complex conjugate of the spectrum of the input signal;
- its impulse response is the time-inverse of the input waveform;
- the matched-filtered output waveform is the autocorrelation function of the input waveform.

2.2 Equivalence of Time/Frequency and Angular/Aperture Domains

The matched filter for a sampled sinusoid consists of summing the samples with unit amplitude weighting, and the resulting time-domain output is:

$$h(t) = \sum_{n=1}^{N} a_n \exp(-j2\pi n / N) \tag{11}$$

It is easy to see that this is exactly equivalent to the sampling by a linear antenna array of an incoming sinusoidal waveform (Figure 1). The resulting radiation pattern of the array steered to the direction of incidence θ_0 has the familiar form:

$$D(\theta) = \frac{\sin\left(\frac{\pi N d}{\lambda}(\sin\theta - \sin\theta_0)\right)}{N\sin\left(\frac{\pi d}{\lambda}(\sin\theta - \sin\theta_0)\right)} \tag{12}$$

where N is the number of elements, λ is the wavelength and d is the interelement spacing.

Thus the array forms a spatial matched filter, matched to the direction of incidence θ_0. This illustrates the equivalence between on one hand the Fourier transform relationship between the time domain and frequency, and on the other the Fourier transform relationship between the aperture domain and the angular (sin θ) domain. Thus all of the processing techniques developed for time domain / frequency domain can equally be applied in the aperture domain / angular domain. These include:

- matched filtering (as described above);
- the effects of the sampling theorem (aliasing); in the angular domain aliasing results in *grating lobes*;
- formation of a set of orthogonal filterbank responses by the Discrete Fourier Transform [10, 11]; in the angular domain the equivalent process is carried out by the Butler Matrix producing a set of orthogonal beams [14];
- weighting to reduce sidelobes (at the expense of loss and of broadening of response); the same weighting functions (Taylor, Chebyshev, …) are usable;
- synthesis of a desired radiation pattern (or spectrum) from a uniformly-spaced set of aperture (or time series) samples [49];
- superresolution techniques;
- adaptive filtering.

2.3 Superresolution Techniques

'Superresolution' is a term used to describe a set of processing techniques which attempt to resolve signals of closer angular separation than the classical Rayleigh λ/D limit (where λ is the signal wavelength and D the array length). An intuitive demonstration that this can be done is provided by considering the 'tree' structure of phase shifters and combiners shown in Figure 2, and known as the 'Davies Beamformer' [17].

In 1979, Schmidt presented one of the earliest, and certainly one of the best-known of the superresolution algorithms, which he named MUltiple SIgnal Classification, or MUSIC [36]. A similar formulation had been published earlier the same year by Bienvenu [7].

Consider an M-element array of arbitrary geometry, with n incident signals $F_1, F_2, \ldots, F_n$ ($n \leq M$). The element signals $X_1, X_2, \ldots, X_M$ can be written as

$$\begin{array}{rcccccccccc} X_1 & = & a_{11}F_1 & + & a_{21}F_2 & + & \ldots & + & a_{D1}F_n & + & W_1 \\ X_2 & = & a_{12}F_1 & + & a_{22}F_2 & + & \ldots & + & a_{D2}F_n & + & W_2 \\ \vdots & = & \vdots & + & \vdots & + & \ldots & + & \vdots & + & \vdots \\ X_M & = & a_{1M}F_1 & + & a_{2M}F_2 & + & \ldots & + & a_{DM}F_n & + & W_M \end{array}$$

or in matrix notation

$$\mathbf{X} = \mathbf{AF} + \mathbf{W} \tag{13}$$

Here the terms W_1, W_2, ... W_M represent the noise at the array elements. This noise may be either internally or externally-generated.

The matrix **A** is known as the *array manifold*, and its coefficients depend on the element positions and directional responses. The j^{th} column of **A** is a mode vector $\mathbf{a}(\theta)$ of responses of the array to the direction of arrival θ_j The mode vectors and **X** can each be visualized as vectors in M-dimensional space, and **X** is a linear combination of mode vectors, where the coefficients are the elements of **F**.

The covariance matrix **R** is formed by averaging a number of 'snapshots' of the element signals

$$\begin{aligned} \mathbf{R} &= \overline{\mathbf{X}\mathbf{X}^*} \\ &= \mathbf{A}\overline{\mathbf{F}\mathbf{F}^*}\mathbf{A}^* + \sigma^2\mathbf{I} \end{aligned} \tag{14}$$

under the assumption that the signals and noise are uncorrelated, and where the elements of the noise vector **W** are zero mean and of variance σ^2.

The covariance matrix can be broken down into its eigenvectors and eigenvalues

$$\mathbf{R} = \sum_{i=1}^{N} \lambda_i \mathbf{e}_i \mathbf{e}_i^* = \mathbf{ELE}^* \tag{15}$$

The eigenvalues λ_i of the covariance matrix will be

$$\lambda_i > \sigma^2 \text{ for } i = 1, \ldots, n, \text{ and } \lambda_i = \sigma^2 \text{ for } i = n+1, \ldots, M \tag{16}$$

The number of incident signals can therefore be determined by inspection of the relative magnitudes of the eigenvalues, or in some situations this information may be known *a priori*.

Consequently, the covariance matrix can be partitioned into an n-dimensional subspace spanned by the incident signal mode vectors and an $M–n$ dimensional subspace spanned by the $M–n$ noise eigenvectors

$$\mathbf{R} = \mathbf{E}_S\mathbf{L}_S\mathbf{E}_S^* + \mathbf{E}_N\mathbf{L}_N\mathbf{E}_N^* \tag{17}$$

where $\mathbf{E}_S$ is the M by n signal subspace and $\mathbf{E}_N$ is the M by $M–n$ noise subspace.

The MUSIC algorithm then estimates the angular spectrum $P(\theta)$ of the incident signals according to

$$P(\theta) = \frac{1}{\mathbf{a}^*(\theta)\mathbf{E}_N\mathbf{E}_N^*\mathbf{a}(\theta)} \tag{18}$$

A large number of other superresolution algorithms have been formulated and evaluated, giving improved performance over the basic MUSIC algorithm. These include search-free methods such as ESPRIT (Estimation of Signal Parameters by Rotational Invariance Technique) and TAM, one-dimensional parameter search methods such as MUSIC and Capon's MVDR, and multidimensional search schemes such as IMP (Incremental MultiParameter), stochastic and deterministic max-likelihood, and WSF. Algorithms of this kind are described in detail in reference [25].

Figure 3 shows an attempt to classify these algorithms, into those which work with arrays of arbitrary geometry and those which are formulated for uniformly-spaced linear arrays. The algorithms are also divided into those based on translational invariance, one-dimensional parameter searches, and multi-dimensional parameter searches.

A particular problem occurs when the incident signals are correlated - such as would be the case with multipath, for example. In this case the MUSIC algorithm does not perform well, and a 'pre-whitening' process is necessary to decorrelate the input signals applied to the algorithm. This may be done by taking successive subaperture samples of the complete array, and using these as the inputs to the algorithm [38].

The description of superresolution presented here has been in terms of the aperture / angular domains, but clearly in view of the discussion of Section 2.2 the process can be applied equally in the time / frequency domains. It is interesting to note that the original description of the MUSIC algorithm includes the polarization domain as well [36].

2.4 Adaptive Filtering

The derivation of the matched filter in section 2.1 assumed a uniform noise distribution. We consider now the situation when the noise is inhomogeneous. Suppose we have an N-element array, of $\lambda/2$ spacing, in an environment of noise (interference and/or jamming) of which the angular distribution, in intensity, is fixed by a function $T(\tau)$ (where τ = sin θ). There is a wanted signal in the direction τ_0. The optimization criterion chosen here is to maximize the ratio between the array gain in this direction, $G(\tau_0)$, and the total noise power T_A received by the antenna. This ratio is sometimes called the 'factor of merit'

$$M = \frac{G(\tau_0)}{T_A} \tag{19}$$

The gain $G(\tau_0)$ is proportional to the square modulus of the characteristic function, which in turn is the Fourier Transform of the set of weight coefficients. We can therefore write:

$$G(\tau_0) = \left| \sum_1^N W_n \exp(j2\pi n\tau_0) \right|^2 \tag{20}$$

We define the 'weight matrix' or 'weight vector' by the column matrix

$$\mathbf{W} = \begin{bmatrix} W_1 \\ : \\ W_N \end{bmatrix} \tag{21}$$

The steering vector defining the pointing direction is written in the same way

$$\mathbf{D}_0 = \begin{bmatrix} 1 \\ \exp\left(j\pi\tau_0\right) \\ : \\ \exp\left(j\pi N\tau_0\right) \end{bmatrix} \tag{22}$$

The gain $G(\tau_0)$ is therefore written

$$G\left(\tau_0\right) = \left|\mathbf{W}^{\mathrm{t}}\mathbf{D}_0\right|^2 \tag{23}$$

(The symbol $\mathbf{W}^{\mathrm{t}}$ denotes the transpose of $\mathbf{W}$).

In the same way as the gain, the noise power received can be expressed in terms of the weight vector $\mathbf{W}$

$$\mathbf{S} = \sum_1^N s_n W_n \tag{24}$$

The set of element signals is

$$\boldsymbol{\sigma} = \begin{bmatrix} s_1 \\ : \\ s_N \end{bmatrix} \tag{25}$$

so we can write

$$\mathbf{S} = \boldsymbol{\sigma}^{\mathrm{t}}\mathbf{W} = \mathbf{W}^{\mathrm{t}}\boldsymbol{\sigma} \tag{26}$$

The noise power is therefore

$$T_A = \overline{\left|\mathbf{S}\right|^2} = \overline{\mathbf{S}^*\mathbf{S}} = \overline{\left(\mathbf{W}^{\mathrm{t}}\boldsymbol{\sigma}\right)\boldsymbol{\sigma}^{\mathrm{t}}\mathbf{W}} = \mathbf{W}^{\dagger}\overline{\boldsymbol{\sigma}^*\boldsymbol{\sigma}^{\mathrm{t}}}\mathbf{W} \tag{27}$$

where $\mathbf{W}^{\dagger}$ is the adjoint matrix of $\mathbf{W}$.

The covariance matrix $\mathbf{R}$ can be recognized in the product $\overline{\boldsymbol{\sigma}^*\boldsymbol{\sigma}^{\mathrm{t}}}$, thus

$$\overline{\boldsymbol{\sigma}^{*}\boldsymbol{\sigma}^{t}} = \overline{\begin{bmatrix} s_1^{*} \\ s_2^{*} \\ \vdots \\ s_N^{*} \end{bmatrix} \begin{bmatrix} s_1 \ \ldots \ s_N \end{bmatrix}} = \begin{bmatrix} \overline{|s_1|^2} & \cdots & \overline{s_1^{*} s_N} \\ \vdots & & \vdots \\ \overline{s_N^{*} s_1} & \cdots & \overline{|s_N|^2} \end{bmatrix} = \mathbf{R} \tag{28}$$

The factor of merit is therefore written

$$M = \frac{G(\tau_0)}{T_A} = \frac{\left|\mathbf{W}^{t}\mathbf{D}_0\right|^2}{\mathbf{W}^{\dagger}\mathbf{R}\mathbf{W}} \tag{29}$$

The problem of the optimum array is now to find a weight vector $\mathbf{W}$ which maximizes the factor of merit M. This reduces to finding the vector $\hat{\mathbf{W}}$ such that the factor of merit is stationary with respect to a perturbation dW. The solution is:

$$\mathbf{R}\hat{\mathbf{W}} = k\mathbf{D}_0 \tag{30}$$

where k is an arbitrary scalar constant.

If the covariance matrix can be inverted, we obtain

$$\hat{\mathbf{W}} = k\mathbf{R}^{-1}\mathbf{D}_0 \tag{31}$$

This says that the optimum weight vector is obtained by forming an estimate of the covariance matrix, inverting it, and multiplying by a steering vector to define the required direction of maximum gain. The estimate of the covariance matrix is formed by averaging a number of 'snapshots' of the element signals, and Reed, Mallett and Brennan [35] showed that the number of samples K must be such that

$$K \geq (2N - 3) \tag{32}$$

This is sometimes known as 'Brennan's law'.

Although this discussion has been in terms of the radiation pattern of an adaptive antenna array, the discussion of section 2.2 shows that it is equally applicable to adaptive Doppler filtering. This formed the basis of Brennan and Reed's classic 1973 paper [12].

2.5 Space-Time Adaptive Processing

Space-Time Adaptive Filtering (STAP) is a two-dimensional combination of adaptive antenna array and adaptive Doppler filtering to suppress clutter and jamming [27]. Figure 4 shows a sideways-looking airborne radar, from which it can be seen that the Doppler shift associated with an echo from an angle θ from boresight is

$$f_D = \frac{2vf_0 \sin\theta}{c} \tag{33}$$

Figure 5 shows a two-dimensional plot of the clutter and jamming, as a function of angle (sin θ extending from −1 to +1) and of Doppler (extending from –PRF/2 to +PRF/2). There is a weak target at boresight, and it can be appreciated from the diagram that two-dimensional filtering is necessary to suppress the clutter and jamming to reveal the target.

The 'STAP data cube' (Figure 6) is thus used to estimate the covariance matrix. One important aspect of research into STAP techniques is to devise efficient ways of computing the inverse of the covariance matrix, since direct inversion is usually impractical. Reduced-dimension STAP (RD-STAP) is one such technique. Further such techniques will be described in the fifth lecture in this series.

3. CLUTTER AND DETECTION

3.1 Introduction

Radar clutter has been studied since the earliest days of radar. A proper knowledge of the statistics of radar clutter is essential in predicting radar detection performance, i.e. in ensuring correct setting of the detection threshold in CFAR (constant false alarm rate) processing, and in determining the clutter residue at the output of Doppler filter processors [8].

For radars of low or moderate resolution, Gaussian statistics have for many years given adequate results, both for land and sea clutter. However, for high resolution radars at low grazing angles, it has been found that clutter pdfs (probability density functions) deviate quite markedly from Gaussian, and consequently that the detection performance predicted by Gaussian clutter models does not agree well with practical experience. This is particularly true for the 'tails' of the distributions, which are exactly the parts which have the greatest effect on the false alarm rate. Furthermore, high spatial resolution radars may be able to exploit the spatial and temporal correlation properties of the clutter, so models which can take this into account can give superior performance. Various models have therefore been proposed and analyzed to give improved performance.

In addition, it is important to understand the effects of clutter inhomogeneities (edges) and discrete scatterers, and of range-ambiguous clutter [4]. The latter may be critical in evaluating the performance of naval radars operating in littoral environments. The fact that clutter can be so variable underlines the idea that knowledge-based techniques should be valuable in using prior information to bring the most appropriate detection algorithms to bear.

The next section provides a brief review of clutter models in current use.

2.2 Clutter Models

Rayleigh model: The simplest model for radar clutter assumes that the clutter echo is the sum of a large number of contributions of similar amplitude and random phase, in which case the Central Limit Theorem indicates that the in-phase (I) and quadrature (Q) components are independent and Gaussian-distributed, in which case the intensity follows a negative-exponential distribution:

$$f_E(x) = \frac{1}{\beta}\exp\left(-\frac{x}{\beta}\right) \tag{34}$$

and the corresponding pdf of the envelope-detected voltage z is Rayleigh:

$$f_R(z) = \frac{2z}{\beta}\exp\left(-\frac{z^2}{\beta}\right) \qquad z \geq 0 \tag{35}$$

Ricean model: If there is an additional non-random component in the clutter echo, the peak of the distribution is shifted so that the most probable value of the received power is not zero. The pdf of the detected envelope can be written as:

$$f(z) = \frac{z}{\psi_0} \exp\left(-\frac{z^2 + A^2}{2\psi_0} \right) I_0\left(\frac{zA}{\psi_0} \right) \tag{36}$$

where $I_0(.)$ is the modified Bessel function of order zero, ψ_0 is the variance of the noise, A is the amplitude of the coherent component, and the ratio of coherent to random scattering is proportional to A^2/ψ_0.

Lognormal model: The lognormal distribution is obtained from the normal distribution using the transformation $x = \ln(y)$. The pdf of the detected envelope is:

$$f(z) = \frac{2}{\sqrt{2\pi}\sigma z} \exp\left[-\frac{1}{2\sigma^2} \left(2 \ln \frac{z}{z_m} \right)^2 \right] \tag{37}$$

where z_m is the median value of z and σ^2 is the standard deviation of $\ln(z)$.

Weibull model: The Weibull pdf [37] is intermediate between the Rayleigh and lognormal distributions:

$$f_w(z) = \frac{\nu}{\beta} \left(\frac{x}{\beta} \right)^{\nu - 1} \exp\left(-\left(\frac{x}{\beta} \right)^{\nu} \right) \tag{38}$$

where β is the scale parameter and ν is the shape parameter. For $\nu = 2$ the expression reduces to the Rayleigh case.

In the 1970s, much research was done on the non-Gaussian characteristics of high-resolution clutter. The lognormal distribution was found to give a better fit than the negative exponential distribution, but still fell short of describing adequately the single point statistics of coherent clutter.

Compound K distribution model: The K-distribution was originally devised in the context of optical scattering, and was subsequently applied in its compound from to radar sea clutter [40-46]. It consists of the product of a modulation component associated with the large scale structure (in the case of the sea surface this represents the long-wavelength swell waves) and Rayleigh-distributed speckle resulting from the coherent addition of contributions from the individual scatterers. More recently, the K-distribution has also been found to give an accurate representation of the statistics of texture in high-resolution SAR images of rural target scenes [34], and even of texture in high-resolution sonar images of the seabed [22].

The Rayleigh distributed speckle component is described by:

$$f(x|y) = \frac{\pi x}{2y^2} \exp\left(-\frac{\pi x^2}{4y^2} \right) \qquad \text{for } 0 < x < \infty \tag{39}$$

and the modulation component is described by the chi-distribution:

$$f(y) = \frac{2b}{\Gamma(\nu)}(b\nu)^{2\nu-1}\exp\left(-b^2y^2\right) \qquad \text{for } 0 < y < \infty \tag{40}$$

where b is a scale parameter and ν is a shape parameter.

Equations (39) and (40) are combined to yield the usual form of the compound K-distribution:

$$f(x) = \frac{4c}{\Gamma(\nu)}(cx)^{\nu} K_{\nu-1}(2cx) \tag{41}$$

where $c = b\sqrt{\frac{\pi}{4}}$ is a scale parameter, ν is the same shape parameter as the chi-distributed modulation, and $K_\nu(.)$ is the modified Bessel function of the third kind of order ν. The shape parameter ν expresses the 'spikiness' of the clutter. For $\nu = \infty$ the expression reduces to the Rayleigh distribution., Low values of shape parameter ν (<1) indicate spiky clutter.

3.3 Sea clutter

The properties of sea clutter will depend on a wide variety of parameters: : the radar parameters (frequency, polarization, resolution (in range and azimuth), incidence angle, …), and the surface parameters (wave height and wavelength, wind speed and direction, presence or absence of 'whitecaps', presence or absence of rainfall on the sea surface, …) and will depend on whether the sea surface is in the open ocean or in the littoral region. Figures 7 and 8 show photographs of the sea surface from Sennen Cove in Cornwall, UK, from which simultaneous radar data was gathered. In Figure 7, corresponding to a significant wave height of 4.3 m, the presence of whitecaps at once suggests that there are individual and discrete scattering events upon the relatively slow modulated surface. In heavier sea conditions (Figure 8), corresponding to a significant wave height of 6.1 m, the whitecaps dominate even more and considerable areas of the scene are shadowed.

The radar frequency was 9 GHz, and it operated in a staring mode, mounted on a clifftop with a grazing angle of 1.5˚. The range resolution is 6 m. Figure 9 shows 6 second blocks of data from this radar (at vertical polarization) as Weibull plots (logarithmic probability of occurrence versus amplitude), displaced for clarity. It is evident that neither the power nor the distribution is stable with time.

Observation of the Doppler spectrum suggests that the clutter returns consist of discrete scatterers with a characteristic lifetime. The upper plot of Figure 10 is a very high PRF Doppler trace over 60 seconds. A series of individual scatterers can be seen to be breaking away from the underlying modulated Doppler spectrum. The middle plot shows a distribution measure of the spikiness of the distribution using the normalised log estimate U. The lower plot shows the proportion of the tails of the Doppler spectrum above the noise level. In this case the underlying Doppler bin distribution is not spiky, rather it is non-stationary exponential.

As an example of the problems faced by a CFAR detector, Figure 11 shows the detection threshold set by Cell Averaging (CA), Cell Averaging Greater Of (CAGO) and Order Statistic (OS) processors operating on simulated K-distributed clutter with shape parameter ν = 0.5 (i.e fairly spiky). The number of reference cells is 32, and the threshold multiplier factor α is set to achieve $P_{fa} = 10^{-4}$. For the OS processor k is chosen as 20. A 15 dB clutter edge is located at range bin no. 240. A number of closely spaced targets of 16 dB signal-to-clutter ration are located between range bins 70 and 95, with isolated targets at range bins 150 and 230.

Several points can be noted. For the CA detector it is apparent that the closely spaced targets raise the detection threshold between range bins 60 and 110 so much that none of the targets are detected. The isolated target at range bin 150 is detected, but the presence of the clutter edge raises the threshold in the vicinity of range bin 240, thereby masking the target at range bin 230. Close examination of the figure also indicates that a false alarm will occur in range bin 246, due to the threshold being biased down by the low region of clutter power still within the CFAR window. It is evident that for the CAGO processor the closely spaced targets are even more comprehensively masked by each other. Again, the isolated target at range bin 150 is detected and the target at range bin 230 is masked by the clutter edge. The clutter spike at sample 246 does not, however, cause a false alarm in the CAGO processor. The OS processor can be seen to resolve the closely spaced targets and exhibits no discernable increase in the threshold in that region. The isolated target at range bin 150 is, of course, detected, and the target at range bin 230 is now detected and is not masked by the clutter edge. This is achieved at the expense of a false alarm at range bin 246 caused by the clutter edge, and almost another false alarm at sample 243. The choice of a higher value of k, around 27 or 28, would eliminate the false alarms at the clutter edge, but would extend the region of target masking caused by the clutter edge to the left, causing masking of the target at range bin 230. It is also apparent that in regions of homogeneous clutter the threshold is lowest for the CA processor and highest for the OS processor, reflecting the nominal loss for these respective processors.

3.4 Land clutter [9]

The properties of land clutter will depend on a wide variety of parameters: the radar parameters (frequency, polarization, resolution (in range and azimuth), incidence angle, …) as with sea clutter, and the surface properties (topography, dielectric properties, vegetation, moisture, wind speed and direction, time of day and season of year, …).

As an example, land clutter data from the BYSON radar has been analyzed [23]. The BYSON radar (now decommissioned) was located at the Malvern site (formerly RSRE, DERA; now QinetiQ), and provided a fully-instrumented flexible experimental facility. It used two modified Siemens Plessey AWS-5 naval radar transmitters, with digital waveform synthesis. The radar is depicted in Figure 12 and its parameters summarized in Figure 13.

Figure 14 shows an example of the result of fitting four of the clutter models described in section 3.2 to measured land clutter data. A number of techniques exist to fit models to measured data, and thereby to estimate the parameters of the model distributions. A standard approach is the maximum likelihood estimator, but no closed-form solution for the K-distribution has been found, so alternative techniques are required. In the work described here the downhill simplex method has been used [33], implemented in Mathematica. The goodness-of-fit in each case was evaluated by computing the mean square difference (MSD) between the model pdf and the measured data:

$$\mathrm{MSD} = \frac{1}{N}\sum_{i=1}^{N}\left(p\left(x_i\right) - f\left(x_i\right)\right)^2 \tag{42}$$

The target scene in this example corresponds to a region at a range of 71.6 km, including a television transmitter mast located at Litchfield. The model giving the best fit (lowest value of MSD) is highlighted. In all cases the K-distribution gives the best fit, and the K-distribution and Weibull models are noticeably superior to the other models. There is little difference between HH and VV polarizations.

Further analysis of the same data (Figure 15) with reference to the corresponding terrain height information (Figure 16) has shown that the clutter statistics can be highly variable [16]. The two swaths shown in Figure 15 include a number of man-made structures such as a motorway (highway) with metal lampposts, power pylons, and glasshouses. A likelihood ratio test for individual range cells was used to classify the

data as exponential clutter (largely shadow), positive values (areas more likely to be an edge), and negative areas (more likely to be IID K), and the result is shown in Figure 17. Many of the 'spiky' areas are related to man-made structures.

The Doppler spectrum of land clutter will depend on the motion of wind-blown trees and other vegetation [9].

3.5 Application of Knowledge-based Processing

The conclusion to be drawn from the preceding discussion is that radar clutter will in general be non-Gaussian and non-stationary both in time and in space. When interference and jamming are present the environment will be even more non-uniform.

Adaptive Doppler filtering of nonhomogeneous clutter: A study of the application of adaptive Doppler filtering to nonhomogeneous clutter [4] considered three types of inhomogeneity:

(i) clutter in which the amplitude and spectral width in each range bin are randomly drawn from spatially invariant parent populations of specified characteristics. This could represent, for example, high-resolution sea clutter or land clutter due to wind-blown fields or trees;

(ii) clutter edges, in which the clutter amplitude and/or spectrum exhibit a step change at some point in the range profile of the clutter. This could typically represent transitions between land and sea clutter or shadowed and illuminated surface clutter;

(iii) clutter which is essentially homogeneous but in which a small number of range bins are corrupted by returns with significantly different amplitude and spectral characteristics, representing point-clutter sources or extraneous targets.

The performance is characterized in terms of the improvement factor (IF) defined as:

$$\mathrm{IF} = \frac{(S/C)_{out}}{(S/C)_{out}} = \frac{\mathbf{w}^H \mathbf{s}\mathbf{s}^T \mathbf{w}}{\mathbf{w}^H \mathbf{R}\mathbf{w}} \tag{43}$$

where **R** is the covariance matrix, as before, **w** is the desired filter weight vector and **s** is the vector of target returns. The IF was calculated for eight edge scenarios, tabulated in Figure 18, and for number of reference bins K = 10, 20 and $K \rightarrow \infty$. The clutter is assumed to have a Gaussian spectrum, with spectral width given by its standard deviation σ_0:

$$H(f) = \frac{1}{\sqrt{2\pi\sigma_0^2}} \exp\left(\frac{-(f - f_c)^2}{2\sigma_0^2}\right) \tag{44}$$

In homogeneous clutter, as $K \rightarrow \infty$ the estimated covariance matrix tends to the exact description of the clutter in the test cell. However, in nonhomogeneous clutter, as $K \rightarrow \infty$ the estimated covariance matrix in general will differ from that in the test cell.

Figure 19 shows the loss in IF around the clutter edge scenarios of Figure 18, and show that the losses can be substantial. The paper [4] goes on to show that prefiltering MTI can restore some of this loss.

Inhomogeneity detector in Space-Time Adaptive Processing: A second example of radar operation in nonhomogeneous clutter environments is in Space-Time Adaptive Processing. A number of different STAP algorithms have been developed [1, 2], and it is evident that no one algorithm is optimal in all scenarios. As the previous example has shown, the way in which the covariance matrix is estimated can have a great influence on the performance.

The concept of Knowledge-Based STAP was therefore developed, in which several different STAP algorithms are provided, with knowledge-based selection of algorithm parameters and selection of secondary data. The selection of the appropriate STAP algorithm for a given scenario is made on the basis of a non-homogeneity detector [1], and Figure 20 shows the basic scheme. The KB-STAP scheme has been extensively evaluated using data from the MCARM testbed.

4. TRACKING

The process of tracking consists of associating a set of detections to a particular target. The detections may be those from a single sensor, or in the general case they may be from a network of different sensors. The classical approach to monosensor tracking follows the stages of track initiation, plot-track correlation, track prediction, track filtering and track termination [19]. Classically the filtering process is provided by the α–β tracker, in which running averages of target position and velocity are maintained, updated at regular intervals. The values of α and β control the 'time constants' of the running averages, and represent a compromise on one hand between the ability to suppress noise, and on the other hand the ability to track target manoeuvres.

It can readily be appreciated that the tracking process offers great scope for adaptive processing and for the use of prior knowledge. The Kalman filter [13] is perhaps a first stage in this; here the filter time constants are varied adaptively according to the target's manoeuvres. There are further possibilities in adaptively varying the filter update interval, and in filters such as the Interactive Multiple Model (IMM), Joint Probabilistic Data Association (JPDA) and Multi-Hypothesis Tracking (MHT). These algorithms will be covered in the tutorial on application of knowledge-based techniques to the tracking function.

5. CONCLUSIONS

This tutorial has attempted to provide an introduction to the application of knowledge-based processing to the general radar problem. We have described the nature of the general radar problem and the basic processing techniques that are used. The fundamental concepts of matched filtering, superresolution and adaptive filtering have been described, emphasizing the equivalence of time/frequency and aperture/angular domains, and introducing the concept of Space-Time Adaptive Processing.

We have described some of the statistical clutter models in common use. It should be emphasized that these are just models, and as such represent an idealization of reality; nevertheless, clutter models can be very useful in predicting radar detection performance. Some practical examples of sea clutter and of land clutter have been presented, which demonstrate quite vividly that clutter is in general non-Gaussian and non-stationary, both in time and space. It is hoped this makes the case for the application of knowledge-based signal processing techniques to the general radar problem.

The two examples of filtering in nonhomogeneous clutter environments are intended to illustrate this further, showing that the performance of the adaptive Doppler filtering algorithm is severely compromised at clutter edges, due to incorrect estimation of the clutter covariance matrix, and how in Space-Time Adaptive Processing a non-homogeneity detector can be used in the choice of the most appropriate STAP algorithm, forming the so-called Knowledge-Based STAP (KB-STAP) processor.

6. ACKNOWLEDGEMENTS

I gratefully acknowledge invaluable discussions with many people from whom I have learned much about radar and signal processing over the years. I would particularly like to mention Chris Baker, DEN Davies, Alfonso Farina, Richard Klemm, Simon Watts, Richard White and Mike Wicks. I am also grateful to the students with whom I have worked on these subjects over the years, in particular Brian Armstrong, Glen Davidson, Jonathan Dunlop and Dominic Walker, and to the organisations, including the UK Ministry of Defence, the UK Engineering and Physical Sciences Research Council, QinetiQ and its predecessors, BAE SYSTEMS, Thales Sensors and AMS, who have supported the various projects.

7. REFERENCES

1. Adve, R., Antonik, P., Baldygo, W., Capraro, C., Capraro, G., Hale, T., Schneible, R. and Wicks, M., 'Knowledge-base application to ground moving target detection', AFRL-SN-RS-TR-2001-185, September 2001.
2. Antonik, P., Shuman, H., Li, P., Melvin, W. and Wicks, M.C., 'Knowledge-based space-time adaptive processing, Proc. *IEEE Radar Conference*, Syracuse NY, May 1997.
3. Armstrong, B.C. and Griffiths, H.D., 'CFAR detection of fluctuating targets in spatially correlated K-distributed clutter'; *IEE Proc*., Vol.138, Pt.F, No.2, pp139–152, April 1991.
4. Armstrong, B.C., Griffiths, H.D., Baker, C.J. and White, R.G., 'Performance evaluation of adaptive optimal Doppler processors in heterogeneous clutter'; *IEE Proc. Radar, Sonar and Navigation*, Vol.142, No.4, pp179–190, August 1995.
5. Benjamin, R., *Modulation, Resolution and Signal Processing in Radar, Sonar and Related Systems*, Pergamon Press, 1966.
6. Benjamin, R. and Griffiths, H.D., 'Aperture-domain signal processing'; *Electronics and Communication Engineering Journal*, Vol.1, No.2, pp71–80, March/April 1989.
7. Bienvenu, G., 'Influence of the spatial coherence of the background noise on high resolution passive methods', *Proc. IEEE International Conference on Acoustics, Speech and Signal Processing*, Washington DC, IEEE Publication No. 79CH1379-7 ASSP, 2-4 April 1979, pp306-309.
8. Billingsley, J.B., Farina, A., Gini, F., Greco, M.V. and Verrazzani, L., 'Statistical analyses of measured radar ground clutter data', *IEEE Trans. Aerospace and Electronic Systems*, Vol.AES-35, No.2, pp579-593, 1999.
9. Billingsley, J.B., *Low Angle Radar Land Clutter: Measurements and Empirical Models*, SciTech / Peter Peregrinus, 2002.
10. Bracewell, R.N., *The Fourier Transform and its Applications*, second edition, McGraw-Hill, 1978.
11. Brandwood, D.H., *Fourier Transforms in Radar and Signal Processing*, Artech House, 2003.
12. Brennan, L.E. and Reed, I.S., 'Theory of adaptive radar', *IEEE Trans. Aerospace & Electronic Systems*, Vol.AES-9, No.2, pp237-252, March 1973.
13. Brookner, E., *Tracking and Kalman Filtering Made Easy*, Wiley-Interscience, 1998.
14. Butler, J.L., 'Digital matrix and intermediate frequency scanning', Chapter 3 in *Microwave Scanning Antennas*, Volume III, (R.C. Hansen ed.), Peninsula Publishing, 1985.
15. Davidson, G. and Griffiths, H.D., 'Wavelet detection of low observable targets within sea clutter', Proc. *RADAR 2002* Conference, Edinburgh; IEE Conf. Publ. No.490, pp238–242, 15–17 October 2002.
16. Davidson, G., Griffiths, H.D. and Ablett, S., 'Statistical analysis of high resolution land clutter', Proc. *RADAR 2002* Conference, Edinburgh; IEE Conf. Publ. No.490, pp434–438, 15–17 October 2002.
17. Davies, D.E.N., 'Independent angular steering of each zero of the directional pattern of a linear array', *IEEE Trans. Antennas & Propagation*, Vol. AP-15, March 1967, pp296-298.
18. Drabowitch, S., Papiernik, A., Griffiths, H.D., Encinas, J. and Smith, B.L., *Modern Antennas*, Chapman & Hall / IEEE MTT, ISBN 0 412 57910 3, 1997.
19. Farina, A. and Studer, F.A., *Radar Data Procesing: Introduction and Tracking* (vol.1), Research Studies Press, May 1985.
20. Farina, A., *Antenna-based Signal Processing Techniques for Radar Systems*, Artech House, 1991.
21. Goldstein, J.S., Guerci, J.R. and Reed, I.S., 'Advanced concepts in STAP', Proc. *IEEE International Radar Conference*, Washington DC, pp699-704, May 2000.
22. Griffiths, H.D., Dunlop, J. and Voles, R., 'Texture analysis of sidescan sonar imagery using statistical scattering models', *Proc. NATO Conference on High Frequency Acoustics in Shallow Water*, Lerici, Italy; SACLANTCEN Conference Proceedings CP-45 (N.G. Pace, E. Poulinquen, O. Bergem and A.P. Lyons eds), pp187–194, 30 June – 4 July 1997.
23. Griffiths, H.D., Fassi, C., Dunsmore, M., Ablett, S. and Walbridge, M., 'Statistical analysis of high resolution land clutter', Proc. *NATO Symposium on Low Grazing Angle Clutter: its Characterisation,*

Measurement and Application, Columbia, MD, USA, 25–27 April 2000; RTO-MP-60, AC/323(SET)TP/12, pp25.1 – 25.10, October 2000.
24. Guerci, J.R., Goldstein, J.S., Zulch, P.A. and Reed, I.S., 'Optimal reduced-rank 3D STAP for joint hot and cold clutter mitigation', Proc. *IEEE Radar Conference*, Boston, pp119-124, April 1999.
25. Haykin, S. (ed.), *Advances in Spectrum Analysis and Array Processing* (vols I and II), Prentice-Hall, 1991.
26. Jakeman, E. and Pusey, P.N., 'Statistics of non-Rayleigh microwave sea echo', Proc. *RADAR'77* Conference, IEE Conference Publication No.155, pp105-109, 1977.
27. Klemm, R., *Space-Time Adaptive Processing*, Peter Peregrinus, 1999.
28. Lee, P., Barter, J., Beach, K., Caponi, E., Hindman, C., Lake, B., Rungaldier, H. and Shelton, J., 'Power spectral lineshapes of microwave radiation backscattered from sea surfaces at small grazing angles', *IEE Proc. Radar, Sonar and Navigation*, Vol.142, No.5, pp252-258, 1995.
29. Lee, P., Barter, J., Caponi, E., Caponi, M., Hindman, C., Lake, B. and Rungaldier, H., 'Wind-speed dependence of small grazing-angle microwave backscatter from sea surfaces', *IEEE Trans. Antennas & Propagation*, Vol.44, No.3, pp333-340, 1996.
30. Lee, P., Barter, J., Lake, B. and Thompson, H., 'Lineshape analysis of breaking-wave Doppler spectra', *IEE Proc. Radar, Sonar and Navigation*, Vol.145, No.2, pp135-139, 1998.
31. Long, M.W., *Radar Reflectivity of Land and Sea*, second edition, Artech House, 1983.
32. Nathanson, F.E., *Radar Design Principles*, Second edition, p355 et seq., McGraw-Hill, 1990.
33. Nelder, , J.A. and Mead, R., 'A simplex method for function minimisation' *Computer Journal*, Vol.7, p308, 1965.
34. Oliver, C.J. and Quegan, S., *Understanding Synthetic Aperture Radar Images*, Artech House, 1998.
35. Reed, I.S., Mallett, J.D. and Brennan, L.E., 'Rapid convergence rate in adaptive arrays', *IEEE Trans. Aerospace & Electronic Systems*, Vol.AES-10, November 1974, pp853-863.
36. Schmidt, R.O., 'Multiple emitter location and signal parameter estimation', Proc. RADC Spectrum Estimation Workshop, RADC-TR-79-63, Rome Air Development Center, Rome, NY, USA, Oct 1979, pp243-258; reprinted in *IEEE Trans. Antennas & Propagation*, Vol. AP-34, March 1986, pp276-280.
37. Sekine, M. and Mao, Y., *Weibull Radar Clutter*, Peter Peregrinus, 1990.
38. Shan, T.J. and Kailath, T., 'Adaptive beamforming for coherent signals and interference', *IEEE Trans. Acoustics, Speech & Signal Processing*, Vol. ASSP-33, No. 3, pp527-536, June 1985.
39. Van Trees, H.L., *Detection, Estimation and Modulation Theory, Part I*, Wiley, New York, 1968.
40. Walker, D., 'Experimentally motivated model for the low grazing angle Doppler spectra of the sea surface', *IEE Proc. Radar, Sonar & Navigation*, Vol.147, No.3, pp114-120, 2000.
41. Ward, K.D., 'Compound representation of high resolution sea clutter', *Electronics Letters*, Vol.17, No.16, pp561-563, August 1981.
42. Ward, K.D., 'A radar sea clutter model and its application to performance assessment', *Proc. RADAR'82* Conference, IEE Conference Publication No.216, pp203-207, 1982.
43. Ward, K.D. and Watts, S., 'Radar sea clutter', *Microwave Journal*, June 1985, pp109-121.
44. Ward, K.D., Baker, C.J. and Watts, S., 'Maritime surveillance radar, Part 1: radar scattering from the ocean surface', *IEE Proc.*, Vol.137, Pt.F., No.2, pp51-62, April 1990.
45. Watts, S., 'Radar detection prediction in sea clutter using the compound K-distribution model', *IEE Proc.*, Vol.132, Pt.F., No.7, pp613-620, December 1985.
46. Watts, S., 'Radar detection prediction in K-distributed sea clutter and thermal noise', *IEEE Trans. Aerospace & Electronic Systems*, Vol.AES-23, No.1, pp40-45, January 1987.
47. Watts, S., Baker, C.J. and Ward, K.D., 'Maritime surveillance radar, Part 2: detection performance in sea clutter', *IEE Proc.*, Vol.137, Pt.F., No.2, pp63-72, April 1990.
48. Wirth, W-D., *Radar Techniques using Array Antennas*, Peter Peregrinus, 2001.
49. Woodward, P.M., 'A method for calculating the field over a plane aperture required to produce a given polar diagram', *J.IEE*, Vol. 93, Pt. IIIA, pp1554-1558, 1946.
50. Woodward, P.M., *Probability and Information Theory, with Applications to Radar*, Pergamon Press, 1953; reprinted by Artech House, 1980.

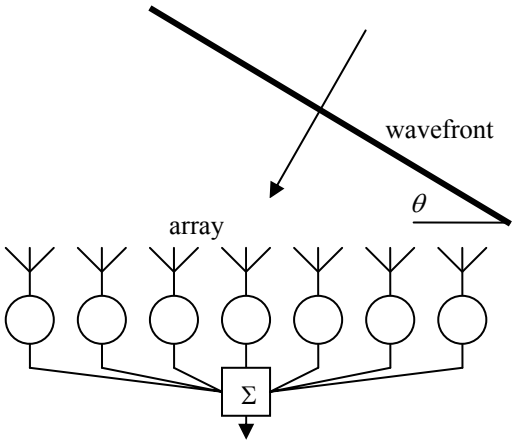

Figure 1. Linear antenna array as a spatial matched filter.

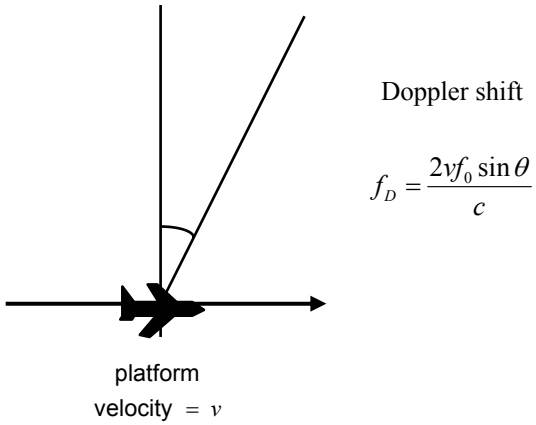

Figure 4. Doppler shift from a sideways-looking airborne radar.

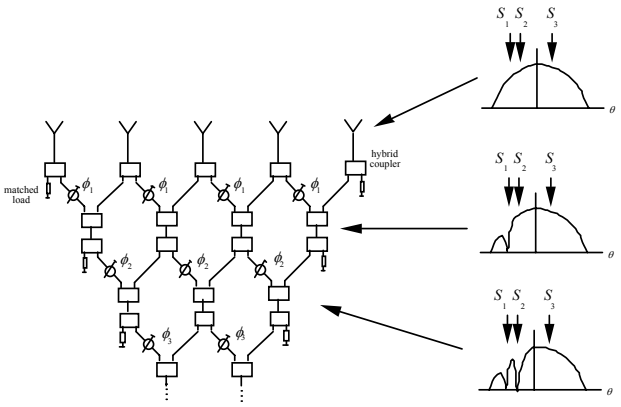

Figure 2. The Davies Beamformer.

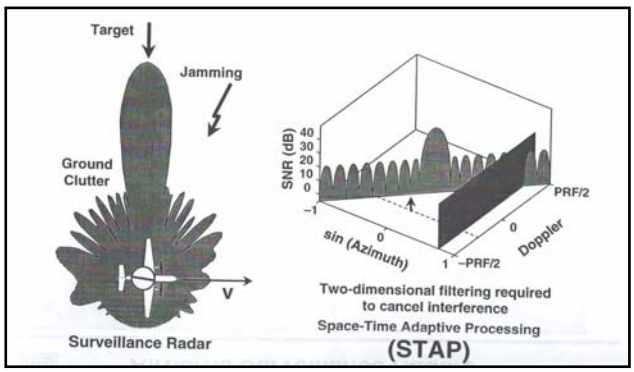

Figure 5. Space-Time Adaptive Processing (STAP): adaptive filtering in angle and in Doppler.

	Arrays of arbitrary geometry	Equi-spaced linear arrays
Translational invariance	ESPRIT [LS, TLS] †	TAM
One-dimensional parameter search	MVDR (Capon) MUSIC (Schmidt)	Maximum Entropy (Burg) minimum norm (KT)
Multi-dimensional parameter search	IMP (Clarke) WSF Stochastic max. likelihood Deterministic max. likelihood	† array must possess at least one translational invariance

Figure 3. Classification of superresolution algorithms.

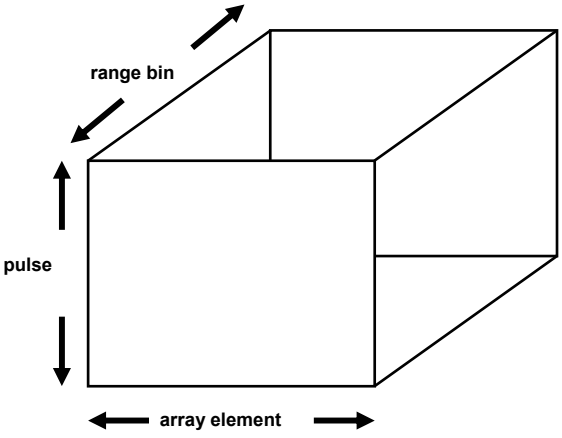

Figure 6. The STAP data cube.

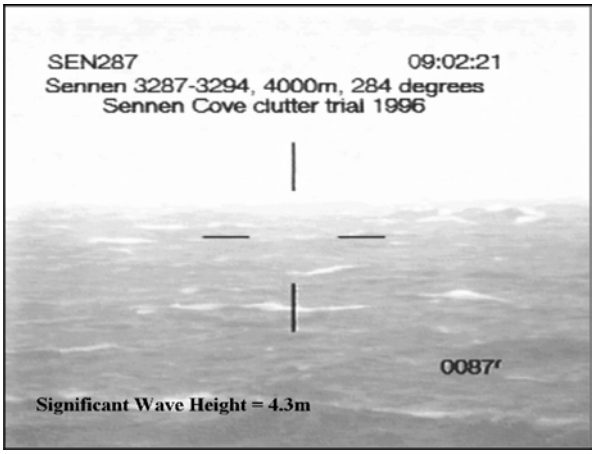

Figure 7. Photograph of sea surface from Sennen Cove, Cornwall, UK; significant wave height = 4.3 m.

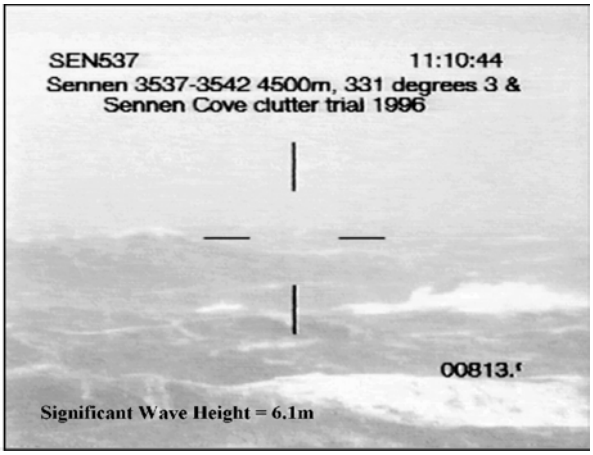

Figure 8. Photograph of sea surface from Sennen Cove, Cornwall, UK; significant wave height = 6.1 m.

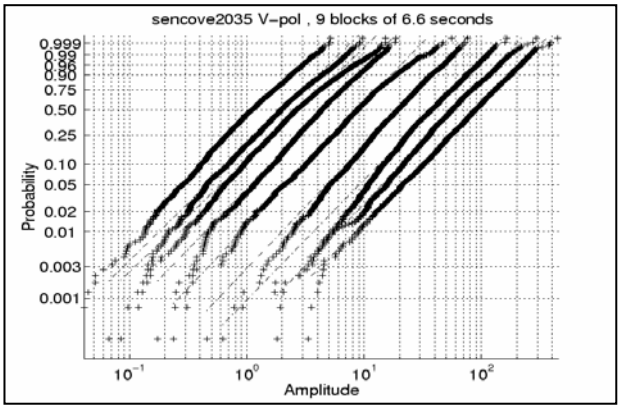

Figure 9. Consecutive Weibull plots of 6 second blocks of V-pol data, displaced for clarity. Neither power nor distribution is stable with time showing 2nd order statistics are necessary.

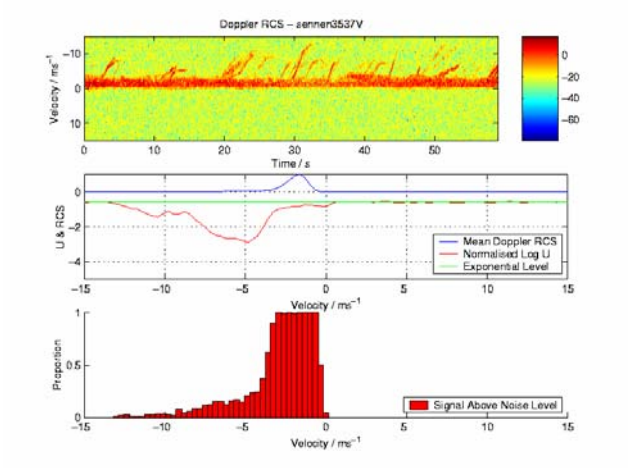

Figure 10. (a) High PRF Doppler trace over 60 second period; (b) distribution measure of spikiness; (c) proportion of tails of the Doppler spectrum above noise level [15].

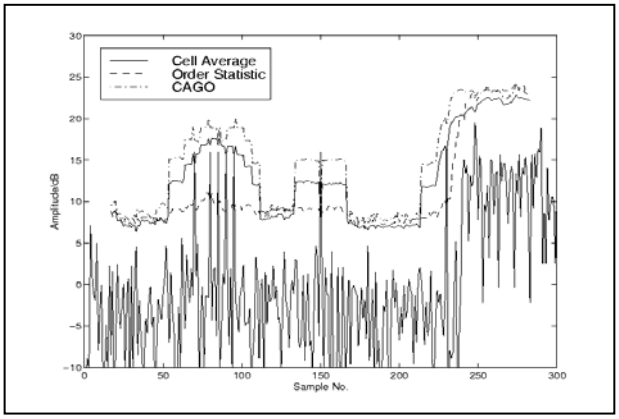

Figure 11. K-distributed noise (ν = 0.5), 32 cell CFAR, 16dB targets multiple @ 70-90, isolated target @ 150, potentially masked @ 230 by 14dB edge at 240 onwards.

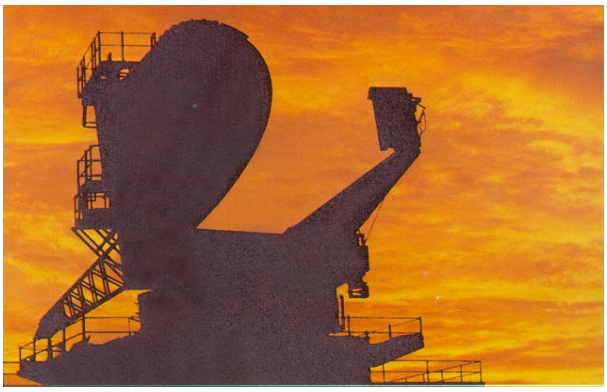

Figure 12. The BYSON radar.

frequency	2.7 – 3.1 GHz, frequency agile
PRF	100 Hz – 10 kHz
antenna gain	46 dBi
horizontal beamwidth	0.5°
vertical beamwidth	1.0°
polarisation	Vertical, horizontal or circular

Figure 13. BYSON radar parameters [23].

l	dist	MSD	parameter values	
HH	Weibull	0.4487	β=7.03E-3	ν=1.5101
	lognormal	8.0164	σ^2=22.796	z_m=2.87E-6
	Ricean	1.6403	ψ_0=2.45E-2	A=3.017E-4
	K-dist	0.3254	ν=1.388	b=53.33
VV	Weibull	0.3969	β=0.0129	ν=1.429
	lognormal	6.0643	σ^2=20.33	z_m=5.18E-6
	Ricean	1.7269	ψ_0=0.031	A=3.05E-4
	K-dist	0.2729	ν=1.164	b=37.85

Figure 14. Fit of Weibull, lognormal, Ricean and K-distribution models to high-resolution land clutter data acquired using BYSON radar [23].

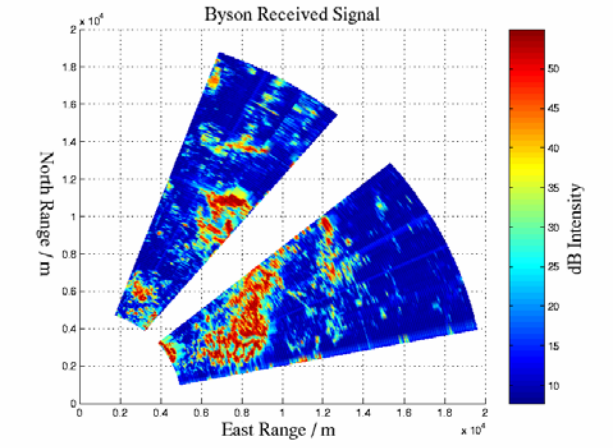

Figure 15. BYSON data (intensity in dB) [16].

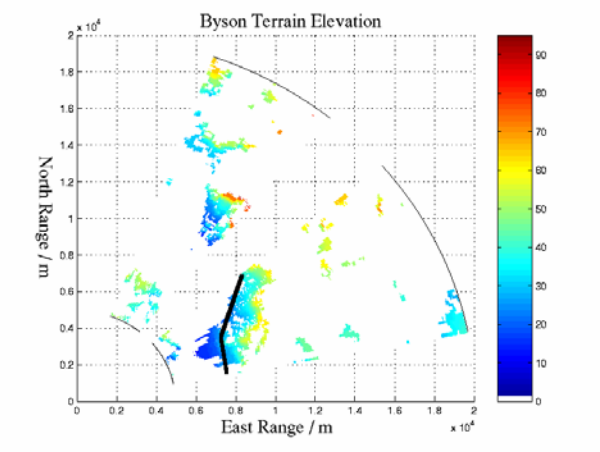

Figure 16. Digital elevation data corresponding to data of Figure 15 [16].

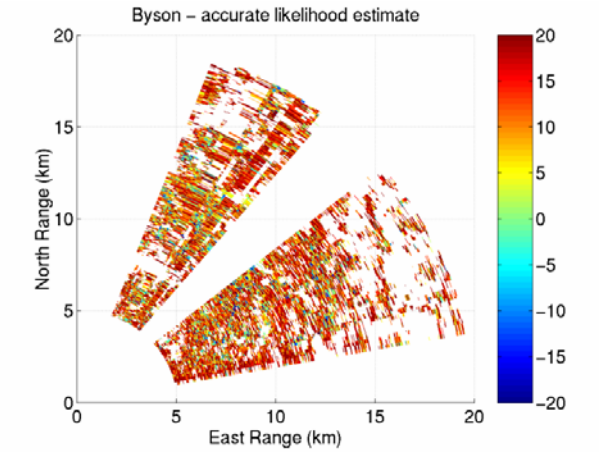

Figure 17. Likelihood ratio ($\log_{10}$) for individual range cells. White areas are classed as exponential clutter (largely shadow), positive values are more likely to be an edge, negative areas are more likely to be IID K. Note the motorway is visible as bright blue [16].

edge scenario	P_1	σ_1	f_{c1}	P_1	σ_1	f_{c1}
1	50	0.02	0	30	0.1	0.2
2	50	0.02	0	30	0.1	0.0
3	50	0.02	0	30	0.1	0.5
4	30	0.02	0	40	0.1	0.2
5	30	0.02	0	40	0.1	0.0
6	30	0.02	0	40	0.1	0.5
7	60	0.02	0	30	0.1	0.0
8	50	0.02	0	30	0.05	0.0

Figure 18. Clutter edge scenarios [4].

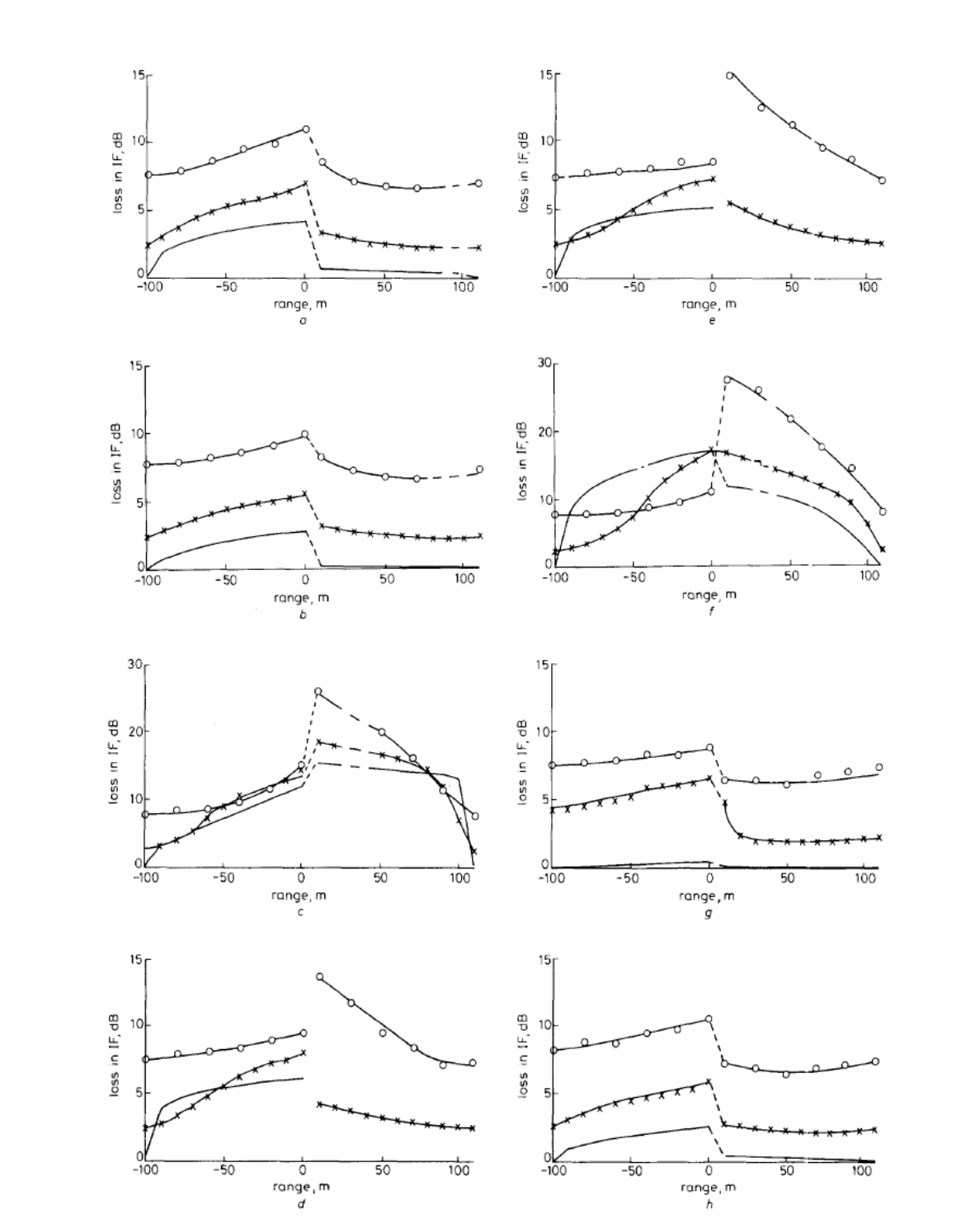

Figure 19. Improvement Factor (IF) loss around clutter edges ($N = 10$) (after [4]).

(a) edge scenario 1
(b) edge scenario 2
(c) edge scenario 3
(d) edge scenario 4
(e) edge scenario 5
(f) edge scenario 6
(g) edge scenario 7
(h) edge scenario 8

×-------× $K = 20$
o-------o $K = 10$
---------- $K \rightarrow \infty$

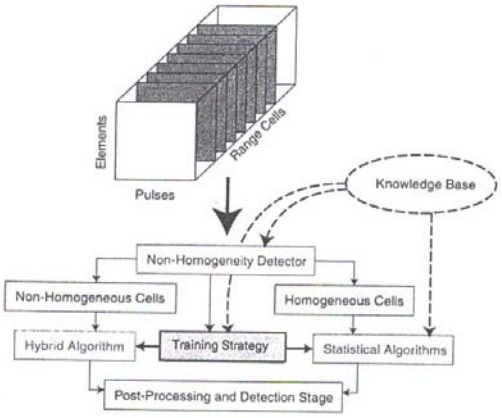

Figure 20. Knowledge-Based STAP (after [1]).

EXPERT SYSTEM APPLICATION TO CONSTANT FALSE ALARM RATE (CFAR) PROCESSOR

Michael C. Wicks, Ph.D.

Air Force Research Laboratory/Sensors Directorate

26 Electronic Parkway

Rome, NY 13441-4514

USA

Email: Michael.Wicks@rl.af.mil

ABSTRACT

An artificial intelligence system improves radar signal processor performance by increasing target probability of detection and reducing probability of false alarm in a severe radar clutter environment. This utilizes advances in artificial intelligence and expert systems technology for the development of data analysis and information (signal) processors used in conjunction with conventional (deterministic) data analysis algorithms to combine radar measurement data (including observed target tracks and radar clutter returns from terrain, sea, atmospheric effects, etc.) with topographic data, weather information, and similar information to formulate optimum filter coefficients and threshold tests. Present fielded radar systems use one CFAR algorithm for signal processing over the entire surveillance volume. However, radar experiments have shown that certain CFAR algorithms outperform others in different environments. The system intelligently senses the clutter environment, and selects and combines the most appropriate CFAR algorithm(s) to produce detection decisions that will outperform a processor using a single algorithm. The invention provides for improved performance through the application of rule-based and data-based expert system computer software technology to CFAR signal processors, thereby improving target detection by reducing processing losses which result from a mismatch between the single, fixed CFAR processor and dynamically changing environment in which a radar must operate.

EXPERT SYSTEM CONSTANT FALSE ALARM RATE (CFAR) PROCESSOR

STATEMENT OF GOVERNMENT INTEREST

The invention described herein may be manufactured and used by or for the Government for governmental purposes without the payment of any royalty thereon.

BACKGROUND OF THE INVENTION

The present invention generally relates to constant false alarm rate (CFAR) signal processors, and in particular, to a CFAR which improves radar signal processor performance by increasing target probability of detection and reducing probability of false alarms in a severe radar clutter environment.

False alarms are a significant problem in wide area surveillance radar. The conflicting requirements for a high probability of detection and a low probability of false alarm are rarely met due to the dynamically changing environment. The typical assumption of a homogeneous, Gaussian, thermal noise like background is routinely violated due to the spatial variation in clutter characteristics and effects of clutter edges, discretes, and multiple targets. Many different CFAR algorithms have been developed to effectively deal with the various types of backgrounds that are encountered. However, any single algorithm is likely to be inadequate in a dynamically changing environment as described

Paper presented at the RTO SET Lecture Series on "Knowledge-Based Radar Signal and Data Processing", held in Stockholm, Sweden, 3-4 November 2003; Rome, Italy, 6-7 November 2003; Budapest, Hungary, 10-11 November 2003; Madrid, Spain, 28-29 October 2004; Gdansk, Poland, 4-5 November 2004, and published in RTO-EN-SET-063.

above. The approach suggested here is to intelligently select the CFAR algorithm or algorithms being executed at any given time, based upon the observed characteristics of the environment. This approach requires sensing the environment, employing the most suitable CFAR algorithm(s), and applying an appropriate multiple algorithm fusion scheme or consensus algorithm to produce a global detection decision.

Adaptive threshold techniques are usually employed to control false alarm rates in varying background environments. The most common of these techniques is Constant False Alarm Rate (CFAR) processing. CFAR processors are designed to maintain a constant false alarm rate by adjusting the threshold for a cell under test by estimating the interference in the vicinity of the test cell. A "cell" is a sample in the domains of interest (eg: range, Doppler, angle, polarization). In general the data operated on by the CFAR processor may be pre-filtered to improve detection performance. This pre-filtering may include Doppler filtering, adaptive space-time processing, pre-whitening, and channel equalization.

Constant False Alarm Rate (CFAR) signal processing for automatic detection radar is an important part of the system design problem. The classical theory is developed under the assumption that detection is to be performed for the targets in the presence of stationary, Gaussian noise with known statistics, i.e. receiver noise. For ground-based radar systems looking high above the near-range clutter this was a valid assumption. For the case of modern, long-range, airborne surveillance radars, the situation is more complicated. The steep grazing angles associated with a look down radar produce far stronger clutter returns than those observed in any ground based radar, effectively masking targets flying above these clutter regions. Clutter changes dynamically as the platform moves such that the processor must effectively deal with clutter edges, discretes, multiple targets and non-Gaussian interference. The general theory for optimum detection in non-stationary, non-Gaussian clutter of interference is not well developed, even when the statistical properties of the environment are known. In an attempt to solve this problem, presently fielded radar systems employ canceller-based signal processing techniques which exploit anticipated differences between target returns and clutter. The classical techniques for automatic target detection in receiver noise are then employed. Non-zero clutter residues at the output of these canceller-based systems degrade the performance of classical detectors, and improved CFAR signal processing is required to achieve the desired probability of detection and probability of false alarm. Historically, the design of filters for clutter cancellation is performed separately from the design or CFAR signal processors. Consequently, detection performance will be suboptimum. Also, the selection of a single filter, and a single CFAR processor, to perform in all environments, will surely be mismatched to the ever changing radar returns, and will result in further degraded performance. The Expert System CFAR (ES-CFAR) Processor solves this problem by intelligently sensing the environment, employing one or more CFAR algorithms for data analysis, and combining results to make detection decisions.

The task of providing a CFAR processor that improves radar signal processor performance by increasing target probability of detection and reducing probability of false alarms in a severe radar clutter environment, is alleviated to some extent by the systems disclosed in the following U.S. patents, the disclosures of which are incorporated herein by reference:

U.S. Pat. No. 5,075,856 issued to Kneizys et al;
U.S. Pat. No. 5,093,665 issued to Wieler;
U.S. Pat. No.5,063,607 issued to FitzHenry el al;
U.S. Pat. No. 4,970,660 issued to Marchant; and
U.S. Pat. No. 4,749,994 issued to Taylor.

The patent to Marchant discloses an accumulated statistics CFAR method and device using integrated data to maximize the probability of target detection for a given false alarm rate. The remaining patents are of interest, but do not disclose improving performance through the application of rule-based and data-based expert system computer software technology to CFAR signal processors, thereby improving target detection by reducing processing losses which result from a mismatch between the single fixed CFAR processor and the dynamically changing environment.

Constant False Alarm Rate (CFAR) processors were developed to maintain a constant average false alarm rate through adaptive threshold control while maintaining adequate target detection performance. The classical Cell

Averaging (CA) CFAR processor assumes a homogeneous, Gaussian, thermal noise environment. It is, in fact, optimum under these conditions. However, in a wide area surveillance radar, these assumptions are routinely violated, presenting a variety of returns whose statistical characteristics are varied and unpredictable and quite unlike those of thermal noise even after filtering. The resulting effect is such that conventional CA CFAR processing may generate excessive false alarms.

The present invention utilizes advances in artificial intelligence and expert systems technology for the development of data analysis and information (signal) processors used in conjunction with conventional (deterministic) data analysis algorithms to combine radar measurement data (including observed target tracks and radar clutter returns from terrain, sea, atmospheric effects, etc.) with topographic data, weather information, and similar information to formulate optimum filter coefficients and threshold tests. Present fielded radar systems use one CFAR algorithm for signal processing over the entire surveillance volume. However, radar experiments have shown that certain CFAR algorithms outperform others in different environments. The invention's system intelligently sense the clutter environment, selects and combines the most appropriate CFAR algorithm(s) to produce detection decisions that will outperform a processor using a single algorithm.

SUMMARY OF INVENTION

The present invention includes both a three-step process and an artificial intelligence system that may be used to suppress false alarms in data of interest. The process begins by collecting data with a sensor system which collects both said data of interest and environmental data. A suitable sensor system is described in the above cited Kneizys et al patent, in which a radar system would collect both radar data and the environmental data (of atmospheric transmittance and background radiance) using the LOWTRAN 7 system.

Next comes the first processing step which entails processing the environmental data to select a best CFAR analysis model from a stored library of CFAR models. This represents the artificial intelligence aspect of the data in which the system automatically changes the selection of the analyses models with changes in the environment.

The process concludes with a second processing step which entails processing the data of interest with the best CFAR analysis model to yield a set of CFAR processed data of interest in which false alarms are suppressed.

As described above, the present invention includes a CFAR processor that improves radar signal processor performance by increasing target probability of detection and reducing probability of false alarms in a severe radar clutter environment. This invention utilizes advances in artificial intelligence and expert systems technology for the development of data analysis and information (signal) processors used in conjunction with conventional (deterministic) data analysis algorithms to combine radar measurement data (including observed target tracks and radar clutter returns from terrain, sea, atmospheric effects, etc.) with topographic data, weather information, and similar information to formulate optimum filter coefficients and threshold tests. Present fielded radar systems use one CFAR algorithm for signal processing over the entire surveillance volume. However, radar experiments have shown that certain CFAR algorithms outperform others in different environments. The invention's system intelligently senses the clutter environment, selects and combines the most appropriate CFAR algorithm(s) to produce detection decisions that will outperform a processor using a single algorithm. The invention provides for improved performance through the application of rule-based and data-based expert system computer software technology to CFAR signal processors, thereby improving target detection by reducing processing losses which result from a mismatch between the single, fixed CFAR processor and the dynamically changing environment in which a radar must operate.

The requirements for high detection probability and low false alarm probability in modern wide area surveillance radars are rarely met due to spatial variations in clutter characteristics. Many filtering and CFAR detection algorithms have been developed to effectively deal with these variations; however, any single algorithm is likely to exhibit excessive

false alarms and intolerably low detection probabilities in a dynamically changing environment. A great deal of research has led to advances in the state of the art in Artificial Intelligence (AI) and numerous areas have been identified for application to radar signal processing. The approach suggested here, discussed in a patent application submitted by the authors, is to intelligently select the filtering and CFAR detection algorithms being executed at any given time, based upon the observed characteristics of the interference environment. This approach requires sensing the environment, employing the most suitable algorithms, and applying an appropriate multiple algorithm fusion scheme or consensus algorithm to produce a global detection decision.

It is an object of the invention to minimize false alarms in data of interest.

It is another object of the invention to provide an artificial intelligence system which varies the selection of CFAR analysis models with changes in circumstances.

These objects together with other objects, features and advantages of the invention will become more readily apparent from the following detailed description when taken in conjunction with the accompanying drawings wherein like elements are given like reference numerals throughout.

DESCRIPTION OF THE DRAWINGS

Fig 1 is a block diagram of a system suing a prior art cell averaging CFAR;

Fig 2 is a simplified block diagram of an ES CFAR:

Fig 3 is a detailed block diagram of an ES CFAR:

Fig 4 is a chart comparing receiver operating characteristics for two CFAR algorithms;

Fig 5 is a chart illustrating the variation in detection performance versus Weibull shape parameter for two arbitrary CFAR algorithms;

Fig 6 is a detailed block diagram of the elements of the preferred embodiment of the ES-CFAR processor;

Fig 7 is a block diagram of an OS CFAR processor used for single-pulse linear detection;

Fig 8 is a block diagram of another embodiment of an ES CFAR processor;

Fig 9 shows a radar system with its data processed by an ES CFAR processor;

Fig 10 is a diagram of an ES-CFAR system using artificial intelligence to perform environmental processing as it selects an appropriate CFAR algorithm;

Fig 11 is a chart illustrating one of the scenarios for simulation analysis, a ring of exponentially distributed clutter is placed around the radar location (marked with the flag); and

Fig 12 is a chart illustrating the detection performance of the expert system CFAR (left hand display) versus cell averaging CFAR (right hand display).

DETAILED DESCRIPTION OF THE PREFERRED EMBODIMENT

The present invention is a CFAR system that applies artificial intelligence techniques in a system that dynamically selects CFAR algorithms and controls CFAR parameters based on the environment, and in doing so, should out-perform a single, fixed CFAR system.

CFAR processors were developed to maintain a constant average false alarm rate through adaptive threshold control while maintaining adequate target detection performance. Fig 1 illustrates a classical Cell Averaging CFAR (CA-CFAR) processor 160 operating on a sliding window 110 of n cells from the output of a linear detector 100. The cell 120 in the center of the window is referred to as the test cell and those on either side are guard cells. Secondary data obtained from the n cells leading and lagging the test and guard cells are averaged to yield an estimate of the interference in the test cell. This estimate is then compared via comparator 190 to the test cell after scaling by an appropriate multiplicative gain factor 150. A detection is declared if the product of the test cell and the multiplicate gain factor exceed the test cell background or interference estimate obtained from the secondary data. This process is repeated for subsequent radar returns in range, angle and Doppler. CA-CFAR was developed for operation in a homogeneous, Gaussian, thermal noise environment, and is optimum under these conditions. However, in wide area surveillance radar, these assumptions are routinely violated, with diverse returns whose statistical characteristics are varied and unpredictable and

quite unlike those of thermal noise, even after filtering. The resulting effect is such that conventional CA-CFAR processing may generate excessive false alarms.

As an introduction to the Expert System CFAR (ES-CFAR) Processor, first consider the theory of target detection. As mentioned above, in Fig 1 a sliding window of n cells from the output of a detector as 100 are applied to a CFAR processor 160. In the case of the Greatest-Of CFAR (GO-CFAR), the leading and lagging windows are compared and the larger of the two is used as the interference estimate. In the case of Ordered Statistic CFAR (OS-CFAR) the cells in the reference window are placed in ascending order and the mth largest value of n cells is selected as the estimate of the interference. This estimate is then compared to the test cell after scaling by an appropriate multiplicative gain factor. A detection is declared if the produce of the test cell and the multiplicative gain factor exceed the test cell background or interference estimate. This process is repeated for subsequent radar returns in range, angle and Doppler.

The classical approach to radar signal processing was developed for target detection by a ground-based radar looking high above near-range clutter. Interference is suppressed by the use of canceller-based filters such as Moving Target Indicator (MTI), assuming pulse to pulse invariance of the ground clutter. Additionally, Doppler processing is employed to further suppress clutter returns and improve Signal to Noise Ratio (SNR). Fast Fourier Transform (FFT) based filtering provides for excellent results. Typically, the output of the zero Doppler filter is ignored. The largest source of the interference is the return from near-in ground clutter, within the first few miles of the radar. At the long detection ranges of interest, ground clutter is almost non-existent and the only limitation to detection is thermal noise, generally accepted to behave as a complex Gaussian random vector. The output of the MTI canceller and/or Doppler filter is processed most appropriately using CA-CFAR.

Now consider modern long range airborne surveillance radars operating in a complicated interference environment. The steep grazing angles associated with down looking radar may produce clutter returns of far greater magnitude than in ground based systems. As such, clutter backscatter often mask returns from targets flying above these regions. Also, clutter statistics change dramatically as the platform moves. For example, within one scan, we may have to content with clutter returns ranging from calm sea which we observe to behave as a Rayleigh distributed random vector, while at other locations within the surveillance volume we may encounter clutter returns from a land sea interface. Since terrain clutter backscatter often behaves as K-distributed random vector, we ultimately must perform detection processing along a clutter edge where the statistics vary unpredictably. Clearly, the classical CA-CFAR detector used in ground based radar is not adequate. Further complicating this problem are spectrally spread sidelobe clutter returns which broaden the Doppler spectrum occupied by clutter, making Airborne Moving Target Indicator (AMTI) less effective. Also, FFT-based Doppler filtering is suboptimum because the clutter returns are no longer confined to the zero Hertz filter. Platform motion and sidelobe returns broaden the clutter spectrum, spreading clutter energy into adjacent Doppler bins. This further complicates detection processing. It is in situations such as this that the use of a single combination of filtering and CFAR algorithms will produce excessive false alarms, because it cannot be designed to be optimum for each and every scenario to which it must be applied. In light of the many constraints imposed upon radar systems, improvements in detection performance are most likely to be a result of advanced processing techniques able to recognize the existence of these situations and apply appropriate processing while effectively maintaining a constant false alarm rate and an adequate detection probability.

The ES-CFAR processor presented here is based upon the combined use of algorithmic and heuristic (artificial intelligence) techniques designed to assess the characteristics of the environment in order to apply the most appropriate filtering and CFAR detection algorithm. The concept and structure of an Expert System is illustrated in Fig 2. Here, input data is compared to a data base where like or similar data sets are identified. These characteristics and descriptors of the data set are analyzed by a knowledge base which utilizes an extensive rulebase to make inferences about the data. These

inferences are then interpreted to ascertain their meaning in the context of the decision problem, and applied under control based upon the nature of the input data. Feedback may also be incorporated where outputs of the control structure are input to the data base providing additional sources of knowledge. The control structure relays decisions and actions to the user. The structure of the Expert System CFAR Processor as well as the many functions performed by it, are based on this design, and are to be discussed below.

Fig 2 is a diagram representing one basic structure of an Expert System which uses a data base 210, a knowledge base 220, a control structure 230 and an interface 240 with the user 250. The control structure 230 is a data processor which will select the use of different CFAR detection algorithms based upon different conditions in the environment. In this case, the input data is compared to a database where like or similar data sets are identified. Descriptors and characteristics of the input data are determined at this point. These characteristics and descriptors of the data sets are analyzed by a knowledge base which utilizes an extensive set of rules to make inferences about the data. These inferences are then interpreted to ascertain their meaning in the context of the problem and applied to a control structure which makes adjustments to the system "being controlled" based upon the input data. Feedback may be incorporated where outputs of the control structure are input to the database providing additional sources of knowledge. The control structure relays decisions and actions to the user.

This Expert System technology can be applied to CFAR detection processing to develop an EX-CFAR Processor as illustrated in Fig 3. The system operates in the same manner as described above, but the knowledge base has been modified to perform functions specific to target detection and false alarm control. For this particular problem, various knowledge sources are available to provide input to the knowledge base. There are basically five functions tob e performed.

First consider the background analysis problem. As a radar returns (data) are processed, one of the first tasks to be performed is determination of the statistical characteristics of the clutter. This entails identifying the probability density function (pdf) of the data as well as the associated parameters of the distribution. Standard histogram techniques, Quantile-Quantile and Percent-Percent (plot) analysis, moment techniques and various hybrid combinations are employed for this analysis.

Next, consider clutter classification (type). Also of importance is the selection of an appropriate CFAR detection algorithm are the physical attributes of the clutter (i.e. urban, sea, desert, etc). For example, extensive research has resulted in numerous clutter and interference moels which associate physical clutter features with particular statistical distribution. In fact, many CFAR algorithms are designed for detection processing in clutter behaving according to these statistical distributions. This a priori knowledge provides the rule base which dictates the use of CFAR algorithm over another in a given interference environment. Knowing the physical and statistical nature of the clutter environment, combined with performance measures for various CFAR algorithms as a function of clutter type, aids in the selection of the most appropriate CFAR algorithm. For example, it was stated previously that in a Gaussian white noise interference environment, CA-CFAR processing is optimum. If we consider performing detection along a clutter edge such as a transition from a thermal noise limited environment to sea clutter limited environment, the same CA-CFAR will exhibit excessive false alarms with a corresponding degradation in detection probability. A more prudent choice may be GO-CFAR which will abate the effects of the clutter edge on our ability to perform CFAR detection processing.

The adaptive filtering algorithm library is also important. As discussed above, various forms of clutter suppression and Doppler filtering schemes are available (MTI cancellers, Doppler Filtering, space-time processing, etc.) but generally only one is used. Here, based on the assessment of the environment, we cannot only choose the most appropriate CFAR algorithm, but also the most appropriate filtering technique to precede the CFAR detector.

A complete library of CFAR algorithms is critical. Many of the rules in the knowledge base control the utilization of CFAR algorithms. For each algorithm in the library, performance under the dynamic conditions of interest to the radar

system engineer must be available. The relative performance of each CFAR algorithm must be quantified as a function of clutter type/statistic, detection probability, false alarm probability and CFAR processing loss. CFAR algorithm performance will vary widely considering the variety of backgrounds likely to be encountered in an airborne radar system. It is for this reason that the library must contain CFAR algorithms with variable parameters such as Cell Averaging, Greatest-Of, Ordered Statistic, and Trimmed Mean. Each of these algorithms exhibit performance advantages that can be exploited in an attempt to maintain an adequate level of detection and false alarm probability. One conventional performance measure of a detector is the receiver operating characteristics (ROC) which is a plot of detection probability versus false alarm probability. Intuitively, one would expect that as detection probability is increased, the threshold must be lowered, and consequently, false alarm probability will be increased. Fig 4 is a sample plot of the ROC for two different CFAR algorithms. This illustrates the very different behavior of the two CFAR algorithms under the same conditions. We may also observe detection performance as a function of pdf, or more specifically, the variation of the parameters of a given pdf. Fig 5 is a plot of detection probability versus Weibull shape parameter for two (arbitrary) CFAR algorithms. Again, we can see the very different behavior of these algorithms under identical background conditions. These are examples of the factors affecting detection and false alarm probability and the extent to which they dictate the use of one CFAR algorithm over another.

Finally, consensus analysis must be considered. After selection of the most appropriate algorithms, detection processing is performed and decisions from the selected CFAR algorithms must be weighted and fused to produce a satisfactory global detection decision.

The knowledge sources are not limited to the five listed above, but may also include exogeneous variables such as temperature, wind speed, and precipitation. These factors are not directly related to target detection, but can certainly play a role in altering the statistics of the background interference we are trying to suppress.

A conceptual diagram of the ES-CFAR System is illustrated in Fig 6. The input is applied to an expert system where analysis (heuristic and algorithmic) produces the statistical and physical characteristics of the data. This information is used in conjunction with a library of CFAR algorithms, containing algorithms such as Cell Averaging, Greatest Of, Smallest Of, Ordered Statistic and Trimmed Mean. Within each of these individual CFAR algorithms there are many subclasses with various combinations of rank, order, window size and multiplicative gain factor. Preceding each of the CFAR algorithms is a filter and detector matched to that particular CFAR algorithm. In this way one ensures that the filtering of radar data corresponds to the method of CFAR detection processing that follows. Based on the characteristics of the input data, the expert system assigns weights to the outputs of the various CFAR algorithms corresponding to their suitability given the input data. The weighted outputs are then summed to produce a cumulative or global detection output. This output could be, in simplest form, the decision of just one of the CFAR algorithms. Alternatively, the output could be more complex such as summation of the weighted outputs of CFAR algorithms. In this way the most appropriate combination of CFAR algorithms and parameters are used to perform CFAR detection processing.

The conflicting requirements for high probability of detection and low probability of false alarm are rarely met in a wide area surveillance radar, due to spatial variations in the clutter. Any single algorithm is likely to be inadequate in a dynamically changing environment. The approach suggested in this paper is to select the filtering and CFAR algorithms being executed at any one time based upon the observed characteristics of the interference. This requires sensing the environment, employing the most suitable filtering and CFAR algorithms, and applying a consensus algorithm to produce a global detection decision. Based on advances in expert systems, adaptive processing and CFAR algorithms, this approach has the potential to provide significant performance improvements to future wide area surveillance radars. Commercially operating systems can also benefit from this technology; FAA air surveillance radars must content with a

very dense target environment where false alarms, missed detections and operator overload are factors which must be tightly controlled to avoid disastrous outcomes in the civilian/commercial travel industry.

The prototype ES-CFAR Processor has been developed on a Sun Sparc Station 4/470 using a commercial-off-the-shelf software development package called G2 by Gensym Corporation. It is a real-time expert system development shell used for Knowledge Base and Inference Engine development. G2 is currently being used in numerous real-time systems including a prototype hydroelectric power generation plant monitoring and control system and is incorporated into software analysis tools on board the National Aeronautic and Space Administration (NASA) Space Shuttle. The ES-CFAR Processor does not currently operate in real time because G2 is performing many extraneous functions which would not be required when utilized in a fielded radar system, such as simulated data generation, performance monitoring, and graphical display. Additionally, the prototype has been developed to provide a great deal of flexibility to emulate a variety of CFAR detection processors as a baseline for performance comparison. Essentially, two CFAR processors (baseline and ES-CFAR) are running simultaneously which would not be required for fielded operation. When a specific candidate radar system is chosen for implementation, a point design configuration can be developed using high speed floating point processor boards.

The prototype ES-CFAR Processor was developed through off-line analysis of radar processing functions, allowing an expert to assess the characteristics of the environment and to apply the most appropriate CFAR algorithm. It is important to be able to accurately identify the statistical characteristics of the background interference. Standard techniques are currently employed for this purpose, although research into a new statistical distribution identification techniques is continuing. Also essential is a library of CFAR algorithms chosen so that the most stable algorithm for detection processing may be chosen for any interference scenario likely to be encountered. An extensive literature search was performed which revealed an abundance of journal articles reporting the existence of more than 40 CFAR algorithms developed to counter the effects of non-homogeneous clutter, interfering targets, clutter edges and Electronic Counter Measures (ECM). The conclusions reached provided insight and directions into those CFAR algorithms that should be implemented in the prototype ES-CFAR Processor. Additionally, these same results helped to formulate the rules incorporated into the expert system which dictated the selection of one CFAR algorithm over another.

The knowledge sources are not limited to the five listed above, but may also include exogeneous variables such as temperature, wind speed, and precipitation. These factors are not directly related to CFAR detection, but can certainly play a role in altering the statistics of the background we are trying to suppress.

There are many ways an ES-CFAR processor could be envisioned, but the preferred embodiment is illustrated in Fig 6. The input data is applied to the expert system where data analysis (heuristic and algorithmic) produces the statistical and physical characteristics of the data. The library of CFAR algorithms consists of a variety of Ordered Statistic CFAR (OS-CFAR) algorithms with varying values of rank and order. There are a total of M such algorithms in the Expert System CFAR Processor. Preceding each of these M OS-CFAR algorithms is a filter and detector illustrated for completeness. Each OS-CFAR in Fig 6 is of this form. Based on the characteristics of the input data, the expert system assigns weights to the outputs of the M CFAR algorithms corresponding to their suitability to the input data. The M weighted outputs are then summed to produce a cumulative or global detection output. This output could be, in simplest form, the output of just one of the M CFAR algorithms. Alternatively, the output could be more complex such as a summation of the weighted outputs of all M CFAR algorithms. In this way the most appropriate combination of rank and order are used to perform CFAR detection processing.

As an example of a possible implementation of the preferred embodiment of the ES-CFAR Processor, let us consider target detection in the presence of a clutter edge. Here, some of the reference cells are occupied by clutter while the rest are occupied by noise only. The single, fixed CFAR algorithm will raise the threshold to an

intolerable level by overestimating the power level of the background. This same high threshold will also decrease the detection probability. In a case such as that it is desirable to vary the parameters of the CFAR algorithm, namely, the window size, order and threshold multiplier for an Ordered Statistic CFAR algorithm. Assuming some knowledge about the background derived from the Clutter Classifier such as number of clutter cells in the reference window, we can select the most appropriate parameters for performing detection processing. Table I lists an illustrative example of the order values that would be selected for an OS-CFAR algorithm with a window size of 32, a target signal-to-noise ratio of 10dB, and designed for a false alarm probability of 0.001 for varying clutter power levels and number of reference cells occupied by clutter. As is evident from the table, where OS(n) is the nth largest data point out of k samples, the knowledge and classification of the clutter plays an important role in intelligently varying the parameters of the CFAR algorithm to meet the design false alarm and detection probabilities.

The Expert System CFAR Processor, ES-CFAR, has the advantages of improved detection performance and false alarm control in the presence of non-Gaussian, non-stationary interference relative to a conventional CFAR processor utilizing a single, fixed CFAR algorithm. By intelligent sensing and classification of environmental interference, the most appropriate CFAR algorithm or combination of CFAR algorithms may be chosen to maximize detection probability while maintaining a satisfactorily low probability of false alarm.

The Expert System CFAR (ES-CFAR) Processor can be implemented in many other ways other than the preferred embodiment described previously. Instead of choosing from a CFAR algorithm library of M different Ordered Statistic CFAR algorithms, the library could consist of multiple CFAR algorithms such as Cell Averaging (CA-CFAR), Greatest-Of (GO-CFAR) and the OS-CFAR mentioned above. Within each of these individual CFAR algorithms there may be subclasses with various combinations of rank and order as described previously, or window size and multiplicative gain factor for CA-CFAR and GO-CFAR. Fig 8 illustrates how this could be implemented. By adding another control line from the expert system to each of the individual CFAR algorithms, the parameters of the CFAR algorithm could be specified in addition to just selecting the CFAR. In this way additional adaptivity can be added to the system to deal with more complex interference scenarios that one may encounter in the dynamically changing environment encountered by a long range, wide area surveillance radar system.

A schematic design of the EX-CFAR Processor is illustrated in Fig 9. Not all functions are fully implemented at this time. The upper portion of the figure 9above the dashed line) depicts the baseline system, representing a typical radar operating with one CFAR algorithm in the signal processor. The remaining portion of the figure (below the dashed line) illustrates the major functional aspects of the conceptual ES-CFAR system. Radar returns, which may be raw data, FFT-Doppler filtered data, or adaptively filtered data, are processed by both systems. Following this filtering operation, the target signal is competing favorably with the background interference. The Baseline Processor performs detection processing on this data using a single, fixed CFAR algorithm. This algorithm may be chosen from any of the CFAR algorithms in the library, but once selected will be used for all detection processing. As the library of CFAR algorithms is expanded, one can emulate the performance of the CFAR detector in any fielded system. The library of CFAR algorithms currently contains Cell Averaging, Greatest Of, Ordered Statistic and Trimmed Mean processors. Below the dashed line, ES-CFAR processing occurs simultaneously with the baseline, using the same input data. At the right side of the figure, the circles indicate Knowledge Sources such as Geographic Data, Radar Location, and User Inputs. In future implementations, map information will be used in conjunction with the radar location and the antenna pointing direction to assess the physical features of the surveillance region (i.e. sea, desert, urban, etc.) The radar returns are processed to extract information concerning the statistics of the clutter. The statistical and feature information form the basis for selection of the most appropriate CFAR algorithm(s) to be used by the ES-CFAR Processor for detection processing. The outputs

of the CFAR algorithm(s) are weighted and fused to produce a global detection decision which is further processed for track initiation. The output of the tracker is fed back as additional knowledge. For example, the tracker may indicate the presence of multiple closely spaced targets. The results of the Baseline and ES-CFAR Processors are then presented respectively on two simulated PPI displays depicting the resultant targets and false alarms. Alternatively, the resultant detection and false alarm probabilities are plotted as a function of time for both the Baseline and ES-CFAR Processors as another indication of performance.

The input data may be either simulated or measured. The simulated data is generated by the expert system according to a surveillance scenario specified by the user. Clutter with various distributions and parameters may be "drawn" on the PPI display. Targets may also be placed within the surveillance area and assigned various cross sections. This provides a controlled means to evaluate the performance of the baseline against that of the ES-CFAR processor. Results are displayed as discussed in the last paragraph. A capability also exists to import data from outside the expert system and process it in the same fashion. This data may be one-dimensional (such as range only) or multi-dimensional (such as range and Doppler). Again the user selects the CFAR algorithm to be used in the baseline and performance is compared to that of the ES-CFAR system which adaptively performs CFAR processing based upon the background.

Extensive testing has been performed on the ES-CFAR Processor in an attempt to compare its performance to a baseline CA-CFAR Processor. This testing has taken the form of both simulated and measured data. In the following paragraphs this testing will be described in more detail showing the dramatic performance improvements to be derived by use of the ES-CFAR processor. This will be followed by a discussion of the potential applicability of ES-CFAR to the AN/APS-145 radar aboard the E-2C Hawkeye as well as potential performance in the presence of ECM.

A total of nine simulated scenarios were developed for analysis by the ES-CFAR Processor. These scenarios were chosen to represent some of the most stressing environments encountered, and included non-Gaussian clutter, interfering targets and clutter edges. One of the scenarios will be described in detail, and the results of the remaining eight will be shown in tabular form. In one of the scenarios for simulation analysis, a ring of Exponentially distributed clutter has been placed around the radar location. See Fig. 11. Fig 11 is a chart illustrating one of the scenarios for simulation analysis, a ring of exponentially distributed clutter is placed around the radar location (marked with the flag). All other range cells contain white noise. This scenario incorporates a target near a boundary between two regions of interference within the typical CFAR reference window. Conventional CA-CFAR will tend to elevate the threshold level in this case because Exponential clutter returns in the leading window are much stronger than the Gaussian noise in the lagging window thus causing the target to be undetected. Statistically identical interference is generated at each beam position so that after several scans a sufficiently large number of data points have been processed to make the selected false alarm probability of 0.001 statistically meaningful. Many detections were reported at each beam position and all occurred in the vicinity of the clutter edge, as it was the edge of the clutter region which was detected and not the target. No detections occurred at the actual range of the target (i.e. in the square). See Fig 12. Fig 12 is a chart illustrating the detection performance of the expert system CFAR (left hand display) versus cell averaging CFAR 9right hand display). This is typically the case when using CA-CFAR to perform detection processing along a clutter edge. False alarms are generated and weak targets near the clutter edge are not detected. The ES-CFAR Processor was able to recognize this discontinuity (clutter edge) as the CFAR window moved in range. The rules in expert system appropriately dictated a change of CFAR processing for better detection performance. The PPI on the left corresponds to the ES-CFAR processor. It displays a large number of detections all occurring within the squares, indicating correct detections.

As mentioned previously, eight other simulated scenarios were run which posed stressing problems such as clutter edges, interfering targets and non-homogeneous clutter. The results of all nine scenarios are listed in Table

I for the Baseline and ES-CFAR processors. As can be seen, the ES-CFAR processor significantly outperformed the Baseline in terms of detection while also maintaining a better false alarm probability.

Using Fig 2.2.2 on page 62 from Barton's modern Radar System Analysis test and the results from Table II on page 34 of this patent application, the improved detection performance and reduced false alarm rate provides for an improvement of 6.4dB over CA-CFAR and 5.7dB over OS-CFAR. This is equivalent to a 50% increase in range in a clutter limited environment.

AIRBORNE MEASURED DATA ANALYSIS AND RESULTS

To verity ES-CFAR performance, a comparison was made at Rome Laboratory using a database of recorded radar returns from an airborne radar system. This data set was collected for another purpose, but it did allow for testing the ES-CFAR Processor in a multiple (interfering) target scenario and in the present of a clutter edge.

The airborne radar is a medium PRF pulsed Doppler system and data was recorded as the antenna swept past the targets of interest. The system PRF is constantly changing during each Coherent Processing Interval (CPI) so that the range ambiguity of this medium PRF waveform can be resolved. The result of each CPI is a two dimensional map of range versus Doppler. Many such range versus Doppler data sets were collected and served as the input to the ES-CFAR Processor. Detection processing in modern airborne radars is via Cell Averaging CFAR. This was the Baseline CFAR algorithm used for performance comparison. The ES-CFAR Processor accepts this data and also processes it using all the CFAR algorithms available in the CFAR Algorithm Library as discussed above. A total of 25 CPIs have been processed in this way for various design values of false alarm probability (0.001, 0.0001, 0.00001, and 0.000001). Table II is a listing of the detection and false alarm results for the four cases corresponding to the four design false alarm probabilities in terms of the resultant values of detection and false alarm probabilities of the Baseline and the Expert System CFAR Processor. It is evident that ES-CFAR improves both detection and false alarm probability and would have significant impact on modern long range surveillance radars.

Obtaining similar improvements by increasing the antenna aperture or transmit power would be prohibitive. In addition, if detection is limited by sidelobe clutter and not thermal noise, a larger power-aperture product alone would likely not improve detection performance.

The U.S. Navy is currently implementing the Group 2 update of the E-2C early warning surveillance platform. Target detection and tracking performance is greatly improved by an upgrade to the General Electric AN/APS-145 radar. Significant improvements have been made to the Detection and Data Processor which provides for automatic radar configuration and performance optimization over heterogeneous ground clutter environments. Based on the E-3 performance analyses accomplished to date, the ES-CFAR processor could provide significant improvement in target detection, tracking and false alarm control over this single CFAR scheme processor, even with its improved adaptive thresholding control. In the near future, we would like to perform an analysis similar to that reported on here to provide an assessment of the ES-CFAR processor performance using actual E-2C data.

Fig 10 presents a functional block diagram illustrating data flow and processing surrounding the new Environmental Processor (EP) function within the Detection and Data Processor. It is the introduction of this processor into the AN/APS-145 which is key to enabling low-risk implementations of the ES-CFAR. We clearly show in Fig 10 where the ES-CFAR integrates into the current processing architecture, and that it takes advantage of the existing data streams. The EP constructs a map of the surveillance volume segmented into cells 4 miles in range by 5.6 degrees in azimuth. Each cell goes through a two-level classification. The course classification determines whether it is land, sea or clear and this categorization is used to invoke subsequent processing modes (e.g. MTI, surface surveillance, bypass). A finer classification estimates potential detection densities, providing input for detection threshold control and multi-scan processing which produces target reports. The ES-CFAR performance would be enhanced by taking advantage of this volume segmentation and environmental characterization, improving

performance over the difficult littoral zones even above that already demonstrated in this paper for the E-3. Introduction of the ES-CFAR as a P3I to the E-2C has the potential to provide dramatic target detection, tracking and false alarm control improvements with manageable (limited scope, low-cost and at low risk) impact on the existing system.

Modern Electronic Warfare (EW) techniques heavily rely upon the ability to deny information to an enemy radar or to deceive the enemy radar by generating false target returns in range, angle or Doppler. The development of modern sensors for Command, Control, Communications and Intelligence (C3I) incorporating advanced Electronic Counter-Counter Measures (ECCM) for robust survivable performance in an EW environment is governed by Department of Defense policy through DoD instruction 5000.2. Robust ECCM techniques are not tailor-designed to address the weaknesses of a particular ECM, but are intended to be effective against a large variety of ECM techniques. While maintaining this effectiveness in the presence of ECM, it is important that the ECCM technique not introduce large performance losses when operating in a non-ECM environment. Additionally, robust ECCM techniques should be nonperishable, remaining undetectable by the enemy, or, at least, not susceptible to additional countermeasures. Modern ECM techniques are designed to degrade the performance of various radar receiver and signal processor functions. For example, detection performance may be degraded in several ways as discussed below. In many cases, these ECM techniques are used to simply preclude detection by an enemy radar and in other cases they are used evasively to break an established track to that weapons cannot be fired accurately. ECM techniques generally take the form of either noise-like (denial) jammers or false target (deception) jammers. These offensive roles are routinely assigned to escort, self-screening and standoff jammers.

The noise-like jammers may be barrage noise, narrow band Doppler noise or responsive spot noise to name a few. These are usually used to defeat the commonly used CA-CFAR detector by generating a statistical discontinuity near the actual location of the target in range, angle or Doppler. This discontinuity causes the CA-CFAR algorithm to over-estimate the required threshold for detection and thus the true target goes undetected. This situation is very similar to clutter edge processing where conventional CA-CFAR performs poorly. The ES-CFAR Processor has been shown to significantly outperform a conventional Baseline CA-CFAR processor in these situations by recognizing this discontinuity and processing the data accordingly. As such, it is logical to conclude that similar benefits could be derived for purposes of Electronic Counter-Counter Measures in a modern radar system via ES-CFAR processing.

Similarly, false target jammers may fall into such categories as false range or Doppler targets, range or velocity gate pull-off or cover pulse. These techniques are commonly used to generate a false target in range or Doppler near the true target location and at a significantly higher Signal-to-Noise ratio (SNR) than the true target. The conventional CA-CFAR will perform poorly in this situation because the larger false target serves to mask the true target signal by elevating the detection threshold so that the smaller true target signal goes undetected. Once this deception has occurred successfully, the false target signal may be moved in range or Doppler so that the range or velocity gate generated by the victim radar is moved from the true location of the target. It is in this way the ECM techniques are used to break a radar track. The ES-CFAR Processor has demonstrated dramatic performance improvements in multiple interfering target scenarios. Because of the similarity of multiple interfering target scenarios to false target jammers, ES-CFAR may provide modern radar systems with added resilience to this type of ECM.

The ES-CFAR Processor has not been evaluated using ECM contaminated data, but the argument given in the previous paragraphs suggests that ECCM improvements are likely to be obtained. By appropriate CFAR algorithm and parameter selection as is currently done in the ES-CFAR Processor, a higher level of ECCM effectiveness is likely to be obtained against many ECM threats.

With the application of an expert system to radar signal processing, demonstrated performance gains have been made possible through the combined use of symbolic and numeric processing. By combining techniques to

assess the interference environment and select the most appropriate algorithms, improved detection probability and false alarm control have been demonstrated in regions of dynamically changing clutter. The next step is to integrate expert systems technology into adaptive space and time signal processing. Given the successful application to CFAR processing described above, effort should focus on applying these techniques to adaptive filtering, the process immediately preceding CFAR detection processing. Significant areas of impact are adaptive MTI filtering, adaptive Doppler processing, and joint adaptive space-time processing. These are means by which radar returns are processed to separate target energy from interference, thus transforming the detection problem from a sub-clutter visibility domain to a super-clutter visibility domain. These methods are powerful in their own right, but each suffers strengths and weaknesses. Combined with an assessment of the interference environment, this can be exploited to select the most appropriate space and time processing algorithm to extract target energy, in conjunction CFAR detection processing.

In an effort to achieve very high sub-clutter visibility, radar designers must strive to closely match the combined space an/or time filtering method and CFAR detection processing technique to the characteristics of the target and interference environment. The characteristics of both the target and the interference have a major impact on parameters such as required degrees of freedom, coherent dwell time, and average sidelobe level. For example, improved adaptive filter performance in a non-homogeneous clutter environment may be achieved through the application of a variety of numerical techniques for secondary data analysis, providing for the formulation of more accurate covariance matrix estimates. Alternatively, an automatic technique for the selection of the most appropriate window function, to be applied to the measurement data prior to non-adaptive filtering, will significantly improve performance in less severe interference environments. An expert system radar signal processor will be developed that implements a library of algorithms for adaptive and non-adaptive angle-Doppler filtering (including secondary data selection) and false alarm control, which are intelligently selected based upon an assessment of the clutter and jammer environment.

Although a large amount of research and development of adaptive processing has been documented in the past two decades, its application to airborne Doppler processing faces the following two challenges. First, the severely non-homogeneous and non-stationary airborne clutter environment demands a very fast convergence rate or the adaptive processor may degrade the CFAR detector performance. A new adaptive Doppler processor called Doppler Domain Localized-Generalized Likelihood Ratio (DDL-GLR) has been developed which has a high potential to offer E-3A and E-2C systems a significant performance improvement. The DDL-GLR processor has a very fast convergence rate with an embedded robust CFAR, and it is computationally very efficient, realizable with an add-on parallel processor and compatible with the existing E-3A and E-2C Doppler processors. The environment assessment features of the ES-CFAR can effectively help the DDL-GLR for the selection of its Regions of Detection Improvement (RODI) as well as determine the right size of the training data set.

A prototype expert system CFAR Processor has been presented which applies artificial intelligence to CFAR detection processing. By assessing the radar interference environment and selecting the most appropriate CFAR algorithm for performing detection processing, a significant performance improvement can be obtained. Dramatic improvements in detection and false alarm probabilities over a conventional CA-CFAR baseline processor have been demonstrated using both simulated data and measurement data from the E-3A. The potential applicability of the ES-CFAR technology to the E-2C was also discussed as was its applicability as a more robust and effective ECCM technique.

While the invention has been described in its presently preferred embodiment it is understood that the words which have been used are words of description rather than words of limitation and that changes within the purview of the appended claims may be made without departing from the scope and spirit of the invention in its broader aspects.

What is claimed is:

1. An artificial intelligence system for suppressing false alarms in data of interest, and which comprises:
   a. Stored library of CFAR models; wherein said stored library of CFAR models comprises an electronic memory containing: a group of CFAR algorithms each with a set of varied parameters defining a set of cell averaging CFAR models (CA-CFAR); a set of greatest of CFAR models (GO-CFAR(); and a set of ordered statistic CFAR models (OS-CFAR);
   b. A sensor system which collects both said data of interest and environment data;
   c. A means for processing said environmental data from the sensor system to select a CFAR analysis model from said stored library of CFAR models; and
   d. A means for processing the data of interest from the sensor system with the CFAR analysis model to yield a set of CFAR processed data of interest in which false alarms are suppressed.
2. An artificial intelligence system, as defined in claim 1, wherein said sensor system comprises a host radar system which outputs radar return signals as said data of interest, and environmental information including atmostpheric transmittance as said environmental data.

2 Claims, 9 Drawing Sheets

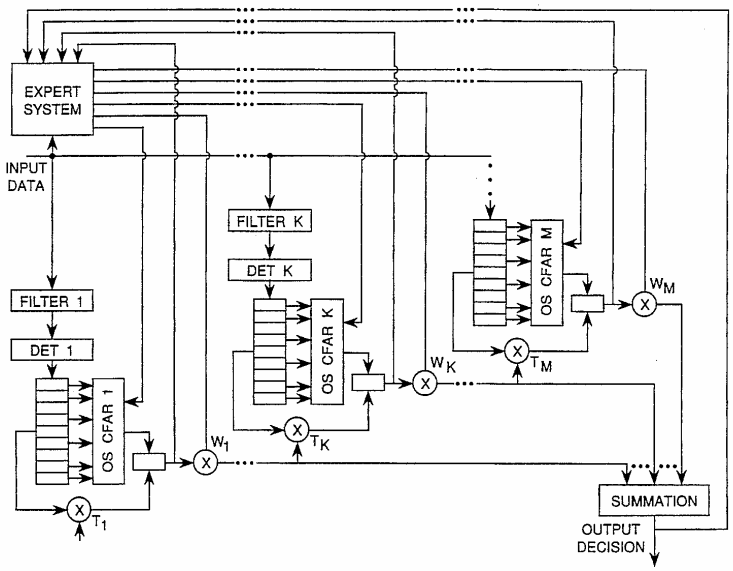

U.S. Patent Mar. 12, 1996 Sheet 1 of 9 5,499,030

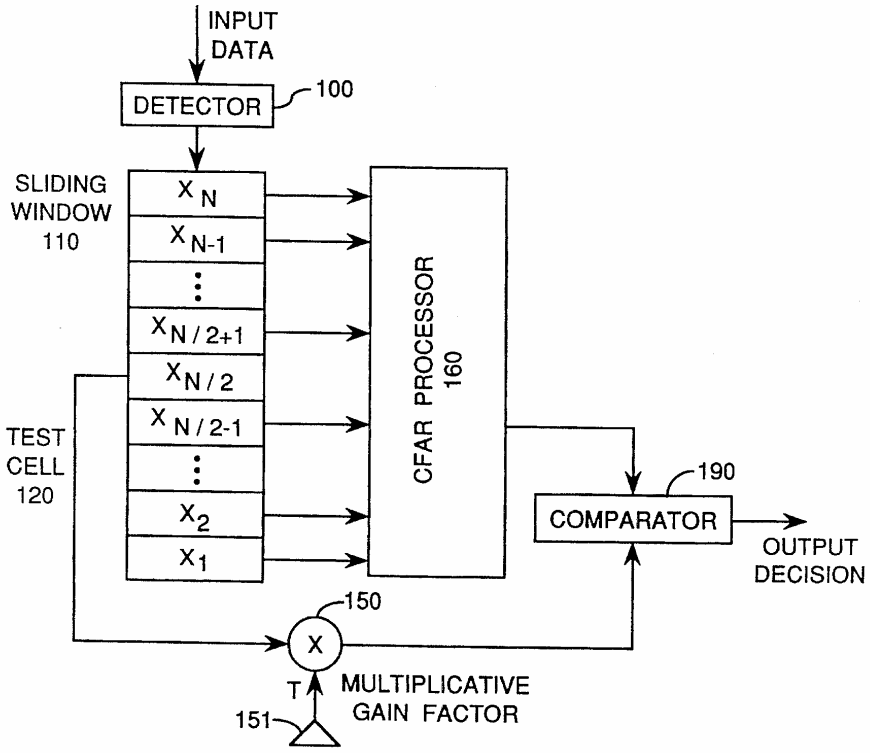

FIG. 1

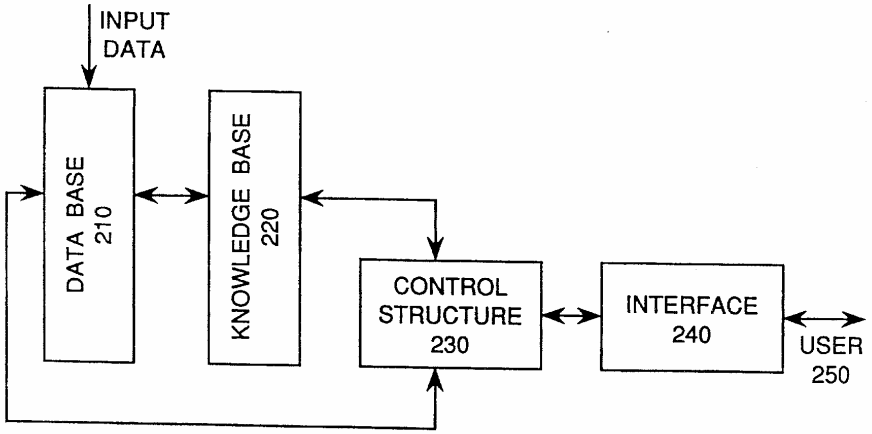

FIG. 2

U.S. Patent Mar. 12, 1996 Sheet 2 of 9 5,499,030

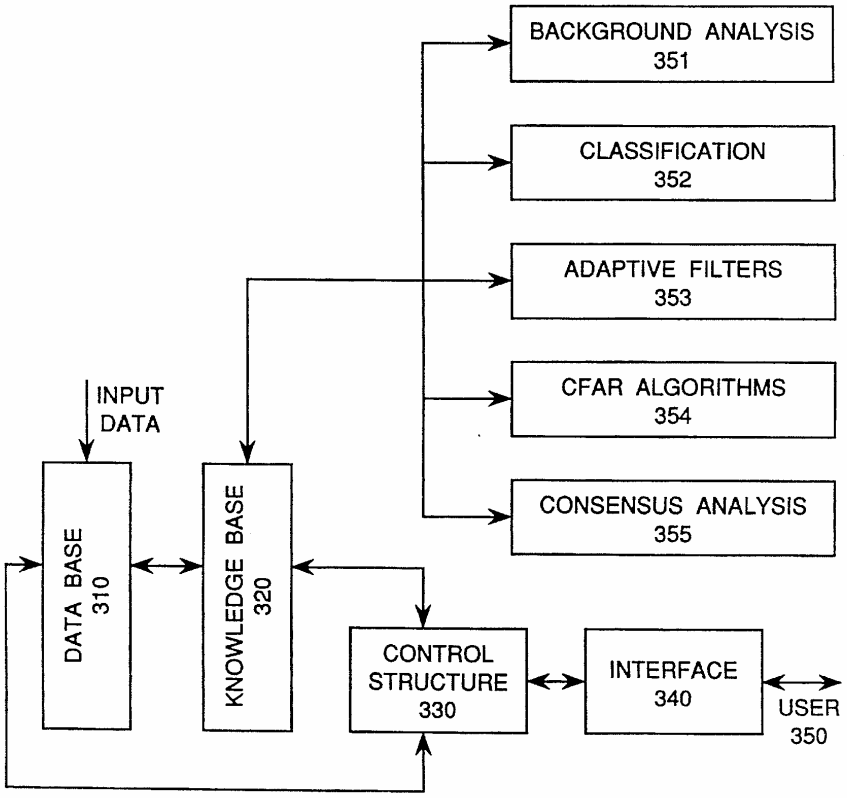

FIG. 3

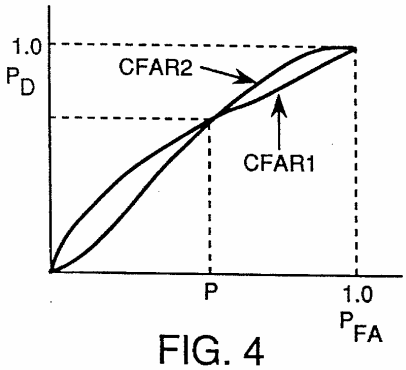

FIG. 4

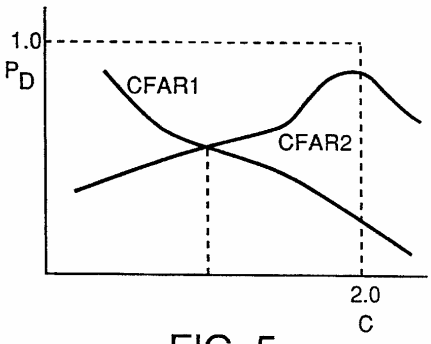

FIG. 5

U.S. Patent Mar. 12, 1996 Sheet 3 of 9 5,499,030

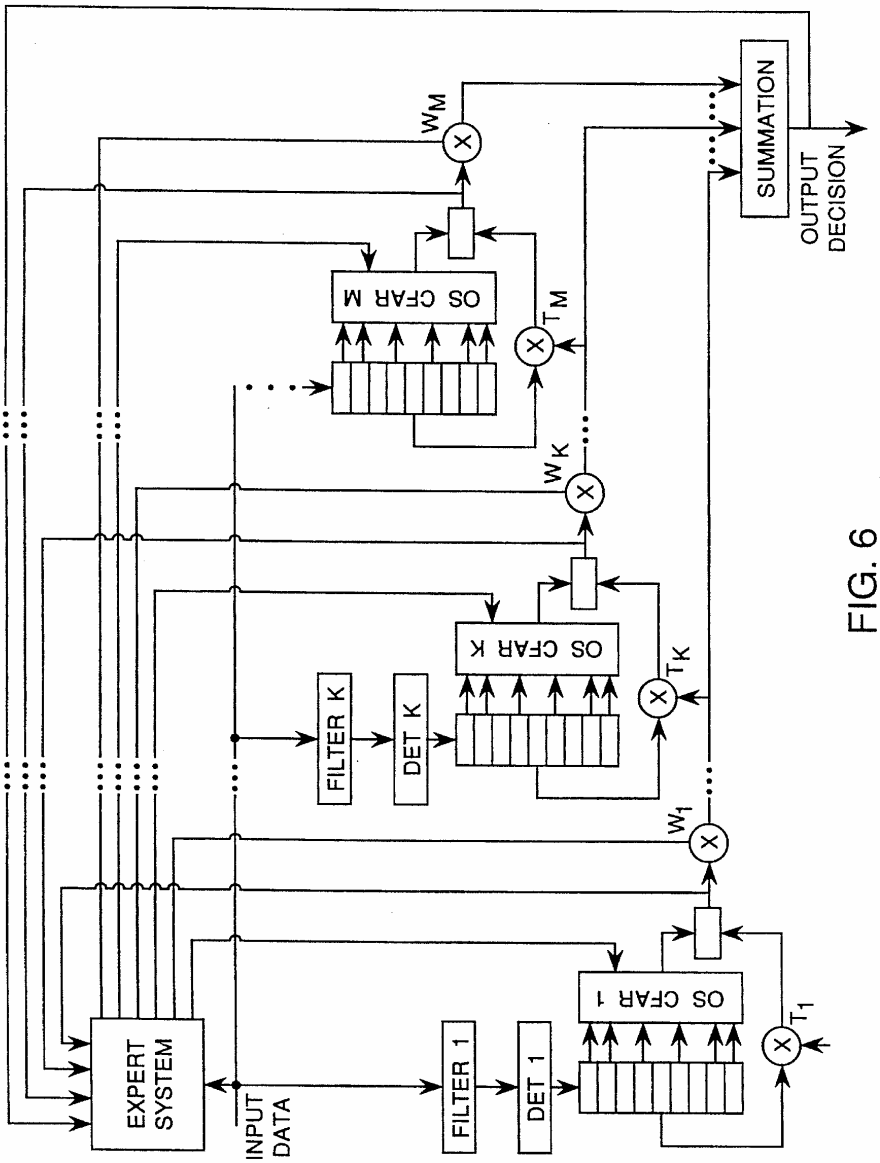

FIG. 6

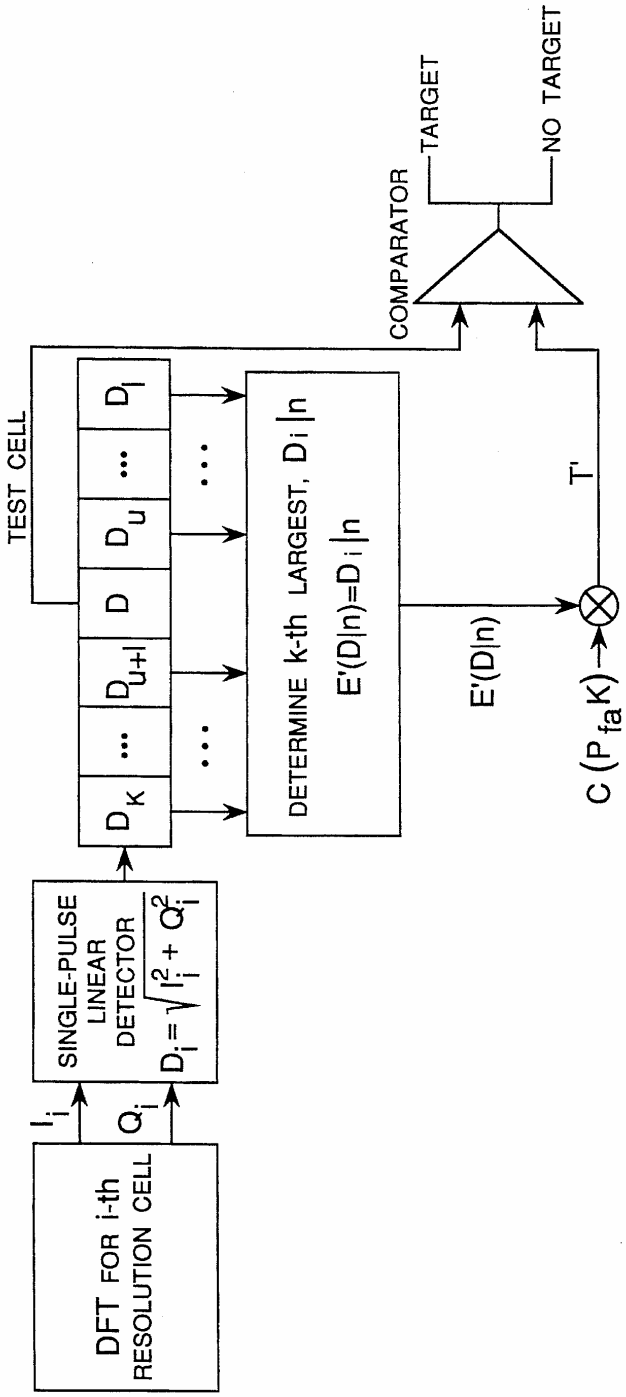
DFT FOR i-th RESOLUTION CELL
I_i
Q_i
SINGLE-PULSE LINEAR DETECTOR
$D_i = \sqrt{I_i^2 + Q_i^2}$
D_K
D_{u+1}
D
D_u
D_l
TEST CELL
DETERMINE k-th LARGEST, $D_i|n$
$E'(D|n)=D_i|n$
E'(D|n)
T'
$C(P_{fa}K)$
COMPARATOR
TARGET
NO TARGET

FIG. 7

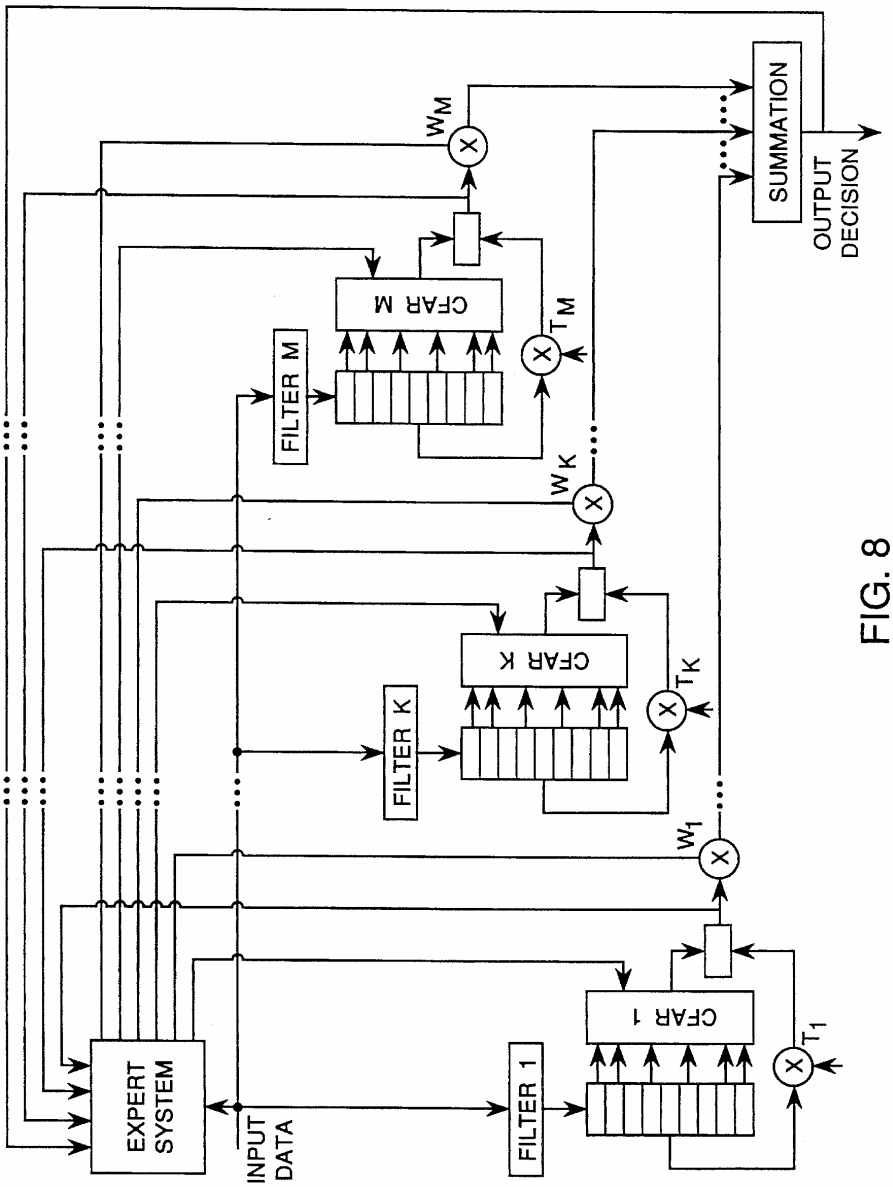
EXPERT SYSTEM
INPUT DATA
FILTER 1
FILTER K
FILTER M
CFAR 1
CFAR K
CFAR M
W_1
W_K
W_M
T_1
T_K
T_M
SUMMATION
OUTPUT DECISION

FIG. 8

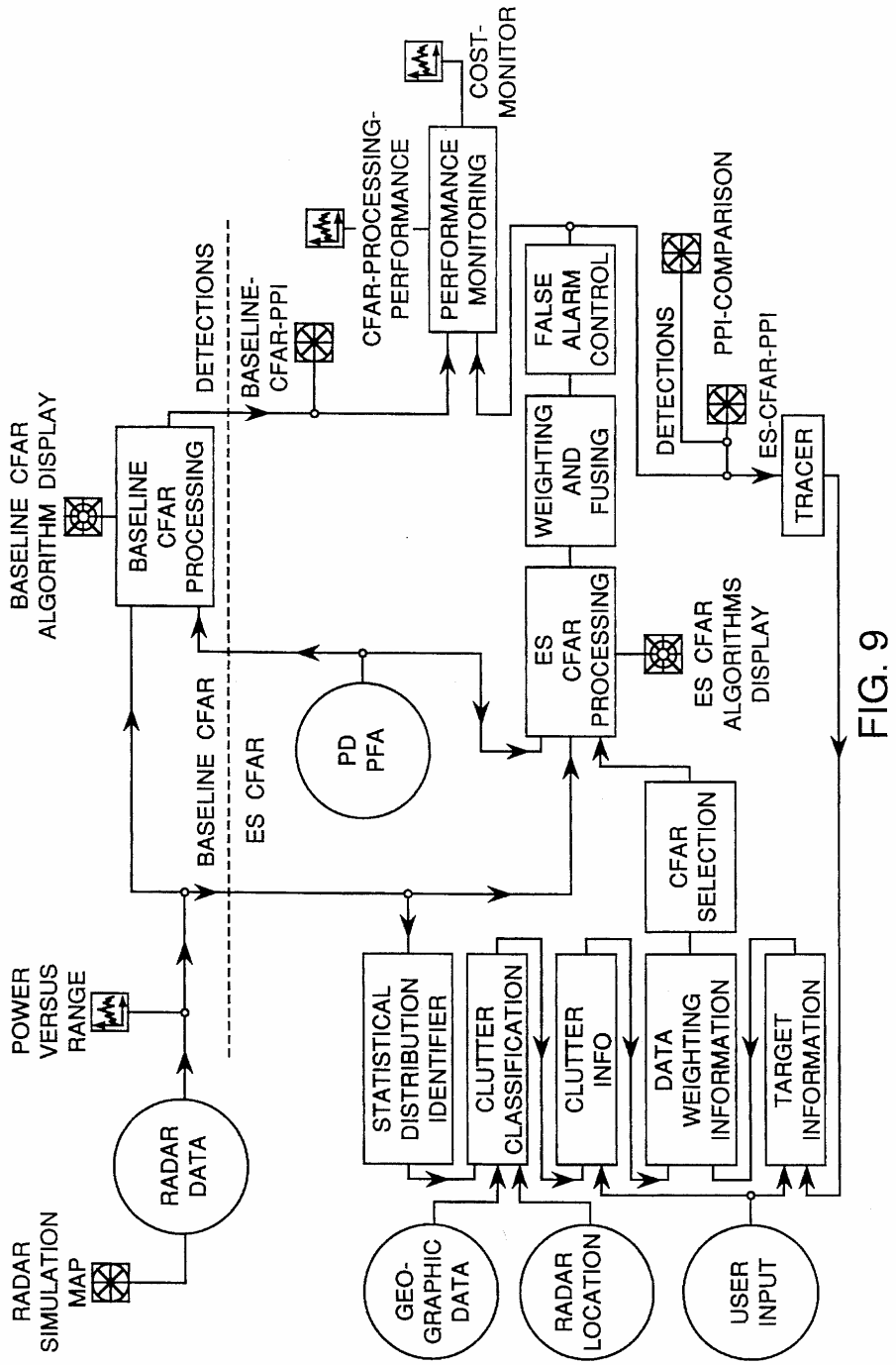
BASELINE CFAR ALGORITHM DISPLAY
BASELINE CFAR PROCESSING
DETECTIONS
BASELINE-CFAR-PPI
CFAR-PROCESSING-PERFORMANCE
PERFORMANCE MONITORING
COST-MONITOR
FALSE ALARM CONTROL
WEIGHTING AND FUSING
DETECTIONS
PPI-COMPARISON
ES-CFAR-PPI
TRACER
ES CFAR PROCESSING
ES CFAR ALGORITHMS DISPLAY
BASELINE CFAR
ES CFAR
PD
PFA
CFAR SELECTION
POWER VERSUS RANGE
STATISTICAL DISTRIBUTION IDENTIFIER
CLUTTER CLASSIFICATION
CLUTTER INFO
DATA WEIGHTING INFORMATION
TARGET INFORMATION
RADAR DATA
RADAR SIMULATION MAP
GEO-GRAPHIC DATA
RADAR LOCATION
USER INPUT

FIG. 9

U.S. Patent Mar. 12, 1996 Sheet 7 of 9 5,499,030

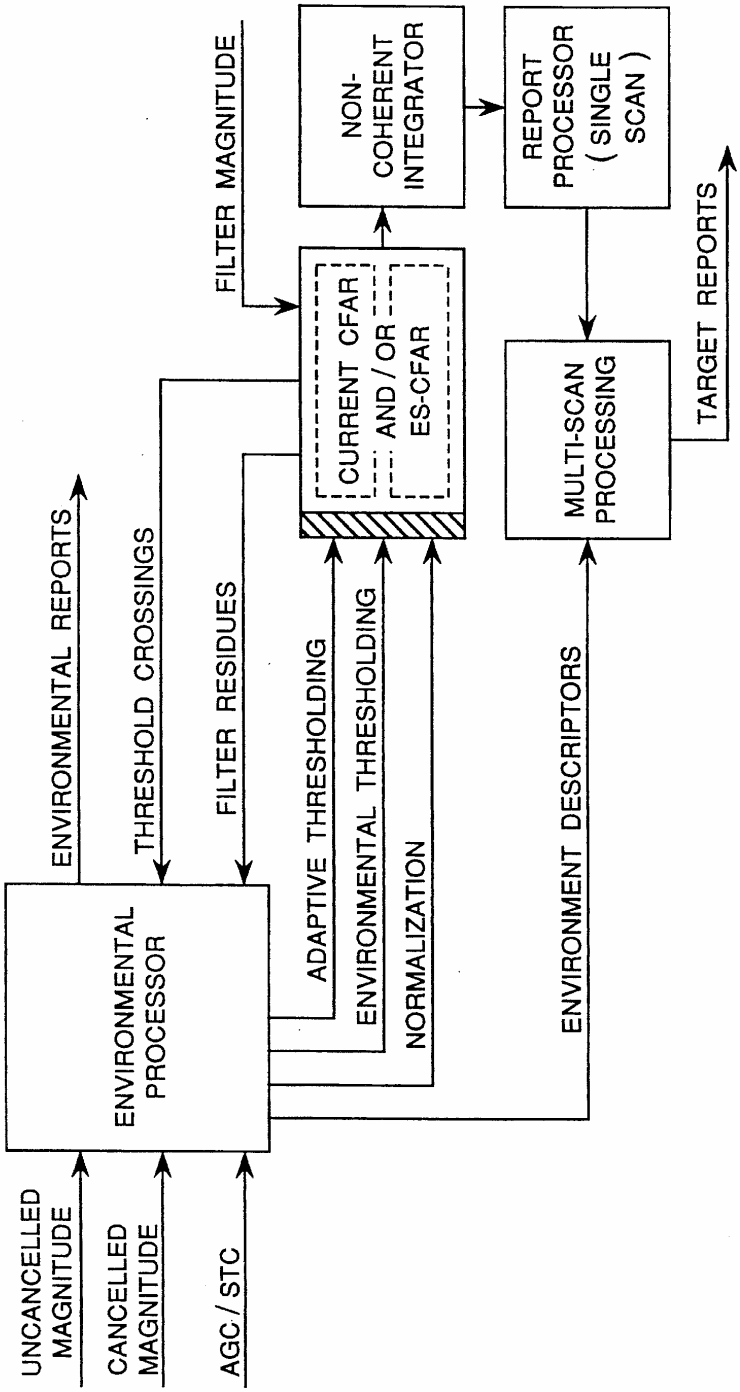

FIG. 10

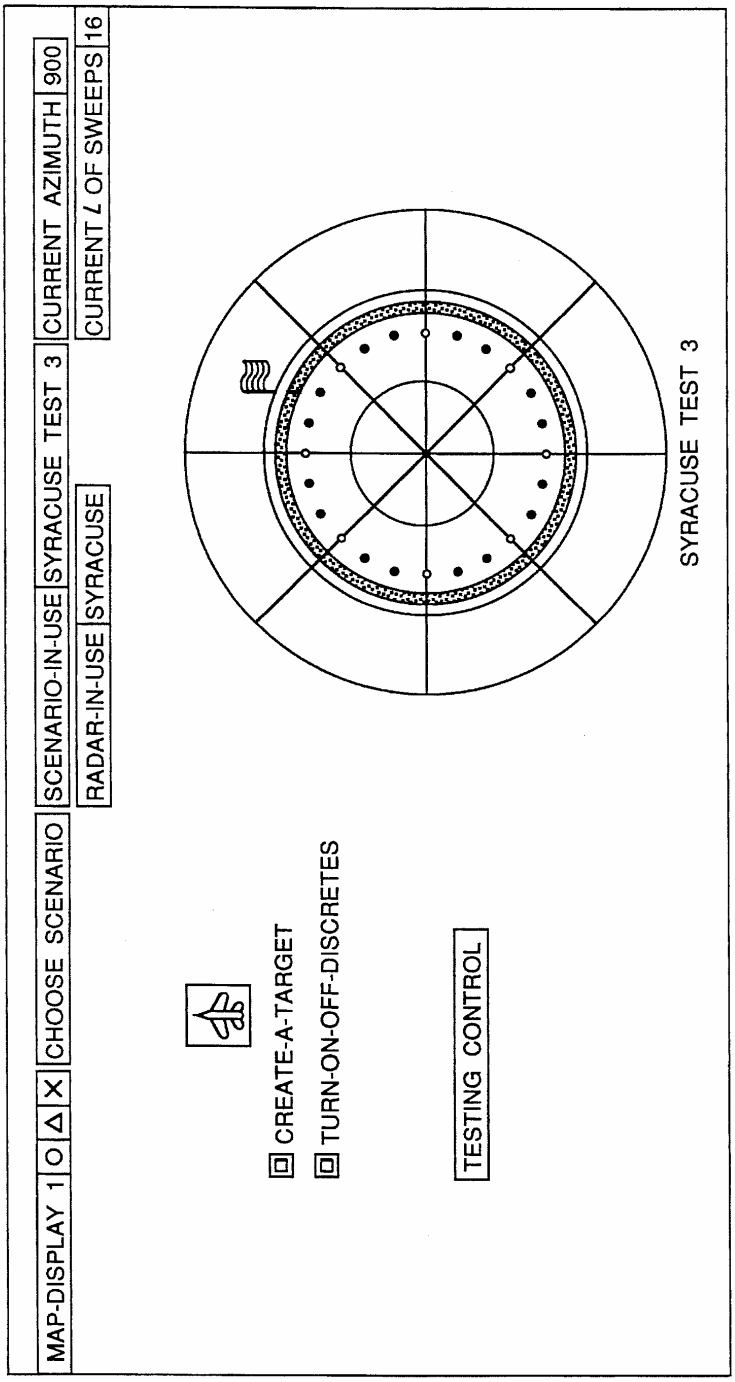
MAP-DISPLAY 1
O
Δ
X
CHOOSE SCENARIO
SCENARIO-IN-USE
SYRACUSE TEST 3
CURRENT AZIMUTH
900
RADAR-IN-USE
SYRACUSE
CURRENT L OF SWEEPS
16
CREATE-A-TARGET
TURN-ON-OFF-DISCRETES
TESTING CONTROL
SYRACUSE TEST 3

FIG. 11

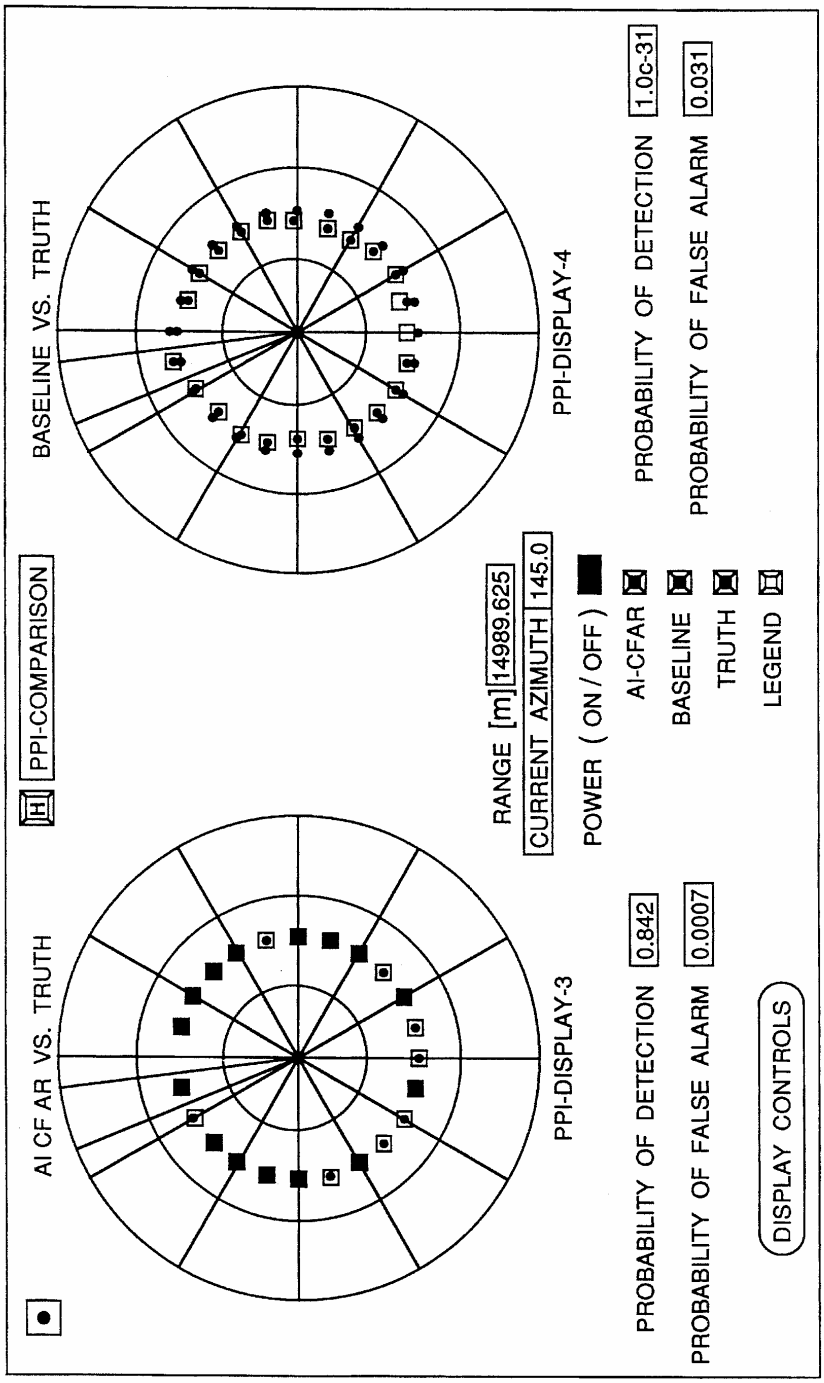
AI CF AR VS. TRUTH
PPI-COMPARISON
BASELINE VS. TRUTH
PPI-DISPLAY-3
PPI-DISPLAY-4
RANGE [m] 14989.625
CURRENT AZIMUTH 145.0
POWER (ON / OFF)
AI-CFAR
BASELINE
TRUTH
LEGEND
PROBABILITY OF DETECTION 0.842
PROBABILITY OF FALSE ALARM 0.0007
PROBABILITY OF DETECTION 1.0c-31
PROBABILITY OF FALSE ALARM 0.031
DISPLAY CONTROLS

FIG. 12

Knowledge-Based Control For Space Time Adaptive Processing

Michael C. Wicks, Ph.D.
Air Force Research Laboratory/Sensors Directorate
26 Electronic Parkway
Rome, NY 13441-4514
USA
Email: Michael.Wicks@rl.af.mil

The material contained in this report was condensed from AFRL-SN-RS-TR-2001-185 In-House Technical Report, September 2001, entitled "Knowledge-Base Application to Ground Moving Target Detection"

Paper presented at the RTO SET Lecture Series on "Knowledge-Based Radar Signal and Data Processing", held in Stockholm, Sweden, 3-4 November 2003; Rome, Italy, 6-7 November 2003; Budapest, Hungary, 10-11 November 2003; Madrid, Spain, 28-29 October 2004; Gdansk, Poland, 4-5 November 2004, and published in RTO-EN-SET-063.

Table of Contents

Acknowledgements

Technical contributors to this report include: R. Adve, P. Antonik, W. Baldygo, C. Capraro, G. Capraro, T. Hale, R. Schneible, and M. Wicks. Typing and Graphics Support was provided by P. Woodard

Executive Summary

The major impact of the research reported herein is the development of an adaptive algorithm that specifically addresses the rejection of discretes in the cell under test competing with all targets; and the rejection of distributed clutter competing with slow moving targets. Discretes can include large fixed clutter returns and multiple moving objects in the sidelobes.

This report discusses the development of space-time adaptive processing (STAP) technology for ground moving target indication (GMTI) applications. Current GMTI systems, e.g. the E-8 Joint STARS, use non-adaptive displaced phase center antenna (DPCA) techniques. The Joint STARS platform has been very successful in certain deployments, such as the Gulf War. So the question naturally arises, why is STAP needed for GMTI?

In theory, DPCA can outperform some (suboptimal) STAP implementations. DPCA may also perform better in highly non-homogeneous environments, where sufficient training data for adaptive systems is not available. However, when hardware and system errors are considered, the performance of DPCA degrades rapidly. For example, phase, and amplitude errors between channels impose a fundamental limit on non-adaptive DPCA processing. Adaptive processing is several orders of magnitude less sensitive to receiver channel errors.

STAP has demonstrated much better clutter rejection than DPCA for high velocity targets. This is because an adaptive null placed in the sidelobe region by STAP is significantly lower than the error sidelobes that limit DPCA performance. On the other hand, DPCA has traditionally provided better performance in the low velocity region, which corresponds to the main beam clutter. The objective of this research is to extend the advantages of STAP in the high velocity region to lower velocity targets. This requires some fundamental re-design of the STAP process. Merely executing the current suite of STAP algorithms in the low-velocity region is inadequate.

This report summarizes past, present and proposed future STAP research. The theme of this research has been to move from AMTI STAP theory to GMTI STAP for real systems. STAP algorithms were developed under several simplifying assumptions. The adaptive weights are determined statistically, based on an estimated interference covariance matrix. This estimation requires a large number of homogeneous data samples, i.e. sample support. In the real world, the received data is non-homogeneous, and the required sample support is not available. Special techniques must be developed to counter spatially non-homogeneous interference. In addition, STAP techniques ignore array electromagnetic effects. This issue is of importance in applying STAP to real arrays.

The research presented here has addressed the issues of sample support and array effects. The sample support required is directly proportional to the number of adaptive weights to be determined. This report presents two algorithms, $\Sigma\Delta$ STAP and Joint Domain Localized (JDL) Processing, that yield excellent interference suppression with a limited number of unknowns. Array effects are addressed for the JDL algorithm through the use of spatial steering vectors that account for array mutual coupling. Using measured data, the examples present significant performance improvements by accounting for array effects. For non-homogeneous scenarios, we present an alternative Direct Data Domain (D^3) processing approach. D^3 algorithms do not estimate a covariance matrix and provide effective suppression of discrete interference. D^3 algorithms do not provide as effective suppression of spatially correlated interference as compared to covariance matrix based techniques.

In non-homogeneous interference, researchers have used a non-homogeneity detector (NHD) to identify the non-homogeneous regions of the radar scene. The radar data cube is divided into homogeneous and non-

homogeneous range cells. Traditional STAP may be applied within the homogeneous cells, though only using homogeneous cells for sample support. However, by definition of statistical algorithms, traditional STAP cannot suppress the non-homogeneous component of interference. This report presents the hybrid algorithm, a combination of D^3 processing and JDL with the benefits of both. The hybrid algorithm provides effective suppression of both discrete and spatially correlated interference. This algorithm is a significant achievement because it (1) rejects discrete clutter in the test cell against which covariance matrix approaches are totally ineffective and (2) outperforms the D^3 by 30dB against distributed mainlobe clutter. This performance combination is unique in STAP.

The sum total of thirty years of research into STAP is that no single algorithm is optimal in all interference scenarios. Our ongoing research moves towards the Knowledge Based STAP (KB-STAP) concept where the adaptive algorithm and its associated training is chosen "intelligently" to best detect weak and slow moving targets. Here we present the use of terrain maps to determine the sample support for the adaptive process. The use of maps allows the adaptive process to choose the best representative sample support to estimate the clutter covariance matrix. This approach is a first step to the development of practical KB-STAP.

1.0 Introduction: Why STAP for GMTI?

Airborne surveillance radar systems operate in a severe and dynamic interference environment. The interference is a sum of clutter, other moving objects, possible deliberate electronic counter measures (ECM) and noise. The ability to detect weak airborne and ground targets requires the suppression of interference in real time. Space-Time Adaptive Processing (STAP) techniques promise to be the best means to suppress such interference.

The processing technique presently employed for GMTI systems is displaced phase center antenna (DPCA). In DPCA the Doppler spectrum of the sidelobe clutter is folded into the mainlobe and centered at zero Doppler, thus minimizing the spread induced by platform motion. Theoretically, in benign interference environments, this technique can outperform advanced adaptive techniques (Figure 1) [1].

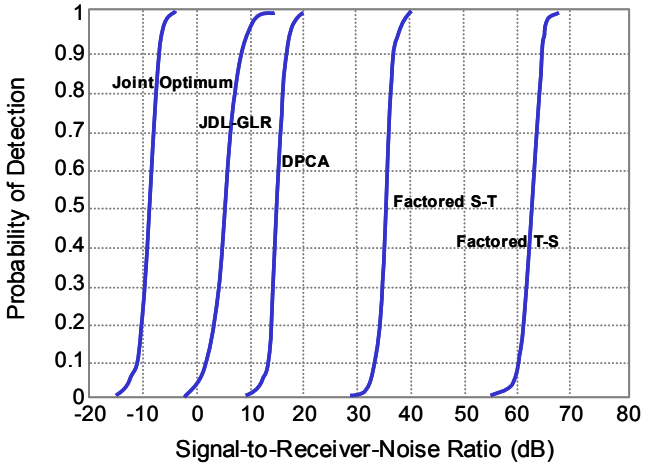

Figure 1: Performance Comparison of Airborne Array Radar Signal Processing Techniques

In practice, however, there are several factors that limit the performance of DPCA. System errors, such as the channel-to-channel mismatch, are the prime limiting factor. In addition, DPCA processing is heavily dependent on an assumed relationship between platform velocity and the radar PRI. Deviation from this relationship leads to severely degraded performance (Figure 2). Furthermore, at any time only a fraction of the array channels is used, i.e. DPCA uses the antenna aperture inefficiently.

In contrast to DPCA, STAP uses the multiple channel receive data vector to determine where to place nulls: spatial nulls for point interference, such as jammers and space-time nulls for extended interference, such as clutter. STAP is therefore effective against all forms of interference, both unintentional and intentional ECM. Furthermore, STAP is much less sensitive (by orders of magnitude) to receiver channel errors.

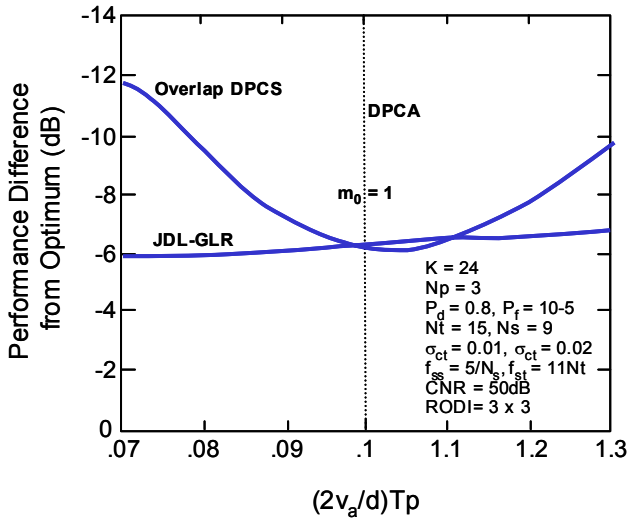

Figure 2: Performance Loss Due to the Velocity-PRI Constraint on Target Detection

For an accurate comparison between processing approaches, hardware errors of actual radars must be considered. Phase and amplitude errors in the multiple channels of the DPCA system impose a basic limit on non-adaptive DPCA processing. On the other hand, STAP is limited by channel mismatch across bandwidth and by processor hardware effects, such as quantization. Traditionally, STAP has been applied to the AMTI mission wherein the high velocity airborne targets are offset from mainbeam clutter in Doppler. For high velocity targets, STAP has demonstrated much better interference rejection than can be obtained with DPCA. This is because STAP can place an adaptive null in the sidelobe region that is significantly lower than the error sidelobes that limit DPCA. The location, depth and width of the null can be determined adaptively based on the interference to be suppressed.

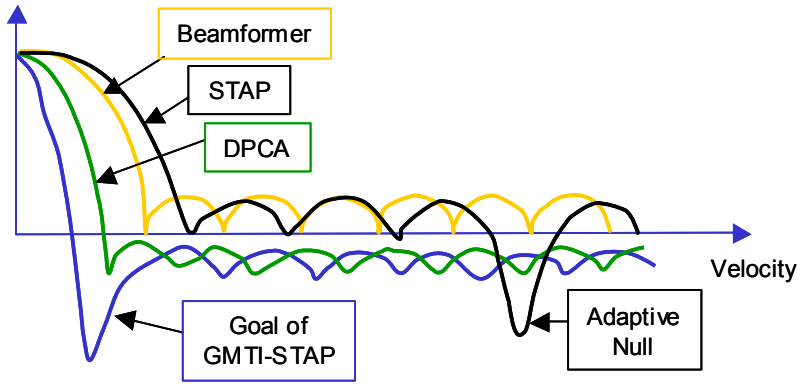

Figure 3: GMTI-STAP Goal

Extensive research into STAP for the AMTI mission, i.e. high radial velocity targets competing with clutter from the antenna sidelobes, has proven its superiority over current non-adaptive processing techniques. Looking to the future, the advantages of STAP for the AMTI mission needs to be extended to the GMTI mission, i.e. slow targets competing with clutter from the antenna mainlobe (Figure 3). This report discusses the approach and progress in that area.

The theme of this report is to present the transition of space-time adaptive processing from AMTI as developed in theory to GMTI in practice. This report presents past, on-going and proposed research to support this transition to practical *knowledge-based adaptive processing* for GMTI. Section 1.0 presents a review of STAP and the issues to be addressed to field STAP. In particular, Section 2.0 presents the concepts of reduced

degrees of freedom (DOF), array effects and non-homogeneous interference scenarios. Section 3.0 presents on-going work in STAP, including the new hybrid algorithm and MAP-STAP. These concepts are developed in support of the Knowledge-Based STAP concept (KB-STAP) as applied to the GMTI problem. Section 4.0 presents proposed research enhancing STAP for the GMTI mission. Both planned near-term activity and possible far-term efforts are discussed.

In this report, italicized letters denote scalars and integers, such as x and N, and lower case bold italic characters denote column vectors, e.g. $\boldsymbol{x}$. Upper case bold italic characters such as $\mathbf{R}$ denote matrices, while subscripts to bold characters represent the entries in the vector or matrix, such as $\mathbf{R}_{nm}$. A superscript ^{T} denotes the transpose and the superscript ^{H} denotes the Hermitian transpose of a vector or matrix.

2.0 Background

The goal of adaptive processing is to weight the received space-time data vectors to maximize the output signal-to-interference plus noise ratio (SINR). Traditionally, the weights are determined based on an estimated covariance matrix of the interference. The weights maximize the gain in the look direction, while placing pattern nulls in the interference directions. This interference plus noise is a combination of clutter, ECM and thermal noise.

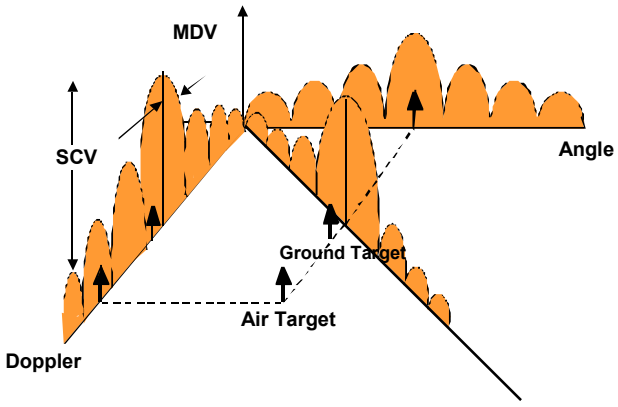

Figure 4 : Angle-Doppler Structure of Clutter

In airborne or space radar, the clutter in a given range cell has a structure determined by the motion of the aircraft platform (Figure 4). The slope of the clutter ridge in angle-Doppler space is determined by the speed of the aircraft. In the AMTI case, the threat target is widely spaced from mainlobe clutter in the Doppler domain and it is possible to use Doppler processing to separate targets from clutter. The limitation on target detection is determined by the sub-clutter visibility (SCV). In the GMTI case, the problem is more difficult since the target is close to the mainbeam clutter in Doppler. Placing a null on mainbeam clutter reduces the gain on target and hence detection performance. The goal of GMTI is to reduce the minimum detectable velocity (MDV), the lowest velocity where a target can be separated from clutter.

Traditionally, the fully adaptive (and optimal) STAP procedure determines the adaptive weights using an estimated covariance matrix, as given by Eqn. (1).

$$\mathbf{w} = \hat{\mathbf{R}}^{-1}\mathbf{s}. \tag{1}$$

In the equation, s sets the "look direction", the direction in angle and Doppler being tested for the presence of a target. Note that s sets the look direction only, while the actual target may be at a different angle-Doppler point close to the look direction. The covariance matrix, R, is estimated by averaging over *secondary data* chosen from range cells close to the range cell of interest (the primary range cell) as given by Eqn. (2) and illustrated in Figure 5.

$$\hat{\mathbf{R}} = \frac{1}{K}\sum_{k=1}^{K} \mathbf{x}_k \mathbf{x}_k^H . \qquad (2)$$

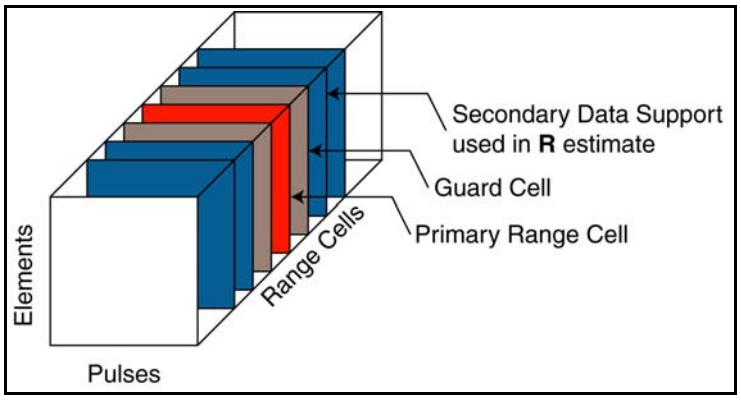

Figure 5 : Estimating the space-time interference covariance matrix

Equations (1) and (2) illustrate the two main difficulties in applying the fully adaptive procedure: the number of degrees of freedom and the assumption of homogeneous data. Underlying several STAP approaches is a third problem, ignoring array effects.

***Computation Load*:** In Eqn. (1) the number of unknowns and size of the covariance matrix directly determines the degrees of freedom. The total computation load rises as the third power of the number of unknowns. Choosing this parameter is therefore crucial to a practical implementation of STAP. In the fully adaptive approach, the number of unknowns is the number of antenna subarrays (N) times the number of pulses (M) in the datacube. The algorithm estimates the NM dimensional covariance matrix of the interference. In practice, an accurate estimate requires about $2NM$ to $3NM$ independent and identically distributed (i.i.d.) secondary data samples [2]. This number is very large making it impossible to evaluate the covariance matrix and the adaptive weights in a reasonable computation time. The goal of STAP research has therefore been to reduce the number of adaptive unknowns, while retaining performance.

Homogeneous Data:

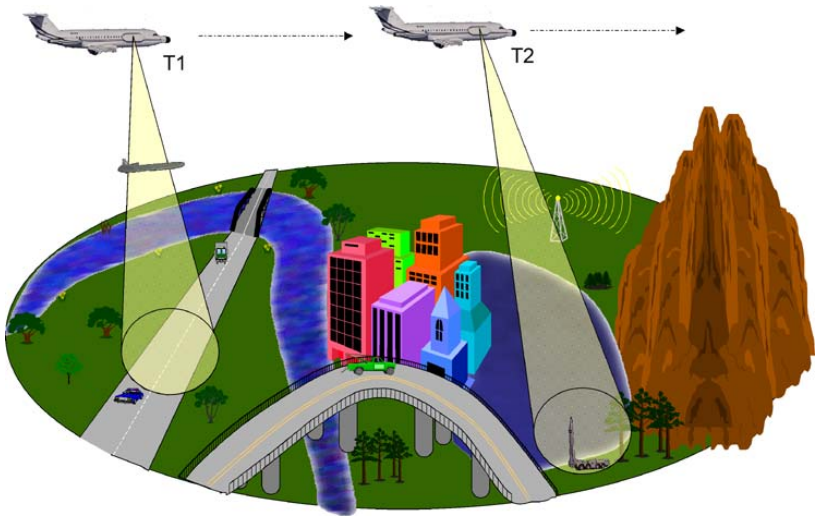

Figure 6: Clutter Non-Homogeneity

Equation (2) estimates the covariance matrix using K secondary data vectors from range bins close to the range cell of interest. The inherent assumption is that the statistics of the interference in the secondary data is the same as that within the primary range cell, i.e. the data is assumed homogeneous. K must be greater than twice the number of unknowns, between $2NM$ and $3NM$ in the fully adaptive case [2]. In practice, it is impossible to obtain a large number of i.i.d. homogeneous secondary data vectors. No clutter scene is perfectly homogeneous and most, if not all, land clutter is sufficiently non-homogeneous to impact performance. In addition, some regions are worse than others: urban clutter, land/sea interfaces (Figure 6). This leads to severely degraded performance.

***Array effects*:** Traditionally STAP algorithms were developed for proof-of-concept, assuming the receiving antenna array is a linear array of isotropic point sensors. In practice, such an array is not feasible and the elements must be of some physical size. This implies that the array not only receives, but also scatters the incident fields, leading to mutual coupling between elements. Additionally, near field scattering off the aircraft body has a significant impact on how the array receives incident signals. Ignoring array effects leads to significantly degraded STAP performance.

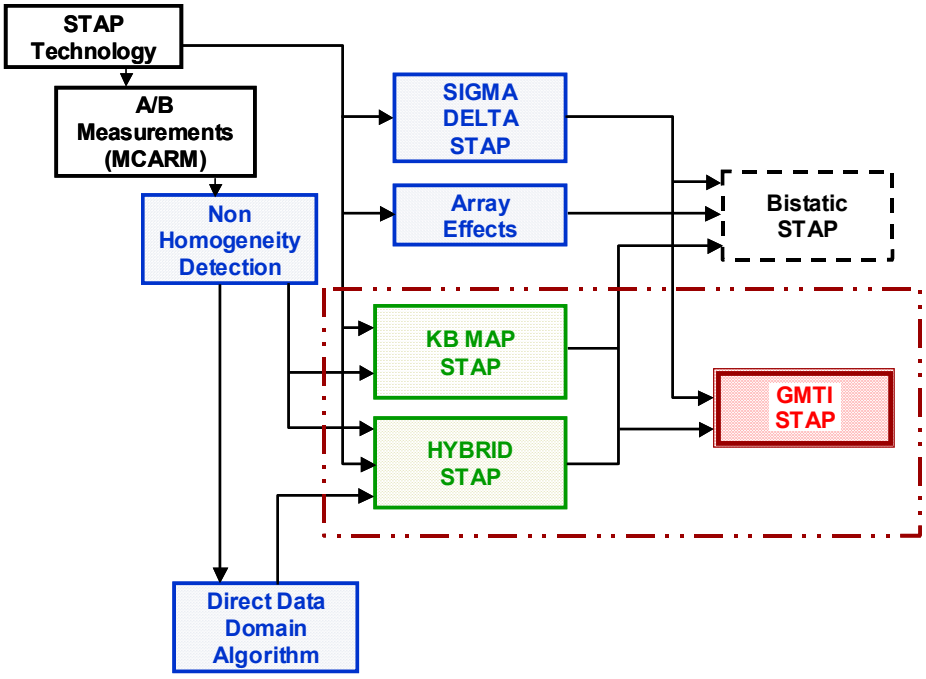

Figure 7: Past and Proposed STAP efforts

Past efforts in STAP have addressed these concerns to enable the transition from theory to practice. Current efforts address the concerns listed in this section while extending STAP to mainbeam clutter rejection and the GMTI problem. In addition, AFRL's expertise is also being extended from monostatic radar to bistatic radar. This report summarizes our approach to addressing these issues for GMTI (Figure 7). The rest of section 2.0 summarizes the approaches developed to mitigate the impact of the above concerns. Section 2.1 presents ΣΔ-STAP and section 2.2 presents Joint Domain Localized (JDL) Processing as reduced rank (low DOF) alternatives to traditional fully adaptive STAP. Section 2.3 presents JDL processing while accounting for array effects, such as mutual coupling and near field scattering from the aircraft body. Section 2.4 presents a non-homogeneity detector to deal with non-homogeneous received data, while section 2.5 presents an alternative, non-statistical, approach to STAP developed specifically for the non-homogeneous data case.

The various techniques presented in this section represent past work in the transition from STAP theory to practice. They form a critical component of any future proposed adaptive surveillance system for GMTI.

2.1 Sigma-Delta STAP

Historically, ΣΔ-STAP was proposed to minimize the number of adaptive degrees of freedom, and consequently, the computation load. However a (possibly) more important property of ΣΔ-STAP is the use of only one sum (Σ) and one or more difference (Δ) beams. For STAP, a phased array with digitized channels is commonly viewed as necessary. Although significant progress is being made on the phased array front-end electronics, the employment of any STAP scheme with a large number of channels imposes its own set of performance requirements. This is particularly true in terms of channel matching. The high performance required of the electronics in these systems thus makes cost an important issue. ΣΔ-STAP addresses this issue of affordability, as well as concerns about the clutter non-homogeneity, channel-to-channel calibration, and response pattern effects [3].

ΣΔ-STAP is unique in that it can be retrofitted onto any antenna with analog sum and difference beams. Antenna engineers have excelled in the design of high performance sum and difference beams, whether for phased array or for reflector antennas [4]. This is particularly true in airborne radars where the sum and difference beams are already implemented for monopulse tracking and/or motion compensation.

In this section, we first present the ΣΔ-STAP principle and algorithms with multiple difference beams. We assume in this work that Wideband Noise Jammers (WNJs) have been suppressed before entering ΣΔ-STAP, by spatial-only processing (e.g., multiple sidelobe cancelers) incorporated with the sum beam and each difference beam [5]. We identify the advantages and limitations of this STAP approach.

2.1.1 ΣΔ-STAP Algorithm Development

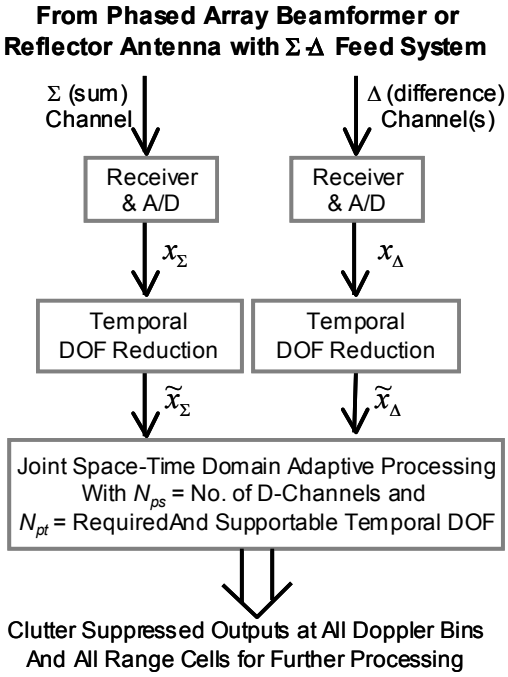

Figure 8: Block Diagram of General ΣΔ-STAP

Figure 8 illustrates the block diagram of general ΣΔ-STAP where the processor's spatial DOF is determined by N_{ps}, the number of Δ-beams. Much of this block diagram follows the general STAP configuration of [3]. The variations from the block diagram of Figure 8 depend only on the choices of the Δ-beams, the temporal DOF reduction approaches, and the joint-domain adaptive filtering-CFAR (constant false alarm rate) algorithms. The algorithm development also makes use of the fact that the Δ-beams have deep central nulls in the look direction.

Note that in the block diagram of Figure 8, the sum and difference channels are digitized as opposed to the individual elements themselves. ΣΔ-STAP treats these channels as equivalent spatial channels and applies adaptive processing to the digitized sum and difference channels. The temporal data from the Σ and Δ channels over the M pulses in a coherent pulse interval (CPI) can be transformed to the Doppler domain, resulting in further DOF reduction.

Let $\mathbf{x}_\Sigma$, a length M data vector, be the sum-channel data of a range cell before the temporal DOF reduction. Let $\mathbf{x}_\Delta$, be the length $N_{ps}M$ stacked delta-channel data, corresponding to N_{ps} Δ-beams, of the same range cell before temporal DOF reduction. If N_{pt} is the number of unknowns in the temporal domain after DOF reduction, the number of DOF is N_{pt}-1. The data after reduction can be expressed as

$$\tilde{\mathbf{x}}_\Sigma = \mathbf{Q}^H \mathbf{x}_\Sigma, \tag{3}$$

and

$$\tilde{\mathbf{x}}_\Delta = \left[\mathbf{I}(N_{ps}) \otimes \mathbf{Q}^H\right] \mathbf{x}_\Delta, \tag{4}$$

where Q is a matrix of order $M \times N_{pt}$ that represents the temporal DOF reduction and ⊗ represents the Kronecker product of two matrices. $\mathrm{I}(N_{ps})$ is the identity matrix of order N_{ps}. $\tilde{\mathbf{x}}_\Sigma$ is the post-reduction sum channel data of order $N_{pt} \times 1$ and $\tilde{\mathbf{x}}_\Delta$ is the post-reduction difference channel data of order $N_{pt}\, N_{ps} \times 1$. The tilde (~) above the data vectors represents the post-reduction data.

Let $\mathbf{s}_t$, $M \times 1$, be the temporal steering vector of a chosen Doppler bin and denote

$$\tilde{\mathbf{s}} = \mathbf{Q}^H \mathbf{s}_t \tag{5}$$

to be the post-reduction temporal steering vector. Denote the stacked data vector

$$\tilde{\tilde{\mathbf{x}}} = \begin{bmatrix} \tilde{\tilde{\mathbf{x}}}_\Sigma \\ \tilde{\tilde{\mathbf{x}}}_\Delta \end{bmatrix}, \tag{6}$$

Note that $\tilde{\tilde{\mathbf{x}}}$ simply represents the sum and difference channels after temporal DOF reduction stacked into a convenient form. The "maximum likelihood" estimate of the correlation matrix can be written as

$$\hat{\mathbf{R}} = \begin{bmatrix} \hat{\mathbf{R}}_{\Sigma\Sigma} & \hat{\mathbf{R}}_{\Sigma\Delta} \\ \hat{\mathbf{R}}_{\Delta\Sigma} & \hat{\mathbf{R}}_{\Delta\Delta} \end{bmatrix}, \tag{7}$$

where

$$\hat{\mathbf{R}} = \frac{1}{K}\sum_{k=1}^{K} \tilde{\mathbf{x}}_k \tilde{\mathbf{x}}_k^H, \tag{8}$$

with $\tilde{\mathbf{x}}_k$, k=1,…K being secondary data samples from nearby range cells. The adaptive weights are then obtained from Eqn. (1) with the covariance matrix replaced by the estimate given in Eqn. (8). The steering vector is replaced by the post-reduction ΣΔ steering vector,

$$\tilde{\mathbf{s}} = \begin{bmatrix} \tilde{\mathbf{s}}_t \\ \mathbf{0} \end{bmatrix}, \tag{9}$$

A target at the primary range cell is declared if the modified sample matrix inversion (MSMI) statistic is above a chosen threshold (η_0).

$$\eta_{MSMI} = \frac{\left|\hat{\tilde{\mathbf{w}}}^H \tilde{\mathbf{x}}\right|^2}{\tilde{\mathbf{s}}^H \hat{\mathbf{R}}^{-1} \tilde{\mathbf{s}}} \underset{H_0}{\overset{H_1}{>}} \eta_0. \tag{10}$$

2.1.2 Numerical Example

As a numerical example, we compare the performance of ΣΔ-STAP with the factored approach (FA-STAP) and conventional non-adaptive pulse-Doppler (PD) processing. The array is comprised of 16 elements, with each CPI comprising 16 pulses. This example uses a single Δ-channel and temporal DOF reduction reduces the 16 pulses to 3 Doppler bins. As such, there are only 6 unknown weights to be determined: the sum and difference beams in space for 3 Doppler bins. The sum pattern is generated using 35dB Taylor weights and the difference pattern using 30dB Bayliss weights. Possible array errors are modeled as complex Gaussian multiplicative random variables at the element and beamformer level. This example uses a 2% magnitude, 2^o phase standard deviation at the element level and a 3% magnitude, 3^o phase standard deviation at the beamformer level. The clutter is modeled as Gaussian interference.

Figure 9 compares potential output SINR versus target Doppler for four cases, the fully adaptive case, ΣΔ-STAP, FA-STAP and traditional, non-adaptive, PD processing [6]. As can be seen, the performance of ΣΔ-STAP is significantly better than both FA-STAP and PD processing. Of special interest is the performance improvement at low Doppler frequencies, which correspond to low target velocities and consequently the GMTI case.

This example illustrates the significant gains associated with ΣΔ-STAP. Working with only a limited set of unknowns, ΣΔ-STAP yields better performance at low Doppler frequencies than algorithms with much higher unknowns (and computation loads). Furthermore, since only the sum and difference beams are used, the algorithm can be applied even if these beams are obtained using analog beamformers.

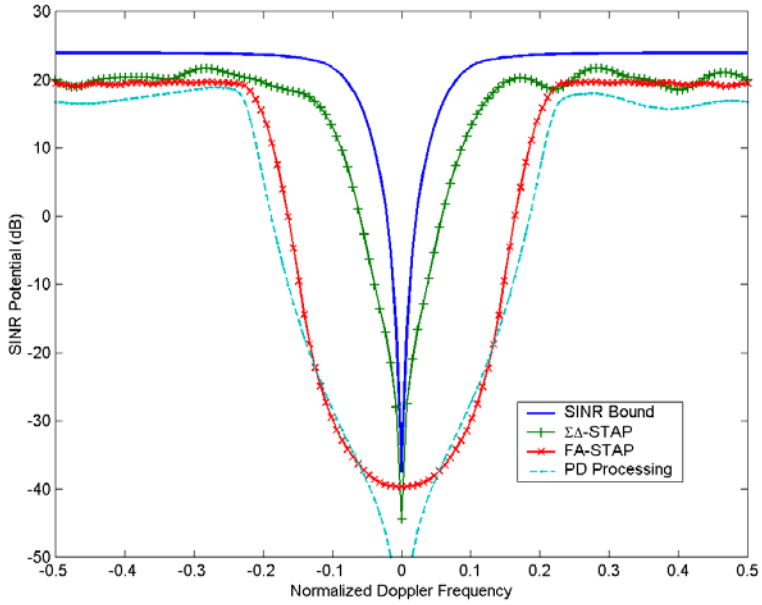

Figure 9: Performance of ΣΔ̃STAP compared to Pulse Doppler processing

2.1.3 Discussions: Advantages and Limitations

We summarize the advantages of the ΣΔ-STAP approach and its limitations. With as few as two spatial channels, Figure 9 shows that the ΣΔ-STAP approach can lead to clutter suppression performance potential higher than other STAP approaches that require many more unknowns and much higher secondary data support. The following includes its advantages (and some limitations) over other approaches:

***Applicability to Existing Systems*:** With other approaches, the application of STAP requires new hardware, from expensive phased arrays to multichannel receivers. In contrast to those approaches, therefore, ΣΔ-STAP can be applied to existing radar systems, both phased array and continuous aperture. It simply requires digitizing the monopulse difference channel, or making relatively minor antenna modifications to add such a channel. Such a relatively low cost add-on can significantly improve the clutter suppression performance of an *existing* airborne radar system.

***Data Efficiency*:** Correlation matrix estimation for ΣΔ-STAP can be performed with fewer than 20 data vectors. This feature provides good performance in severely non-homogeneous environments where many other STAP approaches may break down, regardless how high their performance potentials are with known clutter statistics.

***Channel Calibration*:** Channel calibration is a problem for many other STAP approaches. In order to minimize performance degradation, the channels with many other STAP approaches must be matched across the signal band, and steering vectors must be known to match the array. The difficulty and performance impact of channel calibration has often been underestimated. In contrast, ΣΔ-STAP uses as few as two channels to begin with and its corresponding signal (steering) vector remains of known and simple form as long as the central null of the Δ-beam is correctly placed. Therefore, ΣΔ-STAP greatly simplifies calibration issues in practice.

***Response Pattern*:** STAP has long been known to have hard-to-predict spatial response patterns that are often undesirable in some applications, e.g., very high sidelobe levels in some interference-free regions, loss of mainlobe gain, and significantly shifted mainlobe peak. With only two spatial channels and with the critical

null location of the Δ-beam, ΣΔ-STAP offers much more desirable and predictable response patterns than many other STAP approaches with excessive DOF.

***Computation Load*:** While the trend is toward more affordable computing hardware, STAP processing still imposes a considerable burden which increases sharply with the order of the adaptive processor and radar bandwidth. In this respect, ΣΔ-STAP reduces computational requirements in order N^3 adaptive problems. Moreover, the sparse steering vector can be exploited to further reduce numerical computations.

***Affordability*:** Affordability has long been an issue with STAP-based systems. Analog beamforming and minimization of the number of digitized receiver channels provides a substantial payoff in total system cost. Reliability is increased and maintenance costs are reduced by simplifying system interconnects. ΣΔ-STAP therefore greatly reduces system cost.

***Limitations*:** In the case of Doppler ambiguities, any system with only two (or few) channels will not meet the required DOF for clutter suppression. ΣΔ-STAP is not exceptional in this regard. Additionally, we have established the advantages of the presuppression of WNJs with the needed number of auxiliary channels [5], we do not view that the ΣΔ-STAP is limited to jammer-free applications. However, there is a need for additional hardware for operation in the presence of jammers.

In summary, ΣΔ-STAP is a very natural combination of the traditional antenna-design based approaches and "modern" signal processing based approaches, making the best use of the strengths of each and avoiding their weaknesses. The advantages of ΣΔ-STAP, especially applicability to existing radar systems, far outweigh the limitations of this adaptive processing method.

The next section presents another low computation load algorithm: Joint Domain Localized Processing.

2.2 Joint Domain Localized Processing in the Ideal Case

To overcome the drawbacks of the fully adaptive algorithm, researchers have limited the number of adaptive weights to reduce problems associated with sample support and computation expense. Wang and Cai [7] introduced the JDL algorithm, a post-Doppler, beamspace approach that adaptively processes the radar data after transformation to the angle-Doppler domain. Adaptive processing is restricted to a localized processing region (LPR) in the transform domain, significantly reducing the number of unknowns while retaining maximal gain against thermal noise. The reduced DOF leads to corresponding reductions in required sample support and computation load.

This section develops the JDL algorithm as applied to the case of an ideal array. Based on the assumption of a linear array of equispaced, isotropic, point sensors, the space-time data is transformed to the angle-Doppler domain using a two dimensional Fast Fourier Transform (FFT). Under certain restrictions, this approach is valid because the spatial and temporal steering vectors form Fourier coefficients [8, pp. 12-17]. In order to highlight the restrictions placed on the algorithm by the original formulation, this section clarifies the original development of Wang and Cai [7]. Section 2.3 extends the JDL algorithm to account for array effects and illustrates the performance of the JDL algorithm.

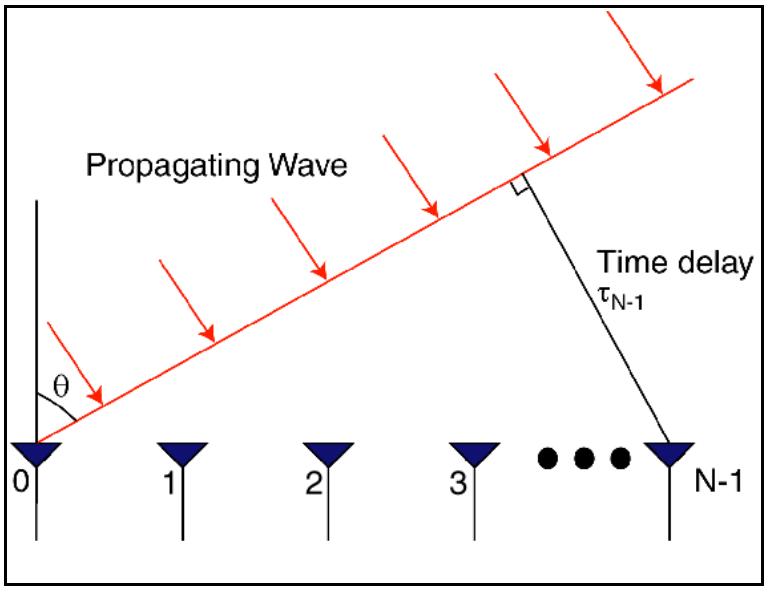

Figure 10: Linear Array of Point Sensors

Consider an equispaced linear array of N isotropic, point sensors as shown in Figure 10. Each sensor receives data samples corresponding to the M pulses in a CPI. Therefore, for each range bin, the received data is a length MN vector x whose entries numbered mN to $[(m + 1) N - 1]$ correspond to the returns at the N elements from pulse number m, where $m = 0, 1,\ldots M - 1$. The data vector is a sum of the contributions from the external interference sources, the thermal noise and possibly a target, i.e.

$$\mathbf{x} = \xi\,\mathbf{s}(\phi_t, f_t) + \mathbf{c} + \mathbf{n} \tag{11}$$

where c is the vector of interference sources, n is the thermal noise and ξ is the target amplitude, equal to zero in range cells without a target. The term $s(\phi_t f_t)$ is the space-time steering vector corresponding to a possible target at look angle ϕ_t and Doppler frequency f_t. The steering vector can be written in terms of a spatial steering vector $a(\phi_t)$ and a temporal steering vector $b(f_t)$ [8],

$$\mathbf{s}(\phi_t f_t) = \mathbf{b}(f_t) \otimes \mathbf{a}(\phi_t), \tag{12}$$

$$\mathbf{a}(\phi_t) = \left[1\; e^{j2\pi f_s}\; e^{j(2)2\pi f_s} \ldots e^{j(N-1)2\pi f_s}\right]^T, \tag{13}$$

$$\mathbf{b}(f_t) = \left[1\; e^{j2\pi f_t / f_R}\; e^{j(2)2\pi f_t / f_R} \ldots e^{j(M-1)2\pi f_t / f_R}\right]^T, \tag{14}$$

where f_s is the normalized spatial frequency given by $f_s = (d/\lambda)\sin\phi_t$, λ the wavelength of operation and f_R the pulse repetition frequency (PRF).

The spatial steering vector $a(\phi)$is the magnitude and phase taper at the N elements of the array due to a far field source at angle ϕ. Owing to electromagnetic reciprocity, to transmit in the direction of ϕ the elements of the array must be excited with the conjugates of the steering vector, i.e. the conjugates of the steering vector maximize the response in the direction ϕ. Transformation of spatial data to the angle domain at angle ϕ therefore requires an inner product with the corresponding spatial steering vector. Similarly, the temporal steering vector b (f) corresponding to a Doppler frequency f is the magnitude and phase taper measured at an

individual element for the M pulses in a CPI. An inner product with the corresponding temporal steering vector transforms time domain data to the Doppler domain. The angle-Doppler response of the data vector x at angle ϕ and Doppler f is therefore given by

$$\tilde{x}(\phi,f) = \left[\mathbf{b}(f) \otimes \mathbf{a}(\phi)\right]^H \mathbf{x}, \tag{15}$$

where the tilde (~) above the scalar x(ϕ,f) signifies the post-transform angle-Doppler domain. Choosing a set of spatial and temporal steering vectors generates a corresponding vector of angle-Doppler domain data.

Equations (12)-(14) show that for an ideal array the spatial and temporal steering vectors are identical to the Fourier coefficients. Based on this observation, the transformation to the angle-Doppler domain can be simplified under two conditions.

- If a set of angles are chosen such that (d/λ sin ϕ) is spaced by $1/N$ and a set of Doppler frequencies are chosen such that (f/f_R) is spaced by $1/M$, the transformation to the angle-Doppler domain is equivalent to the 2D.DFT.
- If the angle ϕ_t corresponds to one of these angles *and* the Doppler f corresponds to one of these Dopplers, the steering vector is a column of the 2-D DFT matrix and the angle-Doppler steering vector is localized to a single angle-Doppler bin (Figure 11).

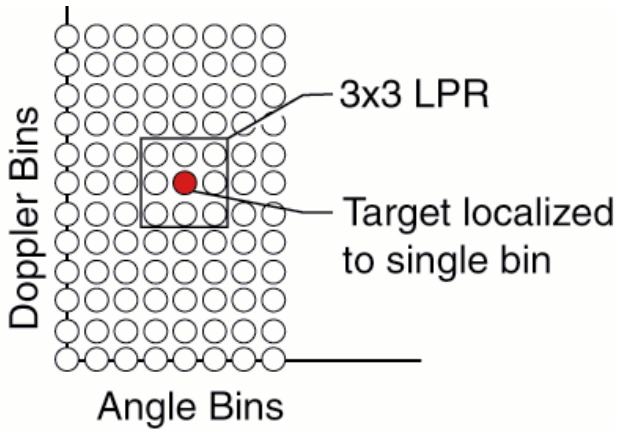

Figure 11: Localized Processing Regions in JDL for η_a - η_d = 3

The JDL algorithm as originally developed in [7] assumes both these conditions are met. This simplification is possible only in the case of the ideal, equispaced, linear array of Figure 10. Owing to beam mismatch, the localization to a single point in angle-Doppler space is only exact for the look steering vector.

As shown in Figure 11, a LPR centered about the look angle-Doppler point is formed and interference is suppressed in this angle-Doppler region only. The LPR covers η_a angle bins and η_d Doppler bins. The choice of η_a and η_d is independent of N and M, i.e. the localization of the target to a single angle-Doppler bin decouples the number of adaptive degrees of freedom from the size of the data cube, while retaining maximal gain against thermal noise. The covariance matrix corresponding to this LPR is estimated using secondary data from neighboring range cells. The adaptive weights are then calculated using Eqn. (1). The estimated covariance matrix $\hat{\mathbf{R}}$ is replaced with $\tilde{\mathbf{R}}$, the estimated *angle-Doppler* covariance matrix corresponding to the LPR of interest. The steering vector s is replaced with the angle-Doppler steering vector $\tilde{\mathbf{s}}$, i.e.

$$\tilde{\mathbf{w}} = \tilde{\mathbf{R}}^{-1}\tilde{\mathbf{s}}. \tag{16}$$

The number of adaptive unknowns is equal to $\eta_a\eta_d$. The steering vector for the adaptive process is the space-time steering vector $\mathbf{s}$ of Eqn. (12) transformed to the angle-Doppler domain. Under the two conditions listed above $\tilde{\mathbf{s}}$ is given by the length $\eta_a\eta_d$ vector

$$\tilde{\mathbf{s}} = [0,0,\ldots,0,1,0,\ldots 0,0]^T. \tag{17}$$

It must be emphasized that this simple form of the steering vector is valid only because the DFT is an orthogonal transformation. The space-time steering vector is transformed to angle-Doppler using the same transformation used for the data.

2.3 JDL Processing Accounting for Array Effects

Sections 2.1 and 2.2 presented two adaptive processing algorithms that address the issue of minimizing the number of adaptive unknowns while maintaining system performance. Reducing the number of unknowns leads to corresponding reductions in required sample support (to estimate the covariance matrix) and computation load (to obtain the adaptive weights). This section addresses a second major concern: the impact of mutual coupling between the elements of the array and the scattering off the aircraft body. The results in this section were published in [9].

When applying the JDL algorithm to measured data, a crucial assumption in the development of [7] is invalid. The elements of a real array cannot be point sensors. Owing to their physical size, the elements of the array are subject to mutual coupling. Furthermore, the assumption of a linear array is restrictive. A planar array allows for DOF in azimuth and elevation. Therefore the Fourier coefficients do not form the spatial steering vector and a DFT does not transform the spatial data to the angle domain. In this case, a DFT is mathematically feasible but has no physical meaning.

In a physical array, the spatial steering vectors must be measured or obtained using a numerical electromagnetic analysis. These steering vectors must be used to transform the space domain to the angle domain. This transformation is necessarily non-orthogonal with a corresponding spread of target information in the angle-Doppler domain. The assumptions listed in Section 2.2, therefore, cannot be met in practice. Earlier attempts to apply JDL to a real array ignored the non-orthogonal nature of the measured spatial transform [10].

This section replaces the DFT-based transformation described in Section 2.2 with a generalized transformation matrix. The key contribution of this new approach is the accounting for the array effects, thereby eliminating the two stipulations on the original JDL algorithm. This formulation can now be applied to physical arrays of arbitrary configuration. The modification results in significantly improved detection performance.

In the JDL algorithm, only data from within the LPR is used for the adaptation process. The transformation from the space-time domain to the angle-Doppler domain is an inner product with a space-time steering vector, an argument that holds true for ideal linear arrays and physical arrays. Mathematically therefore, the relevant transformation to within the LPR is a pre-multiplication with a ($NM \times \eta_a\eta_d$) transformation matrix. The transformation process is

$$\tilde{\mathbf{x}}_{LPR} = \mathbf{T}^H\mathbf{x}. \tag{18}$$

For example, for an LPR of 3 angle bins (ϕ_{-1}, ϕ_0, ϕ_1; η_a=3) and 3 Doppler bins (f_{-1}, f_0, f_1; η_d=3)

$$\mathbf{T} = \left[\mathbf{b}(f_{-1}) \otimes \mathbf{a}(\phi_{-1})\ \mathbf{b}(f_{-1}) \otimes \mathbf{a}(\phi_0)\ \ \mathbf{b}(f_{-1}) \otimes \mathbf{a}(\phi_1)\right.$$
$$\mathbf{b}(f_0) \otimes \mathbf{a}(\phi_{-1})\ \mathbf{b}(f_0) \otimes \mathbf{a}(\phi_0)\ \ \mathbf{b}(f_0) \otimes \mathbf{a}(\phi_1)$$
$$\left.\mathbf{b}(f_1) \otimes \mathbf{a}(\phi_{-1})\ \mathbf{b}(f_1) \otimes \mathbf{a}(\phi_0)\ \ \mathbf{b}(f_1) \otimes \mathbf{a}(\phi_1)\right], \tag{19}$$

$$= \left[\mathbf{b}(f_{-1})\ \ \mathbf{b}(f_0)\ \ \mathbf{b}(f_1)\right] \otimes \left[\mathbf{a}(\phi_{-1})\ \ \mathbf{a}(\phi_0)\ \ \mathbf{a}(\phi_1)\right].$$

In [7], to achieve the simple form of the angle-Doppler steering vector given by Eqn. (17), the use of a low sidelobe window to lower the transform sidelobes is discouraged. However, the use of such a window may be incorporated by modifying the transformation matrix of Eqn. (19). If a length N taper t_s is to be used in the spatial domain and a length of M taper t_t in the temporal domain, the transformation matrix is given by

$$\mathbf{T} = \left[\mathbf{t}_t \bullet \mathbf{b}(f_{-1})\ \ \mathbf{t}_t \bullet \mathbf{b}(f_0)\ \ \mathbf{t}_t \bullet \mathbf{b}(f_1)\right] \otimes$$
$$\left[\mathbf{t}_s \bullet \mathbf{a}(\phi_{-1})\ \ \mathbf{t}_s \bullet \mathbf{a}(\phi_0)\ \ \mathbf{t}_s \bullet \mathbf{a}(\phi_1)\right] \tag{20}$$

where $\bullet$ represents the Hadamard product, a point-by-point multiplication of two vectors.

The angle-Doppler steering vector used to solve for the adaptive weights in Eqn. (16) is the space-time steering vector, transformed to the angle-Doppler domain via the same transformation matrix T, i.e.

$$\tilde{\mathbf{s}} = \mathbf{T}^H \mathbf{s} \tag{21}$$

Note the transformation matrix defined in Eqn. (20) is defined for the chosen Doppler frequencies and angles without any restrictions on their values. No assumption is made about the form of the spatial or temporal steering vectors, i.e. the use of a transformation matrix eliminates the two restrictions of the original JDL formulation.

In the case of a linear array of isotropic point sensors, the ideal steering vectors are obtained from Eqns. (13) and (14). If the angles and Doppler frequencies satisfy the conditions listed in Section 2.2, the transformation matrix T reduces to the relevant rows of the 2-D FFT matrix. The FFT-based formulation is equivalent to choosing a spacing in the angle domain such that $[(d/\lambda)\Delta\sin(\phi)]=1/N$ and in the Doppler domain of $\Delta f=1/M$. Furthermore, if both the look angle and Doppler correspond to one of these angles and Dopplers, the transformed steering vector of Eqn. (21) is equivalent to the steering vector of Eqn. (17). The formulation of [7] is therefore a special, not necessarily optimal, case of the more general formulation presented here.

For a real array, the steering vector associated with a given angle is the measured magnitude and phase taper due to a calibrated far-field source. If measurements are not available, the steering vectors can be obtained from a numerical electromagnetic analysis of the receiving antenna. These steering vectors include array effects and the effects that the aircraft body has on the reception of signals. Usually, even in the case of a real array, the pulses are equally spaced in time and hence the temporal steering vector is unchanged. In the case of a real array, the spatial component in Eqn. (12) must be replaced with a measured steering vector, i.e. the space time steering vector is:

$$\mathbf{s}(\phi_t, f_t) = \mathbf{b}(f_t) \otimes \mathbf{a}_m(\phi_t), \tag{22}$$

where $a_m(\phi_t)$ is the *measured* steering vector corresponding to angle ϕ_t. Similarly the spatial steering vectors in the transformation matrix of Eqns. (19) and (20) must be replaced with the corresponding measured steering vectors.

Melvin and Himed [10] applied the JDL algorithm to measured data and used the measured steering vectors to transform the space domain to the angle domain. In effect, without explicitly stating so, they use a transformation matrix in the spatial domain and a DFT in the temporal domain. The spacing between the angles chosen for the LPR is determined by the available measured steering vectors. The spacing between the Doppler frequencies is fixed by the DFT. Crucially, the resulting change on the angle-Doppler steering vector is ignored and they assume the simplified form of the steering vector in Eqn. (17) is valid. However, the use of a different transform from the spatial domain to the angle domain violates the assumptions listed in Section 2.2.

2.3.1 Multi-Channel Airborne Radar Measurements (MCARM)

The discussion above dealt with applying the JDL algorithm to real arrays by accounting for array and airframe effect. The performance improvements over the original JDL algorithm are presented here using data from the MCARM database.

Figure 12: MCARM Testbed

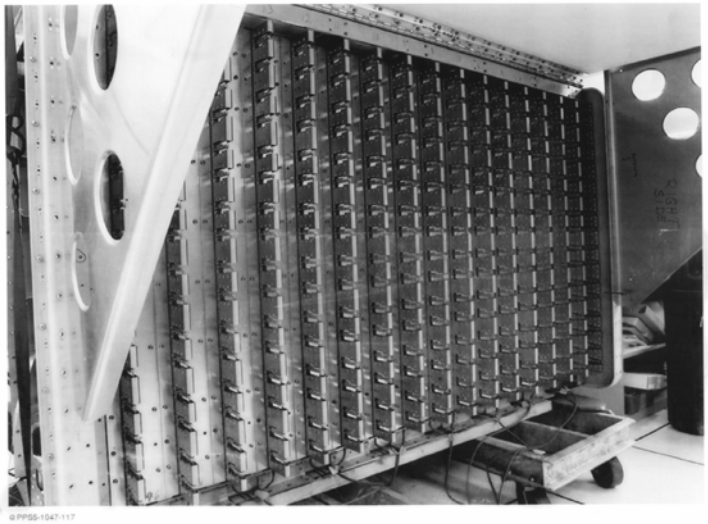

Figure 13: MCARM Antenna Array

The MCARM program had as its objective the collection of multiple spatial channel airborne radar data for the development and evaluation of STAP algorithms for future Airborne Early Warning (AEW) radar systems [11, 12].

Under the MCARM program, some ground moving target indication (GMTI) data was collected with and without vegetation to evaluate foliage penetration (FOPEN). Mono-static data was collected at PRFs of 7 kHz, 2 kHz, and 500 Hz. The MCARM data was collected during flights over the Delmarva Peninsula and the east coast of the US. There were a total of eleven flights with more than 50 Gigabytes of data collected.

The airborne MCARM testbed, a BAC1-11 aircraft, used for these measurements is shown in Figure 12. The sensor is hosted in an aerodynamic cheek-mounted, mounted just forward of the left wing of the aircraft. The L-band (1.24GHz) active array consists of 16 columns, with each column having two 4-element subarrays (Figure 13). The elements are vertically polarized, dual-notch reduced-depth radiators. These elements are located on a rectangular grid with azimuth spacing of 4.3 inches and elevation spacing of 5.54 inches. There is a 20 dB Taylor weighting across the 8 elevation elements resulting in a 0.25 dB elevation taper loss for both transmit and receive. The total average radiated power for the array was approximately 1.5 kW. A 6 dB modified trapezoid weighting for the transmit azimuthal illumination function is used to produce a 7.5° beamwidth pattern on boresight with -25 dB rms sidelobes. This pattern can be steered up to ±60°.

Of the 32 possible channels, only 24 receivers were available for the data collection program. Two of the receivers were used for analog sum and azimuthal difference beams. There are therefore 22 (N=22) digitized channels which, in this work, are arranged as rectangular 2×11 array. Each CPI comprises 128 (M=128) pulses at a PRF of 1984Hz.

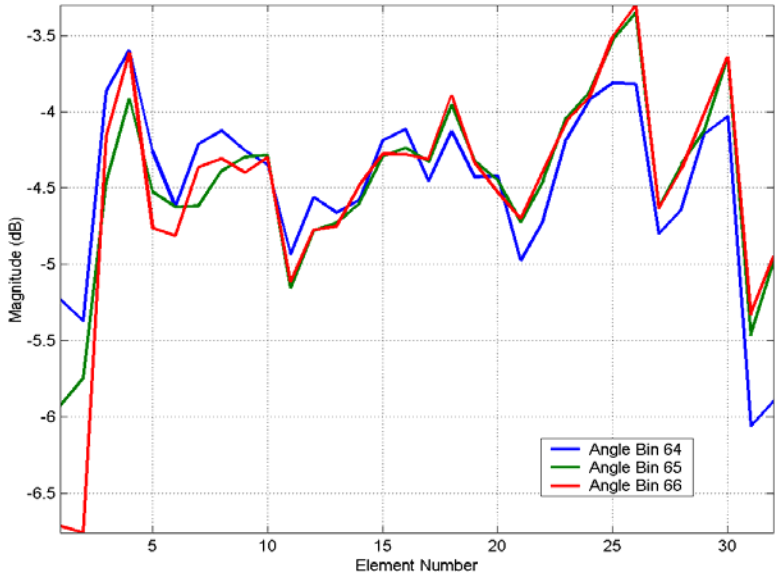

Figure 14: Magnitude of MCARM steering vectors

In the ideal case of a linear array, Eqn. (13) shows that the magnitude of the steering vector is constant at each element. Figure 14 shows the variation in magnitude for the MCARM array. The magnitude varies by as much as 4dB over the 32 elements. This variation is due to the mutual coupling between the elements of the antenna array.

2.3.2 Example 1. Injected target

In the first example, a synthetic target of fixed amplitude, direction, Doppler and range is injected into the MCARM data set. The amplitude and phase variation of the injected target across the 22 channels is obtained from the measured steering vectors. The amplitude of the injected target is chosen such that it remains undetected by non-adaptive pulse-Doppler processing.

JDL processing is performed at the target angle bin, for a few range bins surrounding the injected target and for all Doppler bins. In this example, the figure of merit used to compare the two scenarios is the separation between the MSMI statistic at the target range/Doppler bin and the highest statistic at other range or Doppler bins (the largest false alarm statistic). A large separation implies a large difference between target and residual interference, i.e. improving the ability to detect the target.

In this example, the data from acquisition 575 on flight 5 is used. The parameters of the injected target are: Amplitude = $0.0001\angle 0^o$, Angle bin = 0^o (Broadside), Doppler bin = -9 (-139.5Hz), Range bin = 290

Figure 15 plots the MSMI statistic, as a function of range bin for the two scenarios considered. In the first case, a strong false alarm several dB over the target is clearly visible. In the second case, target clearly stands out over the nearest false alarm. The false alarm is somewhat suppressed, but more crucially, the gain on the target and hence the target statistic is significantly improved. Accounting for the non-orthogonal nature of the steering vectors yields an improvement of 7.1dB.

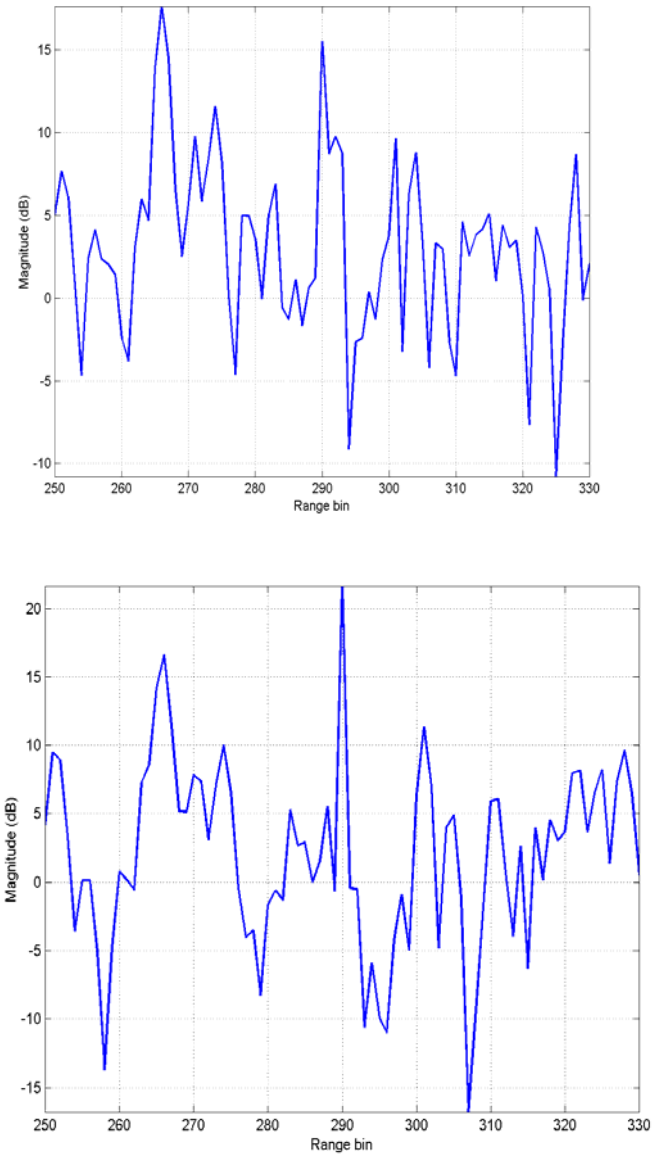

Figure 15: JDL performance before and after accounting for array effects (Injected Target)

2.3.3 Example 2: MTS Tones

On flight 5, acquisition 152 includes clutter and tones from a moving target simulator (MTS) at pre-selected Doppler frequencies. Five tones are received at approximately -800 Hz (0 dB), -600 Hz (-14 dB), -400 Hz (-20 dB), -200 Hz (-26 dB) and 0 Hz (-31 dB). The data in this acquisition are returns from 128 pulses measured across 22 channels. The pulse repetition frequency for this flight was 1984 Hz, hence the separation of 200 Hz corresponds to nearly 13 Doppler bins. Using an acquisition with the MTS allows us to compare the performance of the JDL algorithm in the above scenarios using measured data. The MTS tones are processed like returns from moving targets. The presence of five MTS tones of differing amplitudes makes it difficult to define a unique figure of merit to compare the two scenarios. In this example, a visual inspection is used for comparison.

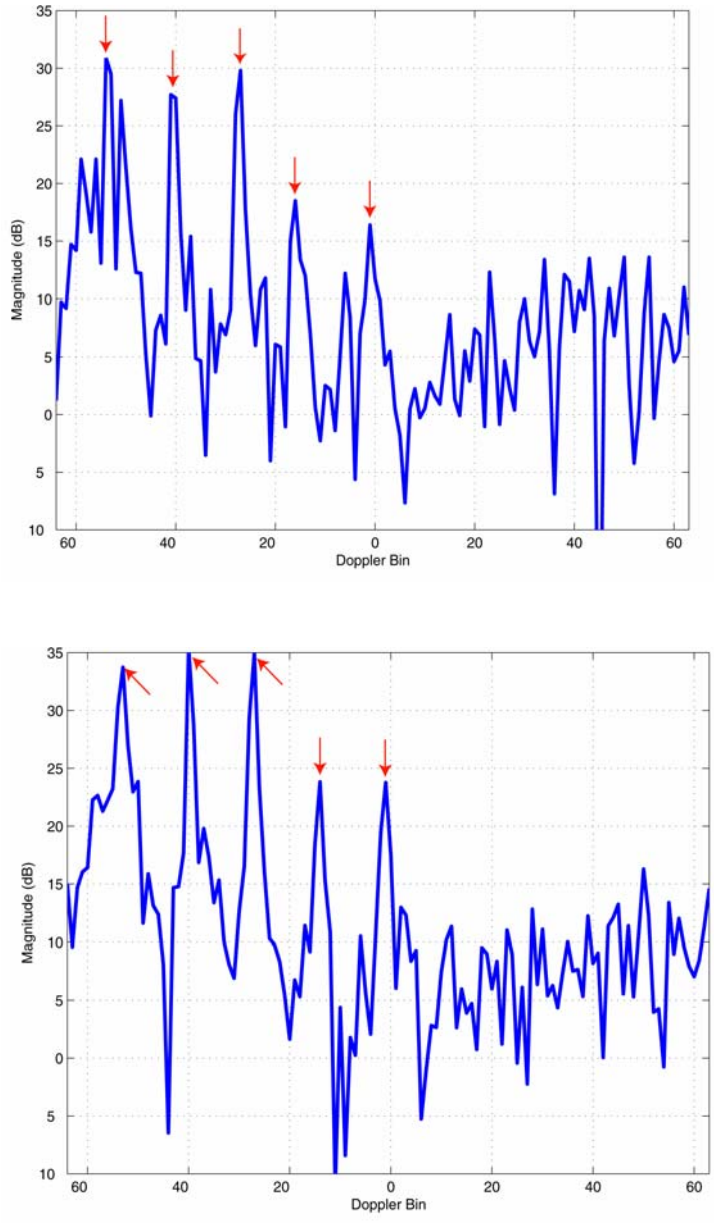

Figure 16: JDL before and after accounting for array effects (MTS Tones)

Figure 16 plots the MSMI statistic versus Doppler bin for the two cases considered. In the first plot, the five tones are clearly visible with the strongest tone at bin -53 spread over Doppler space. A few spurious tones are also visible. The second plot shows the results of the JDL algorithm modified by Eqn. (21). The five tones are clearly visible and the spurious tones are completely suppressed.

Figure 15 and Figure 16 demonstrate the importance of and performance enhancements possible by accounting for array effects. The traditional formulation for JDL ignored the fact that real world arrays are not comprised of isotropic, point sensors. Accounting for the array effects leads to huge improvements in performance, *as applied to measured data.*

2.4 Non-Homogeneity Detection/Knowledge Based Processing

This section presents the third of the key issues that limit the performance of adaptive processing algorithms in real world applications: the non-homogeneous and dynamic background environments typically observed from airborne radar. Non-homogeneous data is the most significant of the three issues that we discuss. Significant processing losses result from mismatches between the environment and the processing algorithms. Recent work has shown that it is essential to sense the actual environment, and then to match end-to-end processing to this environment. Moreover, the processing should be "intelligent"; the radar processor should learn from the environment.

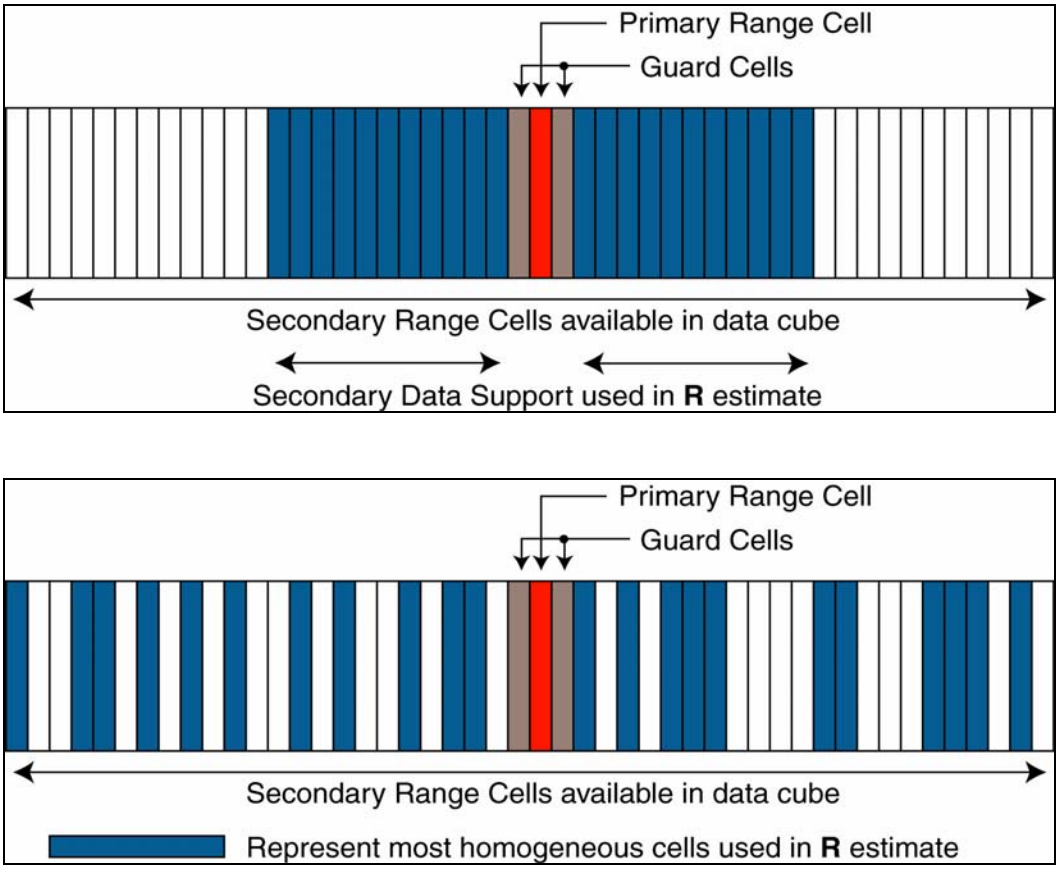

Figure 17: Secondary Data Selection (a) Homogeneous Case (b) Non-homogeneous Case

In the filtering and detection stages of the radar processing chain, training data are selected about the cell under test, and that training data is used to represent the interference in the cell under test. Conventional constant false alarm rate (CFAR) and space-time adaptive processing (STAP) algorithms use a symmetric sliding window about the cell under test in order to select the training data as shown in Figure 17(a). This

assumes that the data is homogeneous and i.i.d. To quote [13] "A data set is termed wide sense homogeneous if the system performance loss can be ignored or is acceptable for a given STAP algorithm. A data set is said to be wide sense non-homogeneous if it is not wide sense homogeneous". In the real world, wide sense homogeneity is routinely violated, leading to sub-optimum performance.

Improved methods are needed to more carefully select processing based on the environment. For detection and filtering, this means better selection of training data, requiring non-symmetric secondary data samples be selected. As shown in Figure 17(b) these secondary data samples must best represent the interference, or at least the homogeneous component of the interference, in a statistical sense.

The non-homogeneity detector (NHD) must be matched to the processing at hand. For example, a non-homogeneity that impacts on the performance of FA-STAP has no impact on the performance of the JDL algorithm if it falls in a natural null of the transformation to the angle-Doppler domain. Transforms to other domains may therefore be necessary. Figure 18 shows non-homogeneity detection in two different domains. In the upper path, range-pulse-element data cubes are transformed into angle-Doppler space for non-homogeneity detection in a two-dimensional LPR. This form of NHD is well suited for the JDL algorithm. In the lower path, a one-dimensional transform is executed and non-homogeneity detection is performed in element-Doppler space. The nature of the data may also dictate whether full- or reduced-dimension adaptive algorithms be executed. If the sample support is severely limited, direct data domain, non-statistical, adaptive algorithms may be required.

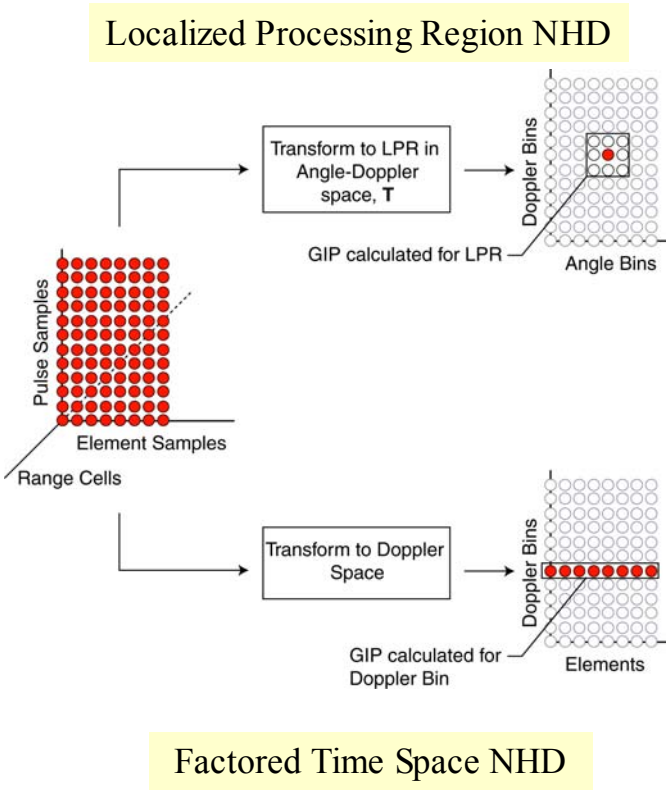

Figure 18: Non-Homogeneity Detection in LPR and in Factored Approaches

Recent developments in non-homogeneity detection allow for better selection of training data. We have been investigating a variety of non-homogeneity detection techniques including application of the Generalized Inner Product and multi-pass STAP. In multi-pass STAP techniques, a first filtering stage serves as the non-homogeneity detector (NHD). A second stage then performs the filtering function. This formulation will be explained in detail later in this report.

Using a NHD provides significant performance improvement over conventional methods. However, once non-homogeneous cells have been identified, how are these cells handled in the filtering and detection processes? By definition, the non-homogeneous cells are not like neighboring cells, so it is not appropriate to use traditional statistical techniques, which estimate the interference in the cell under test by covariance matrix estimation. To address these cases, researchers are continuing to develop hybrid STAP techniques that combine direct data domain (non-statistical) and sample covariance matrix based (statistical) adaptive processing.

2.5 Direct Least Squares Approach

The inability of traditional statistical algorithms to counter the non-homogeneous component of interference motivates research in non-statistical or direct data domain (D^3) algorithms.

In [14] an algorithm is developed that optimizes the signal to interference in a least squares sense for signals at the angle at which a look-direction constraint is established. This method minimizes, in a least squares sense, the error between the received voltages (signal plus interference) and a signal from the assumed angle. This approach does not employ data from outside the radar range cell being evaluated, i.e. this approach does not require secondary data. This makes the D^3 an attractive alternative in non-homogeneous clutter. This is especially true in a severely non-homogeneous clutter environment of urban and land/sea interfaces. The D^3 approach has recently focused on one-dimensional spatial adaptivity [14]. This section introduces a new two-dimensional space-time D^3 algorithm based on the one-dimensional algorithm of [14].

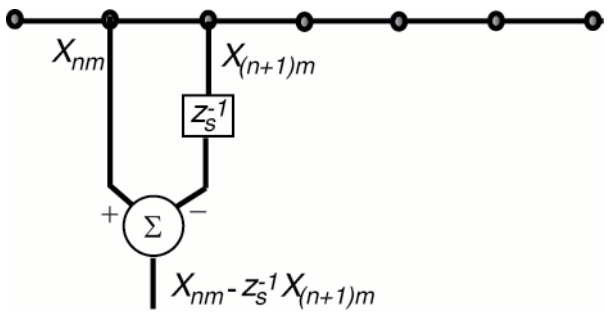

Figure 19: Principle of Direct Data Domain Processing

Consider the N-element uniformly spaced array shown in Figure 19. For a look direction of ϕ_s, the signal advances from one element to the next by the same phase factor $z_s=[\exp(j2\pi\sin(\phi_t)]$. The term obtained by the subtraction operation in Figure 19 is *therefore free of the target signal and contains only interference terms*. The D^3 algorithm minimizes the power in such interference terms while maintaining gain in the direction of the target.

To best present the D^3 algorithm, the data from the N elements due to the M pulses in a CPI is written as a $N\times M$ matrix X whose m^{th} column corresponds to the N returns from the m^{th} pulse, represented by x(m). The data matrix is a sum of target and interference terms. Rewriting Eqn. (11) in terms of matrices

$$\mathbf{X} = \xi\,\mathbf{S}(\phi_t, f_t) + \mathbf{C} + \mathbf{N}. \tag{23}$$

Define the $M\times(N\text{-}1)$ matrix **A** to be

$$\mathbf{A} = \begin{bmatrix} \mathbf{X}_{00} - z_s^{-1}\mathbf{X}_{10} & \mathbf{X}_{10} - z_s^{-1}\mathbf{X}_{20} & \cdots & \mathbf{X}_{(N-2)0} - z_s^{-1}\mathbf{X}_{(N-1)0} \\ \mathbf{X}_{01} - z_s^{-1}\mathbf{X}_{11} & \mathbf{X}_{11} - z_s^{-1}\mathbf{X}_{21} & \cdots & \mathbf{X}_{(N-2)1} - z_s^{-1}\mathbf{X}_{(N-1)1} \\ \vdots & \vdots & \vdots & \vdots \\ \mathbf{X}_{0(M-1)} - z_s^{-1}\mathbf{X}_{1(M-1)} & \mathbf{X}_{1(M-1)} - z_s^{-1}\mathbf{X}_{2(M-1)} & \cdots & \mathbf{X}_{(N-2)(M-1)} - z_s^{-1}\mathbf{X}_{(N-1)(M-1)} \end{bmatrix}, \quad (24)$$

where z_s, as defined earlier, is the phase progression of the *target signal* from one element to the next. Theoretically, the entries of A are interference terms only, though due to beam mismatch there may be some residual signal power. However, unless the target is significantly off the look direction/Doppler, the target signal is effectively nulled. In case the target is significantly off the look direction, it must be treated as interference: in a surveillance radar, targets must be declared only if they are in the look direction. In fact, sidelobe targets are an example of the discrete, non-homogeneous, interference that drives this research.

Consider the following scalar functions of a vector of spatial weights $\boldsymbol{w}_s$.

$$\begin{aligned} G_{\mathbf{w}_s} &= \left|\mathbf{w}_s^H \mathbf{a}_{(0:N-2)}\right|^2 = \mathbf{w}_s^H \mathbf{a}_{(0:N-2)} \mathbf{a}_{(0:N-2)}^H \mathbf{w}_s, \\ I_{\mathbf{w}_s} &= \left\|\mathbf{A}^* \mathbf{w}_s\right\|^2 = \mathbf{w}_s^H \mathbf{A}^T \mathbf{A}^* \mathbf{w}_s, \\ R_{\mathbf{w}_s} &= G_{\mathbf{w}_s} - \kappa^2 I_{\mathbf{w}_s}, \end{aligned} \quad (25)$$

where $\|\cdot\|$ represents the 2-norm of a vector and $a_{(0:N-2)}$ represents the first N-1 entries of the spatial steering vector. In the equation, $A^* w_s$ is used to remain consistent with the term $w_s^H a_{(0:N-2)}$ in that the weights multiply the conjugate of the data.

The term G in Eqn. (25) represents the gain of the weight vector w_s at the look angle ϕ_t, while the term I represents the residual interference power after the data is filtered by the same weights. Hence, the term R is the difference between the gain of the antenna at the look Doppler and the residual interference power. The term κ in the definition of R is an emphasis parameter that will be described later. The D^3 algorithm finds the weights that maximize this difference. Mathematically,

$$\begin{aligned} \max_{\|\mathbf{w}_t\|_2=1} [\mathrm{R}_{\mathrm{w_t}}] &= \max_{\|\mathbf{w}_t\|_2=1} \left[G_{w_t} - \kappa^2 I_{w_t}\right], \\ &= \max_{\|\mathbf{w}_t\|_2=1} \mathbf{w}_t^H \left[\mathbf{a}_{(0:N-2)} \mathbf{a}_{(0:N-2)}^H - \kappa^2 \mathbf{A}^T \mathbf{A}^*\right] \mathbf{w}_t, \end{aligned} \quad (26)$$

where the constraint $\|\mathbf{w}_s\|_2 = 1$ is chosen to obtain a finite solution. Using the method of Lagrange multipliers, it can be shown that the desired temporal weight vector is the eigenvector corresponding to the maximum eigenvalue of the (N-1)×(N-1) matrix $\left[\mathbf{a}_{(0:N-2)} \mathbf{a}_{(0:N-2)}^H - \kappa^2 \mathbf{A}^T \mathbf{A}^*\right]$. This formulation yields a spatial weight vector of length (N-1). The loss of one DOF represents the subtraction operation in defining the entries of A.

Analogous to the spatial adaptive weights, the temporal weight vector w_t is the eigenvector corresponding to the largest eigenvalue of the (M-1)×(M-1) matrix $\left[\mathbf{b}_{(0:M-2)} \mathbf{b}_{(0:M-2)}^H - \kappa^2 \mathbf{B}^T \mathbf{B}^*\right]$, where $b_{(0:M-2)}$ is the vector of the first (M-1) entries of the temporal steering vector defined by Eqn. (14) and B is the N×(M-1) matrix

$$\mathbf{B} = \begin{bmatrix} \mathbf{X}_{00} - z_t\mathbf{X}_{01} & \mathbf{X}_{01} - z_t\mathbf{X}_{01} & \cdots & \mathbf{X}_{0(M-2)} - z_t\mathbf{X}_{0(M-1)} \\ \mathbf{X}_{10} - z_t\mathbf{X}_{11} & \mathbf{X}_{11} - z_t\mathbf{X}_{12} & \cdots & \mathbf{X}_{1(M-2)} - z_t\mathbf{X}_{1(M-1)} \\ \vdots & \vdots & \vdots & \vdots \\ \mathbf{X}_{(N-1)0} - z_t\mathbf{X}_{(N-1)1} & \mathbf{X}_{(N-1)1} - z_t\mathbf{X}_{(N-1)2} & \cdots & \mathbf{X}_{(N-1)(M-2)} - z_t\mathbf{X}_{(N-1)(M-1)} \end{bmatrix} \quad (27)$$

The length NM space-time adaptive weight vector, for look angle ϕ_t and look Doppler f_t is then given by

$$\mathbf{w}(\phi_t, f_t) = \begin{bmatrix} \mathbf{w}_t \\ 0 \end{bmatrix} \otimes \begin{bmatrix} \mathbf{w}_s \\ 0 \end{bmatrix} \quad (28)$$

The zeros appended to the spatial and temporal weight vectors represent the lost DOF in space and time.

The parameter κ above sets a trade off between mainbeam gain and interference suppression. By changing the value of this parameter, it is possible to emphasize one or the other term. In determining the spatial weights, choosing $\kappa = 0$ eliminates the interference term leaving the largest eigenvalue equal to $\left\|\mathbf{a}_{(0:N-2)}\right\|_2^2 = (N-1)$ with the corresponding eigenvector $\mathbf{w}_s = \mathbf{a}_{(0:N-2)} / \left\|\mathbf{a}_{(0:N-2)}\right\|_2$. Therefore, as $\kappa \to 0$ the D^3 weight vector approaches the non-adaptive steering vector used in pulse-Doppler processing.

On the other hand, if κ is chosen to be large, the role of the gain term G is negligible and the weight vector is dependent on the interference terms only. This leads to emphasis on the suppression of interference at the expense of mainbeam gain. In this case, the look direction plays a limited role through the term z_s and the weight vector may vary significantly by range cell.

Note that the adaptive weight vector in Eqn. (28) is obtained using data from the *primary range cell only*. There is no estimation of a covariance matrix and no correlation information required to obtain the adaptive weights. This property gives direct data domain processing its greatest advantage and its greatest disadvantage. The lack of an estimation of correlation allows use of D^3 processing in severely non-homogeneous situations. However, ignoring correlation information limits its ability to suppress correlated interference. A hybrid method to overcome this drawback and combine the benefits of statistical and non-statistical (D^3) processing will be described in Section 3.1.

2.5.1 Performance of D^3 Processing in Non-homogeneous Interference

This section presents a simulation to illustrate the advantages and disadvantages of D^3 processing. This simulation includes the effects of clutter, barrage noise jammers, white noise and a discrete interferer. Table 1 lists the parameters used in the example. The jammer and discrete interferer powers are referenced to the noise level. The clutter power is fixed by the transmit power and the assumed land reflectivity. The clutter and jammers represent correlated interference because these two interference sources are homogeneous across all range cells. Note that the discrete interferer is within the target range cell only, with an offset from the look direction in angle but not Doppler. Matching the non-homogeneity to the target in one domain makes it more difficult for the D^3 algorithm to suppress the non-homogeneity.

Table 1: Parameters for example using simulated data

Parameter	*Value*	*Parameter*	*Value*
Elements (N)	18	Pulses (M)	18
Element Spacing	0.5λ	Pulse repetition frequency	300 Hz
Array Transmit Pattern	Uniform	Uncompressed pulse width	400μs
Mainbeam Transmit Azimuth	0 deg	Transmit power	400kw
Backlobe attenuation	30	Land reflectivity	-3.0dB
Jammer azimuth angles	[-20° 45°]	Jammer powers	[40 dB 40 dB]
Target normalized Doppler (f_t)	1/3	Jammer Elevation angles	[0° 0°]
Doppler of interferer	1/3	Interferer power	40 dB
Angle of interferer	-51°	Thermal noise power	Unity
β (Clutter slope)	1	Number of clutter patches	361

The adapted beam pattern plots presented in this report are the mean patterns over 200 independent realizations. Vertical bars represent the standard deviation over these 200 trials. This method was required because the D^3 algorithm is non-statistical and based solely on a single data set/realization. Operating with the known covariance matrix to obtain an ideal pattern, as possible in statistical algorithms, is not an option.

Figure 20 illustrates the antenna patterns along the target azimuth and Doppler for the JDL algorithm. In the angle plot, note the high sidelobe in the direction of the discrete interferer. The discrete interferer is within the primary range cell and so does not contribute to the covariance matrix estimate and therefore *cannot* be nulled by a purely statistical algorithm such as JDL. However, the angle plot shows the JDL algorithm does place deep nulls in the direction of the white noise jammers at -20° and 45°. The Doppler plot shows the deep null placed at zero Doppler frequency corresponding to mainbeam clutter. These two figures illustrate the effectiveness of the JDL algorithm in suppressing correlated interference such as jamming and clutter. However, they also illustrate the inability of a purely statistical algorithm to suppress point non-homogeneities (discretes).

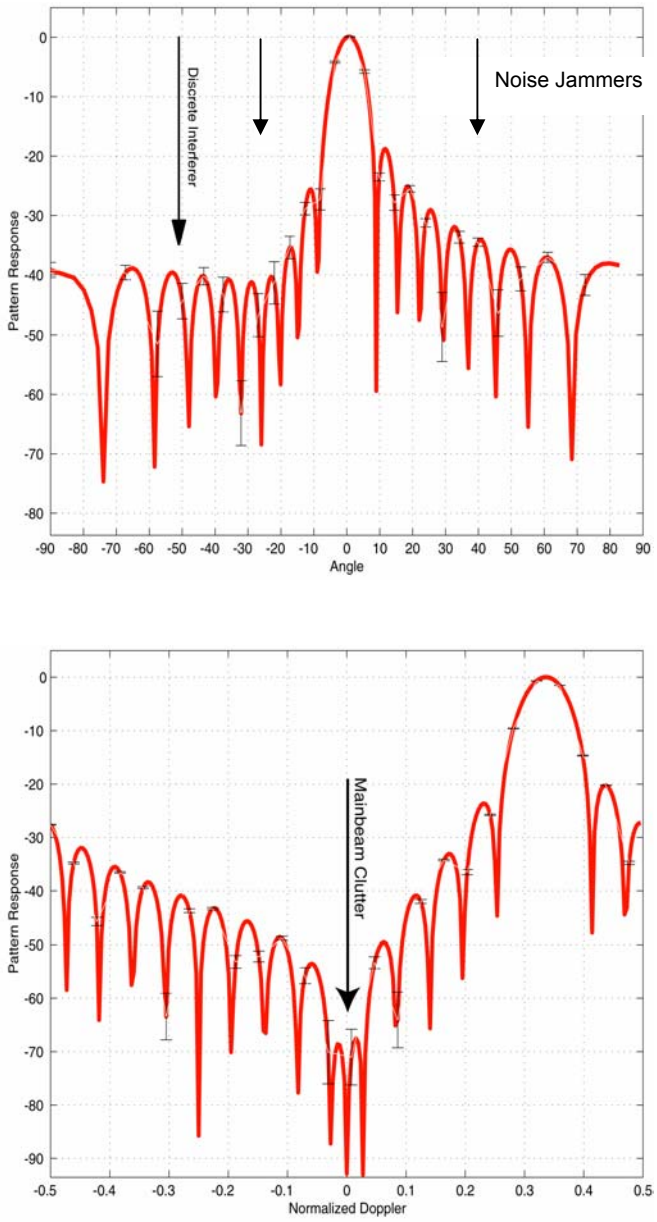

Figure 20: JDL Antenna Patterns at Target Doppler and Azimuth (a) Angle Pattern (b) Doppler Pattern

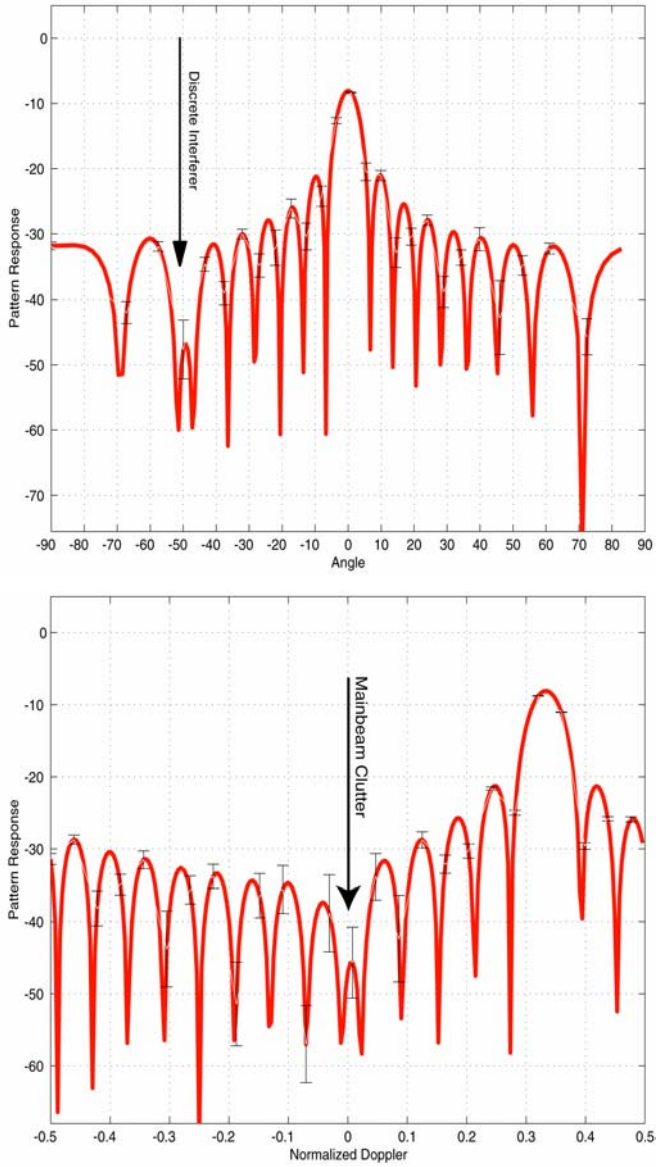

Figure 21: Direct Data Domain Patterns at Target Doppler and Azimuth (a) Angle Pattern (b) Doppler Pattern

Figure 21 plots the antenna patterns resulting from the implementation of the two-dimensional D^3 algorithm. The angle plot shows that the D^3 algorithm places a null in the direction of the discrete interferer. The adapted spatial beam pattern shows a distinct null in the direction of the discrete interferer at –51°, i.e. the algorithm is effective in countering a discrete interferer within the range cell of interest. However, the figure also illustrates the limitations of the D^3 algorithm. The nulls in the direction of the jammers are not as deep as in the case of JDL. The Doppler plot shows a shallow null in the direction of the mainbeam clutter. In summary, D^3 algorithms do not suppress correlated interference as well as statistical algorithms, however they are an excellent processing technique to deal with non-homogeneities. Later in this report, we present results from combining the benefits of D^3 and statistical algorithms.

3.0 GMTI-STAP Status

This section details on-going research. The research presented here is a continuation of the work presented in Section 2.0 addressing some of the issues raised. We developed a hybrid algorithm combining

non-statistical and statistical adaptive processing and use this algorithm to develop the simplest formulation for a comprehensive, practical, approach to STAP. This formulation accounts for all the real world effects listed in Section 2.0.

Section 2.5 discusses non-statistical adaptive processing in non-homogeneous environments, pointing out both the advantages and drawbacks of such an approach. Here we present a unique formulation combining the benefits of non-statistical and statistical processing. This hybrid algorithm, presented in section 3.1, is a two-stage algorithm combining the two approaches. The issues of non-homogeneous data, non-homogeneity detection and the hybrid algorithm lead to a formulation using *Knowledge Based STAP* (KB-STAP). Section 3.2 presents the KB-STAP concept and simplest KB-STAP formulation. The examples presented in this section show the huge improvements in performance over traditional STAP algorithms and prove the importance of the issues raised in this report. Section 3.3 presents further enhancements to KB-STAP, incorporating map data to inform the decision making process within the knowledge base.

3.1 Hybrid (D3/JDL) STAP

Performance degradation of STAP algorithms due to non-homogeneous data occurs in two forms. In one form the secondary data is not i.i.d., leading to an inaccurate estimate of the covariance matrix. For example, the clutter statistics in urban environments fluctuate rapidly with range. To minimize the loss in performance due to non-homogeneous sample support, a NHD may be used to identify secondary data cells that do not reflect the statistical properties of the primary data. These data samples are then eliminated from the estimate of the covariance matrix.

The second form of performance loss is due to a discrete non-homogeneity within the primary range cell. For example, a large target within the test range cell but at a different angle and/or Doppler appears as a false alarm at the look angle-Doppler domain. Other examples include a strong discrete non-homogeneity, such as a large building (corner reflector), in the primary range cell. These false alarms appear through the sidelobes of the adapted beam pattern. The secondary data cells do not carry information about the discrete non-homogeneity and hence a statistical algorithm cannot suppress discrete (uncorrelated) interference within the range cell under test. The example presented in Section 2.5.1 illustrated the impact of such a non-homogeneity.

The inability of statistical STAP algorithms to counter non-homogeneities in the primary data motivates research in the area of non-statistical D^3 algorithms, such as that described in Section 2.4. These algorithms use data from the range cell of interest only, eliminating the sample support problems associated with statistical approaches.

The main contribution of this section is the introduction of a two-stage hybrid STAP algorithm combining the benefits of both non-statistical and statistical methods. The hybrid approach uses the non-statistical algorithm of Section 2.4 as a first-stage filter to suppress discrete interferers present in the range cell of interest. This first stage serves as an *adaptive transform* from the space-time domain to the angle-Doppler domain and is followed by JDL processing in the second stage. The adaptive transform replaces the steering vector based non-adaptive transform used in Section 2.3. The second stage is designed to filter out the residual correlated interference [15].

3.1.1 Two-Stage Hybrid Algorithm

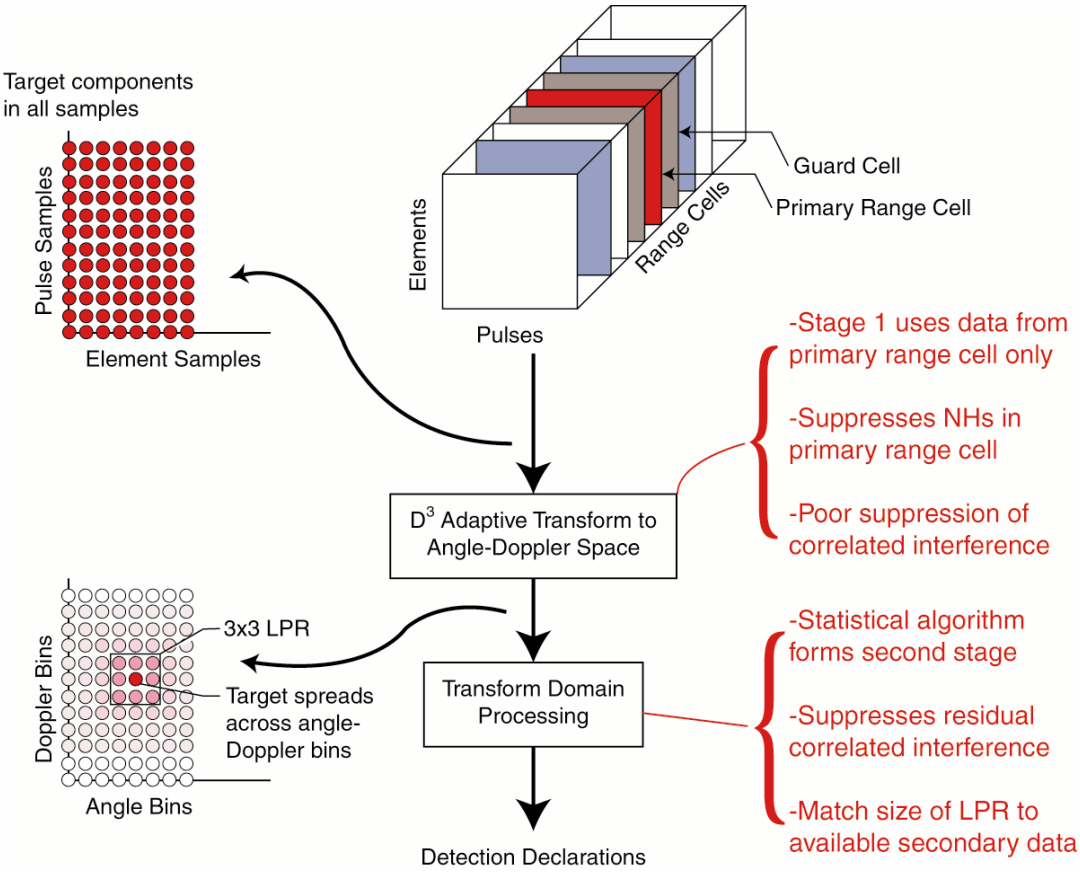

Figure 22: Block diagram of the Two-Stage Hybrid Algorithm

Consider the general framework of any STAP algorithm. The algorithm processes received data to obtain a complex weight vector for each range bin and each look angle/Doppler. The weight vector then multiplies the primary data vector to yield a complex number. The process of obtaining a real scalar from this number for threshold comparison is part of the post-processing and not inherent to the algorithm itself. The adaptive process therefore *estimates the signal component in the look direction* and hence the adaptive weights can be viewed in a role *similar to the non-adaptive steering vectors*, used to transform the space-time data to the angle-Doppler domain.

The JDL processing algorithm begins with a transformation of the data from the space-time domain to the angle-Doppler domain. This is followed by statistical adaptive processing within a LPR in the angle-Doppler domain. The hybrid approach uses the D^3 weights, replacing the non-adaptive steering vectors used earlier. By choosing the set of look angles and Dopplers to form the LPR, the D^3 weights perform a function analogous to the non-adaptive transform. As shown in Figure 22, the D^3 algorithm serves as a first stage *adaptive* transformation from the space-time to the angle-Doppler domain.

JDL statistical processing in the angle-Doppler domain forms the second stage of adaptive processing to filter the residual correlated interference. The D^3 algorithm is used repeatedly with the η_a look angles and the η_d look Doppler frequencies to form the LPR. The space-time data is transformed to the LPR in the angle-Doppler domain using these adaptive weights. Using the D^3 weights from Eqn. (28), the transformation matrix

of Eqn. (20) in Section 2.3 for $(\phi_{-1}, \phi_0, \phi_1; \eta_a = 3)$ and three Doppler bins $(f_{-1}, f_o, f_1; \eta_d = 3)$ is now given by the *MN*×9 matrix

$$\mathbf{T} = \left[\mathbf{w}(\phi_{-1}, f_{-1}) \;\; \mathbf{w}(\phi_{-1}, f_0) \;\; \mathbf{w}(\phi_{-1}, f_1) \right. \\ \mathbf{w}(\phi_0, f_{-1}) \;\; \mathbf{w}(\phi_0, f_0) \;\; \mathbf{w}(\phi_0, f_1) \\ \left. \mathbf{w}(\phi_1, f_{-1}) \;\; \mathbf{w}(\phi_1, f_0) \;\; \mathbf{w}(\phi_1, f_1)\right] \tag{29}$$

This adaptive transformation is noninvertible, resulting in some information loss. However, this information loss may be beneficial. The hybrid algorithm takes advantage of this loss to suppress discrete interferers within the range cell of interest. The advantages associated with the JDL algorithm, such as in reduction in the required secondary data support, carry over to the hybrid algorithm.

The same transformation matrix T is used to transform the primary and secondary data to the angle-Doppler domain. Furthermore, the steering vector s is also transformed to the angle-Doppler domain using this transformation matrix in conjunction with Eqn. (21). Unlike the JDL algorithm, this transformation matrix changes from range cell to range cell. The hybrid algorithm therefore has a significantly higher computation load than the JDL algorithm. The hybrid algorithm forms the adaptive transformation matrix as given by Eqn. (29) for each range cell and then transforms this primary and *associated* secondary data to the angle-Doppler domain. This process is repeated for each range cell.

3.1.2 Example 1: Simulated Data

The first example uses the same data as presented in Section 2.5.1 to illustrate the performance of the D^3 method. There it was shown that the D^3 algorithm can suppress a discrete interference source well, but does not do as well against correlated interference such as white noise jamming and clutter. This example shows the performance of the hybrid algorithm in the same case.

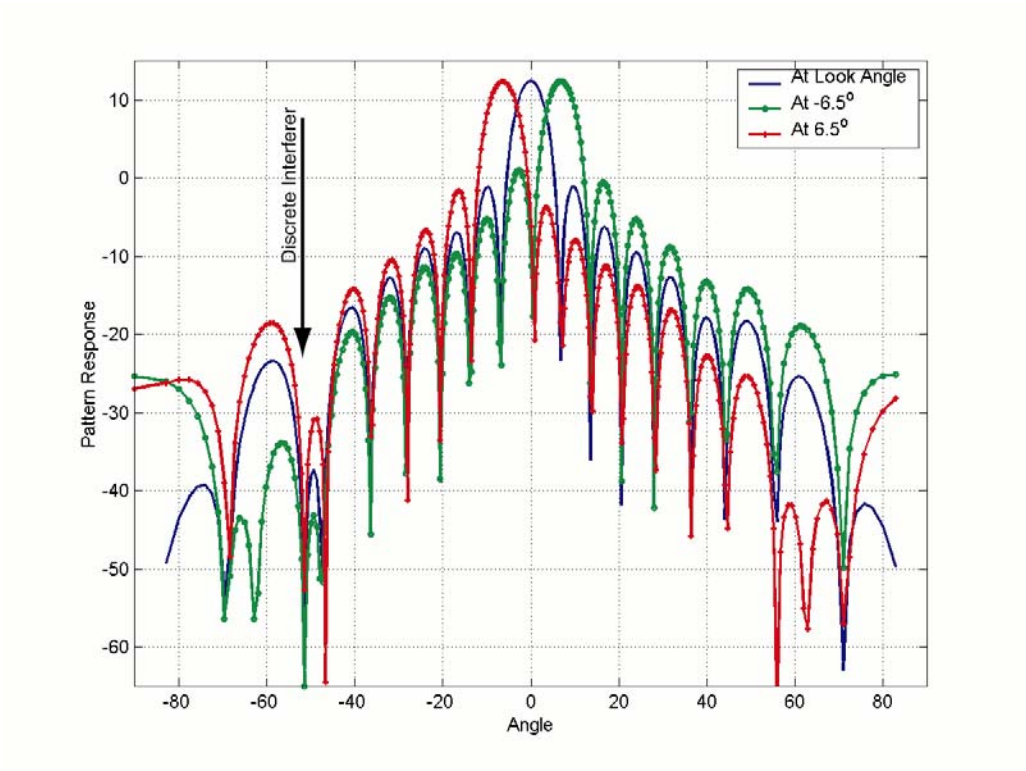

Figure 23: Three D^3 spatial beams used to form LPR

This example uses 3 angle bins and 3 Doppler bins, i.e. 3×3 LPR. The emphasis parameter κ is chosen to be $(NM)^{1/2}$. Figure 23 plots the spatial beam patterns associated with the three beams used to form the LPR in angle-Doppler domain. Note that the three beams are separated by a chosen beamwidth of 6.5^o. All three patterns show a null in the direction of the discrete interferer at angle -51^o. These beams illustrate the benefits of using the D^3 algorithm as the first stage. The algorithm suppresses discrete interference and the data transformed the angle-Doppler domain is free of the effects of discretes in the spatial sidelobes.

Figure 24 plots the antenna beam patterns resulting from the use of the hybrid algorithm. The figure shows that the hybrid algorithm combines the advantages of both statistical and non-statistical adaptive processing. The adapted angle pattern shows deep nulls at -21°, 45°, and -51°, the directions of the two jammers *and the discrete interferer*. Furthermore, the adapted pattern has a deep null at ω=0 resulting in effective nulling of the mainbeam clutter. The hybrid algorithm therefore suppresses correlated interference such as clutter and jamming *and uncorrelated interference such as the strong interferer* in the primary range cell.

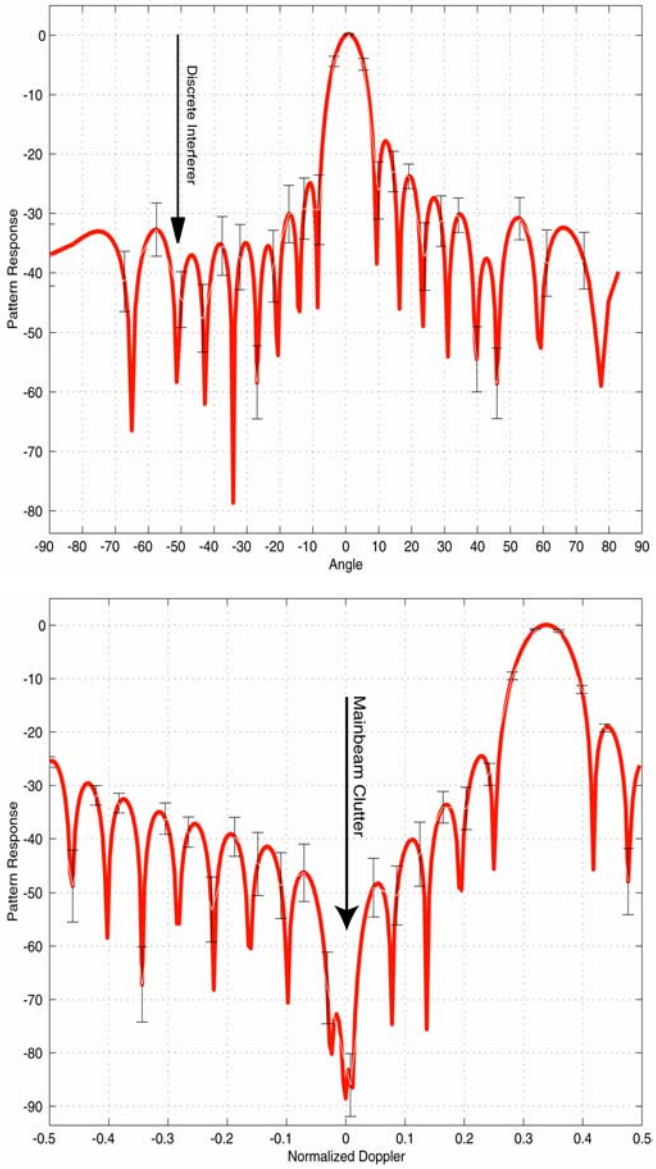

Figure 24: Hybrid Algorithm Patterns at Target Doppler and Azimuth

3.1.3 Applying the Hybrid Algorithm to Measured Data

This section presents two examples of the application of the hybrid algorithm to measured data. The examples use data from the MCARM database. The examples use two acquisitions (acquisitions 575 and 152 on flight 5) to illustrate the suppression of discrete interference in measured data.

Before the hybrid algorithm can be applied to the MCARM database, array effects must be accounted for. The D^3 method was developed in Section 2.5.1 for an equispaced, linear array of point sensors. This allowed for the assumption of no mutual coupling between the elements and that, for each pulse, the target signal advances from one element to the next by a constant spatial multiplicative factor z_s. This, in turn, allowed for the crucial assumption of the elimination of the target signal in the entries of the interference matrix.

The MCARM antenna is an array of 22 elements arranged in a rectangular 2 x 11 grid. For a rectangular array these assumptions are invalid. Furthermore, as shown in Section 2.3.1, a real array is affected by mutual

coupling and the spatial steering vector must be measured. Figure 13 plots an example of the measured steering vectors provided with the MCARM database.

Here we compensate for the mutual coupling using the measured steering vectors (similar to the approach used in Section 2.2 for the JDL algorithm). Equation (13) indicates that the spatial steering vector at broadside ($\phi = 0$) is given by $a(\phi = 0)=[1\ 1 \ldots 1\ 1]^T$. In the absence of mutual coupling, this steering vector at broadside is valid for arrays in *any* configuration. The approach then is to artificially rotate all the data, using the measured spatial steering vector, to force the look direction to broadside. This compensates for the rectangular array configuration and the mutual coupling associated with the look direction. The rotation is achieved by an entry-by-entry division of the received voltages at the array level with the measured spatial steering vector corresponding to the look direction. Using pseudo-MATLAB® notation, this operation can be represented by

$$\hat{\mathbf{x}}(m) = \mathbf{x}(m) ./ \mathbf{a}_m(\phi_t), \tag{30}$$

where $x(m)$ represents the N returns from the m^{th} pulse in a CPI and $a_m(\phi_t)$ represent the measured steering vector corresponding to the look direction ϕ_t. This operation is repeated for all pulses in all range bins.

The division operation of Eqn. (30) forces the effective spatial steering vector for any look direction to be $a(\phi = 0)=[1\ 1 \ldots 1\ 1]^T$. equivalent to broadside in an ideal array. The hybrid method as developed above is applied to the 'rotated' data with broadside as the look direction.

3.1.4 Example 2: Injected Target in MCARM Data

In this example, a discrete non-homogeneity is introduced into the data by adding a strong fictitious target at a single range bin, but not at the look angle-Doppler. Two cases are considered within this example; no injected target and an injected weak target. The first case illustrates the suppression of the discrete non-homogeneity. In the second case, a weak target is injected at the same range bin as the non-homogeneity, but at the look angle and Doppler. This case illustrates the ability of the hybrid algorithm to detect weak targets in the presence of strong discrete non-homogeneities. The data is the same as used earlier in this report to illustrate the performance of the JDL algorithm. In this case, only 22 of the 128 pulses in the CPI are used, i.e. N=22, M=22. The value of the emphasis parameter is $\kappa = (NM)^{3/2}$.

The details of the injected non-homogeneity and weak target are shown in Table 2.

Table 2: Parameters for injected non-homogeneity and target in MCARM Data

Parameter	Non-homogeneity	Target
Amplitude	0.0241	0.000241
Angle bin	35	65 (broadside)
Doppler bin	-3	-2
Range bin	290	290

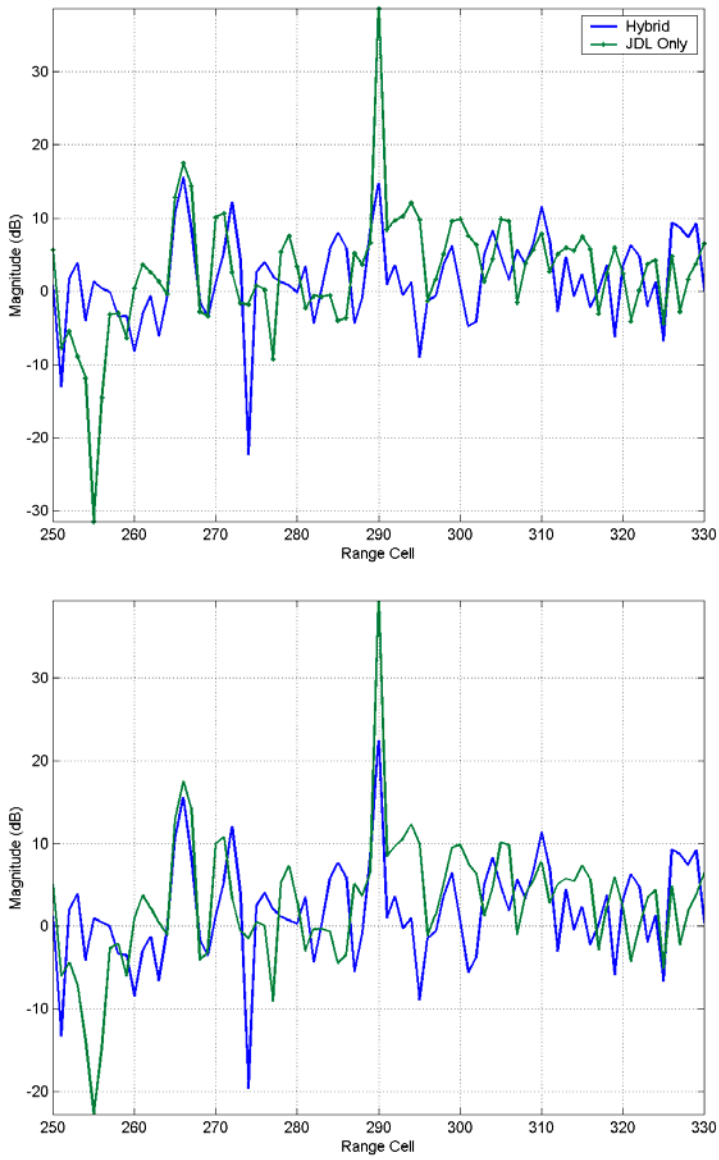

Figure 25: Performance of Hybrid algorithm in countering non-homogeneities: Injected Target (a) With Non-homogeneity, No target (b) With non-homogeneity, With target

The hybrid algorithm is applied to the data from the range bin with the non-homogeneity and surrounding range bins. The output MSMI statistic from the second stage of the hybrid algorithm is plotted as a function of range. In this example, five Doppler bins and five angle bins form the LPR for both the JDL algorithm and the second stage of the hybrid algorithm. One hundred secondary data vectors are used to estimate the 25×25 covariance matrix.

For the case without an injected target, Figure 25(a) compares the output from the JDL algorithm with the output of the hybrid algorithm. As can be seen, the JDL algorithm indicates the presence of a large target in the look direction (angle bin 65). This is because the large non-homogeneity at angle bin 35 and Doppler bin –3 is not suppressed by the statistical algorithm, leading to false alarms at the look direction. On the other hand, the hybrid algorithm shows no target at broadside. The non-homogeneity is suppressed in the first D^3 stage and residual clutter is suppressed in the second JDL stage.

A synthetic target injected at the look direction and Doppler illustrates that sensitivity of the hybrid algorithm to weak targets. The parameters of the weak target are listed in Table 2. Figure 25(b) compares the output of the two algorithms in the case of a strong non-homogeneity and a weak target. The JDL algorithm again shows the presence of a strong target in the look direction. However from Figure 25(a), we know that the strength of the statistic is caused by the non-homogeneity. On the other hand, the plot for the hybrid algorithm shows the statistic at the target range bin is 6.9 dB above the next highest peak.

This example shows that the hybrid algorithm may be use to detect a weak target in the presence of a discrete non-homogeneity within the range cell of interest. This is a unique capability compared to all other STAP approaches.

3.1.5 Example 3: MTS Tones in the MCARM Data:

Certain acquisitions within the MCARM database include signals from a moving target simulator (MTS) at known Doppler shifts. One of these acquisitions was used in Section 2.3.3 to illustrate the benefits of accounting for array effects. In acquisition 152 on flight 5, the MTS tones occur in angle bin 59. In this example, the look direction is set to angle bin 85 for a mismatch (with the MTS direction) and the JDL and hybrid algorithms are applied to the same acquisition. For this look direction, the MTS tones at angle bin 59 act as strong targets at a different angle bin, i.e. discrete non-homogeneities. As in Example 1, two cases are considered; no injected target and a weak injected target. The first case illustrates the suppression of the MTS tones acting as discrete, strong non-homogeneities. The second case illustrates the sensitivity of the hybrid algorithm to weak targets. This example uses all 128 pulses in the CPI, i.e. $N = 22$, $M = 128$. The emphasis parameter for the direct data domain method is set to a large value of $\kappa = (NM)^{3/2}$.

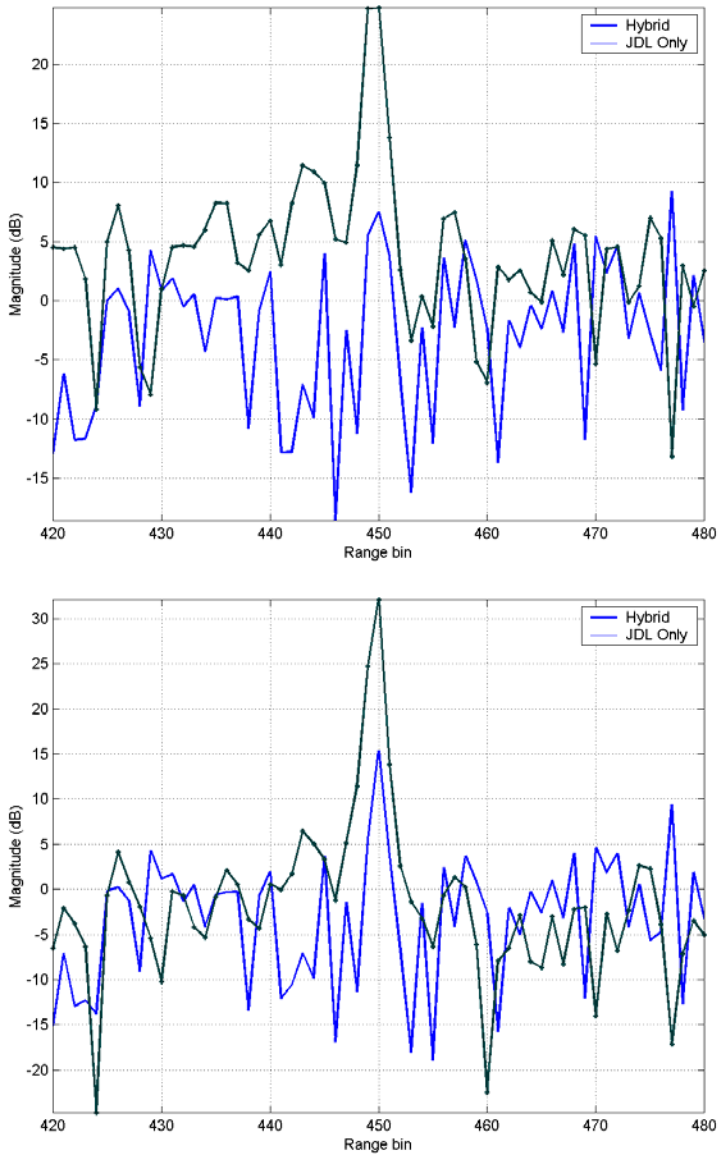

Figure 26: Performance of Hybrid algorithm in countering non-homogeneities: MTS Data (a) With Non-homogeneity, No target (b) With non-homogeneity, With target

In this acquisition, the MTS tones are in range bin 449-450 with the strongest tone at a Doppler corresponding to bin –53 and angle bin 59. The example focuses on the suppression of this tone. Figure 26(a) plots the MSMI statistic of the two algorithms for the case without any artificial injected targets. The JDL algorithm detects a large target at range bins 449 and 450. This false alarm is due to the strong MTS tone at angle bin 59 even though the look direction is set at angle bin 85. The hybrid algorithm, however, suppresses the strong MTS tone, showing no activity at range bins 449 and 450.

Figure 26(b) plots the results of using the two algorithms to detect a weak target injected into range bin 450. The parameters of the weak target are; magnitude: 0.0001, Doppler bin: -53, angle bin: 85. This weak target is easily detected by the hybrid algorithm with the statistic at the target range bin 9.8 dB above the next highest peak.

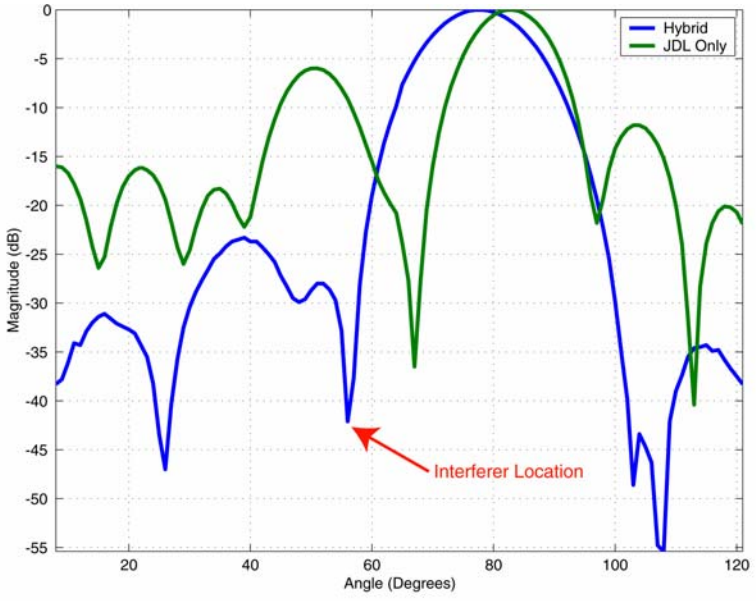

Figure 27: Beam Pattern associated with the Hybrid and JDL methods

The beam patterns associated with the two algorithms illustrate the improvement in using the D^3 algorithm as the first stage of a two-stage hybrid method. Figure 27 plots the spatially adapted beam pattern at the look Doppler frequency for the JDL and hybrid algorithms. The plot for the hybrid algorithm shows the deep null in the adapted pattern of the hybrid algorithm near angle bin 59 while the JDL pattern does not show such a null. In applying the JDL algorithm to the MCARM data acquisition with MTS tones, the strong tones leak through the sidelobes of the adapted pattern, leading to false alarms.

3.1.6 Summary

This section presented the hybrid algorithm, developed specifically for the non-homogeneous data case. Statistical algorithms cannot suppress discrete non-homogeneities because the secondary data possesses no information regarding such interference. The D^3 method, presented earlier, however can suppress such discrete interference. However, performance of D^3 algorithms in homogeneous interference scenarios is inferior to traditional statistical STAP algorithms. Each of these two approaches to STAP has its own area of application.

The proposed two-stage hybrid algorithm alleviates this drawback by implementing a second stage of statistical processing after using the D^3 algorithm as an adaptive transform to the angle-Doppler domain. This algorithm combines the advantages of both the statistical and non-statistical approaches. The D^3 method is particularly effective at countering non-homogeneous interference. The statistical STAP algorithm then improves on the suppression of the residual correlated interference.

Even with *ad hoc* compensation for mutual coupling, the hybrid algorithm shows a significant improvement over statistical methods in suppression discrete non-homogeneities. We anticipate a true evaluation of the mutual coupling would improve the performance of the hybrid algorithm.

3.2 Knowledge Based Processing

The field of Space-Time Adaptive Processing has received much interest in the past 30 years. The sum total of the research is extensive, with several classes of algorithms, some practical and others not so practical.

In addition, interesting new algorithms [16] and algorithms that address particular interference situations [17] are being continually developed. What is clear is that there is no single algorithm that is optimal in all interference scenarios. In a relatively homogeneous scene, an algorithm such as FA-STAP may be best, while in a non-homogeneous scene JDL may be the best or even possibly the D^3 algorithm in an extremely non-homogeneous case. All statistical algorithms require the estimation of a covariance matrix. In a non-homogeneous scene, the choice of the secondary data has a huge impact on the performance of the algorithm. It is essential that in a real world situation the secondary data be chosen properly.

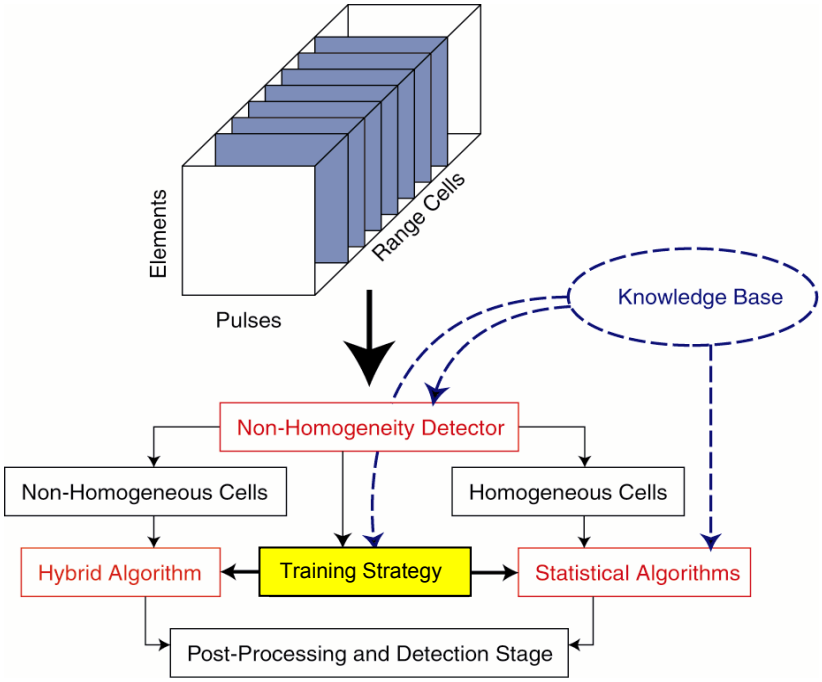

Figure 28: Knowledge Based Space-Time Adaptive Processing (KB-STAP)

This research therefore heads towards the concept of *Knowledge Based STAP* (KB-STAP). KB-STAP [18] chooses the best of several possible STAP algorithms for detection with knowledge-based control of algorithm parameters and selection of secondary data using NHDs. The basic elements of a comprehensive KB-STAP formulation are shown in Figure 28. Any comprehensive algorithm for practical implementation of STAP requires at least three elements: a non-homogeneity detector to separate the received data into homogeneous and non-homogeneous sectors, a statistical algorithm for use within the homogeneous sectors and a hybrid algorithm for use within the non-homogeneous sector. This section presents the performance improvements possible using such a combined scheme [19].

The combined approach is tested using data from the MCARM database. As described earlier, each CPI comprises the data corresponding to 22 digitized channels and 128 pulses at a PRF of 1984 Hz. The datacube comprises 630 range cells, sampled at 0.8μs. Each range bin, therefore, corresponds to 0.075miles. The array operates at a center frequency of 1.24GHz. Included with each CPI is information regarding the position, aspect, velocity and mainbeam transmit direction. This information is used to correlate target detections with ground features.

The example illustrates the issues addressed in this report, namely non-homogeneities and the use of the appropriate processing algorithm in appropriate portions of the radar data cube. Non-homogeneity detection is accomplished using JDL assuming homogeneous data. Any range bin with a statistic above a chosen threshold is considered non-homogeneous. The statistical algorithm is JDL again, though in the second stage only

homogeneous data is used in the sample support. The hybrid algorithm also uses only homogeneous data for sample support in second stage.

This example uses data from acquisition 575 on flight 5. While taking this acquisition the radar platform was at latitude-longitude coordinates of (39.379^o, -75.972^o), placing the aircraft close to Chesapeake Haven, Maryland, near the Delmarva peninsula. The plane was flying mainly south with velocity 223.78mph and east with velocity 26.48mph. The aircraft location and the transmit mainbeam are shown in Figure 29. The mainbeam is close to broadside. Note that the mainbeam illuminates several major highways.

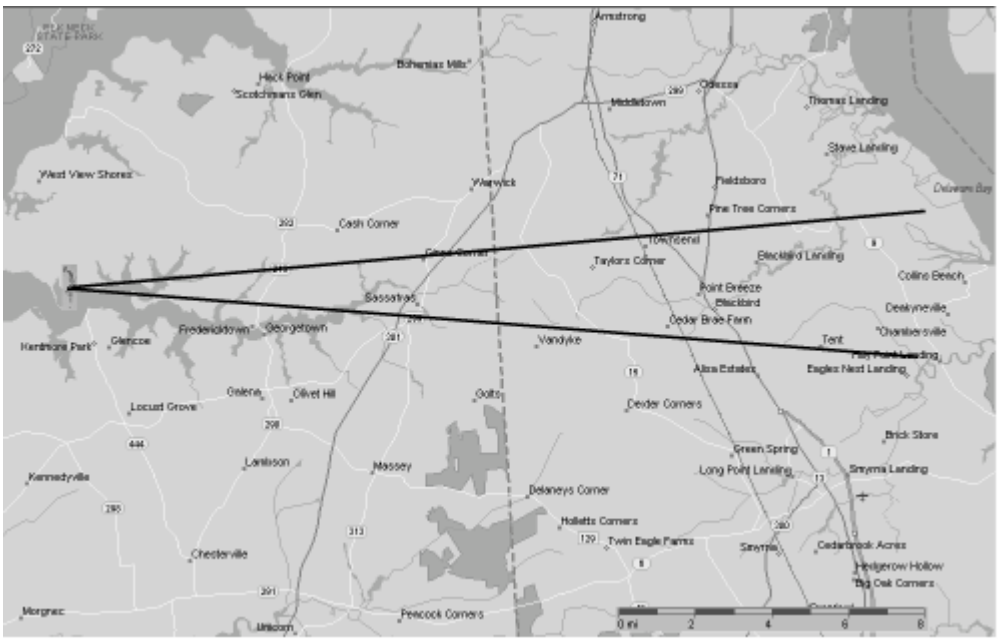

Figure 29: Location and transmit direction of the MCARM Aircraft during the acquisition

In addition to the targets of opportunity on the roadways illuminated by the array, we inject two artificial targets at closely spaced range bins to illustrate the effects of non-homogeneities in secondary training data. Based on the measured steering vectors and chosen Doppler shifts the response of the two simulated targets may be calculated. The artificial targets are injected in range bins 290 and 295. In this acquisition the transmit pulse is zero-shifted to range bin 74, i.e. the targets are at ranges of 16.2miles and 16.575miles respectively. The parameters of the injected targets are:

Table 3: Parameters of the injected targets

Target 1		Target 2	
Amplitude	1×10^{-4}	Amplitude	1×10^{-3}
Range bin	290	Range bin	295
Doppler	Bin –9 ≡ 137.5Hz	Doppler	Bin –9 ≡ 137.5Hz
Angle	1^o	Angle	1^o

Note that the two targets are at the same Doppler frequency and the second target is 20dB stronger than the first.

This example uses 3 angle bins and 3 Doppler bins (a 3×3 LPR) in all stages of adaptivity, including the JDL-NHD. Thirty-six secondary data vectors are used to estimate the 9×9 angle-Doppler LPR covariance matrix. In addition, two guard cells are used on either side of the primary data vector. Based on these numbers, without a NHD stage, range bin 295 would be used as a secondary data vector for detection within range bin 290. The example compares the results of using the JDL algorithm without non-homogeneity detection and the combined approach illustrated in Figure 28.

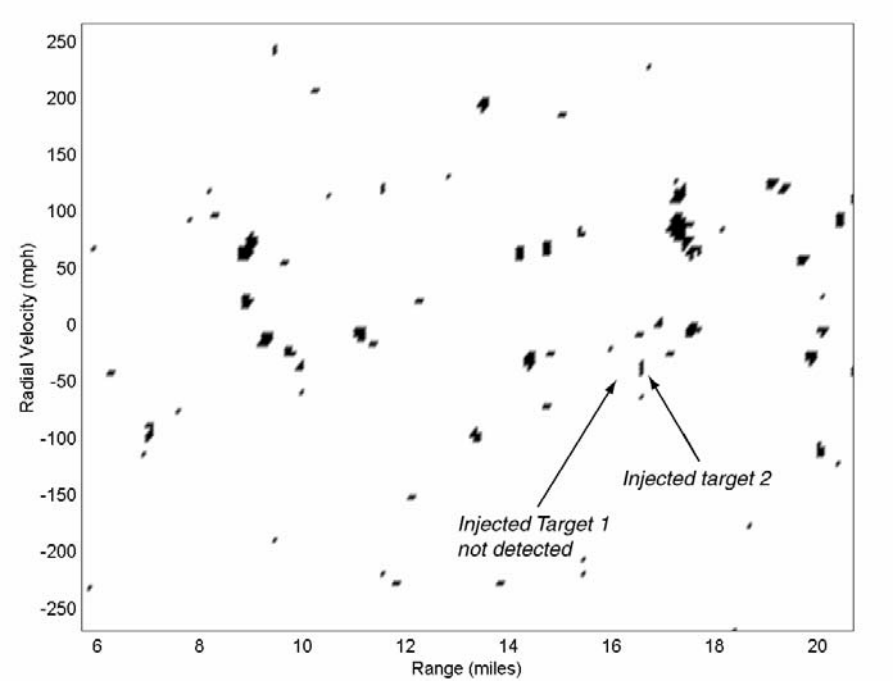

Figure 30 : JDL Processing without accounting for non-homogeneities

Figure 30 presents the results of using the JDL algorithm without any attempt to remove non-homogeneities from the secondary data support. The range-Doppler plot is of the MSMI statistic after applying a threshold. In producing this figure, a threshold of 40 is used, i.e. any Doppler-range bin with a MSMI statistic greater than 40 (amplitude not in dB) is said to contain a target while any Doppler-range bin with a statistic below 40 is declared target free. The plot is for adaptive processing between range bins 150 and 350, i.e. ranges between 5.7 and 20.7 miles and all 128 Doppler bins. Due to platform motion the radar is approaching the declared targets at a speed of 26.48mph.

As is shown later, certain range bins that are declared to contain a target can be correlated with the map in Figure 29 as corresponding to roadways. However, this approach results in several false alarms including several at extremely high radial velocities. In addition, the first injected target at range bin 290 is not detected. This is because of the presence of the larger target at range bin 295 in the secondary data when range bin 290 is the primary data.

Figure 30 clearly illustrates the need for a stage to identify non-homogeneities and eliminate them from the secondary data support. Applying STAP to measured data results in several false alarms and the possibility of targets in the secondary data masking weak targets. The processing structure of Figure 28 addresses this need.

In the implementation used in this paper, a JDL-NHD is used to identify non-homogeneous range cells. A range cell is considered to be non-homogeneous if the JDL-MSMI statistic is above 18.52, significantly lower than the threshold of 40 used to generate Figure 30. Assuming Gaussian interference, using 36 secondary data

vectors to estimate a 9×9 covariance matrix to obtain an MSMI statistic, this threshold corresponds to a false alarm rate of $P_{fa}=10^{-4}$. Note that the true false alarm rate using measured data is significantly higher.

The combined algorithm uses JDL processing in those cells declared homogeneous and hybrid processing in those cells declared non-homogeneous. Again, a 3×3 LPR is used, both in the JDL algorithm and in the Hybrid algorithm. In the second application of the JDL algorithm in homogeneous range cells, only other homogeneous cells are used for sample support. Within the non-homogeneous cells, a hybrid algorithm is used, i.e. the D^3 algorithm is applied 9 times for 3 angle and 3 Doppler look directions, *using the same primary data*. The angle-Doppler data so obtained is used for further JDL processing. Homogeneous cells are used to obtain sample support for the second stage JDL processing.

Figure 31 shows the result of using the combined approach. Notice the significantly fewer false alarms than in Figure 30 when using a purely statistical algorithm without non-homogeneity detection. In essence the hybrid algorithm is applied to all those range/Doppler bins where the JDL-MSMI statistic is greater than 18.52. The use of the hybrid algorithm suppresses the non-homogeneities thereby significantly reducing the false alarms.

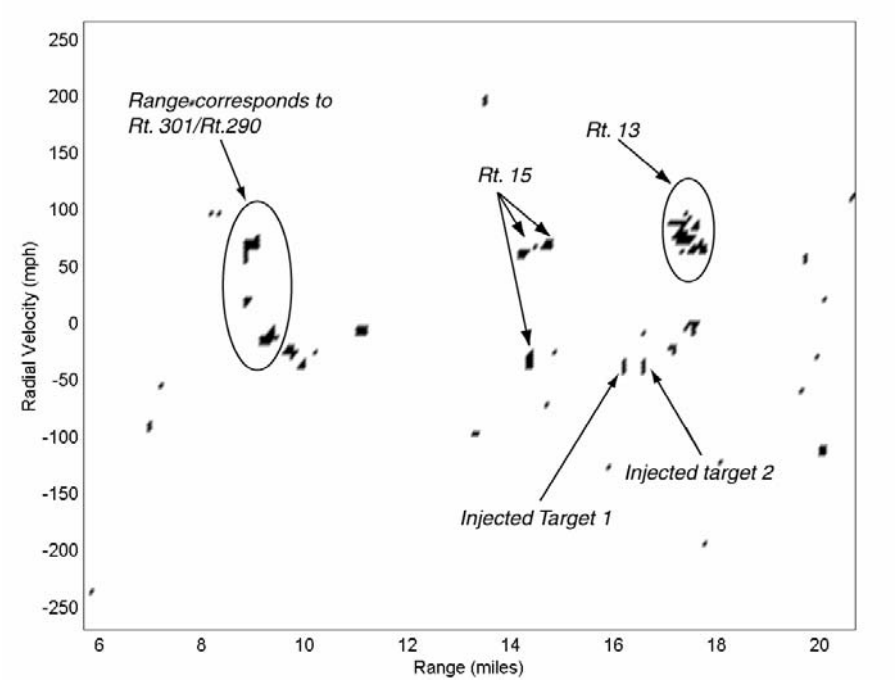

Figure 31: Combined processing accounting for non-homogeneities

In addition, the weaker injected target is detected since the stronger target at range bin 295 is eliminated from the sample support for range bin 290. Furthermore, the range bins of most target detections can be directly correlated with the state highways in Maryland and Delaware. Routes 299 and 301 in Maryland are closely spaced at a range of 9.0 and 9.8 miles. Note that the aircraft is moving due east at a speed of 26.48mph. The ground speed of the targets is therefore approximately 50mph towards and away from the aircraft.

The range of the several target detections at the far range shown in the plot, approximately 20miles, is not immediately attributable to Route 9 in Delaware. At broadside, Route 9 is at a range of 21 miles. The detected targets are between 19.4 and 20.4 miles. However, note that Route 9, north-south at broadside curves and has a short east-west section within the 3dB mainbeam. The distance to this section is between 19.1 and 20.6 miles. These targets are detected at these range bins and are present in both Figure 30 and Figure 31.

At a range of approximately 11 miles is a strong detection. Accounting for the aircraft motion, this detection has zero ground velocity. This corresponds to the town of Van Dyke.

This section has presented a comprehensive approach to STAP incorporating the essential elements of a practical scheme: non-homogeneity detection, a statistical algorithm for STAP in homogeneous cells and the hybrid algorithm for STAP in non-homogeneous cells. The example illustrates the importance of these concepts to the GMTI case. This scheme yields huge performance improvements over the traditional STAP algorithm, as applied to real measured data.

The next section presents a formulation to include *a priori* map data to enhance the KB-STAP concept.

4.0 GMTI-STAP Future Work

Sections 2.0 and 3.0 have presented past and on-going research on the transition of space-time adaptive processing from theory to practice. In particular, concepts including spatial DOF reduction, array effects, non-homogeneous data were presented, finally leading to the KB-STAP concept. Research on MAP-STAP significantly enhances KB-STAP, using *a priori* map data to inform the knowledge base. The adaptive processing concepts developed were applied to AMTI and GMTI.

This section presents proposed future work in the GMTI specific application. GMTI requires that additional attention be paid to the specific problem of low target velocity, with the target signal competing with mainbeam clutter.

4.1 D^3 $\Sigma\Delta$ STAP

This near-term task will develop and evaluate a specific algorithm designed to address both the clutter non-homogeneity and slow velocity issues. STAP has long been known to have hard-to-predict spatial response patterns including very high sidelobes in some interference-free regions, loss of mainlobe gain, and significantly shifted mainlobe gain. These mainlobe impacts will be of much greater importance when addressing the slower targets of the GMTI task and thus must be minimized. The high sidelobes in regions that are evaluated by the secondary data to be interference free will make the algorithm sensitive to even small clutter non-homogeneities. The excellent performance of the $\Sigma\Delta$ algorithm resulted from the low sidelobe of the sum and difference beam systems and the low gain of the difference beam in the direction of the target. These factors give the $\Sigma\Delta$ algorithm a more predictable response pattern.

The work proposed for the near term will be an attempt to combine the advantages of the previous hybrid STAP algorithm (Section 3.1) and the $\Sigma\Delta$ STAP algorithm (Section 4.1) to better address non-homogeneous clutter. In addition the delta channels will be chosen to minimize the impact of the adaptive process on the target return, that is, the low velocity issues.

The previous hybrid STAP algorithm employed a direct data domain (D^3) algorithm for the first stage to suppress discrete non-homogeneities in the range cell under test. This algorithm served as an adaptive transformation from the space-time domain to the angle-Doppler domain and was followed by a statistical STAP algorithm to filter residual correlated interference. The D^3 algorithm constrained the antenna gain in the direction of the target in angle and Doppler space. If the target is not exactly at the center of the antenna mainbeam the target return can be attenuated by this D^3 process. A version of the D^3 algorithm has been developed which maximizes the antenna gain across the antenna mainbeam to overcome this attenuation [21].

In this new algorithm a D^3 process will be developed to constrain both a sum beam and a difference beam across the transmit mainbeam and to use these sum and difference beams as the first stage of a hybrid algorithm with a statistical algorithm as the second stage. Multiple delta beams pointing in different angles within the sum beam will be investigated.

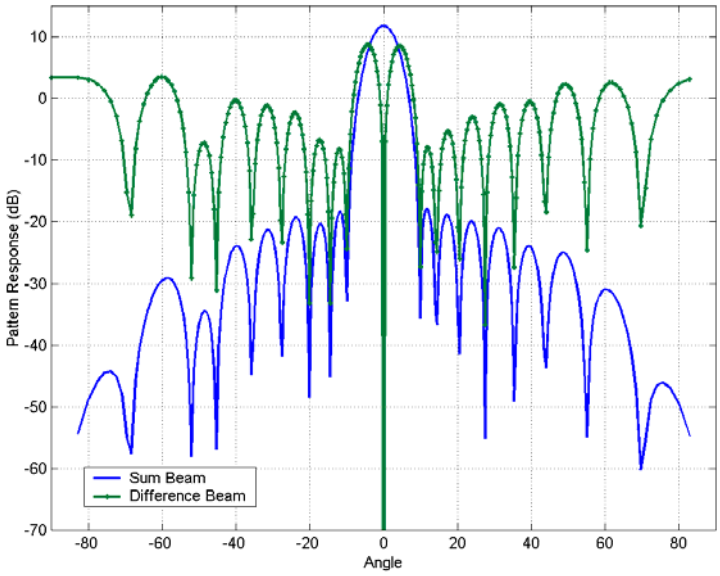

Figure 32: Sum and Difference D^3 Beam Patterns

The work of developing a rigorous formulation in evaluating these beams has only just begun. Figure 32 illustrates the results of a simple formulation extending the hybrid formulation to the $\Sigma\Delta$ case. The example presented uses 18 elements and 18 pulses in the CPI. An artificial non-homogeneity is injected at angle bin -51^o, while the look angle is maintained at 0^o. As can be seen, both the sum and difference channels place a null in the direction of the discrete interference, while maintaining the desired response at the look angle. The sum channel places maximal gain in the look direction, while the difference (delta) channel places a null at the look direction.

The results shown in Figure 32 are preliminary, but show the promise of investigating a D^3 $\Sigma\Delta$ STAP formulation. The work of formalizing the process of obtaining these sum and difference weights is on going and will continue in the near future.

In the longer term, this D^3 $\Sigma\Delta$ algorithm can be improved by incorporating two concepts: first, MAP-STAP can be used to determine the best data samples to be used for statistical processing in the second stage. Second, the location of the mainbeam clutter ridge is determined *a priori* by the motion of the aircraft platform. This information can be exploited by using a *constrained* D^3 algorithm which places a null (in the Doppler domain) at this mainbeam clutter location. This approach should improve the ability of the D^3 algorithm to suppress correlated mainbeam clutter.

4.2 Additional Algorithms

The major difference between GMTI adaptive filtering algorithm and the existing AMTI adaptive filtering work is that the clutter competing with the target is coming from angles that are in the antenna mainbeam or near-in sidelobes whereas AMTI clutter is at angles in farther out sidelobes. Thus the potential for significant impact on the target return is greater for GMTI than it was for AMTI. The focus of filtering algorithm development will be on algorithms that minimize that effect. Additional effort on hybrid algorithms with new versions of the D^3 algorithm for the first stage is planned.

Knowledge-based (KB) processing has been shown to improve both the filtering and detection stages of radar signal processing. In both cases the KB part of the processing is accomplishing similar functions: selection of optimum algorithm and selection of secondary data for the algorithm chosen. The integration of KB processing for the two stages including feedback from detection to filtering has potential for additional improvement in overall performance. Integrated KB adaptive filtering and detection/CFAR will be developed in future efforts.

4.2.1 Evolutionary Algorithms

The selection of the best STAP algorithm for a particular real-world environment is difficult because of the large number of possibilities and because the environment does not satisfy the independent and identical distribution condition that would make theoretical solution of the problem possible. Knowledge-based approaches that address the actual environment have been shown to perform better than theoretically optimum algorithms in these real-world environments. But these KB approaches can not be analyzed from basic principles and there are so many possibilities that comparison of all of them appears difficult.

Expert system and knowledge-based technology has also been shown to have significant payoff for the other steps in radar signal processing (detection/CFAR, tracking) in these same real-world environments [18]. Each step in the signal processing has been investigated separately and the algorithms tested for performance at that phase. Since there are dependencies between the performance in step of the processing of the previous steps, it seems reasonable that integrated KB processing with feedback between stages could have better performance than algorithms developed for each step separately. Integrated end-to-end signal processing will have a much greater number of algorithm options because more filtering algorithms can be combined with most detection algorithms and those combinations can be combined with most tracking algorithms.

5.0 References

[1] *M.C. Wicks, A Comparative Study of Space-Time Processing for Airborne Radar, Ph.D. Thesis, Syracuse University, May 1995.*

[2] *I.S. Reed, J. Mallet, and L. Brennan, "Rapid convergence rate in adaptive arrays",* IEEE Trans. on AES*, vol. 10, no. 6, pp. 853-963, December 1974.*

[3] *H. Wang, "Space-Time Adaptive Processing for Airborne Radar", in* Digital Signal Processing Handbook*, V. Madisetti and D. Williams* eds.*, CRC Press 1997.*

[4] *S.M. Sherman,* Monopulse Principles and Techniques*, Artech House, 1984.*

[5] *J. Maher, Y. Zhang and H. Wang, "Space-Time Adaptive Processing with Sum and Difference Beams for Airborne Radars,"* Proc. SPIE's 13th Annual International Symposium on AeroSense*, vol. 3704, pp. 160-169, Orlando, FL, April 1999.*

[6] *R.D. Brown, R.A. Schneible, H. Wang, M.C. Wicks, Y. Zhang "STAP for Clutter Suppression with Sum and Difference Beams",* IEEE Trans. on AESS, April 2000*.*

[7] *H. Wang and L. Cai, "On adaptive spatial-temporal processing for airborne surveillance radar systems",* IEEE Transactions on AES, *vol. 30, No. 3, pp. 660-669, July 1994.*

[8] *J. Ward, "Space-time adaptive processing for airborne radar", Tech.Rep. F19628-95-C-0002, MIT Lincoln Laboratory, December 1994.*

[9] *R.S. Adve, T.B. Hale and M.C. Wicks, "Joint Domain Localized Adaptive Processing in Homogeneous and Non-homogeneous Environments. Part I: Homogeneous Environments", To appear in* IEEE Proc. on Radar, Sonar and Navigation*. Accepted for publication November 1999.*

[10] *W.L. Melvin and B. Himed "Comparative analysis of space-time adaptive algorithms with measured airborne data", In* Proceedings of the 7th International Conf. on Signal Processing Applications & Technology*, Boston, MA, October 1996.*

[11] *D.K. Fenner and W.F. Hoover Jr., "Test Results of a Space Time Adaptive Processing System for Airborne Early Warning Radar",* Proc. IEEE National Radar Conference*, pp. 88-93, Ann Arbor, MI, May 1996.*

[12] *"Multi-Channel Airborne Radar Measurements (MCARM) Final Report", vol. 1 of 4, MCARM Flight Test, Contract F30602-92-C-0161, for Rome Laboratory/USAF, by Westinghouse Electronic Systems.*

[13] *H.H. Chang, "Improving Space-Time Adaptive Processing (STAP) Performance in Nonhomogeneous Clutter", Ph.D. thesis, Syracuse University, August 1997.*

[14] *T.K. Sarkar and N. Sangruji, "An Adaptive Nulling System for a narrow band signal with a Look Direction Constraint Utilizing the Conjugate Gradient method",* IEEE Trans. on AP*, vol. 37, no. 7, pp. 940-944, July 1989.*

[15] R.S. Adve, T.B. Hale and M.C. Wicks, "Joint Domain Localized Adaptive Processing in Homogeneous and Non-homogeneous Environments. Part II: Non-Homogeneous Environments", To appear in IEE Proc. on Radar, Sonar and Navigation*. Accepted for publication December 1999.*

[16] J.S. Goldstein, J.R. Guerci, I.S. Reed, "Advanced Concepts in STAP", Proc of 2000 IEEE International Radar Conference*, Washington, DC, pp.699-704, May 2000.*

[17] J.R. Guerci, J.S. Goldstein, P.A. Zulch, I.S. Reed, "Optimal Reduced-Rank 3D STAP for Joint Hot and Cold Clutter Mitigation", Proc. of the1999 IEEE National Radar Conference*, Boston, MA, pp. 119-124, April 1999.*

[18] P. Antonik, H. Shuman, P. Li, W. Melvin, M. Wicks, "Knowledge-based Space-Time Adaptive Processing", Proc. of the1997 IEEE National Radar Conference*, Syracuse, NY, May 1997.*

[19] R.S. Adve, T.B. Hale, M.C. Wicks, P. Antonik, "Ground Moving Target Indication Using Knowledge Based Space Time Adaptive Processing", Proc of 2000 IEEE International Radar Conference*, Washington, DC, pp.735-740, May 2000.*

[20] G. T. Capraro, C. T. Capraro, and D. D. Weiner, "Knowledge Based Map Space Time Adaptive Processing (KBMapSTAP)", AFRL-SN - unpublished final report.

[21] R. Schneible, "A Deterministic Least Squares Approach to STAP", Ph.D. thesis, Syracuse University, May 1996.

APPLICATION OF KNOWLEDGE-BASED TECHNIQUES TO TRACKING FUNCTION

A. Farina
Chief Technical Office
AMS (Alenia Marconi Systems)
Via Tiburtina Km. 12.400, 00131 Rome, Italy
e.mail: afarina@amsjv.it

Key words: tracking, knowledge based systems, knowledge based tracker, context data exploitation, A-SMGCS: Advanced Surface Movement Guidance and Control System, GMTI: Ground Moving Target Indication.

1. SUMMARY

This paper describes the application of Knowledge-Based System (KBS) to tracking. Section 2 paves the way to the new technology by discussing the following topics: historical survey of stochastic filtering theory; overview of tracking systems with some details on mono-sensor and multi-sensor tracking, evolution of filtering logics, evolution of correlation logics, and presentation of recent findings on non linear filtering (e.g.: unscented Kalman filter, particle filter) theory which go beyond the classical Kalman filtering. After this introduction to the current state of the art, Section 3 discusses the new technology referred to as "knowledge-based tracker": a tracker that exploits a-priori knowledge (e.g.: map data) to gain improved performance. Three applications follow: the first refers to the A-SMGCS (Advanced Surface Movement Guidance and Control System) for traffic control on the surface of an airport (section 4); in this case the target tracker is enhanced by exploiting the knowledge of the aerodrome map with runways, taxiways etc. The sensor is a high resolution surface based radar. The theme of section 5 is the tracking of ground moving or stationary vehicles using an airborne GMTI radar. Here we need to take care of the constraints imposed by the terrain (for which only uncertain data might be available), road networks and regions that could be not-trafficable. These information, also in this case, lead to finite support for the distribution of the target state; the classical Kalman filter doesn't work well and KBS tracker is needed. The last application (section 6) refers to tracking of airborne target masking itself in blind Doppler: these are Doppler frequency bands where the target cannot be detected due to the presence of MTI to reject ground clutter from radar echoes. This is a strategy that the pilot of an aircraft may implement to mask himself to an enemy radar. It is shown that particle filter can fruitfully exploit the a-priori information on blind Doppler thus keeping the probability of target track maintenance at a reasonable level also when the target pursues this masking strategy. An extensive list of references (section 9) is helpful to the Reader for a deeper insight to the many interesting topics of radar.

2. INTRODUCTION

The core of a tracking system is the filtering algorithm. The next section provides some historical notes on the stochastic filtering theory. Then an overview of the state of the art of tracker follows. Also more recent findings on stochastic filtering are discussed.

2.1 HISTORICAL SURVEY OF STOCHASTIC FILTERING THEORY

The well established discipline of estimation theory concerns the problem of deducing the values of a set of unknown parameters from the information given by set of measurements whose values depend on the unknown parameters. As a consequence, it provides valuable solutions to many practical problems in the fields of telecommunications, automatic control, signal and data processing, including tracking with radar and sonar. Estimation theory has its origin in the early work of Gauss [1] and Legendre [2] stimulated by astronomical studies. It was further developed by the contribution of Fisher [3], who introduced the concept of maximum likelihood estimate, and by Kolmogorov's subsequent assessment [4] of probability and random process

Paper presented at the RTO SET Lecture Series on "Knowledge-Based Radar Signal and Data Processing", held in Stockholm, Sweden, 3-4 November 2003; Rome, Italy, 6-7 November 2003; Budapest, Hungary, 10-11 November 2003; Madrid, Spain, 28-29 October 2004; Gdansk, Poland, 4-5 November 2004, and published in RTO-EN-SET-063.

theory. The relevant work by Wiener [5] introduced and solved the problems of linear filtering and prediction for stationary random processes, described in terms of their power spectral densities; Wiener afforded also the non linear filtering problem [6]. Y. W. Lee, a Ph.D. student of Wiener at MIT did relevant contributions on the explanation of Wiener's theory and tackled various engineering problems related to practical application of the work; for instance, He and His students realised the first analogue correlator machine built in 1940s for calculation of the first- and second-order correlation functions of signals required by the Wiener theory [7]. The mathematical difficulties underlying Wiener's solution motivated the research of a recursive time-domain approach, first by Levinson [8] and then by Kalman and Bucy [9], [10] who approached the estimation problem with modern system theory. They employed the concept of state-transition models for dynamic systems. A fundamental historical and theoretical review of linear filtering, which also provides extensive bibliography, is [11]; for R. Kalman biography see [12]. Probably it is less known the contributions that was given to the theory of stochastic filtering by Peter Swerling; recently Eli Brookner in his book [13] has dedicated an appendix ("Comparison of Swerling's and Kalman's formulation of Swerling-Kalman filters" , written by P. Swerling) to this aspect of the stochastic filtering history.

2.2 AN OVERVIEW OF TRACKING SYSTEMS

Surveillance is typically provided by a network of sensors (heterogeneous or not) (see figure 1): netting is deployed to extend the radar coverage, to increase the opportunity of detection and to increase the robustness of the track. In fact the viewing of a target from different aspect angles tends to reduce target fades, glint and terrain masking effects. In military applications, the possible frequency and spatial diversity, coupled with the ability to triangulate on jammers, provide electronic counter-countermeasure (ECCM) capability. In defence systems especially, various types of radar co-operate with other sensors such as infrared cameras, receivers for passive radio reconnaissance and laser systems. The combination gives rise to the so-called multi-sensor (MST) configuration. Depending on the level at which the merging of data is used, MST can be divided into the two following main classes: distributed and centralised. The distributed architecture (see figure 2) is characterised by the use of a computer at each site performing the mono-sensor tracking function on the measurements of a single radar. The mono-sensor tracks are then transmitted to a single data-processing centre which combines them in order to establish a single multi-sensor track for each target. The centralised architecture (see figure 3) is characterised by the use of a single data processor to which sensor measurements instead of tracks are transmitted from the sites. These measurements are processed so as to obtain a single multi-sensor track for each target. This architecture has the features of: reducing tracking errors because of the higher rate of sampling the target path, improves the robustness of the established track using tracking algorithms with variable data rate, requiring more powerful processing resources. A basic parameter to be considered in the selection of the architecture and the comparison of performance is the degree of overlap of the sensor coverage. If the degree of overlap is very small, the advantages of the data redundancy are limited, on average, to small areas and few targets. In this case the overall system performance is almost independent of the type of the architecture: thus the selection is mainly determined by the cost.

Mono-sensor tracking

In a radar (the sensor mainly considered in this paper) the cascade of signal processor, data extractor and data processor depicted in figure 4 is ultimately a bandwidth compressor. It receives data at a high rate (e.g.: the bandwidth of radar signal, which is in the order of also tens of MHz) and processes the signal in such a manner that a relatively low data rate (several Hz) is achieved. This feature is pictorially indicate by the narrowing of the arrows moving from the left to the right of the cascaded processors. At the same time, there is a progressive discrimination between useful and clutter/interference data, by means of a stepwise decision process. The information handled by the processing chain is progressively manipulated into a form which allows easier decision making by the user. In fact, the raw video signal contains many false echoes. The data extractor isolates the useful target and the data processor identifies the target (possibly labelled with a code), determines the target velocity and additional parameters which are presented on a tabular display. A further observation can be made regarding the increase of the time span in which processing is performed through the cascade. The signal processor involves only few pulses, the data extractor some adjacent groups of pulses and

the data processor consecutive radar scans. In other words, the memory of the processing increases on moving from left to right in figure 4 [14].

In this paper we will focus on tracking which is implemented in the data processor block of figure 4. Tracking, from a classical point of view, can be defined as the set of algorithms which, when applied to the radar detections acquired during successive scans, allows:

- recognition of a pattern of successive detections as pertaining to the same target,
- estimation of the kinematics parameters (position, velocity and acceleration) of a target, thus establishing a so-called "target track",
- extrapolation of the track parameters,
- distinguishing of different targets, also on the basis of additional attributes (e.g.: IFF: Identification Friend or Foe, shape, electro magnetic signature) and thus establishing a different track for each target,
- distinguishing of false detections (caused by intentional or natural interference) from true targets,
- adaptive refinement of the threshold setting of the signal processor in order to make the radar more or less sensitive in the different spatial directions, depending on the content of a map of false detections refreshed on a scan-to-scan base,
- scheduling of the track dwells of a phased-array radar in order to follow a manoeuvring target with constant accuracy and to interleave in an optimum manner the tracking phases with search looks and other radar functions,
- efficient managing of the detections and/or the tracks provided by the different radar sets of a netted system looking at the same portion of the controlled space, in order to provide a better picture of the latter.

The working principle of the classical tracking procedure can be explained as follows [14]. Tracking evolves through the following logic steps: track initiation, plot-track correlation, track prediction, track filtering, track termination. The interconnections among these basic tracking functions are shown in figure 5. First of all a track must be established (track initiation). An estimation of the initial kinematics state of the target (say its position and velocity) can usually be obtained from two consecutive target returns. The target velocity is obtained by the ratio of the position displacement to the radar scan time. This simple procedure is not reliable if false plots are present. It is then necessary to use a longer string of plots to initiate as tracks only those sequences that are consistent with the expected behaviour of target. On the next scan, it is desired, if possible, to capture the return signal from the same target and associate it with the track (plot-track correlation logic). Suppose the target to be moving with constant speed; the position of the target on the next scan can be predicted (track prediction logic) using the current estimates of its position and velocity. However, there may be inaccuracies in these estimates, and there is also a random element due to plot noise in the position at which the plot is expected to occur on the next scan. Thus, in searching for the next target return, allowance for these errors must be made. This can be achieved by deploying a search area centred on the predicted position; a plot found within the search area is associated with the established track. The size of the search area is determined by estimates of errors in position and velocity, as well as by the amount of plot noise. The search area must be large enough to render it highly probable that the next target return will fall inside it. But also, its size should be kept minimal, since if false plots are present, a large search area will on average capture more false plots. This aggravates association problems since in the event that more than one plot falls inside the search area, it is not known which plot emanates from target. The above search procedure applies only to non manoeuvring target. The approach is simply extended in principle to allow for target manoeuvres. Some limits on target's capacity to manoeuvre are assumed; in the simplest case, this may merely be its maximum acceleration. The manoeuvring capability of target can be expressed as a manoeuvre gate surrounding the predicted position, such that, ignoring effect of estimation and plot noise errors, the target must be found at some point inside this gate on the next scan. There are now two sources of discrepancy between the predicted position and the actual position of the next target plot, namely: that due to estimation errors and noise, and due to possible manoeuvres. The total search area should be formed by allowing for the occurrence of the worst discrepancies from each of these sources – loosely speaking, the noise gate (i.e. the search area used for a non-manoeuvring target) and the manoeuvre gate are "added" to obtain a final search gate. Assume that the next target plot is successfully associated with the established track. It now remains to update and improve the estimates of the target's position and velocity using the newly acquired plot (track filtering logic). This operation is

accomplished by a digital filter which determines the error between the measured and predicted position of plot and presents the smoothed position and velocity of the target at the output. Details on plot-track correlation and filtering logics are given in the following. The evolution of smoothing and correlation logic runs in parallel with the continuous increase in availability of computer processing power.

Evolution of filtering logic's

A list of techniques is the following: $\alpha-\beta$ filter, fixed weights filter, variable weights filter, Kalman filter, IMM (Interactive Multiple Model) filter. The use of fixed-parameter filters avoid the necessity of iteratively calculating new coefficients at every scan and thus greatly reduces the computational load of the filter. This is the first algorithm employed to track a target and, on account of its simplicity, is still used in practical applications, however its performance might be poor. Variable weights filters take into account the prediction uncertainty of the track in its different life stages and generally produce acceptable performance: gains are pre-evaluated and stored in a look-up table so that computational requirements remain low. They assume a constant measurement error and a fixed update interval. The Kalman filter (the successor of the Wiener filter) is a non-stationary filter in which both the estimate and its covariance are described by recursive equations. The Kalman filter can be suitably implemented by a feedback scheme embedding a replica of the system model. Weights are evaluated on line and take into account measurement and prediction errors: the derived load is definitely higher than that of the previous techniques. Adaptivity to sudden changes in the system model (e.g. manoeuvres,..) is a fundamental quality of a filter, i.e. the capacity of providing good filtering of measurement noise (which can be achieved with a narrowband filter) and simultaneously promptness in following sharp manoeuvres (wide bandwidth). Adaptivity at this point requires some kind of manoeuvre detector to determine the onset time of the manoeuvre and heuristics to quickly accommodate the parameters of the filter to the sudden change (see figure 6). When the position displacement d (|associated plot - predicted state|) is larger than a threshold T (dependent on the noise level), the Kalman filter gain K is suitably increased of a quantity dependent on the displacement. The multiple model (MM) and its more powerful successor, the IMM filter, have intrinsic adaptivity (see figure 7). IMM is a variable bandwidth filter which automatically adapts to target dynamics: it requires the selection of a set of models representative of target motion. The IMM algorithm selects each time the combination of the target models which best fits the measurement data and by appropriate mixing of these different models, each of which is a Kalman filter, it produces the best representation of the target model. IMM has been conceived by H. Blom and Y. Bar-Shalom [15]; further evolution of the theory has produced the variable-structure (VS) IMM [16] which will be used in the following sections 4 and 5.

Evolution of correlation logics

A list of techniques is the following: nearest neighbour (NN), local optimum, global optimum, PDA (Probabilistic Data Association), JPDA (Joint Probabilistic Data Association), Multi-scan correlation (MHT: Multiple Hypothesis Tracking). Nearest neighbour solutions are still widely used and attractive for their low computational requirements: a global optimum approach must certainly be preferred. However they suffer from severe drawbacks in dense and noisy environments. JPDA was developed as a way of achieving acceptable performance in dense clutter environments. Miss-correlation is effectively contrasted by evaluating the probability of each plot-to-track association and then updating the track with a weighted sum of the plots. The approach is time consuming and so many sub-optimal schemes have been developed to reduce its computational load. Multi-scan approaches are certainly the most performant: they allow to defer the final association decision until data relative to subsequent scans is available. They are time consuming since a set of hypotheses over several scans is maintained for each track. Combinatorial optimisation and more powerful processors make multi-scan approaches now feasible.

Most tracking systems in use today employ some type of nearest neighbour correlation and $\alpha-\beta$ adaptive or Kalman filtering with manoeuvre detection. These logics have been refined and improved through the years and produce a sound and consistent picture of the area under surveillance. In order to exploit the additional processing power now available, sophisticated though time consuming algorithms are being investigated, benchmarked and used in practice. IMM, JPDA, MHT and combinations of these techniques represent the new

avenue to pursue. In air defence applications, correlation is the greatest concern. Miss-correlation can completely invalidate the filtering process and so resources should be focused on the data association problem. A computationally intensive MHT algorithm (see figure 8) coupled with simple yet efficient dynamic modelling of target motion has been extensively tested. Manoeuvres are modelled by increasing the process noise of the target model. Several levels of gating are performed to cut down processing time. Results show that the load deriving from an MHT approach can be mastered [17], [18]. In air traffic control applications, correlation is less critical and so resources may be concentrated on the filtering. More accurate modelling of target dynamics (for instance, via IMM and VS-IMM) can improve the kinematics estimates, even though the improvement is dependent on the quality of data.

The performance of the newly-conceived IMM + MHT solution [19], [20] has been investigated: the algorithm seems very promising and its performance should be more than simply the mere combination of the advantages of IMM and MHT, due to the tight coupling of the filtering and correlation components. A diagram of the IMM-MHT tree is shown in figure 9: the tree is a multi-layer tree, with one separate layer for each model of the IMM filter; each layer interacts with all other layers relatively to the same plot according to the IMM logic; multi-layer fusion is enforced, i.e. for each sequence of plots the result is a unique track hypothesis and its scoring is a weighted average of the likelihood at the different layers. The whole IMM + MHT solution provides a flexible framework which can be adapted to the application at a superior level, e.g. in a civilian applications reducing the depth of the multi-scan technique and increasing the number and the modelling of targets and in a defence application the depth of the multi-scan technique can be increased and the modelling made accurate as appropriate. The customisation is also dependent on the available processing resources. IMM plays a relevant role also in the identification phase of surveillance; more precisely, tracking and identification can be jointly performed as explained, for instance, in [21].

Multi-sensor tracking

This is a lively area of research and practical applications. References [22] and [23] illustrate the principle and design of architectures like the ones depicted in Figures 2 and 3. Reference [22] also reports one of the first practical implementations of multi-radar tracking for air traffic control systems in late ‘70s and early ‘80s. Application of tracking to multistatic radar systems is described in [24]. More recent investigations dealing with fusion of radar track and ESM (Electronic Support Measures) tracks are reported in [25] to [28].

2.3 BEYOND KALMAN FILTERING

This section illustrates new recent findings in non linear stochastic filtering theory that are beyond the classical Kalman filter theory. Here we summarise recent findings in non linear stochastic filtering theory that go beyond the classical Kalman filtering; these results allow us to deal with filtering problems characterised by non linear dynamic state equations as, for instance, in the case of tracking a ballistic missile on re-entry (see: [29] to [32]) and to tackle non linear measurement equations as, for instance, in the bearings only tracking problem [33]. The general problem of non-linear non-Gaussian has the optimum estimation which requires the calculation of the entire probability density function (pdf) of the dynamic state $\mathbf{x}_k$ conditioned to the whole set of available measurements $\mathbf{Z}_k = \{\mathbf{z}_1, \mathbf{z}_2, ..., \mathbf{z}_k\}$. To this end one should solve a non-linear stochastic partial differential equation (the Fokker-Plank-Kushner equation); this task is practically impossible except for few cases as the linear-Gaussian that brings to the Kalman filter and the Benes filter [34] which is a truly non linear case. In general, it is necessary to resort to analytical approximation; the most used is the Extended Kalman filter (EKF) which, however, can perform poorly in some cases. A modern and more powerful approximation is the Unscented Kalman filter (UKF); another approach which is truly close to the optimum is the particle filtering (PF). In the following a summary of the UKF and PF is offered.

Unscented Kalman filter

Similar to EKF, the UKF is a recursive minimum mean square error (MMSE) estimator. But unlike the EKF, the UKF does not approximate the non linear equations (dynamic and/or measurement). Instead it uses the true non linear model and approximates the pdf of the state vector [35]. This density, however, is still assumed

Gaussian (in reality it is not, because of non linear dynamics/measurement equations) and is specified by $2n_x+1$ deterministically chosen samples or sigma points (n_x being the dimension of the state vector). The choice of the sigma points guarantees an accurate prediction of the mean and covariance up to the third order for Gaussian priors. The prediction step of the UKF is performed as follows. The unscented transformation [35] first computes the sigma points based on the values of the filtered state vector and the corresponding covariance matrix: $\hat{\mathbf{x}}_{k/k}, \mathbf{P}_{k/k}$. The sigma points are then propagated through the non linear functions and from them the predicted state and its covariance are computed. An application example of UKF is the tracking of ballistic target on re-entry where only the dynamic equation is non linear [29].

Particle filter

Sequential Monte Carlo (SMC) methods lead to estimate of the complete pdf. The approximation is centred on the pdf rather than compromising the state space model. They are known as particle filters, SIR (sequential importance re-sampling), bootstrap filters, Monte Carlo filters, condensation etc. The PF estimates the entire posterior density of the state vector as it evolves over time. PF has the advantage of being able to handle any functional non linearity and system or measurement noise of any distribution. As the number of random samples used in the filters becomes very large, they effectively provide an exact, equivalent representation of the required pdf. Estimates of moments (such as mean and covariance) or percentiles of the state vector pdf can be obtained directly from the samples. The MMSE estimate is then calculated as the mean of the posterior density. The central idea is to represent the required density by a set of random samples (particles) [36], [37]. As the number of particles grows to infinity, the representation of the required density becomes exact. In practice we work with a finite, preferably small number of particles, and the optimality of the PF is lost. Nevertheless in many practical applications the PF has demonstrated superior performance compared to other non linear filters [32] and [38]. Let the posterior density $p(\mathbf{x}_k, \mathbf{Z}_k)$ be represented by a set of random samples (particles) $\mathbf{X}_k = \{\mathbf{x}_k(i) : i = 1,2,...,N\}$. The PF is an algorithm which propagates and updates the set $\mathbf{X}_k$ to a new set of random samples $\mathbf{X}_{k+1}$ which is approximately distributed as the posterior density $p(\mathbf{x}_{k+1}, \mathbf{Z}_{k+1})$. The particular PF scheme we have tested, for instance in [32], is based on the sequential importance re-sampling scheme [36] with the regularisation step to avoid impoverishment problem [39]. In the prediction step, all the N particles from $\mathbf{X}_k$ are passed through the state equation. The weights associated with each predicted particle are computed as the normalised likelihood based on the observation $\mathbf{z}_{k+1}$. In the re-sampling step, the predicted particles are jittered using the Epanechnikov kernel and selected with the probability equal to their weights [39]. Note that for the case of non linear dynamics and linear measurements (as in the case of tracking a re-entry ballistic target), one could design a more efficient PF based on the optimal importance density [37]. Note also that the KF corresponds to (one) particle filter. Other examples of PF applications are: tracking in clutter, tracking with intermittent decoys, group target tracking, bearings only tracking, multiple target tracking and data fusion [40], etc. Some of the PF capabilities are: the algorithm is parallelisable, incorporates realistic models, incorporates prior and context information (terrain shadowing, manoeuvre capabilities), integrates with decision processes [41]. One problem that the PF has is the computational load much higher than the one related to EKF and UKF. To have a flavour of the computational load of PF with respect to EKF and UKF refer to the tracking of ballistic target [29]. A thorough analysis of the computational load of PF and how to mitigate the curse of dimensionality with a careful design of PF is reported in [42].

Cramer-Rao lower bound for non linear/nonGaussian filtering problems

Non linear filters based on approximations generate estimates which are more or less affected by these approximations and deviate from the ideal exact solution. Quality evaluation of the non linear filters is a complex problem of non linear estimation. The knowledge of a lower bound for the mean square error of an estimate can give an indication of estimator performance limitations, and consequently it can be used to determine whether imposed performance requirements are realistic or not. It can also assist in ranking the approximated solutions at hand. Cramer-Rao (CR) bound, defined as the inverse of the Fisher information

matrix is an extremely useful tool in the estimation of constant and deterministic parameters. The CR bound can be applied also to the estimation of random parameters. More relevant is a recent result which refers to the recursive calculation of the CR for stochastic processes in the frame of non linear/non Gaussian filtering theory [43]; an extension of the theory also to dynamic systems with unknown parameters is described in [44]. A further extension to the case in which the measurement is achieved with detection probability less than 1 is reported in [45]. Applications of this theory to practical filtering problems are described in [34] and [29] to [31].

References on tracking

A number of key texts to which the Reader can refer for deeper analysis on target tracking are the following. In addition to [14] and [22], perhaps the first text on target tracking, more recent books are [46] to [50] just to mention a few. Publications on tracking frequently appear on the Trans. of IEEE-AES, on the Proc. of IEE-RSN and on Information Fusion (Elsevier). Conferences that contain papers on tracking are those on radar organised by IEEE and IEE; also the recent series of "Fusion" conferences promoted by the International Society for Information Fusion (ISIF) is rich of such type of papers.

3. KNOWLEDGE BASED TRACKER

Let distinguish between tracking of ground moving targets and tracking of flying targets (aircraft, helicopters, etc.). Theory and application examples are developed for both cases: Sections 4 and 5 are devoted to tracking of surface moving targets, while Section 6 refers to tracking of aircraft. Prior information that can be exploited are map features used to predict shadowed areas in the target flight path, to compute the likelihood of a target manoeuvre to avoid known obstacles (e.g.: turns to avoid elevated terrain) and correlate target paths with road and rail maps. Shadow regions may be due to jamming, line of sight blockage, severe clutter, ground traffic, tangential target velocity (i.e.: portion of track perpendicular to radar line of sight to create zero Doppler region, see Section 6), etc.

The intelligent control of surveillance radar system has great potential in many aspects such as resource allocation and management, signal processing and tracking [51]. Air Force Research Laboratory in US has been among the first R&D institution to prove in 1989 the efficacy of knowledge based tracker (KBT) showing improved tracking performance through the use of external knowledge sources. The KBT receives detections, target, clutter, jammer and contextual information: these are exploited to select track filtering algorithms and correlation gates. One question of interest is to which degree the knowledge about local radar environment could enhance the ability of the tracking processor to maintain multiple tracks through areas of shadowing, clutter and other sources of interference. Also it is important to define knowledge-based rules for the KBT. Both questions have been answered by Air Force Research Laboratory in US; here we report a brief account of some of the findings described in [51], [52] and [53].

KBS allows us to use *proactive tracking* in lieu of classical *reactive tracking*. Proactive tracking anticipates target manoeuvres due to obstacles, coasts tracks in shadowed regions, identifies possible ground moving targets and clutter discrete. A manoeuvre anticipation rule was developed and tested using a priori map information of target's proximity to an obstacle, 1g manoeuvre was added into tracker's plant covariance matrix several scans before the tracker would normally respond to the target's manoeuvre. The resulting performance of proactive tracker was seen to be superior to the normal reactive tracker operating on the same data. Not only were the peak, mean and standard deviation of tracking error smaller, but the stability of the proactive filter was also better [51], [52] and [53]. In more general terms, the proactive tracker uses information from sources such as digital terrain maps, radar clutter and interference maps, and target priority assessments to determine the nature of the threat, evaluate the local environment, anticipate the target's actions, and enhance the prediction of target's location for the next radar observation. A conventional tracker reacts to target manoeuvres, missed detections etc. As a consequence, there can be significant errors in the predicted target location, especially when manoeuvres occur. Additionally, the uncertainty ellipsoid about the predicted target position will become large if data-to-track association cannot be made. This will result in

correspondingly larger target acquisition windows for subsequent scans, which can cause incorrect data-to-track associations and susceptibility of false alarms, and will require the use of additional radar resources for maintaining target tracks. Here a comparison between reactive and proactive trackers. The reactive tracker is characterised as follows: uncertainty ellipses remain small before manoeuvre begins, position errors become large during target turns, manoeuvre gate is triggered by poor prediction of target location, Kalman filter gain remains high for significant length of time. As opposite the proactive tracker is characterised as follows: Kalman filter gain is increased earlier manoeuvre begins, ellipse area is initially larger than for reactive tracker, there is a quick recovery after manoeuvre. Rules are also developed for multi-target association logic. In the case of proactive tracker the association logic uses local environment data and includes manoeuvre hypothesis; in the case of reactive tracker the association logic normally uses the nearest report assignment for the track [51], [52] and [53].

Concerning the correlation gates, three types have been devised. 1st type: single elliptical gate centred on the predicted point and oriented along range/cross-range. Its size depends on both measurement error and selectively injected manoeuvre noise that is added to the prediction covariance matrix. Association occurs when the measurement falls within the gate. 2nd type: two gates are used: a measurement gate (oriented along range/cross-range, its size depends only on measurement noise) and a manoeuvre gate (oriented along track/cross-track, its size depends only on the prediction covariance matrix). Association for this case occurs when the measurement falls inside either gates. 3rd type: it is similar to the 2nd type with the exception that measurement gate is positioned on the measured data point and manoeuvre gate is centred on the predicted position. Association occurs when the measurement ellipse intersects the manoeuvre ellipse.

The following data are available to KBT: measured target coordinates, target priority, digital topography and terrain cover maps with road overlays and locations of large stationary discrete, clutter maps generated by the radar providing absolute clutter-to-noise power ratio data and detection threshold relative to system noise level overlays, radar parameters, tracking data from other sensors (including radar, IFF, ESM, GPS). These data are stored in a data base which is dynamic because the data will change with time and need to be updated.

The KBT functional flow is sketched as follows [51], [52] and [53]. 1. detection validation: test for discrete, ground traffic, etc. from map information of highways, railways, digital terrain models and geographic information system. 2. potential manoeuvre contour: determine locus of points that defines physically possible target manoeuvres. 3. anticipated manoeuvre conditions: evaluate data base to identify conditions for which target manoeuvre will probably occur. Adopt KBT by increasing filter gain prior to manoeuvre. 4. deterministic manoeuvre conditions: evaluate data base to identify conditions for which manoeuvres must occur. Position data-to-track association windows accordingly. 5. coast/demote track state: base decision for state demotion on data base information (CFAR level, obscuration, etc.). 6. update data base: performed at end of every radar scan.

Here an example of few (out of some tens) knowledge based rules. *Manoeuvre/obstacle rule*: both α–β and Kalman filters do a good job with targets that move along a constant heading with a fixed speed. Deviation from a straight path cause prediction errors to occur and can ultimately result in a dropped track. Therefore it is important, whenever possible, to anticipate target manoeuvres by several scans. This allows time to make such adjustments as increasing the gate size and filter gain, or using shaped gate to allow for across track deviations cause by target turning. If a target approaches an obstacle whose across-track extent is H, a manoeuvre can be anticipated to occur within a time extent no longer than T_{max}. Assume a constant target speed v and a maximum possible acceleration A_{max}, this extent is: $T_{\max} = \frac{\rho}{v}\cos^{-1}(1-\frac{H}{\rho})$ where $\rho = \frac{v^2}{A_{\max}}$ denotes the radius of curvature of a target turn required to clear the obstacle. Somewhere within this time period the tracker should apply its manoeuvre logic. *Shadow rule*: provides a means of preserving firm tracks that enter regions shadowed from radar line of sight. If the predicted track gate centre falls within a designed shadow region, both the track state and the gate size are frozen. Upon emerging from shadow the state promotion resumes and the gate size will not be allowed to exceed a maximum value. *Discrete rule*: by tagging large radar returns, or discrete, the radar processor can exclude regions containing them from its covariance matrix element formation and thereby not use up limited degrees of freedom on their cancellation. The discrete rule allows the tracker to coast through

any region containing one of these tagged returns and to essentially ignore it. If a known discrete falls within a track gate, that track will be treated as if in a shadow and will not be updated.

The performance of KBT are measured by: number of correct tracks, number of dropped tracks, number of incorrect tracks. Based upon these numbers and the contextual data the KBT will adjust its rules and thresholds to increase its performance. A suitable knowledge based controller incorporates software to dynamically update the knowledge domain data base to indicate object identifications and level of confidence and to extract features.

The KBT provides the system's knowledge based controller with: 1) a very accurate prediction of each target's location and kinematics for an ensuing radar dwell, and 2) knowledge of target's line of sight visibility, the competing clutter conditions and interference at the predicted location so that the optimal radar parameters and adaptive processing algorithm can be applied.

4 APPLICATION TO A-SMGCS

The Advanced Surface Movement Guidance and Control System (A-SMGCS) is an integrated airport management system consisting of different functions (surveillance, control, guidance and routing) to support the safe, orderly and expeditious movement of aircraft and vehicles on aerodromes under all circumstances with respect to visibility conditions, traffic density and complexity of the aerodrome layout. Figure 10 depicts the scheme of a generic A-SMSGCS with several heterogeneous sensors (radar, GPS, multilateration) to acquire kinematical and feature information on moving aircraft and vehicles (bus, car) on the surface airport.

Surveillance function is an essential element of any A-SMGCS. A combination of visual surveillance, Surface Movement Radar (SMR) and voice messages is currently used by controllers to monitor all movements. The monitoring of aircrafts and vehicles is also currently a significant function performed by pilots and vehicle drivers. As visibility reduces, the ability of controllers and pilots to carry out visual surveillance becomes increasingly impaired. Problems for controllers become significant when the movement area cannot be adequately seen from the control tower. For pilots and vehicle drivers their capability becomes seriously impaired when the visibility falls below 400 m. Improvement of surveillance function to overcome the above mentioned problems is one of the key requirements of an A-SMGCS. The surveillance therefore should provide identification and accurate positional information of all movements in the area, consisting of apron (area on an airfield for manoeuvring or loading), the manoeuvring area and runway strip.

The above surveillance requirements are challenging because of the A-SMGCS environment: airports have many obstacles that might block the line of sight causing blind spots and shadows, there are different targets (aircrafts and ground vehicles), different target dynamics, minimal distance between targets, presence of ground, weather and angel clutter (e.g.: due to slow moving flocks of birds), presence of spurious phenomena like multipath, target glint, reflections (typical reflectors are ground obstructions such as aircraft hangars, apron and terminal areas, buildings, towers and adjacent hills or mountains) and target echoes from cars and trains on the roads and railways close to the airport. In this scenario a traditional ATC (Air Traffic Control) tracking algorithm [14] is not sufficient to avoid the growth of false tracks (generated by false plots), ghost tracks (tracks initiated on object target reports and updated with false target reports), swap tracks (tracks updated with plots corresponding to a different object, which occur when two or more objects are in close proximity) and flying angel tracks (primary radar echo caused by a moving atmospheric refraction, atmospheric in homogeneity, insects, birds etc.).

For these reasons, the tracking algorithm of the A-SMGCS needs to be improved, and the following steps are tackled: upgrade the single sensor tracking algorithm; improve the multi sensor tracking performance by a suitable fusion of the data provided by the different A-SMGCS sensors deployed in the aerodrome. This section illustrates an enhancement of the single sensor tracking algorithm. The upgrade is based on the exploitation of the knowledge of airport map data into the tracking algorithm itself. In an airport, the radar targets (aircraft, vehicles) move along the road and runway network. The result is a constrained target kinematics depending on the target state: i.e. when the target is on the airport surface, its position indirectly

contains also some kinematical information; this knowledge can be exploited by the tracking algorithm to reduce the uncertainty of the target state and consequently to improve the accuracy of the predicted target state.

The tracking algorithm can then include the road local configuration to improve the tracking prediction phase ([54], [55]). To include constraints, the Interactive Multiple Model (IMM) approach can be considered ([17], [20] and [56]). The IMM enriches the class of Multiple Model (MM) approach to tracking. The MM methods are based on the fact that the behaviour of the target cannot be properly characterised by only one model during all the time; rather, a finite number of different models should be taken into account. The interaction between the different models is controlled by a transition probability matrix.

However, the constrained IMM approach to the A-SMGCS tracking brings to the simultaneous use of large number of different models because of the complexity of the road network and of the possibility of several different target manoeuvres on the whole airport area. If the constraints due to the road network are used, the classical IMM approach is not suitable, because it brings two problems: (i) if the number of models is too high, the IMM does not work properly because the interaction between the models induces a sensible performance degradation; (ii) the computational load grows with the number of models and it could be unaffordable.

A Variable Structure IMM (VS-IMM) ([16], [54] and [57]) can be used to overcome these two problems. The VS-IMM algorithm is an IMM with a variable set of models and a variable transition probability matrix. The set of models and the transition probabilities of the VS-IMM are updated taking into account the map of the airport and the tracking estimation of the previous step. Each model has associated a section of the airport area in which it is active and, during the tracking of a target, only a few models corresponding to the possible local kinematics are active, reducing the performance degradation due to the model interactions and the computational load of the classical IMM algorithm.

A VS-IMM tracking algorithm, based on the knowledge of the road network of the airport, has been considered in a realistic simulated A-SMGCS scenario; in [58] it has also been applied to real data recorded in the Malpensa (It) airport. The performance of the VS-IMM has been compared to the ones obtained by other tracking approaches, like the classical EKF (Extended Kalman Filter) and two IMM algorithms with different number of constrained models.

Unconstrained tracking

The state vector $\mathbf{s}(k)$ of the EKF includes the position of the target in the Cartesian coordinates, the velocity in the polar coordinates and the turn rate:

$$\mathbf{s}(k) = \left[x(k) \quad y(k) \quad v(k) \quad h(k) \quad \dot{h}(k)\right]^{\mathrm{T}} \tag{1}$$

where x and y represent the target position, v is the module of the velocity, h is the heading and $\dot{h}$ is the turn rate. Technical literature shows that the choice of this set of variables brings to good performance [59]. The target kinematics is represented by the following system of discrete time not linear equations:

$$\begin{aligned} \mathbf{s}(k+1) &= \mathbf{A}(\mathbf{s}(k)) \cdot \mathbf{s}(k) + \mathbf{w}(k) \\ \mathbf{z}(k) &= \mathbf{H} \cdot \mathbf{s}(k) + \mathbf{n}(k) \end{aligned} \tag{2}$$

where: $\mathbf{A}(\mathbf{s}(k))$ is the following not linear transition matrix (T is the radar scan time):

$$\mathbf{A}(\mathbf{s}(k)) = \begin{bmatrix} 1 & 0 & \cos\left(h(k) + \dot{h}(k) \cdot T\right) & 0 & 0 \\ 0 & 1 & \sin\left(h(k) + \dot{h}(k) \cdot T\right) & 0 & 0 \\ 0 & 0 & 1 & 0 & 0 \\ 0 & 0 & 0 & 1 & T \\ 0 & 0 & 0 & 0 & 1 \end{bmatrix} \tag{3}$$

w is a vector representing the total uncertainty on the target kinematics, which it is assumed dependent on the module of the target velocity, the heading and the turn rate. In the simulations reported in the article, the following values of the uncertainties have been chosen:

$$\sigma_v = 1 \ \ m/s \quad \sigma_h = 2° \quad \sigma_{\dot{h}} = 1°/s \tag{4}$$

the standard deviations on x and y are derived by equation (4); $\mathbf{z}$ is the measurement vector; **H** is the matrix that relates the state to the measurements:

$$\mathbf{H} = \begin{bmatrix} 1 & 0 & 0 & 0 & 0 & 0 \\ 0 & 1 & 0 & 0 & 0 & 0 \end{bmatrix} \tag{5}$$

and $\mathbf{n}$ is the measurement error with zero mean and a suitable covariance matrix [14].

Constrained tracking

Constraints can be implemented by imposing relationships between the state variables. There are several ways of doing this; in this study the method presented in [55] has been selected. This method consists in modifying the prediction phase of the models used by the IMM algorithm in such way that a suitable relationship between the state variables is satisfied:

$$\mathbf{C} \cdot \mathbf{s}(k) = \mathbf{c} \tag{6}$$

The unconstrained EKF presented in the previous section has been modified introducing the following constraints based on the local road configuration:

1. if the road is straight and forms an angle θ_0 with the x-axis, the equation (6) becomes:

$$\begin{bmatrix} 0 & 0 & 0 & 1 & 0 \end{bmatrix} \cdot \mathbf{s}(k) = \pm\theta_0 \tag{7}$$

   where the choice of the sign depends on the crossing direction;
2. if there is a curved path with curvature radius R, the equation (6) becomes:

$$\begin{bmatrix} 0 & 0 & 1 & 0 & \pm R \end{bmatrix} \cdot \mathbf{s}(k) = 0 \tag{8}$$

where the choice of the sign depends on target turn which may be clockwise or counter clockwise.

IMM and VS-IMM

The IMM tracking algorithm uses a set of M state equations, corresponding to M different models, in parallel during the prediction phase:

$$\begin{aligned} \mathbf{s}_m(k+1) &= \mathbf{A}_m(\mathbf{s}_m(k)) \cdot \mathbf{s}_m(k) + \mathbf{w}_m(k) \\ \mathbf{z}_m(k) &= \mathbf{H}_m(k) \cdot \mathbf{s}_m(k) + \mathbf{n}_m(k) \end{aligned} \quad m = 1, \cdots, M \tag{9}$$

where the m indicates one of the hypothesised target models. The interaction between the models of the IMM is managed by a Markov chain represented by a matrix whose elements are the probabilities p_{ij} of switching from model i to the model j (transition probabilities):

$$\mathbf{P_T} = \{p_{ij}\} = \{P\{m = j \mid m = i\}\} \tag{10}$$

The IMM algorithm is divided in four phases: interaction, prediction, filtering and combination. In the interaction phase, the solutions of each model corresponding to the previous step are mixed to form the initial

states of the IMM models; the mixing is performed taking into account the mode probabilities and the transition probabilities p_{ij}. In the prediction phase, the transition matrix of each model is applied to the initial state to obtain a new set of predicted states. Each predicted state is then filtered using the residual error, that is the difference between prediction and measurement. The mode probability is calculated by means of the likelihood value, that is derived by the residual error probability density function assuming it is Gaussian. The estimated state of the whole IMM tracking algorithm is finally obtained by linearly combining the filter estimated states of all the models; each state is weighted by the corresponding mode probability.

The IMM algorithm uses a fixed set of models and fixed transition probabilities. The VS-IMM instead has a variable set of models and variable transition probabilities: model set and transition probability up-date phase precedes the interaction [54]. This phase is based on the estimation of the target state of the previous algorithm step and on the map of the area controlled by the radar. All the state variables can be exploited in the above mentioned phase; here only the target position has been considered.

Simulated scenario

Figure 11 shows a section of the Venice (It) airport selected for the simulation. It includes two runways and three taxiways; each of them labelled with a number. In the considered scenario an aircraft has just landed and it is going from runway 2 to the apron. The route and kinematics of the aircraft is as follows: it moves along runway 2 with an acceleration of –2 m/s2; it successively performs a manoeuvre with a turn rate of about 1°/s entering taxiway 1 with 5m/s of speed; it moves along taxiway 1 with a 5 m/s velocity; it then performs a manoeuvre with turn rate of about 4.4°/s entering taxiway 2; it crosses the runway 1 entering the taxiway 3 with a 5 m/s velocity uniform motion and it finally moves along taxiway 3 with a 5 m/s constant speed.

An SMR with a scan time T=1 s intercepts the aircraft in the points of trajectory reported in Figure 11. Each point is labelled with a number indicating the radar frame in which the trajectory point is intercepted. Random noise has been added to the measured position to simulate the extraction of the radar raw data. A standard deviation of 10 m for the range measurement and of 0.2° for the azimuth one have been considered.

Simulation results

The following tracking algorithms have been considered:

- an EKF without constraints;
- an IMM with four models: three constrained ones matched respectively to runway 2, taxiway 1 and 3 and an unconstrained one for the manoeuvres;
- an IMM with seven models: three constrained ones matched respectively to runway 2, taxiway 1 and 3; two constrained ones matched to the manoeuvres effectively performed by the airplane during the trajectory; a constrained one matched to a centripetal manoeuvre that the airplane will not perform ("not performed manoeuvre") and, finally an unconstrained model;
- a VS-IMM with the same seven models of IMM, whose map-based activity areas are shown in Figure 12: the model matched to runway 2 is active in the area 1; the one matched to taxiway 1 is active in the area 3; the one matched to taxiway 3 is active in the area 5; the one matched to the first airplane manoeuvre is active in the area 2; the one matched to the second airplane manoeuvre is active in area 4; the model matched to the "not performed manoeuvre" is present in the bank of filters but is never active in the considered airport section (it might be active in another section); the unconstrained model is always active.

The accuracies of the estimated target states obtained by the tracking algorithms have been compared by averaging the results of 10000 independent Monte Carlo trials. Figure 13 shows the mode probabilities of the IMM with four models. The point marked, the cross marked and the circle marked curves correspond respectively to the models matched to runway 2, taxiway 1 and taxiway 3; the asterisk marked curve is associated to the unconstrained model. It can been seen that there is a correct behaviour of the IMM; the tracking algorithm in fact uses the models that best approximate the target kinematics along the trajectory. In

particular, because the IMM has not constrained models matching the two manoeuvres, during such part of the trajectory the tracking algorithm uses the unconstrained model.

Figure 14 shows the mode probabilities of the IMM with seven models. The point marked, the cross marked and the circle marked curves, like the IMM with only four models, are associated respectively to the models matched to runway 2, taxiway 1 and taxiway 3; the plus sign marked and the triangle-right marked curves correspond to the models matched to the two manoeuvres performed by the aircraft; the triangle-left marked curve corresponds to a manoeuvre that is not performed and the asterisk marked curve is associated to the unconstrained model. It can been seen that the increased number of models does not always guarantee the selection of the model that best approximates the target kinematics. In particular, the results show two causes of performance degradation: when the target is crossing runway 1, the IMM uses the correct model only with the first plots, and it erroneously mixes the other models with the rest of the plots; the IMM gives a higher importance to the model approximating the first aircraft manoeuvre (plus sign marked curve) also when the aircraft is moving along taxiway 1 (cross marked curve).

Figure 15 shows the mode probabilities of the VS-IMM. The models and the marks are the same as the IMM. It can be seen that the map-based activity areas bring to a sensible improvement in the selection of the correct model with respect to the IMM with seven models. The VS-IMM has a behaviour similar to the IMM with four models when the target is crossing a runway or taxiway; when the target is manoeuvring, the VS-IMM, after using for a few plots the unconstrained model, selects the model that best approximates the target kinematics.

Figure 16 shows the standard deviations of the target position estimate along the x-coordinate. It can be noted that the IMM with four models and the VS-IMM estimation are more accurate than the EKF ones during the whole trajectory, thanks to the use of the constraints and to the correct selection of the models. The IMM with 7 models is instead less accurate than the EKF when the target is crossing runway 1, because of the incorrect selection of the model.

In [58] a comprehensive set of performance curves is shown to display the standard deviations of the target velocity in polar coordinates (module and heading) and the target turn rate. It can be seen that the IMM with seven models is not always better than the EKF. The VS-IMM instead brings a sensible improvement along the whole trajectory with respect to all the other algorithms. The best estimation is definitely provided by the VS-IMM. The same reference describes also interesting results concerning the processing of recorded live data from Malpensa (It) airport.

In this section a map-based VS-IMM algorithm for the tracking of targets with the SMR data of the A-SMGCS has been proposed. The tracking algorithm has been tested and compared to an EKF and two IMM algorithms in a realistic simulated scenario and on real data. The obtained results demonstrate the benefits brought by the VS-IMM approach. The VS-IMM has shown a more effective management of the constrained models and better accuracy in the estimation of the target position, velocity and turn rate than the EKF and the IMM approaches.

5 APPLICATION TO GMTI

Airborne surveillance of ground moving or stationary vehicles using the GMTI (Ground Moving Target Indicator) radar was proved extremely successful from an operational point of view [60]. A number of large-scale programs have included the GMTI radar for tracking ground moving targets. The GMTI radar sensor plays an important role in situation awareness of the battlefield, surveillance, and precision tracking of ground targets [54], [62]-[67]. A special Session on Ground Target Tracking and Classification (organised by M. Mallick and A. Marrs) is held during the Fusion 2003 Conference, Australia in July 8-11, 2003. Tracking of ground targets is far more complex than that of air targets due to the constraints imposed by the terrain, for which only uncertain data is available. Ground targets in many cases move on road networks [63] and avoid regions that are not-trafficable; but they can also move off-roads. This leads to finite support for the

distribution of the target state. Therefore, popular filtering algorithms such as the KF with Gaussian distributions and the EKF for non linear filtering problems are not suitable in certain cases. GMTI radar platforms have a number of drawbacks; since the GMTI radar platform operates at a standoff distance from the surveillance area, the terrain, trees and buildings can often occlude the radar line-of-sight. Also GMTI data collection is usually interrupted during the turn of the aircraft. This Section summarises some techniques to build up tracks by exploiting GMTI radar data. This topic is a bit different from one previously discussed in Section 4; for instance, here the targets can manoeuvre and can move off-roads. Here we summarises the main finding of two key references [54] and [67].

Reference [54] is probably the first that has introduced the VS-IMM estimator for tracking groups of ground targets on constrained paths using GMTI data obtained from an airborne sensor. It is assumed that targets move along highways with varying obscuration due to changing terrain conditions. The roads can branch, merge and cross. Some of the targets may also move in open field. The key discovery illustrated in [54] is that the constrained motion estimation problem is handled using an IMM estimator with varying mode sets depending on the topography. The number of models, their types and their parameters are modified adaptively based on the estimated position of target and the corresponding road/visibility conditions. As said in [54], this topography based variable structure mechanism eliminates the need for carrying all the possible models throughout the entire tracking period as in the standard IMM estimator. The specification of the road map with visibility conditions can be summarised in a table which specifies each road segment, the waypoints, the visibility condition, the indication whether it is possible to enter or exit.

A working example is the following. In VS-IMM the filter modules are adaptively modified, added or removed depending on the terrain topography. For example, the added uncertainty at junctions is handled by temporarily augmenting the IMM mode set with modes that represent motion long all possible roads. These additional IMM modes are removed from the mode set after the target passes the junction. At each scan the structure of the estimator for every target is modified individually based on the known topology of the surveillance region and the predicted location of the target. This enables the estimator to handle the variations in the possible motions across the target and along time for each target.

Another issue that has been addressed in [54] is the plot-track association logic. Known algorithms are (see Section 2.2): NN, PDA, JPDA and MHT. Assignment algorithms are also effective in data association for multi-target tracking in clutter environment [61]. Here the data association is formulated as an optimisation problem where the cost function to minimise is a combined likelihood function of the estimated states. The association of the elements of the latest measurement to those in the track list is called assignment with time-depth 1 results in a two-dimensional assignment. A higher order assignment where the latest S-1 scans of measurements are associated with the established track list (from time k-S+1 where k is the current time, i.e., with sliding window of time depth S-1) results in a S-dimensional assignment [61]. In the context of constrained motion it is interesting to check whether higher order assignment yields better association by using topographic history, i.e. by considering not only the topography at the currently predicted position but also the conditions at the previously estimated positions of target. This brings to a VS-IMM based on multidimensional assignment. It has been shown that the S-dimensional assignment requires quasi-polynomial time for computation thus allowing the only systematic implementation of MHT [54].

Here we briefly summarise the mathematical model for on-road/off -road motion. Unlike an off-road-capable target, which is free to move in any direction, the motion of an on-road-only target is highly directional along the road. To handle the motion along the road the concept of directional noise is introduced in [54]. The standard motion model assumes that the target can move in any direction and, therefore, use equal process noise variances in both the x and y directions. This means that for off-road targets the motion uncertainties in both directions are equal. For on-road targets, the road constraint means more uncertainty along the road than orthogonal to it. Thus the IMM module representing on-road motion consists of process noise components along and orthogonal to the road, rather than along x and y directions as in the standard model. Indicating with ψ, measured from the y axis, the direction of the road along which the motion model is matched, indicating with σ_a and σ_0 the standard deviations of the process noise components along the road and orthogonal to the

road, we have: $\sigma_a >> \sigma_0$ which contrasts with the $\sigma_x = \sigma_y$ for off-road motion model. Since the estimate is carried out in x-y coordinates, the variances of the process noise components of along and orthogonal to the road need to be converted into a covariance matrix $\mathbf{Q}$ in that frame:

$$\mathbf{Q} = \begin{bmatrix} -\cos\psi & \sin\psi \\ \sin\psi & \cos\psi \end{bmatrix} \begin{bmatrix} \sigma_0^2 & 0 \\ 0 & \sigma_a^2 \end{bmatrix} \begin{bmatrix} -\cos\psi & \sin\psi \\ \sin\psi & \cos\psi \end{bmatrix} \tag{11}$$

The same references also presents models for junctions, entry/exit conditions and obscuration condition.

Simulation results refer to a complex scenario with a network of roads and 120 targets in nine groups of different characteristics [54]. Four algorithms are compared: IMM with 2-D and 3-D assignment and VS-IMM with 2-D and 3-D assignment. The performance clearly show that the best is the VS-IMM with 3-D assignment followed by the VS-IMM with 2-D assignment. The fixed IMM which consisted of two baseline models in addition to a third second order model performed worse than the VS-IMM. This is because the VS-IMM is able to handle the on-road/off-road transition and the change from one road to another more smoothly than the fixed IMM by anticipating the changes. Also, once that the target begins to move along a particular road, the VS-IMM, which uses a model matched to the road, yields better course estimate than the fixed IMM which uses an open field model.

Reference [67] tackles the problem of incorporating non standard information (road maps and terrain related visibility conditions) by resorting to the PF (see Section 2.3). Exploiting non-standard information leads to highly non Gaussian pdf and conventional trackers do not properly work. Since PF has no restrictions on the types of models, including noise distributions used, one can incorporate non-standard information available through maps and velocity constraints by modelling them as suitable constraints on the state. As said in Section 2.3, PF is routinely used for recursive state estimation; extension to MM has also been reported in the recent literature. Reference [67] combines the VS-IMM concept with the PF technique giving rise to the new algorithm called variable structure multiple model particle filter (VS-MMPF). The key features of the VS-MMPF are that the number of models active at any particular time and the state transitions vary depending on the current state and the topography. Simulation results compare the VS-IMM and the VS-MMPF for a single target moving on a network of roads. It is shown that VS-MMPF provides 65% improvement in tracking accuracy with respect to the VS-IMM for a road target. With speed constraints knowledge the advantage in rms error grows up to 77% [67].

6. APPLICATION TO TRACKING OF TARGETS HIDDEN IN BLIND DOPPLER

This section is fully derived by [68] with permission of the Authors. Most combat aircraft are equipped with some form of electronic warfare intelligence system, such as electronic support measures (ESM) or a radar warning receiver (RWR). These systems in general detect nearby RF emissions, process them in real-time, and report to the pilot the direction of arrival of each RF emission and the identity of its source. In a hostile environment, there are various electronic protection (EP) measures available to the pilot that can hide the aircraft's true position from the enemy radar, such as noise jamming, deceptive ECMs, chaff, etc. One of the simplest and most effective EP measures against any CW or pulse Doppler radar is to hide in the radar Doppler blind zone (DBZ). The blind Doppler are the bands of Doppler frequency falling within the MTI rejection notches covering the regions around zero Doppler and the integer multiples of the PRF. MTI filters out the ground clutter and the ground moving targets from the radar echoes. MTI cut-off frequency can be up to plus or minus 80 knots in airborne radars. Hiding in the blind Doppler is aided by the on-board ESM or the RWR, since either system indicates to the pilot the direction of the enemy radar. The pilot can then manoeuvre to reduce the aircraft's radial velocity by flying tangentially with respect to the enemy radar. Hiding in the blind Doppler is only a temporary measure, but it often causes a loss of track. Once the target comes out of the blind Doppler a new track has to be initiated and the target has to be again identified. By the time the new track is established, the target could be lost again because it hides once again in the blind Doppler. With the

standard Kalman-type filters it is difficult to exploit prior knowledge of the geographical or sensor limitations, such as the position extent of the blind Doppler zones. These effects introduce gross non linearity in the form of "hard edges" on probability distributions. The "hard constraints", however, can be fairly easily incorporated into the framework of sequential Monte Carlo (SMC) estimation techniques. Reference [68] compares two filters, the EKF and the PF, for tracking an airborne target which temporarily hides in the DBZ. Both filters assume a constant velocity target motion with some process noise to handle the possible maneuvers. The EKF is tracking the target using only radar measurements (target range, azimuth, and range rate obtained from Doppler). The PF, in addition to the radar measurements, exploits prior knowledge of the DBZ limits.

The true target state at a discrete time t_k is $s_k = [x_k \quad \dot{x}_k \quad y_k \quad \dot{y}_k]^T$, where x_k, y_k are the position and $\dot{x}_k, \dot{y}_k$ are the velocities of the target in Cartesian coordinates. The polar measurements of the target location at t_k (range r_k and azimuth θ_k), obtained from a radar, are conveniently converted into the Cartesian system [14]. The target motion model is the constant velocity (CV) model, with an appropriate level of process noise to deal with possible maneuvers. The state dynamics is linear equation; while the measurement equation is non linear because of the presence of the radial speed $\dot{r}_k$ [68]. The detection probability of radar is as follows:

$$P_D(s_k) = \begin{cases} P_d \rightarrow if: \left| \dfrac{x_k \dot{x}_k + y_k \dot{y}_k}{\sqrt{x_k^2 + y_k^2}} \right| \geq L_0 \\ 0 \rightarrow otherwhise \end{cases} \tag{12}$$

where L_0 is the limit of the DBZ and P_d is a positive constant less than or equal to unity (i.e.: the actual radar detection probability when the target is visible). The problem is to investigate the performance of a standard EKF, which ignores the existence of the DBZ, against the PF which uses the prior knowledge of L_0 in eq. (12). The latter was developed using SMC techniques mainly because any nonstandard form of information (such as prior knowledge of L_0) can be easily incorporated into the framework of SMC estimation.

In [68] a PF is outlined which allows information about the DBZ limits to be directly utilized in the tracking process. By doing this we have a situation where receiving no measurement actually conveys useful information about the probable target location and velocity. A string of periods with no measurement is then strongly indicative of a target maneuvering in the blind zone and the particles spread out to cover the possible trajectories and locations where this is possible and effectively wait for the target to appear out of the blind zone. Hence we expect increased probability of track maintenance. The basic idea to build the PF is to have one set of particles restricted to motion within the DBZ and the other set able to move unrestricted. The two sets of particles are used to hedge between the two possible motions. Details and pseudo-code of the PF are in [68].

The performance of the candidate algorithms is measured by the probability of track maintenance; Monte Carlo simulation is run to make these evaluations. To define a track loss, a track score S is suitably defined [68]. The following target trajectory is considered (see Figure 17). The target is at first going radially toward the radar at a speed of 800 km/h. Then it makes a 3g turn to its right and continues the tangential motion with respect to radar for about 25 s. Finally the target makes another 3g turn and moves again towards the radar with a high range-rate. Note that while the target is in the DBZ (the second leg of the target motion), there are no target measurements. The parameters of the radar model used in simulation are as follows: the sampling interval is T_s=2 s; the error statistics for radar measurements are $\sigma_r = 250m$, $\sigma_{\dot{r}} = 3m/s$, and $\sigma_\theta = 1°$; the DBZ limit is L_0=100 km/h; the probability of detection is P_d=0.9. Note that the track score is calculated in such a way that if the first measurement after the reappearance of the target from the DBZ is not gated, the track is lost. In the Monte Carlo run concerning the EKF, not shown here, the track has been lost [68]. Figure 17 illustrates the result obtained with the PF. Because of the proper shape of the validation region, the first measurement after the reappearance of the target from the DBZ falls inside the gate of the particle filter. The shape of this gate, just before the crucial moment (at time108 s) is indicated by a cloud of particles in Figure 17a. Note that the shape of the cloud (which resembles an arc) accurately represents the uncertainty associated

with the target position. As a result, the PF does not lose the track – the track score S_k, after dipping to the value of 0.1recovers quickly to 1 which is its maximum allowed value. Additional interesting simulation results are reported in the key reference [68].

The problem of tracking a target occasionally bidden in the blind Doppler of a radar has been investigated. It has been demonstrated that by using prior knowledge of the limits of the DBZ, one can design a tracker which will perform better, in terms of track continuity, than a tracker which ignores this prior information. The concept has been proven using a particle filter, mainly because any non standard information (such as blind Doppler) can be easily incorporated into the framework of sequential Monte Carlo estimation.

7. CONCLUSIONS

In this paper we have described the new technique of knowledge based tracker (KBT). After an extensive review of the state of the art of tracking system, attention has been put on the use of a-priori knowledge in designing a tracking filter with the aim of improving tracking performance. Three application examples have been presented to illustrate the efficacy of KBT. Other applications are of interest like the use of geographic map for radar tracking in littoral environment (i.e.: near the coast-line).

8. ACKNOWLEDGEMENTS

The author expresses his thanks to the following colleagues: G. Golino and L. Ferranti (AMS, Italy), B. Ristic and N. Gordon (DSTO, Australia), S. Coraluppi (Nato-Saclant, Italy) for co-operation in some of the paper topics.

9. REFERENCES

[1] F. C. Gauss, “Theoria motus corporum coelestiorum in sectionibus conics solem ambientum”, Hamburg, 1809 (translation: Dover, New York, 1963).
[2] A. M. Legendre, “Methode de moindres quarres pour trouver le milieu le plus propable entre les resultats des differentes observations”, Mem. Inst. France, pp. 149-154, 1810.
[3] R. A. Fisher, “On an absolute criterion for fitting frequency curves”, Messenger of Math., pp. 41-155, 1912.
[4] A. N. Kolmogorov, “Foundations of the theory of probability”, Spinger, New York, 1933.
[5] N. Wiener, “Extrapolation, interpolation, and smoothing of stationary time series”, Cambridge, MA, Technology Press and New York, Wiley, 1949.
[6] N. Wiener, “Non linear problems in random theory”, Cambridge, MA, Technology Press and New York, Wiley, 1958.
[7] C. W. Therrien, “The Lee-Wiener Legacy”, IEEE Signal Processing Magazine, November 2002, pp. 33-44.
[8] N. Levinson, “The Wiener root-mean-square error criterion in filter design and prediction”, J. Math. Phys., vol. 25, pp. 261-278, 1947.
[9] R. E. Kalman, “A new approach to linear filtering and prediction problems“, Journal of Basic Eng., Trans. ASME, Ser. D, vol. 82, no. 1, pp. 35-45, 1960.
[10] R. E. Kalman, R. S. Bucy, “New results in linear filtering and prediction theory“, Journal of Basic Eng., Trans. ASME, Ser D, vol. 83, no. 3, pp. 95-108, 1961.
[11] T. Kailath, “A view of three decades of linear filtering theory”, IEEE Trans. On Information theory, vol. IT-20, no. 2, pp. 146-179, 1974.
[12] R. Kalman biography: www.math.rutgers.edu/~sontag/ftp_dir/rek.
[13] E. Brookner, “Tracking and Kalman filtering made easy”, Wiley Interscience, 1998.
[14] A. Farina, F.A. Studer, “Radar Data Processing. Introduction and Tracking” (Vol. I). Researches Studies Press. England, May 1985.

[15] H. Blom, Y. Bar-Shalom, "The interacting multiple model algorithm for systems with Markovian switching coefficients", IEEE Trans. on Automatic Control, vol. AC-33, pp. 780-783, August 1988.

[16] X. R. Li, "Engineer's guide to variable-structure multiple-model estimation for tracking. Ch. 10", http://ece.engr.uno.edu/isl/PublicationsBySubjects.htm.

[17] M. De Feo, A. Graziano, R. Miglioli, A. Farina, "IMMJPDA versus MHT and Kalman filter with NN correlation: performance comparison". IEE Proceedings on Radar, Sonar and Navigation (Pt. F), vol. 144, no. 2, April 1997, pp. 49-56.

[18] R. Graziano, R. Miglioli, A. Farina, "Multiple hypothesis tracking vs. Kalman filter with nearest neighbor correlation. Performance comparison". AGARD MSP 3rd Symposium on "Tactical Aerospace C^{3}I in Coming Years", Lisbon, Portugal, 15-18 May 1995, published in CP-557, pp. 25-1, 25-11.

[19] R. Torelli, A. Graziano, A. Farina, "IM^{3}HT algorithm: a joint formulation of IMM and MHT for multitarget tracking". Invited Paper, Proceedings of European Control Conference, ECC97, Vol. 3 "Estimation", Pt.1 WE-A F1, p. 750, Bruxelles, July 1-4, 1997.

[20] R. Torelli, A. Graziano, A. Farina, "IM3HT algorithm: A joint formulation of IMM and MHT for multi-target tracking", European Journal of Control, vol. 5, 1999, pp. 46-53.

[21] A. Farina, P. Lombardo, M. Marsella, "Joint tracking and identification algorithms for multisensor data", Proc. of IEE, RSN, vol. 149, no. 6, December 2002, pp. 271-280.

[22] A. Farina, F.A. Studer, "Radar Data Processing. Advanced Topics and Applications" (Vol. 2). Researches Studies Press, England, January 1986.

[23] A. Farina, "Sensor netting for surveillance and use of related emerging technologies". Proc. of the 1987 Rome AFCEA European Symposium, May 6-8, 1987, pp. 49-57.

[24] A. Farina, "Tracking function in bistatic and multistatic radar systems". Special issue on bistatic and multistatic radar, IEE Communication, Radar and Signal Processing, Pt. F, Vol. 133, no. 7, December 1986, pp. 630-637.

[25] A. Farina, B. La Scala, "Methods for association of active and passive tracks for airborne sensors". International Symposium on Radar, IRS98, Munich, 15-17 September 1998, pp. 735-744.

[26] A. Farina, R. Miglioli, "Association between active and passive tracks for airborne sensors". Signal Processing, 69, 1998, pp. 209-217.

[27] B. La Scala, A. Farina, "Effects of cross-covariance and resolution in track association", 3rd Intl. Conference on Fusion, Fusion 2000, Paris , July 10-13, 2000, pp. WeD1-10 to WeD1-16.

[28] B. La Scala, A. Farina, "Choosing a track association method", Information Fusion Journal, vol. 3, issue 2, June 2002, pp. 119-133.

[29] A. Farina, B. Ristic, D. Benvenuti," Tracking a ballistic target: comparison of several non linear filters", IEEE Trans on Aerospace and Electronic Systems, vol. 38, issue no. 3, July 2002, pp. 854-867.

[30] B. Ristic, A. Farina, D. Benvenuti, "Tracking a ballistic re-entry object: performance bounds and comparison of non-linear filters", IDC-2002, Adelaide, Australia, 11-13 February 2002, pp. 259-264.

[31] A. Farina, D. Benvenuti, B. Ristic, "Estimation accuracy of a landing point of a ballistic target", Proc. of Intl. Conf. Fusion 2002, Washington DC, May 2002, pp. 2-9.

[32] B. Ristic, A. Farina, D. Benvenuti, M. S. Arulampalam, "Performance bounds and comparison of non-linear filters for tracking a ballistic object on re-entry", Proc. of IEE, RSN, to appear, 2003.

[33] A. Farina, "Target tracking with bearings-only measurements". Signal Processing, vol. 78, no. 1, October 1999, pp. 81-78.

[34] A. Farina, D. Benvenuti, B. Ristic," A comparative study of the Benes filtering problem", Signal Processing, vol. 82, no. 2, February 2002, pp. 133-147.

[35] S. Julier, J. Uhlmann, H. F. Durrant_Whyte, "A new method for the non linear transformation of means and covariances in filters and estimators", IEEE Trans. on Automatic Control, vol. AC-45, no. 3, pp. 477-482, March 2000.

[36] N. Gordon, D. Salmond, A. Smith, "Novel approach to nonlinear/nonGaussian Bayesian state estimation", IEE Proc. F, Radar Signal Process, 1993, vol. 140, no. 2, pp107-113.

[37] M. S. Arulampalam, S. Maskell, N. Gordon, T. Clapp, "A tutorial on particle filters for on line nonlinear/nonGaussian Bayesian tracking", IEEE Trans. on Signal Processing, vol. 50, no. 2, February 2002, pp. 174-188.

[38] A. Doucet, N. de Freitas, N. J. Gordon, editors, "Sequential Monte Carlo methods in practice", New York: Springer-Verlag, January 2001.
[39] C. Musso, N. Oudjane, F. Legland, "Improving regularised particle filters", in [38].
[40] C. Hue, J.-P. Le Cadre, P. Perez, "Sequential Monte Carlo methods for multiple target tracking and data fusion", IEEE Trans. on Signal Processing, vol. 50, no. 2, pp. 309-325.
[41] N. Gordon, D. Salmond, "Sequential Monte Carlo methods for tracking", at an IEE Colloquium on Kalman filtering - applications and pitfalls, March 2001. Available on the WWW.
[42] F. Daum, J. Huang "Curse of dimensionality and particle filters", Proc. of the IEEE Aerospace Conference, Big Sky, Montana (USA), March 2003.
[43] P. Tichavsky, C. Muravchik, A. Nehoray, "Posterior Cramer-Rao bounds for discrete-time nonlinear filtering", IEEE Trans on Signal Processing, vol. 46, 1998, pp. 1386-1396.
[44] M. Simandl, J. Kralovec, P. Tichavsky, "Filtering, predictive, and smoothing Cramer-Rao bounds for discrete-time nonlinear dynamic systems", Automatica, vol. 37, 2001, pp. 1703-1716.
[45] A. Farina, B. Ristic, L. Timmoneri, "Cramer-Rao bound for nonlinear filtering with $P_d < 1$ and its application to target tracking", IEEE Trans on Signal Processing, Vol. 50, issue 8, August 2002, pp. 1916-1924.
[46] Y. Bar-Shalom, T. Fortmann, "Tracking and data association", Academic Press, 1988.
[47] S. Blackman, "Multiple-target tracking with radar applications", Artech House, 1986.
[48] Y. Bar-Shalom, X-Rong Li, "Multitarget-multisensor tracking: principles and techniques", YBS, 1995.
[49] P. Bogler, "Radar principles with applications to tracking systems", John Wiley & Sons, New York, January 1990.
[50] D. Halls, J. Llinas, "Handbook of multisensor data fusion", CRC, 2001.
[51] Y. Salama, R. Senne, "Knowledge-based applications to adaptive space-time processing. Volume I: Summary", AFRL-SN-TR-2001-146 Vol. I (of Vol. VI), Final Technical Report, July 2001.
[52] C. Morgan, L. Moyer, "Knowledge-based applications to adaptive space-time processing. Volume IV: Knowledge-based tracking", AFRL-SN-TR-2001-146 Vol. IV (of Vol. VI), Final Technical Report, July 2001.
[53] C. Morgan, L. Moyer, "Knowledge-based applications to adaptive space-time processing. Volume IV: Knowledge-based tracking rule book", AFRL-SN-TR-2001-146 Vol. V (of Vol. VI), Final Technical Report, July 2001.
[54] T. Kirubarajan, Y. Bar Shalom, K. R. Pattipati, I. Kadar, "Ground target tracking with variable structure IMM estimator", IEEE Trans. on Aerospace and Electronic Systems, vol. 36, no. 1, January 2000, pp. 26-46.
[55] D. Simon, T. L. Chia, "Kalman filtering with state equality constraints", IEEE Trans. on Aerospace and Electronic Systems, vol. 38, no. 1, January 2002, pp. 128-136.
[56] S. Coraluppi, C. Carthel, "Multiple-Hypothesis IMM (MH-IMM) filter for moving and stationary targets", Proc. Fourth International Conference on Information Fusion, August 2001, Montreal, Canada.
[57] X.R. Li, Y. Bar Shalom, "Multiple Model Estimation with Variable Structure" IEEE Trans. on Automatic Control, vol. 41, no. 4, April 1996.
[58] A. Farina, L. Ferranti, G. Golino, "Constrained tracking filters for A-SMGCS", Proc. of Fusion 2003, July 8-11, 2003, Cairns, Queensland, Australia.
[59] F. Gustafsson, A.J. Isaksson, "Best choice of coordinate system for tracking coordinate turns", Preprints 35th IEEE CDC, pp. 3145-3150, Kobe, Japan, 1996.
[60] J.N. Entzminger, Jr., C.A. Fowler, and W.J. Kenneally, "JointSTARS and GMTI, past, present and future", IEEE Trans. Aerospace and Electronic Systems, Vol. 35, pp. 748-761, April 1999.
[61] S. Deb, M. Yeaddanapudi, T. Kirubarajan, K.R. Pattipati, Y. Bar-Shalom, "A generalised S-dimensional assignment for multi-sensor multitarget state estimation", IEEE Trans. Aerospace and Electronic Systems, Vol. 33, no. 2, pp. 523-538, April 1997.
[62] T. Kirubarajan, Y. Bar-Shalom, "Tracking Evasive Move-Stop Targets with and MTI Radar Using a VS-IMM Estimator", Signal and Data Processing of Small Targets: Proc. SPIE, Vol. 4048, pp. 236-246, Orlando, FL, April 2000.

[63] T. Kirubarajan, Y. Bar-Shalom, K.R. Pattipati, I. Kadar, B. Abrams, E. Eadan, "Tracking ground targets with road constraints using an IMM estimator", Proc. IEEE Aerospace Conference, March 1998.

[64] S. Coraluppi and C. Carthel, "Multiple-Hypothesis IMM (MH-IMM) Filter for Moving and Stationary Targets", Proc. Fourth International Conference on Information Fusion, August 2001, Montreal, Canada.

[65] M. Mallick, "Maximum Likelihood Geolocation using a Ground Moving Target Indicator (GMTI) Report", Proc. IEEE Aerospace Conference, March 2002, Big Sky MT, USA.

[66] M. Mallick and Y. Bar-Shalom, "Nonlinear Out-of-sequence Measurement Filtering with Applications to GMTI Tracking", Signal and Data Processing of Small Targets: Proc. SPIE, Vol 4048, Orlando, Florida, April 2002.

[67] M. S. Arulampalam, N. Gordon, Orton, B. Ristic, "A variable structure multiple model particle filter for GMTI tracking". Proceedings of the Fifth International Conference on Information Fusion. FUSION 2002. (IEEE Cat.No.02EX5997). Int. Soc. Inf. Fusion. Part vol.2, 2002, pp.927-34 vol.2. Sunnyvale, CA, USA.

[68] N. J. Gordon, B. Ristic, "Tracking airborne targets occasionally hidden in the blind Doppler", Digital Signal Processing, vol. 12, no. 2/3, April/June2002, pp. 383-393.

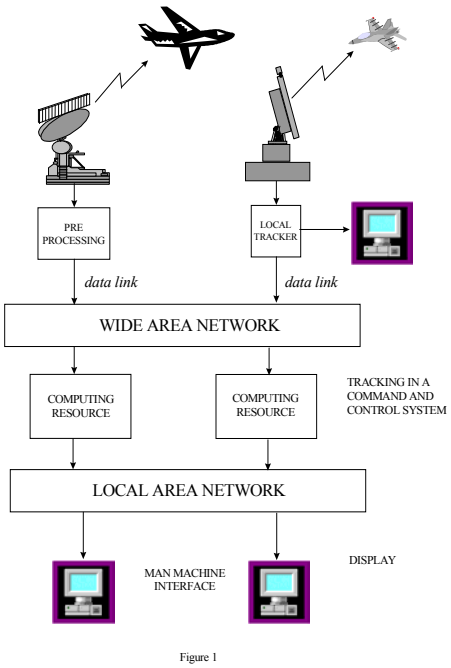

Figure 1: Generic scheme of a tracking system.

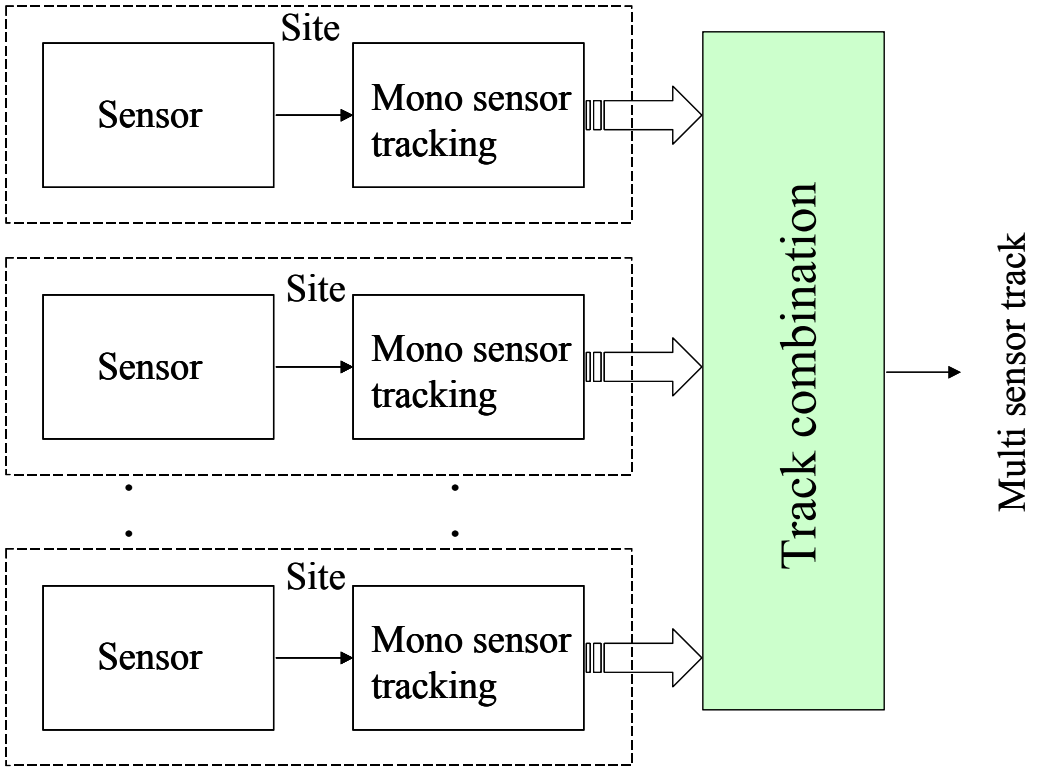

Figure 2: MST with distributed architecture.

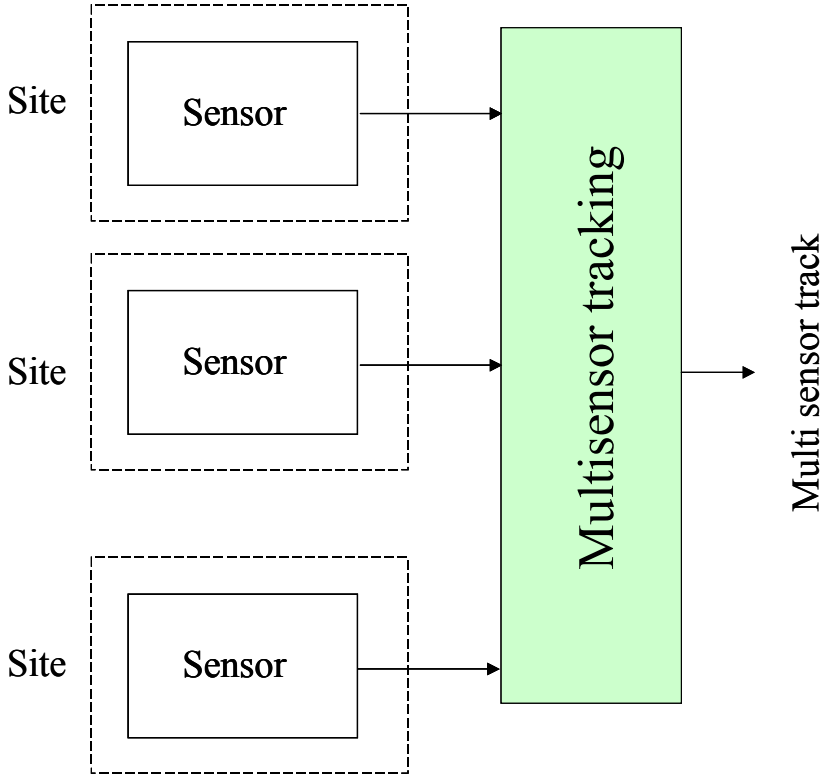

Figure 3: MST with centralised architecture.

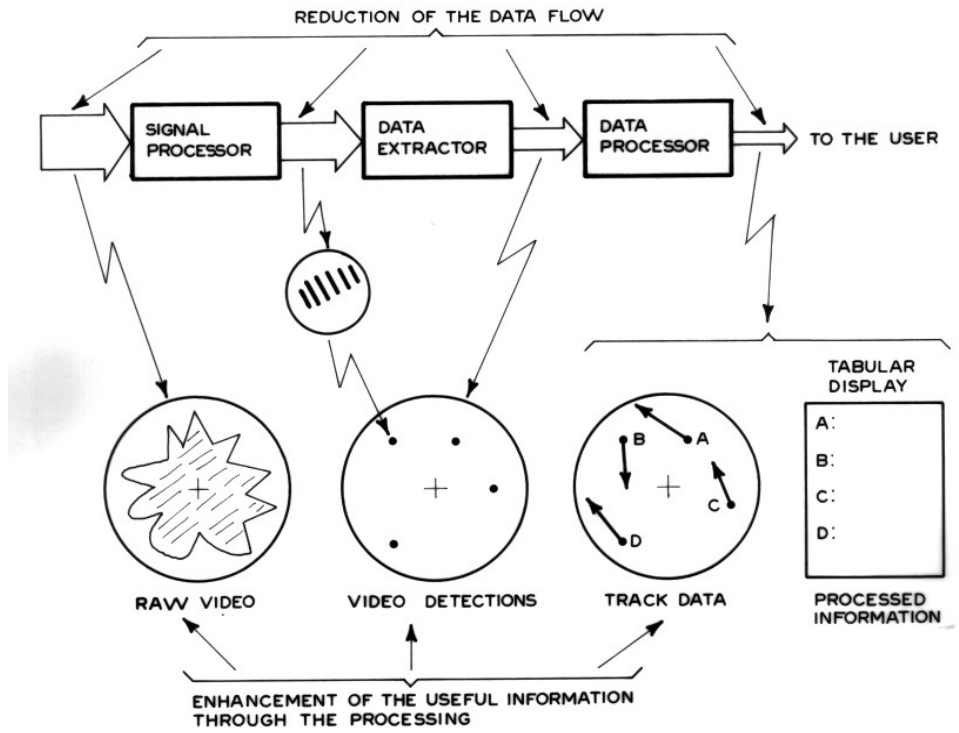

Figure 4: Functions performed in the radar receiving phase. From Farina, Studer [14]

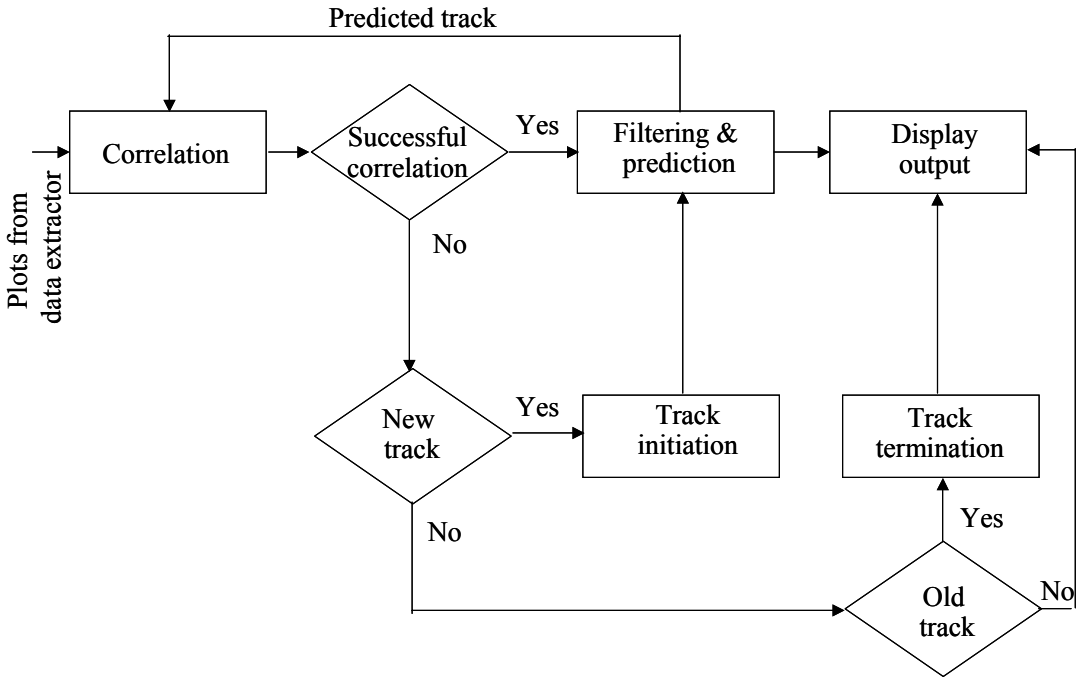

Figure 5: Basic functions of tracking procedure. From Farina, Studer [14].

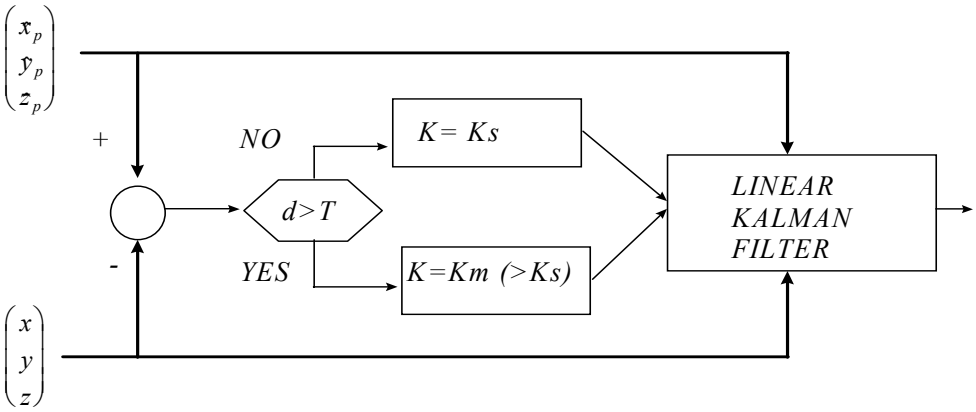

Figure 6: Adaptive Kalman filter with manoeuvre detection logic.

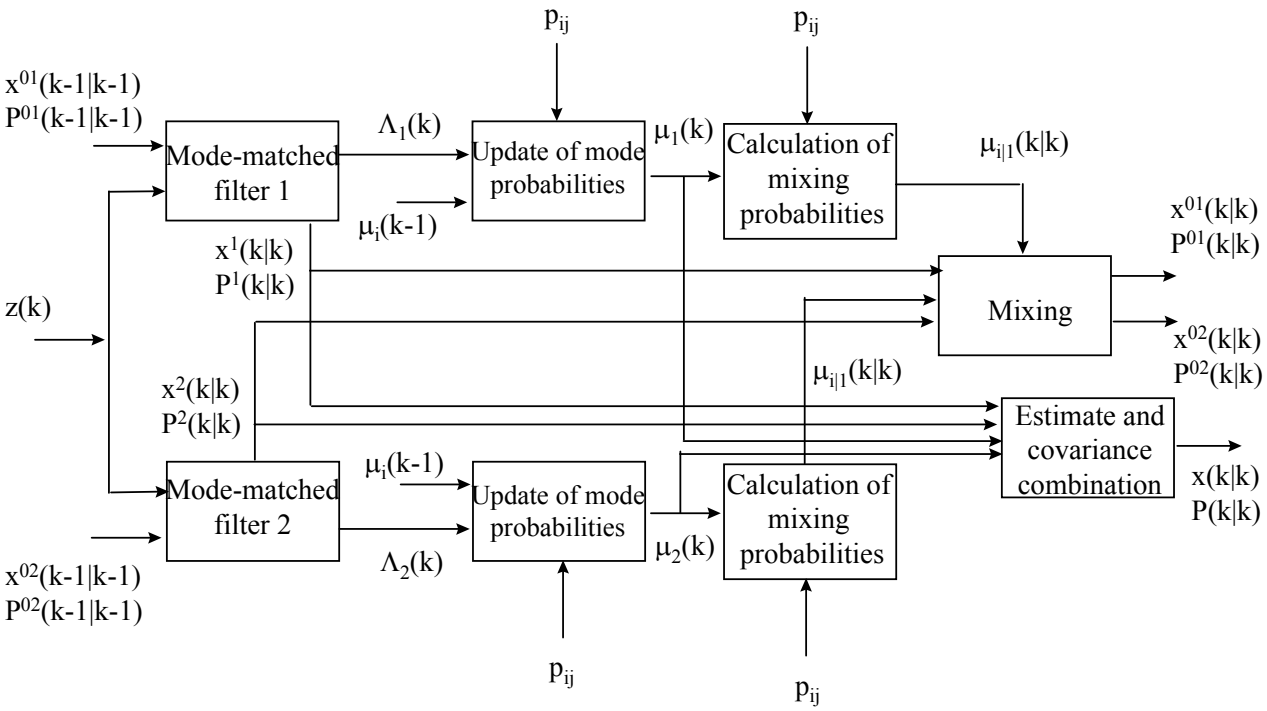

Figure 7: IMM filter (for details, see [17]).

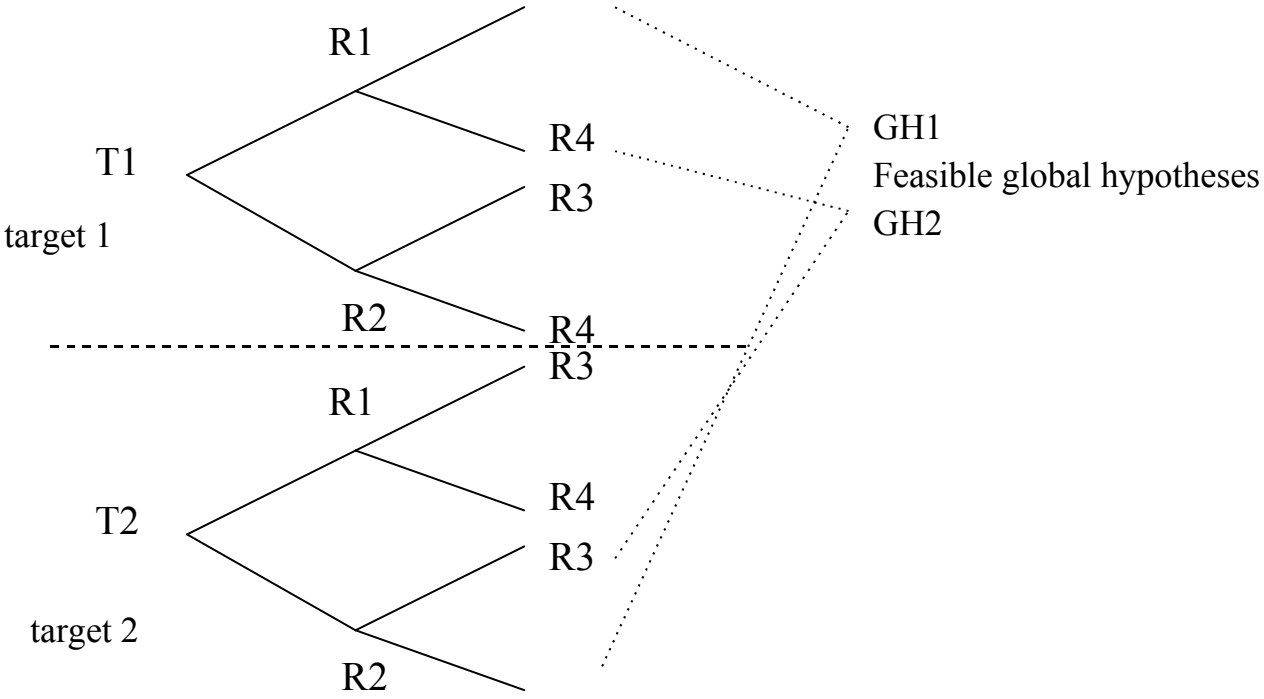

Figure 8: MHT tree (for details, see [18]).

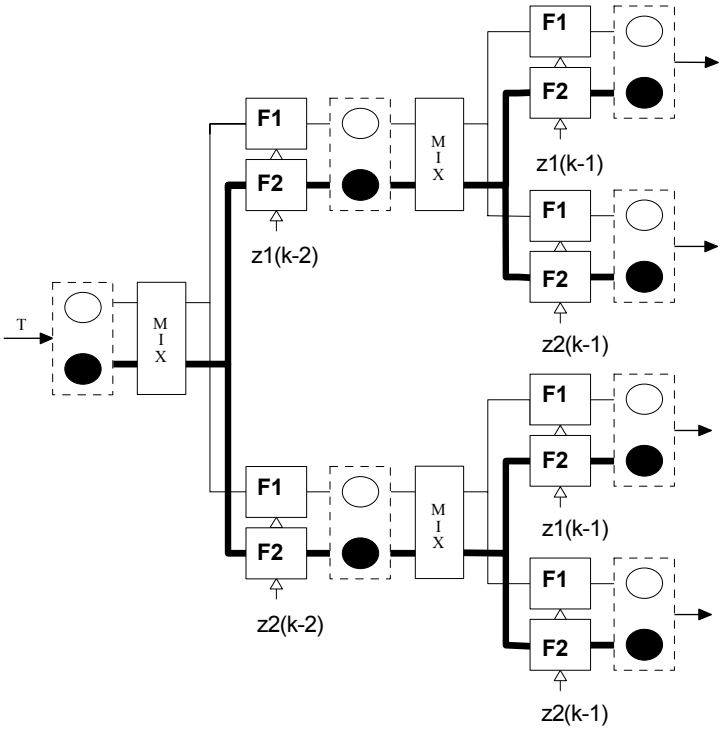

Figure 9: IMM-MHT tree (for details, see [19] and [20]).

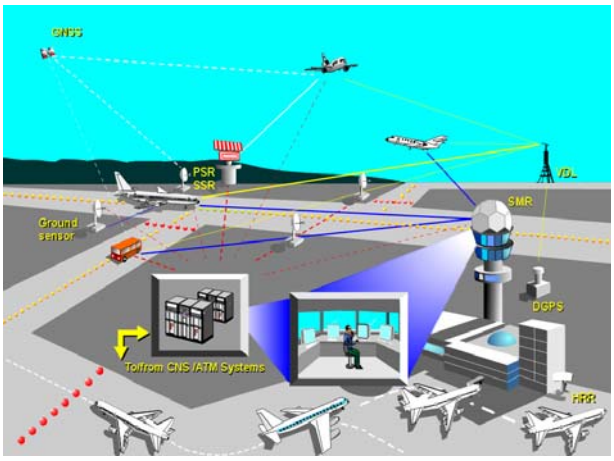

Figure 10: A-SMGCS in a multi-sensor context.

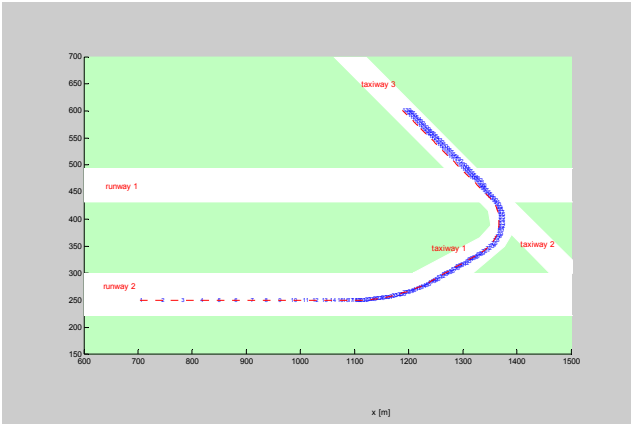

Figure 11: Simulated trajectory of landed aircraft going to apron (section of Venice (It) airport).

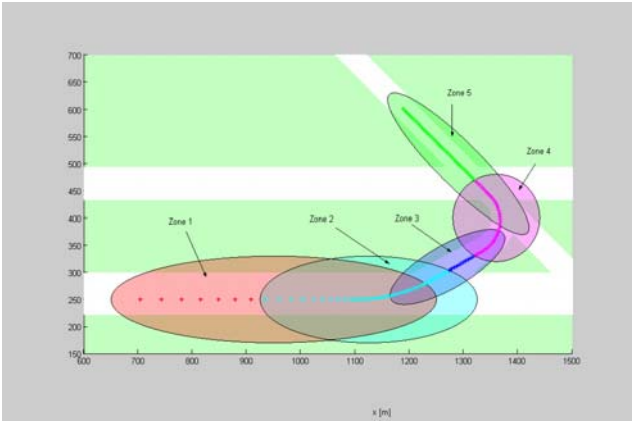

Figure 12: Areas in which the VS-IMM modes are active.

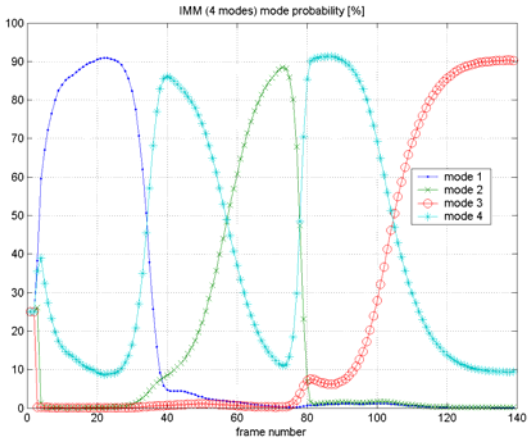

Figure 13: Mode probabilities of IMM with four models along the trajectory of Figure 10.

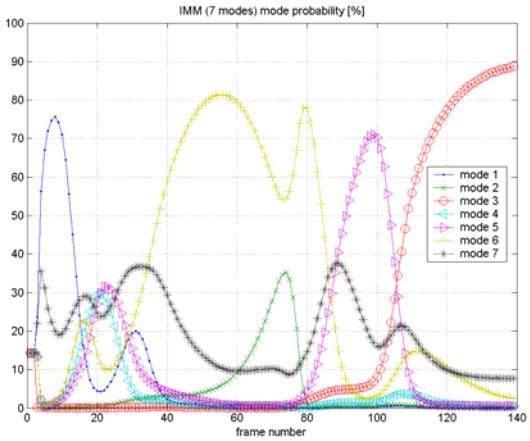

Figure 14: Mode probabilities of IMM with seven models along the trajectory of Figure 10.

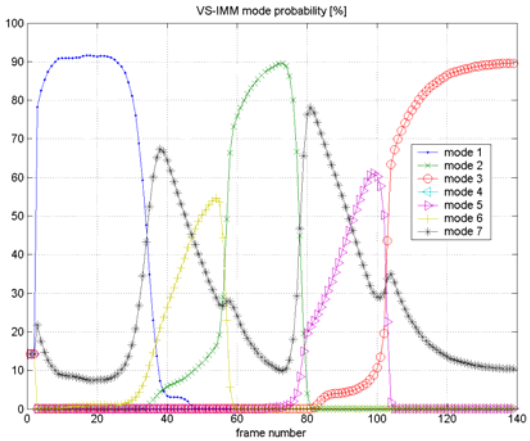

Figure 15: Mode probabilities of VS-IMM along the trajectory of Figure 10.

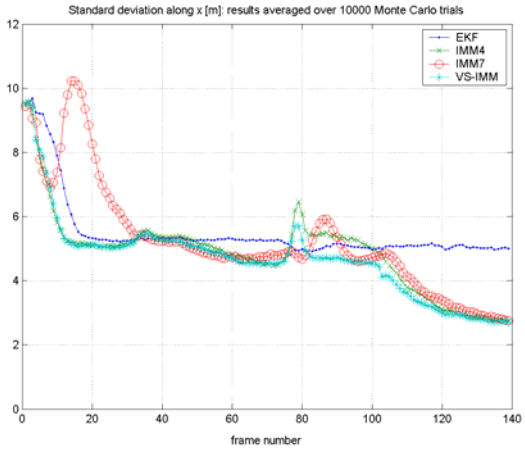

Figure 16: Standard deviation (m) of the target position error along the x-axis for the trajectory of Figure 10.

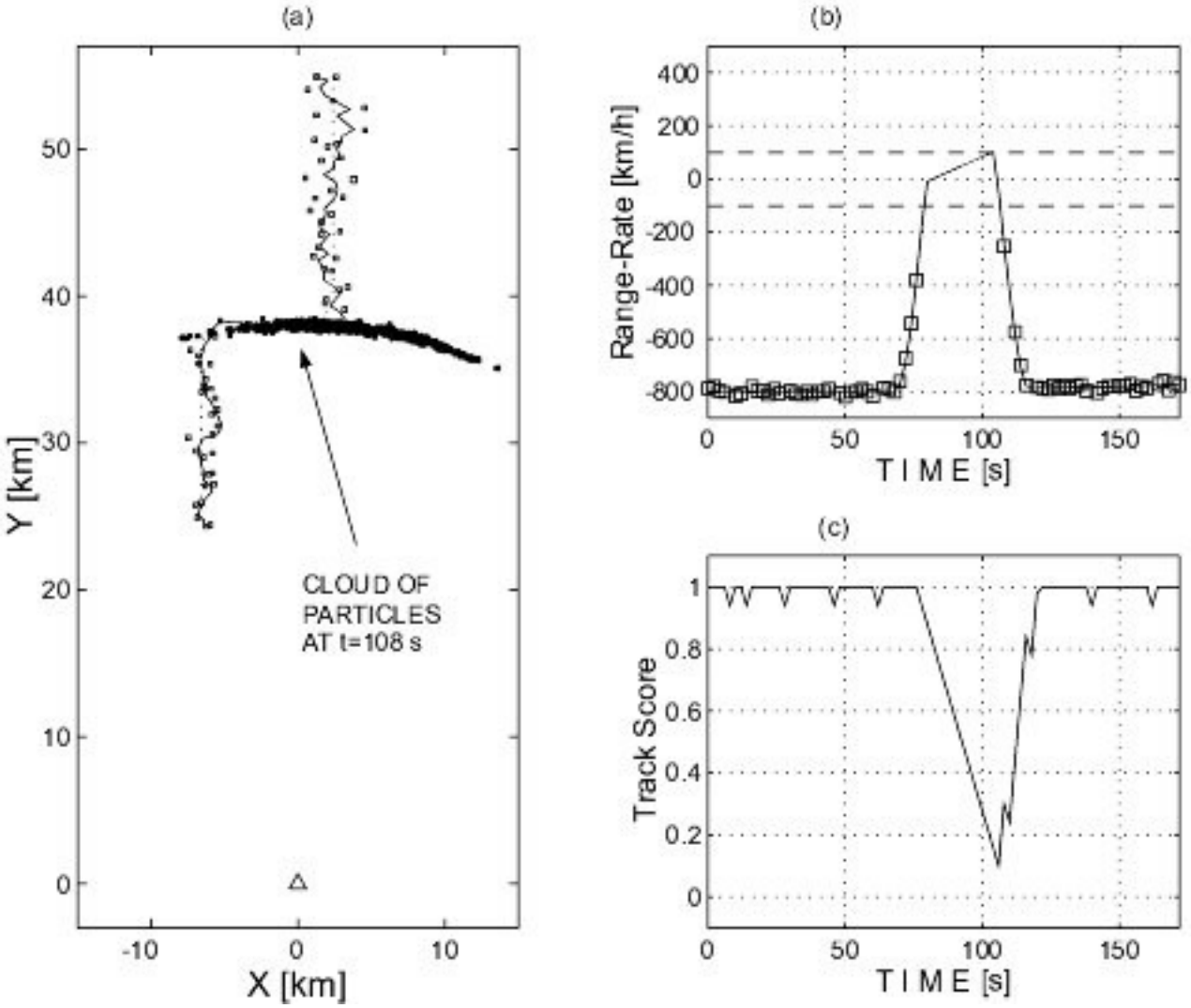

Figure 17: The PF in action : (a) state estimation (solid line) with a cloud of particles at t=108 s ; (b) the range-rate ; (c) the track score S_k. (Reproduced from [68] with permission of the Authors N. Gordon, B. Ristic).

IMPACT OF KNOWLEDGE-BASED TECHNIQUES ON EMERGING TECHNOLOGIES

H.D. Griffiths
Head, Department of Electronic and Electrical Engineering
University College London
Torrington Place, London WC1E 7JE, UK
Tel: +44 20 7679 7310; fax: +44 20 7388 9325; email: h.griffiths@ee.ucl.ac.uk

Keywords: radar, signal processing, adaptive arrays, multifunction phased array radar, resource management, waveform diversity, bistatic radar, synthetic aperture radar, knowledge-based systems.

SUMMARY

This tutorial provides a discussion of the application of knowledge-based processing techniques to emerging technologies. Following the third of the tutorials in this series we interpret knowledge-based processing as the use of adaptivity and the exploitation of prior knowledge in such a way as to choose the optimum processing method in each case. We interpret 'emerging technologies' as novel applications, such as multifunction phased array radars, waveform diversity, bistatic and multistatic radars, and synthetic aperture radars. Firstly, we consider the potential of electronically-steered phased array antennas and the associated signal processing techniques. This is followed by a description of knowledge-based processing in the task scheduling in a multifunction phased array radar. It is shown that prior information on targets can be used to control parameters such as update rate and dwell time. Next, we consider waveform diversity, which may be considered to be a development of multifunction phased array radar, in which a radar may simultaneously radiate and receive different signals in different directions for different purposes. Such a scheme may entail adaptivity in the angular domain, in the time domain and in the coding domain (and conceivably in other domains as well), and the use of knowledge-based techniques in this processing has obvious attractions. Two examples are discussed: the first is target-matched illumination, which shows that there is an optimum waveform for the detection of a given target in a given environment, and the second is interpolation between two (or more) spectral bands to give the effect of a signal of very high bandwidth, and hence very high range resolution. Next there follows a discussion of the application of knowledge-based techniques to bistatic and multistatic radar, including the use of information on waveform properties in passive coherent location (PCL), tracking in multistatic radar, and 'spatial denial' as a waveform diversity technique to prevent the exploitation by an enemy of a radar as a bistatic illuminator. Finally, an example is given of the use of 'context' in target detection in synthetic aperture radar imagery, exploiting the fact that targets of interest will tend to be parked in groups close to hedges and the edges of woods rather than individually in the middle of open ground. Useful improvements in detection performance are obtained.

1. INTRODUCTION

This tutorial provides a discussion of the application of knowledge-based processing techniques to emerging technologies. Following the third of the tutorials in this series we interpret knowledge-based processing as the use of adaptivity and the exploitation of prior knowledge in such a way as to choose the optimum processing method in each case. Knowledge-based systems form part of the subject of artificial intelligence, in which a knowledge base is used to guide an inference engine to make its processing decisions. We interpret 'emerging technologies' as novel applications in the radar domain, such as

Paper presented at the RTO SET Lecture Series on "Knowledge-Based Radar Signal and Data Processing", held in Stockholm, Sweden, 3-4 November 2003; Rome, Italy, 6-7 November 2003; Budapest, Hungary, 10-11 November 2003; Madrid, Spain, 28-29 October 2004; Gdansk, Poland, 4-5 November 2004, and published in RTO-EN-SET-063.

multifunction phased array radars, waveform diversity, and bistatic and multistatic radars, and synthetic aperture radars.

The first topic considered is the potential of electronically-steered phased array antennas and the associated signal processing techniques. These concepts are manifest in the multifunction phased array radar, in which electronic scanning may be employed both on transmit and receive, allowing adaptive control of waveform, PRF and dwell time, and performing a variety of surveillance and tracking tasks. Knowledge-based processing may be used to control the scheduling of tasks in such a radar, showing how prior information on targets can be used to ensure that the most critical tasks are performed first.

The next topic is waveform diversity, which may be considered to be a development of multifunction phased array radar, in which a radar may simultaneously radiate and receive different signals in different directions for different purposes (which may include communications or ECM as well as strictly radar). Such a scheme may entail adaptivity in the angular domain, in the time domain and in the coding domain (and conceivably in other domains as well), and the use of knowledge-based techniques in this processing has obvious attractions. Two examples are discussed: the first is target-matched illumination, which shows that there is an optimum waveform for the detection of a given target in a given environment, and the second is interpolation between two (or more) spectral bands to give the effect of a signal of very high bandwidth, and hence very high range resolution.

The third topic is the application of knowledge-based techniques to bistatic and multistatic radar, including the use of information on waveform properties in passive coherent location (PCL), tracking in multistatic radar, and 'spatial denial' as a waveform diversity technique to prevent the exploitation by an enemy of a radar as a bistatic illuminator.

Finally, an example is given of the use of 'context' in target detection in synthetic aperture radar imagery, exploiting the fact that targets of interest will tend to be parked in groups close to hedges and the edges of woods rather than individually in the middle of open ground. Useful improvements in detection performance are obtained.

2. MULTI-PHASED ARRAYS

The third lecture in this series has shown how antenna array signal processing techniques may be applied in radar, and particularly how these techniques are equivalent to those in the time / frequency domain. These properties and processing techniques include:

- matched filtering;
- the effects of the sampling theorem (aliasing); in the angular domain aliasing results in *grating lobes*;
- formation of a set of orthogonal filterbank responses by the Discrete Fourier Transform; in the angular domain the equivalent process is carried out by the Butler Matrix producing a set of orthogonal beams;
- weighting to reduce sidelobes (at the expense of loss and of broadening of response); the same weighting functions (Taylor, Chebyshev, …) are usable;

- synthesis of a desired radiation pattern (or spectrum) from a uniformly-spaced set of aperture (or time series) samples;
- superresolution techniques;
- adaptive filtering.

The most useful of these properties, when used in the radar function, is undoubtedly the latter one, and the use of adaptive arrays and (particularly) STAP have already been described at some length.

One of the earliest array signal processing techniques is that of monopulse [14], which can give higher angular resolution than the classical Rayleigh limit, avoiding the echo fluctuations that would occur with more than one pulse. Other examples include multiplicative arrays and aperture synthesis [14]. Another example (on transmit) is the 'crosseye' jamming technique, which presents a wavefront with an abruptly-changing phase to deceive an incoming tracking radar.

The following section describes some more modern applications of antenna array signal processing, and in particular some to which knowledge-based approaches may be applied.

3. ELECTRONICALLY AGILE BEAM FORMING

The electronically-steered phased array is one of the key subsystems in a modern radar, and the properties and processing techniques referred to in the previous section are fundamental. The use of individual phased array modules (Figure 1) allow all of the advantages of reliability ('graceful degradation') and flexibility. Figure 2 shows the MESAR (Multifunction Electronically-Scanned Array Radar) testbed developed over the past twenty years of more as a testbed for many of the concepts of phased array radar.

Even greater flexibility may be provided by direct digital synthesis of the signal at the array element. High-speed digital hardware is now sufficiently cheap that this can be straightforward. Such a digitally-generated signal can incorporate the phase shifts necessary to steer the beams, both in respect of the transmit signal and the receiver local oscillator. The modulation on the transmitted signal may also be varied adaptively, to allow techniques such as target-matched illumination to be used.

Further, amplifier linearization techniques, such as the outphasing method due to Chireix [12] are being developed to allow multiple signals to be fed through a single power amplifier with minimal distortion and intermodulation, hence allowing a single aperture to be shared between radar, communications and other functions.

3.2 Knowledge-Based Techniques in Multifunction Phased Array Radars

A multifunction radar is able to perform several different functions such as tracking, surveillance, missile guidance, kill assessment, all sharing the same antenna system. The greatest benefit of such a radar is its flexibility to undertake all these functions, changing the radar parameters such as waveform, frequency, pulse compression, dwell time and beam shaping, in order to cope well with all the different environments and operational scenarios. The functions consist of set of individual tasks that are competing for radar resources at any give instant. Because of this, the allocation of the radar resources must be executed efficiently by a resource manager to provide good performance of the overall system.

Two important processes must be done to allow adequate resource management. The first is the prioritization of the tasks that must be performed. The second is the scheduling that consists of forming a queue of tasks in a time line to be executed by the radar.

Some work has been done over the last years in order to design efficient scheduling algorithms. Casar-Corredera and Izquierdo-Fuente [31] proposed a scheduling process to interleave the tasks using a neural network. Strömberg and Grahn [45] developed two approaches for scheduling tracking and surveillance tasks. The first was based on operations research theory, and the other was based on temporal logic using artificial intelligence. Orman et al. [36] developed an algorithm using the concept of on-line coupled-task scheduling. The algorithm considers that between the pulse transmission time and the pulse reception time of a radar transmission, there is an idle time that could be used for interleaving new tasks. They suggested some heuristics to deal with this scheduling aspect. Another approach was developed by Stafford [44] and was based on the concept of timebalance. The functions to be performed by the radar should be divided into several tasks and jobs and a timebalance scheme was used to define which task or job should be scheduled next. The timebalance indicated how much time the radar owed to a function (surveillance, tracking etc). If a task was late, its time balance should be positive; if a task was due to be executed at a given time *t*, at *t* its timebalance should be zero; finally, if a task was early, its timebalance should be negative. Finally, Vine [48] proposed the use of fuzzy logic to introduce concepts such as dangerous and friendly in the scheduling process to resolve conflicts between tasks when the radar system is operating in an environment that leads to an overload situation.

All these approaches have in common the idea the tasks must have priorities associated to them and the decision-making will be done based on these priorities. The performance of the proposed schedulers is similar when the radar system is operating in a non-stressing situation and there are available radar resources to be allocated to functions. The difference between them becomes evident when the environment changes and there are not additional radar resources left. The schedulers will have to select the tasks that will be undertaken based on their priorities and lower priority tasks may be deferred.

Ranking the functions in priority order is usually determined *a priori* according to the previous knowledge of the tactical situation of the environment in which the radar is operating and to the experience of the radar engineer. These priorities should change during the operation of the radar under automatic control algorithms.

Figures 3 and 4 show the difference of the performance of scheduling algorithms considering the same number of targets under track but with different priorities between coverage areas. In the first case, the priority of region of coverage 3 is greater than the priority of regions of coverage 1 and 2. Because of this, the performance of surveillance in the region of coverage 3 is the last to be affected when the available radar resources are extinguishing. In the second case, the performances of surveillance in the three regions are proportionally degraded in the same situation. The schedulers used on these systems are based on the proposals of Orman et al. and Stafford, respectively.

An important aspect is that not only the scheduler but also the radar functions must be efficiently designed to avoid demanding unnecessary radar resources. For example, the tracking function should request updates only when they are important to keep the track of the targets. An adaptive tracking filter requests track updates based on the dynamics of the targets, on their degree of threatening etc. The more uncertainty there is about the targets, the more often requests will be generated in order to update the data about them. An analogous conclusion can be made when considering the surveillance function. The more uncertainty there is about the environment, the more often requests will be generated to collect data about it. Therefore, the previous knowledge of the tactical situation of the environment and the targets affects the performance of radar resource manager and the overall performance of the radar system.

Figures 5 and 6 show the influence of the previous knowledge of the identity of two targets in how often updates are performed by the radar. The targets are aircraft flying on the same trajectory. An adaptive Kalman filter was used to perform the tracking of the targets.

4. WAVEFORM DIVERSITY

4.1 Introduction

Waveform diversity may be considered to be a development of multifunction phased array radar, in which a radar may simultaneously radiate and receive different signals in different directions for different purposes (which may include communications or ECM as well as strictly radar). The concept is shown pictorially in Figure 9. Such a scheme may entail adaptivity in the angular domain, in the time domain and in the coding domain (and conceivably in other domains as well), and the use of knowledge-based techniques in this processing has obvious attractions.

In the succeeding paragraphs we discuss two important aspects of waveform diversity, namely *target-matched illumination*, in which it is shown that there is an optimum waveform for the detection of a given target, and spectral interpolation, which allows very high range resolution to be obtained from two (or more) spectrally-disjoint bands.

4.2 Target-matched Illumination

Principle: The concept of the matched filter was developed by Gjessing [21-23] and by Bell [2] to consider the optimum waveform for the detection of a target of a given range profile against a noise background. The target is characterized in terms of its impulse response as a function of delay time (i.e. range), which will also be a function of aspect angle (and therefore which in practice would require a library of target impulse responses versus aspect angle). The concept has been extended by Guerci and Pillai [19, 25, 30, 38] to include the detection of a target against nonhomogeneous noise, and also to the problem of discriminating different targets.

The problem is posed as follows (Figure 7) using the notation adopted by Guerci. The radar transmits a signal $s(t)$ towards a target, whose impulse response is $h_T(t)$. The echo signal $y(t)$ is the convolution of s(t) with $h_T(t)$. To this is added noise $n(t)$, so the received signal is

$$r(t) = \left(s(t) \otimes h_T(t)\right) + n(t) \tag{1}$$

where $\otimes$ denotes the convolution operator.

The receiver is characterized by its impulse response $h_R(t)$. The problem is then to choose $s(t)$ and $h_R(t)$ to maximise the signal-to-interference ratio, which can be expressed in mathematical terms as follow:

$$y_0 = \max_s \max_h \rho(t_0) \tag{2}$$

where

$$SINR = \rho(t_0) = \frac{y_s^2(t_0)}{\left\langle y_0(t_0)\right\rangle^2} \tag{3}$$

y_s is the signal component of the output and y_o is the component contributed by interference and noise.

The first step is to maximise the SNIR working on the receiver. Once the optimal impulse response of the receiver, $H_{MF}(t)$, has been determined, it follows (Figure 7) that :

$$SNIR_0 = \frac{1}{\sigma_w^2}\int_{Ti}^{Tf} \left| y_w(t) \right|^2 dt = f\left(s(t)\right) \tag{4}$$

where T_i and T_f are the time boundaries of the receiver and $y_w(t)$ is the signal echo after the whitening filter.

At this stage, the problem is to maximise SNIR at the instant of detection t_0 over the input signal $s(t)$ of finite energy and duration. Grouping the expressions for both whitening filter and matched filter:

$$h(t) \equiv h_T \otimes h_w(t) \tag{5}$$

Using this, the integral in (4) can be written

$$\int_{T_i}^{T_f} \left| y_w(t) \right|^2 dt = \int_0^T s(\tau_1).\int_0^T s^*(\tau_2).K^*(\tau_1,\tau_2)d\tau_2 d\tau_1 \tag{6}$$

where

$$K(\tau_1,\tau_2) \equiv \int_{T_i}^{T_f} h^*(t-\tau_1)h(t-\tau_2)dt \tag{7}$$

The solution must satisfy a homogeneous Fredholm integral of the second kind with Hermitian kernel:

$$\lambda_{\max} s_{opt}(t) = \int_0^T s_{opt}(\tau)K(t-\tau)d\tau \tag{8}$$

This principle can be extended to different models including signal dependent noise (clutter) [38] In this case, one must take the non-linear term into account in the signal to interference plus noise equation:

$$SINR_0 = \frac{\left| \frac{1}{2\pi}\int_{-\infty}^{+\infty} H_R(\omega)H_T(\omega)S(\omega).e^{-j\omega T_f} d\omega \right|^2}{\frac{1}{2\pi}\int_{-\infty}^{+\infty} \left|H_R(\omega)\right|^2.\left(G_n(\omega)+G_c(\omega)\left|S(\omega)\right|^2\right).d\omega} \tag{9}$$

where

$G_n(\omega)$ is the additive noise spectrum
$G_c(\omega)$ is the clutter spectrum
$H_T(\omega)$ and $H_R(\omega)$ are the transmitter and receiver spectrum respectively

From the above model, we can derive three main cases:

1. the clutter is non significant compared to the additive noise $G_c(\omega) << G_n(\omega)$
2. the additive noise is non significant regards to the clutter $G_c(\omega) >> G_n(\omega)$
3. clutter and noise are of equivalent power $G_c(\omega) \sim G_n(\omega)$

Unlike the first two cases, which can be solved by the previous method, the third one (clutter and noise) has been studied by Guerci using an iterative procedure [38].

Applications: Potential applications of matched illumination are:

- identical target resolution (Figure 8)
- target identification
- target tracking/tagging
- target aspect uncertainty

Further issues: The matched illumination has been obtained using information about the system under experiment. A straightforward problem is related to the ability of obtaining and processing the information in such way that it can be used for real applications. As a result, many papers dealing with classification algorithms are being published these days. In parallel with the development of knowledge based techniques is that of the pattern recognition. These methods are being developed to overcome the need for large libraries, and suggest that it is possible to characterize a target by isolating the influence of the strongest scatterers on the target signature.

Assuming a target can be described as a structure of scattering centres, the matched illumination can be applied to these sub-targets. Assuming these scattering centres are of relatively simple geometry, the required library would be much smaller. Furthermore, the extraction of intuitive scattering centres may lead to a fast method of recognition if part of an adaptive process. This method would combine both matched illumination (applied to major scattering centres in this case) and classification algorithm that would define the scattering centres to be extracted for a fast recognition.

4.3 Spectral interpolation

Another technique of interest is interpolation between two (or more) spectral bands to give the effect of a signal of very high bandwidth, and hence very high range resolution. The technique was originally proposed and demonstrated by workers at MIT Lincoln Labs [13], and demonstrated on S-band and C-band data from the COBRA JUDY shipborne radar system, to obtain high range resolution target profiles.

The scheme may be regarded as an extension of the superresolution techniques described in the third lecture of this series. It models the spectral signals in each sub-band with an all-pole model:

$$M\left(f_n\right) = \sum_{k=1}^{P} a_k p_k^n \tag{10}$$

Following the notation of [13], the lower and upper sub-bands contain N_1 and N_2 samples respectively , so the sample index n ranges from $n = 0, \ldots, N_1-1$ for the lower sub-band and $n = N-N_2, \ldots, N-1$ for the upper sub-band. The poles p_k characterize the relative ranges and frequency decay of the individual scattering centres. The sub-bands can be mutually cohered by fitting a separate all-pole model to each sub-band and adjusting the models until they are consistent.

Next, forward-prediction matrices for the lower and upper sub-bands are constructed:

$$\mathbf{H}_1 = \begin{pmatrix} s_0 & \cdots & s_{L-1} \\ \vdots & \ddots & \vdots \\ s_{N_1-L} & \cdots & s_{N_1-1} \end{pmatrix} \quad \text{and} \quad \mathbf{H}_2 = \begin{pmatrix} s_{N-N_2} & \cdots & s_{N-N_2+L-1} \\ \vdots & \ddots & \vdots \\ s_{N-L} & \cdots & s_{N-1} \end{pmatrix} \tag{11}$$

These are decomposed using singular value decomposition:

$$\mathbf{H}_1 = \mathbf{U}_1\mathbf{S}_1\mathbf{V}_1^{'} \quad \text{and} \quad \mathbf{H}_2 = \mathbf{U}_2\mathbf{S}_2\mathbf{V}_2^{'} \tag{12}$$

where the prime denotes the Hermitian operator. The **S** matrices contain the singular values; the **U** and **V** matrices contain the corresponding eigenvectors. Thus the all-pole model parameters can be estimated as follows:

1. The singular value matrices $\mathbf{S}_1$ and $\mathbf{S}_2$ are used to estimate the model orders P_1 and P_2 for the two sub-bands;
2. P_1 and P_2 are used to partition $\mathbf{V}_1$ and $\mathbf{V}_2$ into orthogonal subspaces: a signal-plus-noise subspace and a noise subspace. A modified root-MUSIC algorithm is applied to estimate the signal poles for each sub-band;
3. The all-pole model amplitude coefficients a_k are determined by using a linear least-squares fit to the measured data;
4. The resulting sub-band signal models are adjusted to optimally match.

The paper presents results using 12 – 18 GHz radar data, reduced to two 1 GHz sub-bands (13 – 14 GHz and 16 – 17 GHz) and successfully reconstructs the missing spectral data.

5. BISTATIC, MULTISTATIC AND NETTED RADAR

5.1 Introduction

Bistatic radar systems have been studied and built since the earliest days of radar. As an early example, the Germans used the British Chain Home radars as illuminators for their *Klein Heidelberg* bistatic system. Bistatic radars have some obvious advantages. The receiving systems are passive, and hence undetectable. The receiving systems are also potentially simple and cheap. Bistatic radar may also have a counter-stealth capability, since target shaping to reduce target monostatic RCS will in general not reduce the bistatic RCS. Furthermore, bistatic radar systems can utilize VHF and UHF broadcast and communications signals as 'illuminators of opportunity', at which frequencies target stealth treatment is likely to be less effective.

Bistatic systems have some disadvantages. The geometry is more complicated than that of monostatic systems. It is necessary to provide some form of synchronization between transmitter and receiver, in respect of transmitter azimuth angle, instant of pulse transmission, and (for coherent processing) transmit signal phase. Receivers which use transmitters which scan in azimuth will probably have to utilize 'pulse chasing' processing.

The combination of a number of transmitters and receivers in both monostatic and bistatic configurations, to form a netted radar system, offers the possibility of a further domain – the angular domain centered on the target – to exploit. Thus multistatic and netted radars are an area of considerable current interest.

The properties of bistatic radar have been described in detail by Willis [49, 50] and by Dunsmore [15]. Jackson [32] has analyzed the geometry of bistatic radar systems, and his notation (Figure 11) has been widely adopted.

From this:

$$r_2 = \frac{\left(r_1 + r_2\right)^2 - L^2}{2\left(r_1 + r_2 + L\sin\theta_R\right)} \tag{13}$$

Contours of constant bistatic range are ellipses, with transmitter and receiver as the two foci.

The bistatic radar equation is derived in the same way as the monostatic radar equation (Figure 12):

$$\frac{P_r}{P_n} = \frac{P_t G_t G_r \lambda^2 \sigma_b}{(4\pi)^3 r_1^2 r_2^2 k T_0 B F} \tag{14}$$

The factor $1/(r_1 r_2)$, and hence the signal-to-noise, has a minimum value for $r_1 = r_2$. Thus the signal-to-noise ratio is highest for targets close to the transmitter or close to the receiver.

Doppler shift depends on the motion of target, transmitter and receiver (Figure 13), and in the general case the equations are quite complicated [32, 50].

In the case when only the target is moving the Doppler shift is given by:

$$f_D = \left(\frac{2V}{\lambda}\right) \cos\delta \cos(\beta/2) \tag{15}$$

5.2 Application of Knowledge-based Signal Processing to Bistatic, Multistatic and Netted Radar

Knowledge-based techniques may have several applications in bistatic and (particularly) multistatic radar systems. In a passive coherent location (PCL) system using broadcast or communications signals, the ambiguity behaviour of the waveform depends significantly on the type of signal and the modulation.

The waveform properties of a variety of PCL illuminators (VHF FM radio, analogue and digital TV, digital audio broadcast (DAB) and GSM at 900 and 1800 MHz) have been assessed at University College London by digitizing off-air waveforms and calculating and plotting their ambiguity functions [28, 29]. The receiving system was based on a HP8565A spectrum analyzer, digitizing the 21.4 MHz IF output by means of an Echotek ECDR-214-PCI digitizer card mounted in a PC. The system has the advantage of great flexibility, since the centre frequency and bandwidth of the receiver can be set by the controls of the spectrum analyzer. The rather high noise figure of the spectrum analyzer is not a disadvantage, since all of the signals are of high power and propagation is line-of-sight.

Figure 14 shows typical ambiguity functions derived using this system of (a) BBC Radio 4 at 93.5 MHz, for which the programme content is speech (an announcer reading the news), and (b) a digital audio broadcast (DAB) signal at 222.4 MHz. Both show range resolution appropriate to their instantaneous modulation bandwidths (9.1 and 78.6 kHz respectively), though the difference in the sidelobe structure is very evident, showing that the digital modulation format is far superior because the signal is more noise-like. Furthermore, it has been found that for analogue modulation formats the ambiguity performance depends strongly on the instantaneous modulation. Thus music with high spectral content (such as orchestral or rock) is significantly better than music with low spectral content. Figure 15 tabulates the ambiguity performance in this respect of various forms of modulation. Also, and for the same reasons, with speech, the ambiguity performance during pauses between words is poor.

This suggests that knowledge of the ambiguity performance of different sources may be used with advantage. Monitoring, in real time, of the instantaneous modulation of sources could be used to select the optimum sources.

Another aspect where knowledge-based techniques will be valuable is in multi-sensor tracking. Knowledge of the instantaneous resolution (in range and Doppler) in this way will indicate the appropriate way to

combine the individual detections from each sensor. The knowledge-based tracking techniques discussed in the sixth of these lectures will be relevant here.

5.3 Bistatic Spatial Denial

Another example of waveform diversity is the use of multiple transmitted waveforms from an airborne platform to deny the use of the radar as a bistatic illuminator [16]. Figure 16 shows the geometry, in which the radar transmits a signal towards the target. A hostile bistatic radar system attempts to 'hitchhike' off the radar, but requires a coherent reference signal for synchronization. Conventional methods to prevent the interception of the direct path signal include low sidelobe antennas, physical isolation, and the use of spread spectrum waveforms. In this technique the radar can radiate a suitably coded 'masking signal', which denies the coherent reference to the bistatic receiver (Figure 17).

The problem is therefore one of finding a radar waveform $u_r(t)$ with suitable ambiguity function, and a masking waveform $u_m(t)$ which is orthogonal to the radar waveform over the full range and Doppler domain. The waveforms may be pulsed, quasi-CW or CW. Further, the radar waveform is radiated at a power P_t via a radiation pattern $F_r(\theta)$, and the masking waveform $u_m(t)$ at a power P_m via a radiation pattern $F_m(\theta)$, and we require $F_r(\theta)$ and $F_m(\theta)$ to be spatially orthogonal, over the full bandwidth of the radar.

The overall performance of the scheme is quantified in terms of two parameters: (i) the degree of masking of the radar signal by the masking signal, and (ii) the degree of suppression of echoes (from targets or from clutter) of the masking signal in the channels of the radar receiver.

The performance of waveform codes is quantified in terms of their auto-ambiguity [52] and cross-ambiguity [39] functions:

$$\left|\chi(\tau, f_D)\right|^2 = \left|\int_{-\infty}^{\infty} u_r(t) u_r^*(t-\tau) \exp(j2\pi f_D t) dt\right|^2 \tag{16}$$

$$\left|\chi_{r,m}(\tau, f_D)\right|^2 = \left|\int_{-\infty}^{\infty} u_r(t) u_m^*(t-\tau) \exp(j2\pi f_D t) dt\right|^2 \tag{17}$$

Several different waveform codes have been analyzed in this way, including co-channel chirp waveforms of opposite slope [20], pseudo-random binary sequences [27], and Costas codes [11, 24]. For this work the Costas signal is adopted for the host radar waveform because it yields a thumbtack-shaped ambiguity function with a relatively low pedestal. For a fixed number of frequency hops within a radar pulse there are many different hopping patterns that result in essentially the same thumbtack-shaped ambiguity function. Hence, different frequency hopping patterns can be utilized to further complicate the coherent reference estimation task of the non-cooperative radar.

The first approach to the design of radiation pattern is to use a linear array for the radar, with the masking signal radiated via N additional elements which form an interferometer. The two interferometric elements are driven separately with an independent waveform generation, timing and control circuit. Ideally, the interferometer antenna pattern will overlay the sidelobes of the host radar main antenna pattern with minimal overlay of the radar main beam. This will mask that portion of the host radar signal emitted through the radar sidelobes denying a coherent reference signal to a non-cooperative bistatic receiver.

Figure 18 shows the azimuthal radiation pattern of the interferometer array factor for N = 4 and 5. We notice major lobes at α =0° and 180° as well as major lobes or nulls at α =±90° for N odd or even respectively. In the case where nulls appear at α =±90° we notice something of particular interest. The

derivative of the array factor at $\alpha = \pm 90°$ is zero, which means that the nulls at those angles have zero slope. This makes those particular nulls broader than the rest of the nulls. To avoid self-jamming of the radar waveform, it may be desirable to steer the interferometer pattern such that the main beam of the host radar is centered in this broad null. To achieve this interferometer steering and obtain a broad null at $\alpha = 0$ we place the interferometer on the *y*-axis keeping the linear array of the main radar along the *x*-axis. Assuming that the interferometer elements spacing is measured in units of half wavelength $d_{IFM} = k_s\,(\lambda/2)$ we notice that a broad null exists at $\alpha = 0°$ only for odd k_s. This is shown in Figure 19 for $k_s = 7$. In this case broad nulls occur broad side to the main radar antenna in both the horizontal and vertical planes guaranteeing the orthogonality property between radar and masking signal. Since the interferometer excitation is likely to be considerably smaller than the radar excitation, placement of the broad null of the interferometer at the center of the main beam of the radar is likely to be an effective technique from preventing the interferometer signal from interfering with the desired radar target returns.

Notice that as the number of interferometer elements *N* increases, both the broad null as well as the spacing between sidelobes widens, thereby decreasing masking coverage in the direction of a potential non-cooperative radar. One possible method to overcome this deficiency is to change the configuration of the interferometer so as to form a triangle with three elements. This pattern is more irregular, but does have increased coverage despite being at a lower amplitude.

The second approach uses an *N*-element linear antenna array. Suppose initially that the array is fed by a Butler Matrix [9] (Figure 20). This generates a set of spatially-orthogonal antenna beams, each of the form

$$|E| = \frac{1}{N}\frac{\sin(N\psi/2)}{\sin(\psi/2)} \tag{18}$$

with

$$\psi = \frac{kd}{\lambda}\sin(\theta - \delta) \tag{19}$$

where d is the element spacing, λ is the wavelength, $k = 2\pi/\lambda$, θ is the azimuth angle and δ is the angle of the maximum of the particular beam. For an *N*-element array

$$\delta_m = \frac{(2m-1)\pi}{N} \tag{20}$$

so the normalized far-field pattern of the m^{th} beam is

$$E_m = \frac{1}{N}\frac{\sin N\{(kd/2)\sin\theta - [(2m-1)/N](\pi/2)\}}{\sin\{(kd/2)\sin\theta - [(2m-1)/N](\pi/2)\}} \tag{21}$$

The orthogonality of this set of beams is maintained over a broad bandwidth, dictated by the hardware of the Butler Matrix, but typically an octave or more. In order for this to be so, the beamwidths and directions of the beams must change with frequency. The beams have a first sidelobe level of –13.2 dB, which is rather high for radar purposes; the sidelobe level can be lowered by an amplitude taper across the array in the usual way, but this destroys the orthogonality condition. The set of beams may be steered electronically by a set of phase shifters, either at the antenna elements or at the beam ports.

Suppose that one of the central beams is used for the radar, both for transmitting and receiving. One or more of the remaining beams is used to radiate the masking signal or signals, at an appropriate relative power level. Furthermore, if the radar signal and masking signal(s) were to be generated at the beam ports

of the Butler Matrix by direct digital synthesis, which could include the effect of phase shifts to steer the beams electronically, then since the signals radiated from each element are simply weighted combinations of the beam port signals, the element signals may be calculated and generated directly, without any need for the Butler Matrix hardware.

To evaluate the performance of a given system it is necessary to specify a value for the degree of masking. In practice this will vary with direction θ, so may be specified as a peak value or as a mean averaged over the sidelobe region of $F_r(\theta)$. Thus we define

$$L(\theta) = \frac{P_r F_r(\theta)}{P_m F_m(\theta)} \tag{22}$$

with P_m and P_r the power levels at which the masking and radar signals are transmitted. This is the radar signal to masking signal ratio for the case of an adversary listening from a particular angle θ. This ratio depends on the geometry of the antennas used and their radiation pattern. The required degree of masking represents a compromise on one hand by the need to disrupt the coherent reference, and on the other hand not to disrupt the operation of the radar. From a knowledge of the effect of ECM, a value of about 13 dB is likely to be adequate. The value of L at $\theta = 0$ (i.e. at the centre of the host radar main lobe) will obviously take negligible values, first because of the broad null of the masking signal at this angle and secondly because of the coding of the signals. An adversary could only recover the radar signal if listening from that specific direction.

The suppression of the masking signal in the radar receiver will include the echoes received from the target and clutter. The masking signal levels will be further suppressed because the filter at the receiver is matched to the radar signal. The echo of the masking signal is relative to $P_m F_m$. Similarly the echo of the radar signal is relative to $P_r F_r$. These are received by the radar antenna pattern which for the present we will consider to be the same as the transmit radar pattern. The following two expressions can thus be written down:

$$S_m = P_m F_m(\theta_{TAR}) F_r(\theta_{REC}) \tag{23}$$

$$S_r = P_r F_r(\theta_{TAR}) F_r(\theta_{REC}) \tag{24}$$

These are applied to the matched filter for the radar signal. The degree of suppression of the masking signal is therefore:

$$R(\theta) = \frac{P_m F_m(\theta_{TAR}) F_r(\theta_{REC}) \int_{-\infty}^{\infty} u_m(t-\tau) u_r^*(t) e^{j2\pi f_D t} dt}{P_r F_r(\theta_{TAR}) F_r(\theta_{REC}) \int_{-\infty}^{\infty} u_r(t-\tau) u_r^*(t) e^{j2\pi f_D t} dt} \tag{25}$$

where:

P_m is the power level of the transmitted masking signal;

P_r is the power level of the transmitted radar signal;

$F_m(\theta_{TAR})$ is the Doppler shifted echo of the masking signal from the target;

$F_r(\theta_{TAR})$ is the Doppler shifted echo of the radar signal from the target;

$F_r(\theta_{REC})$ is the radar signal at reception;

$\int_{-\infty}^{\infty} u_m(t-\tau)u_r^*(t)e^{j2\pi f_D t}dt$ is the response to the masking signal of the filter matched to the radar signal (cross ambiguity function);

$\int_{-\infty}^{\infty} u_r(t-\tau)u_r^*(t)e^{j2\pi f_D t}dt$ is the response to the radar signal of the filter matched to the radar signal (auto ambiguity function).

Figure 22 shows a typical result, corresponding to P_r/P_m = 10 dB, for the interferometer scheme and for the Costas-coded signal whose ambiguity function is depicted in Figure 21. The plot shows the degree of suppression of the masking signal in the radar receiver, according to equation (25), as a function of range and of angle. It can be seen that, within the main lobe of the radar antenna pattern the masking signal is suppressed to a very low level, both because the masking signal radiation pattern has a null in that direction, and also because the orthogonality of the masking signal code to the radar signal is very high at zero Doppler (boresight). Outside the main lobe region the degree of suppression is about 30 dB. A different value of P_r/P_m would simply shift this characteristic up or down.

6. SYNTHETIC APERTURE RADAR

High-resolution synthetic aperture radar is now widely used for military surveillance as well as in geophysical remote sensing applications. Whilst huge volumes of image data are readily generated, one of the major challenges is to extract information from those images in a reliable and efficient manner, and Oliver and Quegan's book [35] is devoted to this problem. The use of prior information in a knowledge-based approach is clearly attractive.

Conventionally, the target detection problem is tackled by comparing the value of the image pixel under test against the statistical distribution of the surrounding pixels. If the observed value of the pixel is unlikely to occur as a result of the clutter, then a target is declared to be present. This forms the basis of classical CFAR algorithms. Blacknell [7] has considered the use of what he calls 'context' in this problem. Thus the likelihood of a target being present will be influenced by the image context – for example, military vehicles will tend to be parked in groups close to hedges and the edges of woods rather than individually in the middle of open ground. This contextual information can be exploited by allowing the target probability $P(t)$ to vary as a function of spatial position, depending on the context. This will mean that the detection threshold used in the likelihood ratio test will vary with spatial position, and hence the false alarm rate will not be constant over the scene.

Following Blacknell's description and notation [7], consider a particular image position at which the target probability is $Q(t) = \alpha P(t)$, where $P(t)$ is the target probability associated with a nominal probability of false alarm, P_{FA}. Then the value x_α above which a target is declared is:

$$P_b(x_\alpha) \cong cQ(t) = \alpha cP(t) = \alpha P_b(x_0) \tag{26}$$

and the probability of false alarm is given by:

$$P_{FA}(\alpha) = \int_{x_\alpha}^{\infty} P_b(x)dx \tag{27}$$

For SAR images, the standard background model is given by the negative exponential distribution, which describes the speckle fluctuations that arise in coherent imaging systems:

$$P_b(x) = \frac{1}{\mu_b}\exp\left(-\frac{x}{\mu_b}\right) \tag{28}$$

which gives a probability of false alarm of

$$P_{FA} = \exp\left(-\frac{x_0}{\mu_b}\right) \tag{29}$$

and hence a pixel intensity threshold of

$$x_0 = -\mu_b \ln\left(P_{FA}\right) \tag{30}$$

Thus, given a modified target probability, manipulation of the above equations gives the modified pixel intensity threshold:

$$x_\alpha = x_0 - \mu_b \ln(\alpha) \tag{31}$$

and the modified probability of false alarm

$$P_{FA}(\alpha) = \exp\left(-\frac{x}{\mu_b} + \ln(\alpha)\right) = \alpha P_{FA} \tag{32}$$

The technique was demonstrated using simulated data. Three types of contextual information were considered: the terrain type, the proximity of hedges, and the proximity of other targets. Military targets are more likely to travel through fields than through woods, so terrain type is relevant. Also, military vehicles will tend to travel in groups and will be parked near hedges rather than in the open, to make detection more difficult.

The results showed consistent improvements in detection rates, with a 13±1% increase in the number of targets detected when all of the contextual influences considered were present. Blacknell states: 'The challenge for the future is to quantify in statistical terms the contextual influences in a real SAR scene and to trial the detection scheme against realistic military deployments of targets'.

7. CONCLUSIONS

The examples presented in this tutorial have attempted to show the great potential of knowledge-based processing techniques in future-generation radar systems. The examples presented – in multifunction phased array radar, target-matched illumination and spectral interpolation (as examples of waveform diversity), bistatic radar, and synthetic aperture radar, have all attempted to show how prior information on the target scene and the targets themselves can be exploited.

A further comment is that advances in processing and algorithms are far easier to incorporate in practical radar systems than advances in hardware. A radar system with a planned lifetime of (say) twenty years can be designed so that new algorithms can be incorporated straightforwardly, rather than with radical, expensive modifications.

8. ACKNOWLEDGEMENTS

I gratefully acknowledge invaluable discussions with many people from whom I have learned much about radar and signal processing over the years. I would particularly like to mention Chris Baker, David Blacknell, DEN Davies, Alfonso Farina, Richard Klemm, Simon Watts, Richard White, Mike Wicks and Nick Willis. I am also grateful to the students with whom I have worked on these subjects over the years, in particular Hervé Borrion, Joe Butler, Shirley Coetzee, Glen Davidson, Ioannis Fotinopoulos, Sergio Miranda, Dominic Walker and Aric Whitewood, and to the organisations, including the UK Ministry of Defence, the US Air Force Office of Scientific Research, the UK Engineering and Physical Sciences Research Council, QinetiQ and its predecessors, BAE SYSTEMS, Thales Sensors and AMS, who have supported the various projects.

9. REFERENCES

1. Adve, R., Antonik, P., Baldygo, W., Capraro, C., Capraro, G., Hale, T., Schneible, R. and Wicks, M., 'Knowledge-base application to ground moving target detection', AFRL-SN-RS-TR-2001-185, September 2001.
2. Bell, M., 'Information theory and radar waveform design', *IEEE Trans. Information Theory*, Vol.39, No.5, pp1578-1597, 1993.
3. Berry, P.E. and Fogg, D.A.B., 'On the use of entropy for optimal radar resource management and control', (to be presented at First Australian International Radar, Conference, Adelaide, 3 – 5 September 2003.
4. Billingsley, J.B., *Low Angle Radar Land Clutter: Measurements and Empirical Models*, SciTech / Peter Peregrinus, 2002.
5. Blacknell, D., 'Target detection in correlated SAR clutter', *IEE Proc. Radar, Sonar and Navigation*, Vol.147, No.1, pp9-16, February 2000.
6. Blacknell, D., 'Statistical target behaviour in SAR images', *IEE Proc. Radar, Sonar and Navigation*, Vol.147, No.3, pp143-148, June 2000.
7. Blacknell, D., 'Contextual information in SAR target detection', *IEE Proc. Radar, Sonar and Navigation*, Vol.148, No.1, pp41-47, February 2001.
8. Brennan, L.E. and Reed, I.S., 'Theory of adaptive radar', *IEEE Trans. Aerospace & Electronic Systems*, Vol.AES-9, No.2, pp237-252, March 1973.
9. Butler, J.L., 'Digital matrix and intermediate frequency scanning', Chapter 3 in *Microwave Scanning Antennas*, Volume III, (R.C. Hansen ed.), Peninsula Publishing, 1985.
10. Butler, J.M., Moore, A. and Griffiths, H.D., 'Multifunction radar resource management for the tracking function', Proc. *RADAR'97* Conference, Edinburgh; IEE Conf. Publ. No. 449, pp568–572, 14–16 October 1997.
11. Costas, J.P., 'A study of a class of detection waveforms having nearly ideal range-Doppler ambiguity properties', *IEEE Trans. Information Theory*, Vol.IT-28, No.4, pp600-604, July 1982.
12. Cripps, S.C., *RF Power Amplifiers for Wireless Communications*, Artech House, 1999.
13. Cuomo, K.M., Piou, J.E. and Mayhan, J.T., 'Ultra-wideband coherent processing', Special issue of *The Lincoln Laboratory Journal* on Superresolution, Vol. 10, No.2, pp203-221, 1997.
14. Drabowitch, S., Papiernik, A., Griffiths, H.D., Encinas, J. and Smith, B.L., *Modern Antennas*, Chapman & Hall / IEEE MTT, ISBN 0 412 57910 3, 1997.
15. Dunsmore, M.R.B., 'Bistatic radars', chapter 11 in *Advanced Radar Techniques and Systems* (G. Galati ed.), Peter Peregrinus, 1993.
16. Ertan, S., Wicks, M.C., Antonik, P., Adve, R., Weiner, D., Griffiths, H.D. and Fotinopoulos, I., 'Bistatic denial by spatial waveform diversity', Proc. *RADAR 2002* Conference, Edinburgh; IEE Conf. Publ. No.490, pp17-21, 15 – 17 October 2002.
17. Farina, A. and D'Addio, E., 'Overview of detection theory in multistatic radar', *IEE Proc.*, Vol.133, Pt.F., No.7, pp613-623, December 1986.
18. Farina, A., *Antenna-based Signal Processing Techniques for Radar Systems*, Artech House, 1991.
19. Garren, D.A., Osborn, M.K., Odom, A.C., Goldstein, J.S., Pillai, S.U. and Guerci, J.R., 'Enhanced target detection and identification via optimized radar transmission pulse shape', *IEE Proc. Radar, Sonar and Navigation*, Vol.148, No.3, pp130-138, June 2001.
20. Giuli, D., Fossi, M. and Facheris, L., 'Radar target scattering matrix measurement through orthogonal signals', *IEE Proc*, Pt.F., Vol.140, No.4, pp233-242, August 1993.
21. Gjessing, D.T., 'Adaptive techniques for radar detection and identification of objects in an ocean environment', *IEEE J. Ocean Engineering*, Vol.6, No.1, pp5-17, 1981.
22. Gjessing, D.T., *Target Adaptive Matched Illumination Radar: Principles and Applications*, Peter Peregrinus, 1986.
23. Gjessing, D.T. and Saebboe, J., 'Bistatic matched illumination radar involving synthetic aperture and synthetic pulse for signal to clutter enhancement and target characterization', Proc. 2001 CIE International Conference on Radar, Beijing, pp20-24, 15 – 18 October 2001.

24. Golomb, S.W. and Taylor, H., 'Construction and properties of Costas arrays' *Proc. IEEE*, Vol.72, No.9, pp1143-1163, September 1984.
25. Grieve, P.G. and Guerci, J.R., 'Optimum matched illumination-reception radar', US Patent S517522, 1992.
26. Griffiths, H.D. and Carter, S.M., 'Provision of moving target indication in an independent bistatic radar receiver', *The Radio and Electronic Engineer*, Vol.54, No.7/8, pp336-342, July/August 1984.
27. Griffiths, H.D. and Normant, E., 'Adaptive SAR beamforming network', European Space Agency Contract Report, Contract No. 6553/89/NL/IW, ESA Technical and Publications Branch, ESTEC, Noordwijk, 1990.
28. Griffiths, H.D., Baker, C.J., Ghaleb, H., Ramakrishnan, R. and Willman, E., 'Measurement and analysis of ambiguity functions of off-air signals for passive coherent location', *Electronics Letters*, Vol.39, No.13, pp1005-1007, 26 June 2003.
29. Griffiths, H.D., 'From a different perspective: principles, practice and potential of bistatic radar', (to be presented at First Australian International Radar, Conference, Adelaide, 3 – 5 September 2003.
30. Guerci, J.R., 'Optimum matched illumination-reception radar for target classification', US Patent S5381154, 1995.
31. Izquierdo-Fuente, A. and Casar-Corredera, J.R.; 'Optimal radar pulse scheduling using a neural network', Proc. *IEEE International Conference on Neural Networks*, 1994.
32. Jackson, M.C., 'The geometry of bistatic radar systems' *IEE* Proc., Vol.133, Part F., No.7, pp604-612, December 1986.
33. Morgan, C. and Moyer, L., 'Knowledge base applications to adaptive space-time processing, volume IV: knowledge-based tracking', AFRL-SN-RS-TR-2001-146 Vol.IV, July 2001.
34. Morgan, C. and Moyer, L., 'Knowledge base applications to adaptive space-time processing, volume V: knowledge-based tracker rule book', AFRL-SN-RS-TR-2001-146 Vol.V, July 2001.
35. Oliver, C.J. and Quegan, S., *Understanding Synthetic Aperture Radar Images*, Artech House, 1998.
36. Orman *et al.*, 'Scheduling for a multifunction phased array system', *European Journal of Operational Research*, No. 90, 1996.
37. Pell, C. and Hanle, E. (eds), Special Issue of IEE Proceedings Part F. on Bistatic Radar; *IEE Proc.*, Vol.133, Pt.F., No.7, December 1986.
38. Pillai, S.U., Oh, H.S., Youla, D.C. and Guerci, J.R., 'Optimum transmit-receiver design in the presence of signal-dependent interference and channel noise', *IEEE Trans. Information Theory*, Vol.46, No.2, pp577-584, March 2000.
39. Rihaczek, A.W., *Principles of High Resolution Radar*, McGraw-Hill, New York, 1969; reprinted by Artech House, Norwood, MA, 1996.
40. Salama, Y. and Senn, R., 'Knowledge base applications to adaptive space-time processing, volume I: summary', AFRL-SN-RS-TR-2001-146 Vol.1, July 2001.
41. Salama, Y. and Senn, R., 'Knowledge base applications to adaptive space-time processing, volume VI: knowledge-based space-time adaptive processing (KBSTAP) user's manual and programmer's manual', AFRL-SN-RS-TR-2001-146 Vol.VI, July 2001.
42. Schuman, H., 'Knowledge base applications to adaptive space-time adaptive processing, volume II: airborne radar filtering', AFRL-SN-RS-TR-2001-146 Vol.II, July 2001.
43. Schuman, H., 'Knowledge base applications to adaptive space-time adaptive processing, volume III: radar filtering rule book', AFRL-SN-RS-TR-2001-146 Vol.III, July 2001.
44. Stafford, W.K.; 'Real time control of a Multifunction Electronically Scanned Adaptive Radar (MESAR)', IEE Colloquium on Real Time Management of Adaptive Radar Systems, June 1990.
45. Strömberg D. and Grahn P.; 'Scheduling of tasks in phased array radar', Proc. *IEEE International Symposium on Phased Array Systems and Technology*, 1996.
46. Tsao, T., Slamani, M., Varshney, P., Weiner, D., Schwarzlander, H. and Borek, S., 'Ambiguity function for a bistatic radar', *IEEE Trans. Aerospace and Electronic Systems*, Vol.33, No.3, pp1041-1051, July 1997.
47. Van Trees, H.L., *Detection, Estimation and Modulation Theory, Part I*, Wiley, New York, 1968.

48. Vine, M. T.; 'Fuzzy logic in radar resource management', *Multifunction Radar and Sonar Sensor Management Techniques* (Ref. No. 2001/173), IEE, 2001.
49. Willis, N.J., 'Bistatic radar', chapter 25 in *Radar Handbook* (second edition), (M.I. Skolnik ed.), McGraw-Hill, 1990.
50. Willis, N.J., *Bistatic Radar*, Artech House, 1991.
51. Wirth, W-D., *Radar Techniques using Array Antennas*, Peter Peregrinus, 2001.
52. Woodward, P.M., *Probability and Information Theory, with Applications to Radar*, Pergamon Press, 1953; reprinted by Artech House, 1980.

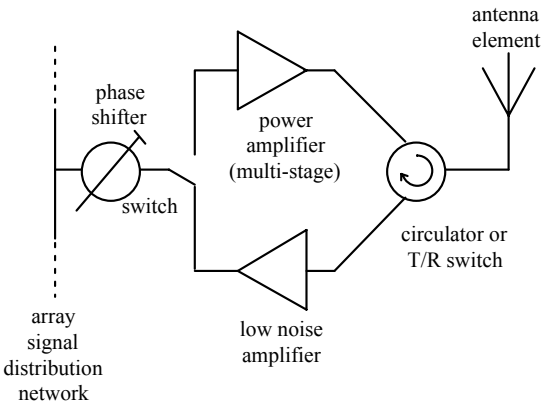

Figure 1. Block diagram of a typical phased array module.

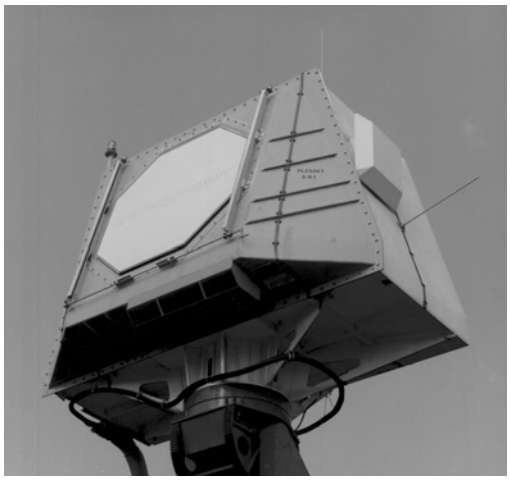

Figure 2. The MESAR (Multifunction Electronically Scanned Adaptive Radar) active phased array radar.

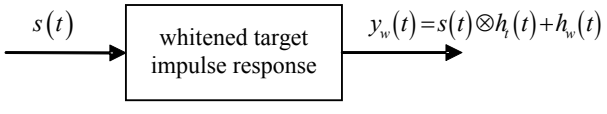

Figure 7. Whitening of the target impulse response in target-matched illumination.

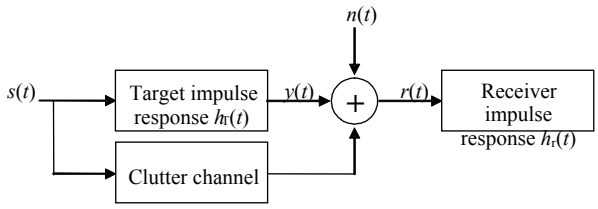

Figure 8. Target-matched illumination with signal-dependant noise (clutter).

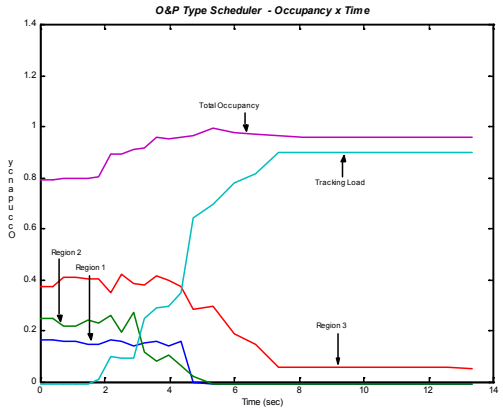

Figure 3. Regions of coverage with different priorities.

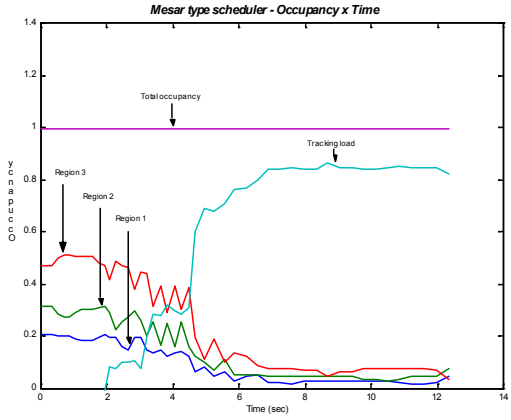

Figure 4. Regions of coverage with the same priorities.

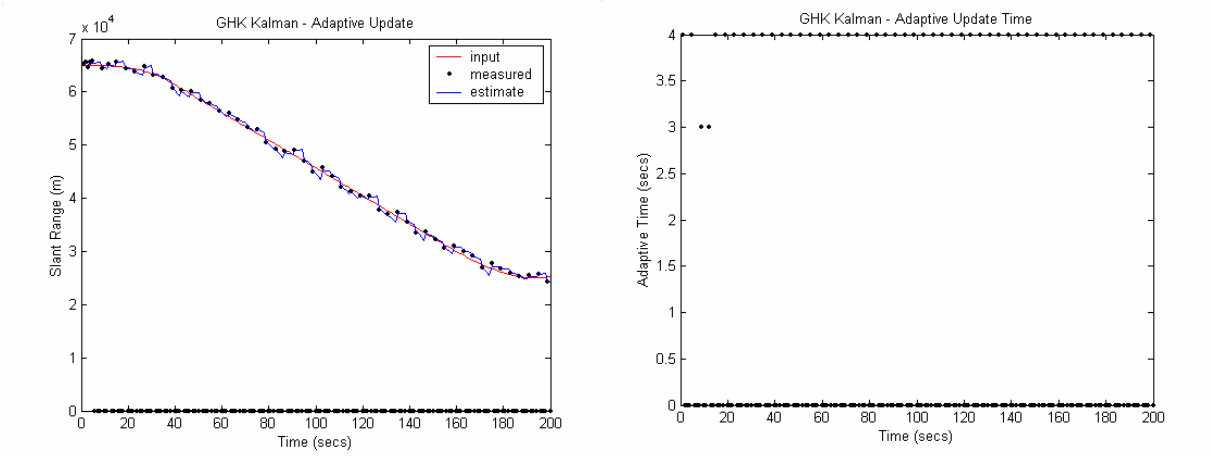

Figure 5 - Tracking of a friendly target

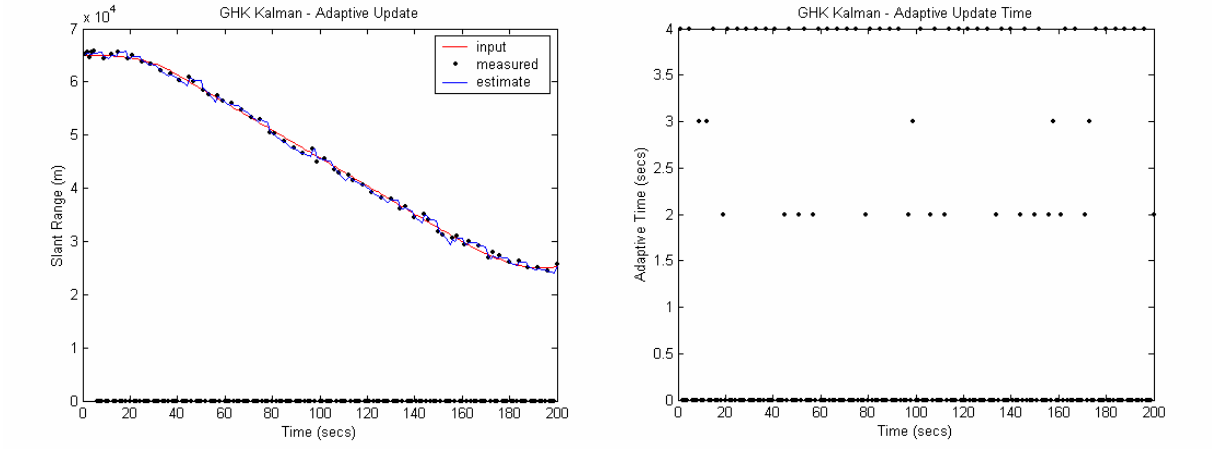

Figure 6. Tracking of an enemy or an unknown target

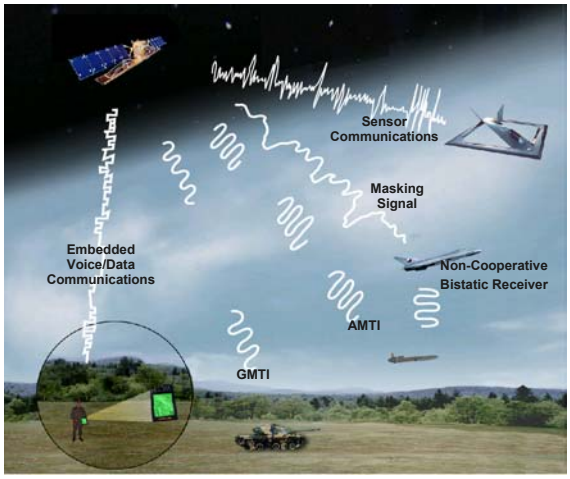

Figure 9. Concept of waveform diversity (after [16]).

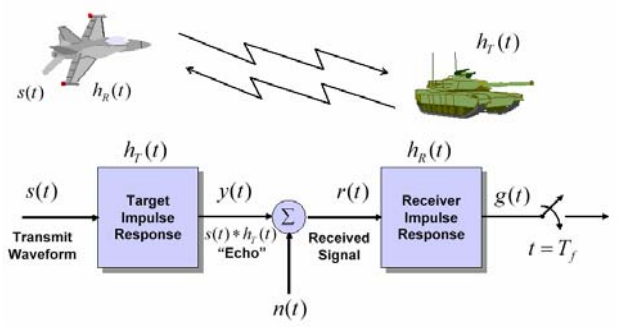

Figure 10. The target-matched illumination problem (after Guerci [38]).

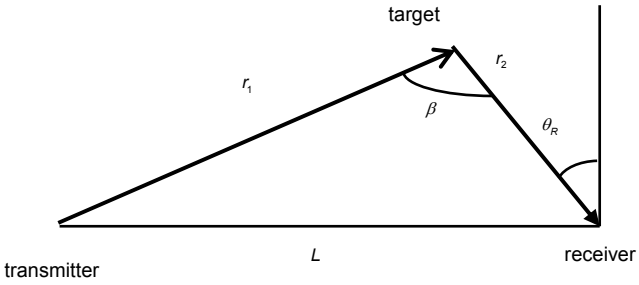

Figure 11. Bistatic radar geometry.

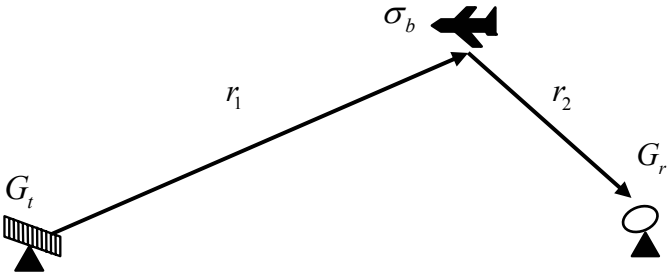

Figure 12. Bistatic radar equation.

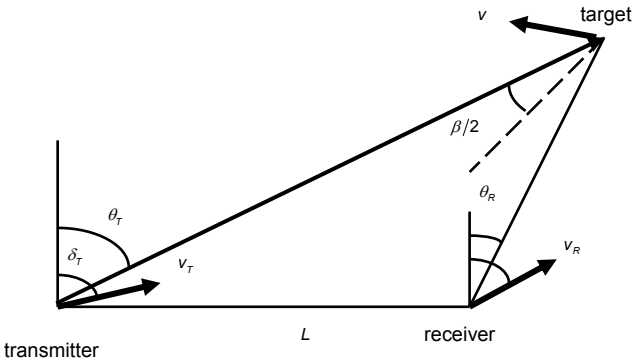

$$\beta = \theta_T - \theta_R$$

Figure 13. Bistatic Doppler (after Jackson [32]).

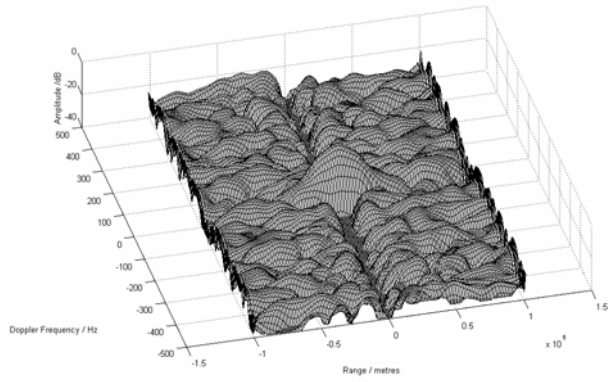

(a)

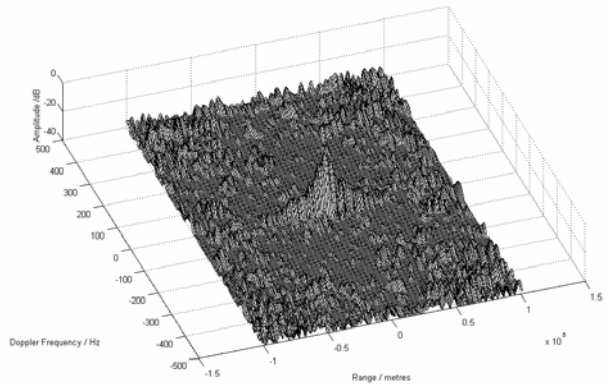

(b)

Figure 14. Typical ambiguity functions: (a) BBC Radio 4 transmission (93.5 MHz) and (b) digital audio broadcast transmission (222.4 MHz).

signal	frequency (MHz)	range resolution (km)	effective bandwidth (kHz)	peak range sidelobe level (dB)	peak Doppler sidelobe level (dB)
FM radio: speech (BBC Radio 4)	93.5	16.5	9.1	–19.1	–46.5
FM radio: classical music	100.6	5.8	25.9	–23.9	–32.5
FM radio: rock music (XFM)	104.9	6.55	22.9	–12.0	–26.0
FM radio: reggae (Choice FM)	107.1	1.8	83.5	–27.0	–39.5
DAB	219.4	1.54	97.1	–11.7	–38.0
Analogue TV: chrominance sub-carrier	491.55	9.61	15.6	–0.2	–9.1
Digital TV (DVB-T)	505.0	1.72	87.1	–18.5	–34.6
GSM 900	944.6	1.8	83.3	–9.3	–46.7
GSM 1800	1833.6	2.62	57.2	–6.9	–43.8

Figure 15. Properties of ambiguity functions of various types of broadcast and communications signals.

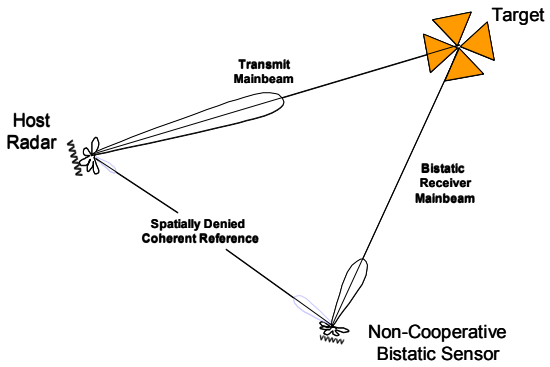

Figure 16. Non-cooperative bistatic receivers require a coherent reference from the host illuminator.

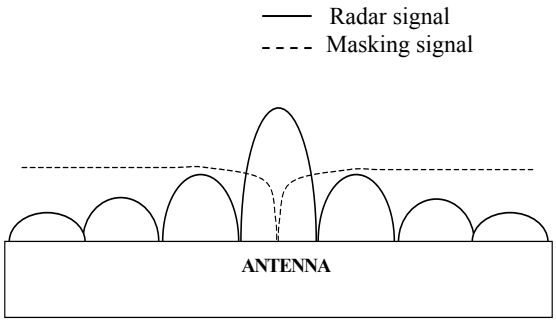

Figure 17. Radar and masking signal radiation patterns.

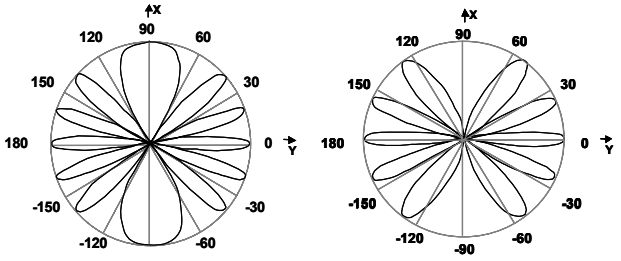

Figure 18. Azimuthal radiation pattern for a) N=4 and b) N=5

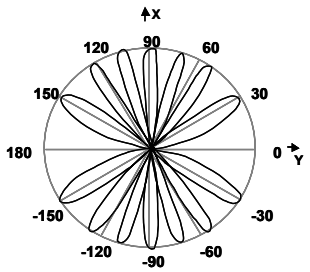

Figure 19. Azimuthal radiation pattern for steered interferometer and k_s=7.

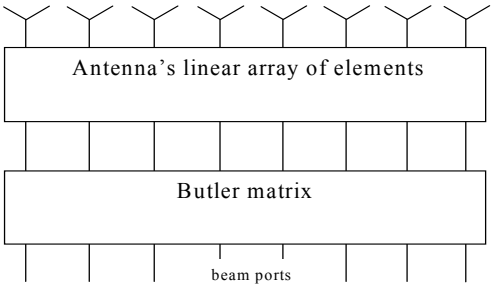

Figure 20. Linear array and Butler matrix

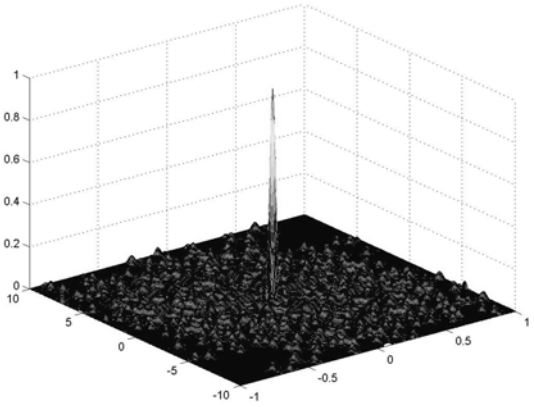

Figure 21. Auto-ambiguity function of a Costas signal for N=30 (linear scale).

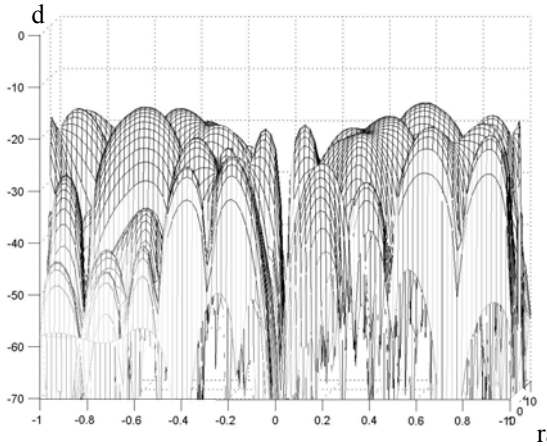

Figure 22. Degree of suppression of masking signal in the radar receiver (for interferometer scheme and for Costas coded signal of Figure 21 with P_r/P_m = 10 dB).

Integrated End-to-End Radar Signal & Data Processing With Over-arching Knowledge-Based Control

Dr. Gerard T. Capraro
Capraro Technologies, Inc.
311 Turner Street – Suite 410
Utica, NY 13501
USA
Email: gcapraro@caprarotechnologies.com

Abstract

This paper provides information related to integrating Knowledge Based (KB) techniques within the filtering, detection, tracking and target identification portions of an airborne radar's processing chain. We will present multiple information sources and how they can be used to enhance a radar's performance for end-to-end signal and data processing.

Introduction

In our previous paper we presented material for understanding some of the basic elements regarding knowledge bases and artificial intelligence (AI). In this paper we wish to present a design of an intelligent airborne radar system that processes information from the end-to-end, i.e. filter, detector and tracking stages of a surveillance radar. Can we build new radar systems that can dynamically change its processing given information from other sensors, outside sources, weather data, etc.? We believe that we can. The computing clock rates for computers have been doubling approximately every 18 months. Today's commercial off the shelf computers have clock rates exceeding 3 GHz. We believe that the computing power is available to insert sophisticated "rules/logic" within radar signal and data processing.

The following section will pick up where we left off in our first paper, dealing with ontologies. A global view of interfacing multiple platforms of sensors and the integration of sensors on one platform will be discussed. The next section will describe the major knowledge base components of an airborne intelligent radar system (AIRS). The next section will provide an overview of how the AIRS processes data within different states. The following section will provide a knowledge base tracking algorithm with memory thereby providing information helpful for target identification and terrain resolution. The last section provides our summary.

A Global View

The performance of our sensor systems can be enhanced by dynamically controlling a sensor's algorithms dependent upon a changing environment. The sharing of information in real time with other sensors is also a major plus. It has been shown in this lecture series that if an airborne radar system knows about certain features of the Earth (e.g. land sea interfaces) and its surroundings then it can use this information intelligently and increase its performance. A radar system can perform better with information from other sensors, e.g. sensor fusion. It could perform better if it knew where potential jammers were located and their characteristics.

However, if an airborne radar is going to share and receive information from multiple sources then it must be able to communicate and understand the information. A solution for the exchange of information between heterogeneous sensors is for each sensor to publish information based upon shared ontologies. In this manner when a sensor publishes its track data multiple sensors receiving this information will be able to interpret its contents without ambiguity. Accomplishing this will require that certain basics be established. We must have an accepted method of defining the Earth's geometry such that every element on the Earth, air

Paper presented at the RTO SET Lecture Series on "Knowledge-Based Radar Signal and Data Processing", held in Stockholm, Sweden, 3-4 November 2003; Rome, Italy, 6-7 November 2003; Budapest, Hungary, 10-11 November 2003; Madrid, Spain, 28-29 October 2004; Gdansk, Poland, 4-5 November 2004, and published in RTO-EN-SET-063.

or space's positions are all defined within the same coordinate system. That each element is time synchronized with the same clock and all communications are time stamped.

Each transmission of information between sensors must depict its time and its coordinates. In addition if it is sharing track or target data it must specify their unique identifier, its velocity, pitch, yaw, and role and meta data describing the transmitted raw data along with encryption/decryption keys. The unique identifier will allow the receiving sensor to acquire, within its resident database management system (DBMS), all of the sender's radar characteristics. The description of these data can be defined by ontologies such that all the sensor platforms will correctly understand the information provided. Sensor characteristics include such things as nomenclature, power output, bandwidth, frequency, antenna pattern, pulse width, pulse repetition frequency (PRF), etc. Platform characteristics as to the position of the antenna on the platform, number of elements, the pattern of the elements, the pointing vector of the radar, etc. We need an ontology for defining these data and numerous rules so that the information published by any sensor can be understood correctly by the receiving sensor to perform functions such as sensor fusion, track correlation, and target identification.

Sharing information between sensors on the same platform is also required, especially if one or more sensors are adaptively changing its waveform parameters to meet the demands of a changing environment. Figure 1 depicts a hypothesized intelligent sensor system. Each of the sensors has its own signal and data processing functional capability. In addition to this capability we have added an intelligent processor to address fusion between sensors, communication between sensors, and control of the sensors. The goal is to be able to build this processor so that it can interface with any sensor and communicate with the other sensors using ontological descriptions via the intelligent platform network. The intelligent network will be able to coordinate the communications between the sensors on board and to off platform sensor systems. There are approaches we can exploit to build this system by using fiber optic or wire links on board the platform. Radio frequency (RF) links using Bluetooth or 802.11 technologies can be exploited for linking these sensors on board the platform. Between platforms other technologies may be exploited such as mobile internet protocol over RF communications links. The communications issues need to be addressed for the sharing of information and for minimizing the potential of electromagnetic (EM) fratricide. The intelligent platform should determine if there is EM interference (EMI) potential when a sensor varies their antenna's main beam pointing vector, or changes its PRF and may thereby cause interference to a receiving sensor. Rather than have each sensor on a platform operate as an independent system we need to design our platform as a system of sensors with multiple goals managed by an intelligent platform network that can manage the dynamics of each sensor to meet the common goal(s) of the platform. This is one of the major goals we are pursuing under our sensors as robots initiative. This initiative is addressing attended and un-attended sensor platforms.

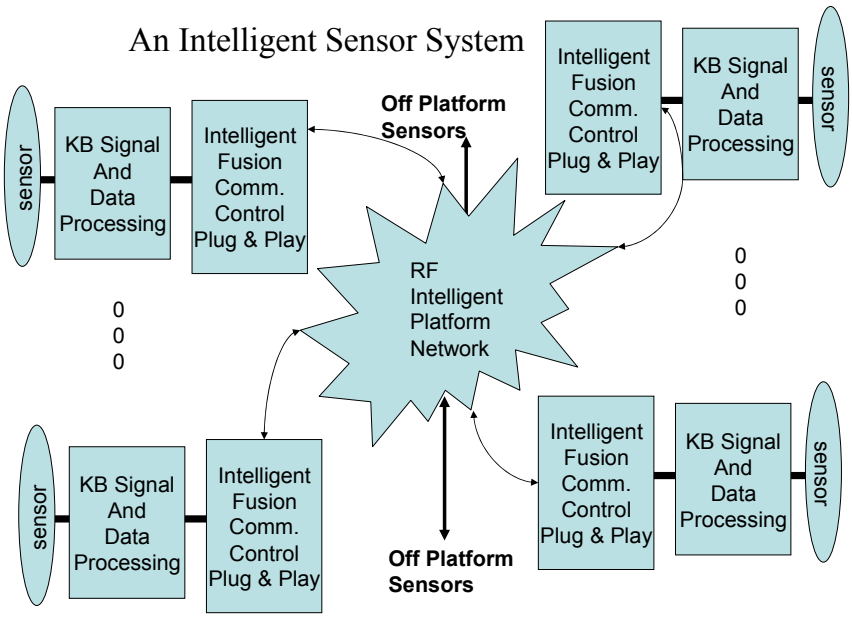

Figure 1. An Intelligent Sensor System

An Airborne Intelligent Radar System (AIRS)

The KB signal and data processing portion shown in figure 1 may represent one radar sensor system. If this sensor system is built using knowledge based techniques then there exists intelligence to control its own processing. A modified design obtained from the KB Space Time Adaptive Processor (KBSTAP) effort (2) is shown in figure 2. In this section we will describe the major components of this knowledge base radar design. In the figure we have labeled the major components as processors with the knowledge base controller as the major integrator for communications and control of the individual processors. These processors operate independently and cooperatively. They can be implemented on a separate computer or on the same computer and operate as separate software processes. The knowledge base controller (KBC) receives information from many sources. Data about the radar, its frequency of operation, antenna configuration, where it is located on the aircraft, etc. is provided by the block labeled in figure 2, configuration information. The map data is preloaded before each mission for estimating clutter returns and for registering its location relative to the Earth and with other sensor platforms. It is also preloaded with its flight profile data and is updated continuously from the platforms navigation system. It also will receive information from the intelligence community both before a mission and throughout the mission. During flight, the KBC will receive information about weather, jammer locations, requests for information, discrete locations, fusion information, etc. We are assuming that the radar system is aboard a surveillance aircraft flying a known and repeatable path over the same terrain. Therefore it can learn by monitoring the performance of different algorithms over repeatable passes of terrain.

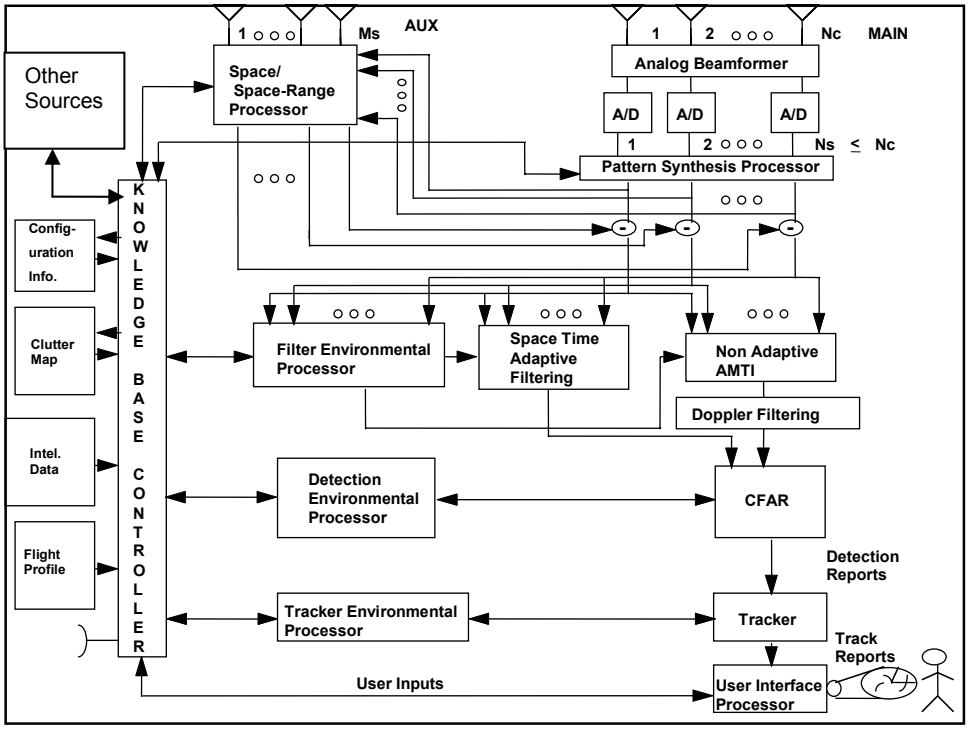

Figure 2. An AIRS Architecture

The KBC performs the overall control functions of the AIRS. It assigns tasks to all processors, communicates with outside system resources, and "optimizes" the system's global performance. Each individual processor "optimizes" its individual performance measures, e.g. signal-to-noise ratio and probability of detection. The tracker with the KBC, for example, "optimizes" the number of correct target tracks and "minimizes" the number of missed targets, incorrect tracks, and lost tracks. The KBC handles all interrupts from the User Interface Processor, assigns tasks to the individual processors based upon user requested jobs, generates information gathered from sources to enhance the performance measures of the individual processors, works with other sensors and outside sources for target identification, and provides the User Interface Processor periodic and aperiodic data for answering queries and requests from the user.

Space/Space Range Processor (SSRP), Pattern Synthesis Processor (PSP), Filter Environmental Processor (FEP) and KBC Interfaces

The KBC will provide geographical information e.g. it will periodically provide the direction the receiver is looking, clutter maps, the location of the emitter, locations of hot clutter jammers, locations of direct jammers or electromagnetic interference sources, and discretes. The KBC will also provide tasks to the SSRP, PSP and FEP. It will for example, task each of the sources of "interference" be reduced by a defined amount. Sources of interference will be prioritized. The SSRP, PSP, and FEP once tasked, will implement and control their own algorithms and processing. The processors will optimize the KBC's request given the number of available degrees of freedom and their physical operational constraints.

The KBC will provide control and operational requests based upon global optimization considerations and/or input directions from the user. For example, the user may want to execute multiple algorithms and compare their results. This may require parallel processing on the same set of data. The user may wish to restrict portions of algorithms from being executed e.g. the user may task the AIRS to compare the performance with and without pattern synthesis. These different tasks will require the KBC to direct the control of each processing stage to operate in a parallel processing mode. Figure 3 illustrates eight different parallel processing modes that will occur when restricting no more than two different algorithms per

processing stage. This approach of executing parallel algorithms, as directed by the user, will allow AIRS to learn which algorithms perform better under identical conditions.

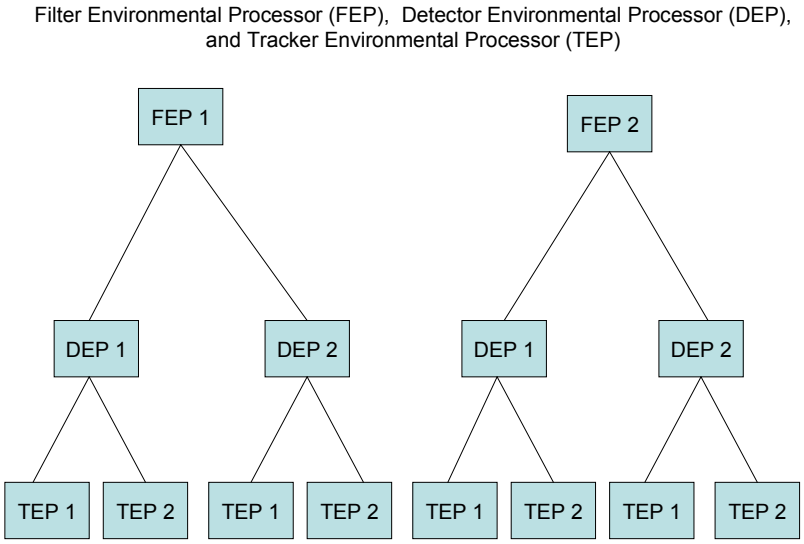

Figure 3. Parallel Algorithms

The results of the KBC's tasks will be reported to the KBC, as a joint or cooperative accomplishment of the three processors. The amount of interference cancellation obtained for each interference source will be reported by the FEP. The information will include the amount of dB attenuation per interference source, whitening, and gain loss. All three processors (SSRP, PSP, FEP) will report to the KBC, the algorithms used and their parameter values.

The three processors' general operating procedure is to use all of their available resources while attempting to exceed KBC tasks. If the resultant global performance measures are not met then the KBC can change the tasks to these processors during the next iteration.

Detection Environmental Processor (DEP) and KBC Interface

The KBC provides the DEP filter output data, clutter map data and results from the tracker such as the degree of belief or weights/importance of previously detected targets. This information allows the DEP to choose its models for the next iteration of data. For instance, the algorithm may adjust its threshold if a high priority target is entering a different clutter background.

The KBC directs the DEP through tasks as discussed in the previous stage. For instance, if the detection process was performed within the filtering stage then the KBC will either "shut down" the DEP or request it to run parallel processes on data obtained from the filter processor. Consider figure 4 where FEP1 incorporates detection and FEP2 does not.

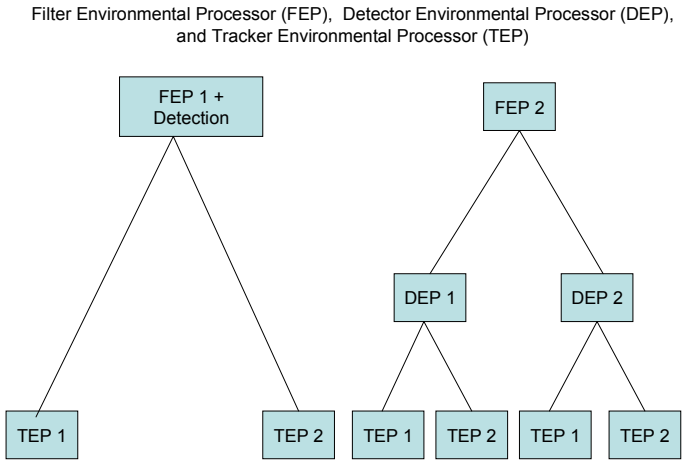

Figure 4 Bypassing the Detection Processor

The results of the KBC's tasks will be communicated back to the KBC. Probability of detection, probability of false alarm, algorithms used, and their parameter values will be reported to the KBC.

Tracker Environmental Processor (TEP) and KBC Interface

The KBC provides data to the TEP that are not contained in the detection data provided by DEP e.g. priority of targets/tracks. The KBC provides control information to the TEP similarly as discussed above based upon parallel processes, choices of algorithms and their parameters, and any definitive requests made by the user.

The TEP will report back to the KBC for each process, each track's probability, the probability of missed tracks or lost tracks, and additional performance measures associated with the algorithms used and their parameter values.

User Interface Processor (UIP) and the KBC Interface

The KBC provides data and receives control from the user via the UIP. Directed by the user the KBC will task the Process Manager and Data Manager (not shown in figure 2) to pre-configure the computers and algorithms for each of the above processors for the next flight iteration or CPI. It will provide information related to intermediate results, performance measures, how AIRS arrived at its solutions, and assist the UIP in configuring the antenna and processors.

Configuration Information and KBC Interface

The exchange between the Configuration Information and the KBC contains for example data regarding the radar, the radar's location, antenna, and transmitter characteristics. Some of these data can be modified by the user and are pre-stored in the Data Manager and accessed via the UIP.

Clutter Map and KBC Interface

The Clutter Map is defined given the flight profile of the aircraft. This file contains those parameters required by the AIRS' algorithms obtainable from actual terrain files such as land use land clutter (LULC), digital elevation model (DEM) and digital line graph (DLG) databases. These data are provided by

the US Geological Survey (USGS). These data will be stored in an environmental data file and accessed via the Data Manager along with clutter map data computed on the fly during flight.

Intelligence Data and KBC Interface

Intelligence community data are provided to the AIRS. These data may contain the location of jammers, a jammer's parameters, target parameters and a target's kinematics. These data will be used by different AIRS' algorithms and knowledge sources.

Flight Profile and KBC Interface

Flight profile data are stored and maintained in a database via the Data Manager. These data contain parameters required by AIRS' algorithms.

Antenna and KBC Interface

This antenna represents the communications link to outside sources for gathering and providing information during flight.

AIRS State Processing

AIRS is a dynamic system, i.e. it changes its processing dependent upon its goals and the environment. This section provides an overview of a hypothetical AIRS and its operation during changing conditions. AIRS' processing begins by loading its computers with pre-flight mission, intelligence, and terrain data. The process will go through four states; pre-flight, initial transient state, correlation/performance/assessment/learning state, and steady state. Steady state probably won't occur until the aircraft (A/C) flies at least one to two race tracks over the same area. The initial transient state will take 4 to 20+ CPIs before tracks can be formed and AIRS starts identifying interrogation-friend-or foe (IFF) related tracks. The intermediate state: to correlate discretes, objects, shadow regions, and jammers, evaluate performance measures and set thresholds, and deciding which objects require nulling, how much nulling, and when nulling should occur. Table 1 provides a brief description of the four different states and the functions of the KBC, its performance processor, and the three main radar intelligent system processors (filter, detector and tracker). We have partitioned the KBC into two processor functions: one to control the AIRS and one to monitor and report its performance throughout its different stages.

System States Versus Processors	**Pre-Flight**	**Initiate System & Initial Transient States (4 to 20+ CPIs)**	**Correlation, Assessment, Learning (1 to 2 Complete Tracks of a Defined Scene/Area)**	**Steady State**

K B Performance Processor	1- Locate and load all Potential Discretes, Clutter Boundaries, Shadow Regions, Jammers, Obstacles - Set System Parameters	6- Monitor System	11- Correlate Discretes, Clutter Boundaries, Shadow Regions, Potential Jammers, Obstacles - Evolve Rules - Insert Synthetic Targets - Measure Performances	16- Insert Synthetic Targets - Measure Performances - Change Rule Sets Accordingly
K B Controller	2- Locate and load all Potential Discretes, Clutter Boundaries, Shadow Regions, Jammers, Obstacles - Set System Parameters	7- Initiate System and Monitor	12- Correlate Discretes, Clutter Boundaries, Shadow Regions, Potential Jammers, Obstacles - Evolve Rules	17- Measure Performances - Change Rule Set Accordingly
Intelligent Filter Environmental Processor	3- Define initial settings and performance measure thresholds	8- Execute Non-STAP Algorithm - Compute No of Secondary Rings - Run NHD - Compute Beam Performance, Determine Null Weights - Determine STAP feasibility	13- Compute Number of Sec. Rings, Run NHD, Compute Beam Performance Measures, Set Nulls, Determine When and Where STAP is Feasible - Evolve Rules	18- Measure Performances - Change Rule Set Accordingly
Intelligent Detector Environmental Processor	4- Define initial settings and Thresholds for Pfa	9- Compute and Adjust Thresholds for Pfa	14- Compute Detections – Re-compute and Adjust Pfa Thresholds - Evolve Rules	19- Measure Performances - Change Rule Set Accordingly
Intelligent Tracker Environmental Processor	5- Locate all Potential Discretes, Clutter Boundaries, Shadow Regions, Jammers, Obstacles - Define initial settings and performance measure thresholds	10- Initiate Tracks - Compute Performance Measures (Number of Correct Tracks, Number of Dropped Tracks, Number of Incorrect Tracks)	15- Correlate FAA Data with Tracks - Compute Performance Measures - Number of Tracks, Number of Dropped Tracks, Number of Incorrect Tracks - Evolve Rules	20- Measure Performances - Change Rule Set Accordingly

Table 1. AIRS States Versus Processors

1-2. Pre-Flight for KB Processors

The hypothesized location of discretes, clutter boundaries, shadow regions, potential jammers, and obstacles are loaded into AIRS. This can be performed in at least two ways.

a. Load the location of all these entities into one table and as AIRS begins learning it will find detections that it will try to correlate with entities in the table. As they are verified, their status will be changed from hypothesized to identified and their parameters updated accordingly. As new entities are found they will be entered into the table as hypothesized and when verified, with detections from more than one race track, they will be upgraded to identified.

b. Load all hypothesized entities into separate tables based upon their type (i.e. discretes, obstacles, shadow regions, aircraft, etc.) and as they are verified they will be marked identified and their parameters updated. As new entities are found they are placed into a general table and as they are verified they can be moved to their proper table.

The classification and storage of the different entities can be done in many ways. Consider the following relations as one example.

Road Traffic (Road ID #, LL1, LL2, LL3, . . . , LLn, Priority, Confidence (= 0 when first loaded, i.e. hypothesized))

LLi implies latitude and longitude of points on the Earth that defines a straight line approximation of a road.

Discretes (Discrete ID #, LL1, LL2, …, Priority, Confidence (= 0 when first loaded))

A discrete may require one or more latitude and longitude points to describe its position, e.g. a steel bridge.

Clutter Types (Clutter Type ID #, LL1, LL2, LL3, . . . , LLn, Priority, Confidence (= 0 when first loaded))

The location points define the boundaries for different clutter types, such as urban, forest, ocean, etc. Every point within a boundary is modeled as the same type of clutter. This describes the homogeneous clutter model for choosing secondary data for STAP.

For shadow or obstacle type (Shadow/Obstacle ID #, LL1, LL2, LL3, . . . , LLn, Maximum Height, Priority, Confidence (= 0 when first loaded),)

The Location points describe the base of the shadow or object.

In addition, if we know from intelligence sources where jammers are located we may enter them similarly as we have for discretes.

3. Pre-Flight Intelligent Filter Processor

These data represent antenna characteristics that will not change during flight, e.g. number of antenna elements and their configuration, antenna tilt angle and pointing direction, and location of the antenna on the A/C. It also contains the initial radar parameters, e.g. pulse repetition frequency (PRF), transmitter frequency, size of the data cube, and bandwidth of signal. The performance thresholds for evaluating antenna beam distortion are also initialized.

4. Pre-Flight Intelligent Detector Processor

These data represent data that are initialized but are not necessarily fixed, e.g. range resolution, Doppler resolution, top percentile for trim mean constant false alarm rate (TM-CFAR), and bottom

percentile for TM-CFAR. Performance measure data are also set such as probability of false alarm thresholds for normal, low and very low levels of interest.

5. Pre-Flight Intelligent Tracker Processor
   This state has similar data requirements as the pre-flight KB processor states [1-2]. All three processors have access to the same data. This state also sets the tracker processor performance measures and parameters, e.g. number of correct tracks, number of dropped or lost tracks, and kinematics of potential targets.

6. KB Performance Processor and Initiate System and Transient State.
   The processor will monitor the AIRS queues for number of potential targets and registration of obstacles, discretes, clutter boundaries, shadow regions, and jammers.

7. KB Controller and Initiate System and Transient State.
   The processor will initiate the antenna processing and monitor the system queues, auxiliary data correlations, feedback from the different processors, system errors, number of potential targets and registration of obstacles, discretes, clutter boundaries, shadow regions, and jammers.

8. Intelligent Filter Processor and Initiate System and Transient State.
   Execute non-STAP algorithm, determine the secondary rings for each cell under test given the stored terrain features, run the non-homogeneous detector (NHD) algorithm if necessary, compute beam performance, and compute antenna weights based upon hypothesized KBC nulling tasks. Note for this state we don't want to distort the antenna beam pattern but gather data so the KBC can determine if nulls should be placed in the direction of interferers and whether STAP is feasible.

9. Intelligent Detector Processor and Initiate System and Transient State.
   The processor will implement thresholds as assigned, will default to the standard detection cell averaging algorithm, and use standard window sizes unless the cell of interest is at a clutter boundary.

10. Intelligent Tracker Processor and Initiate System and Transient State.
    To initiate a track requires multiple CPIs. This process is just beginning. Correlations with objects and shadow regions have begun, performance measures are computed, (number of correct tracks, number of dropped tracks, and number of incorrect tracks) and tracks are formed. It reports tracks and potential correlations with other entities.

11. KB Performance Processor and Correlation, Assessment, and Learning State.
    This processor will use the correlations obtained by the KB Controller [in state 12] for the first portion of its processing, i.e. until it has correlated or discounted all the discretes, clutter boundaries, road traffic, and shadow regions with a high degree of confidence. Once this task is completed the processor will insert synthetic targets of varying sizes and velocities to test the performance of the AIRS. During the second complete scan of an area the KB performance processor will be able to determine if the performance measures have improved. Based upon these results the performance processor may place targets in other locations and/or direct the controller where they should or should not use STAP.

12. KB Controller and Correlation, Assessment, and Learning State.
    There are two levels of correlation required: 1.) position of the above entities within a defined range ring and 2.) the power level at the receiver given the distance to the entity. Note the definition of the range rings relative to the Earth contain different entities as the A/C moves. In addition, as the A/C moves different entities may require nulling, the AIRS may or may not want to place a null in their direction. Correlating entities by power may be done as defined by the following relations.

    Road Traffic Power (Road ID #, Peak Power divided by average peak power over a defined window, for CPI #). Correlations are performed by a road object correlator algorithm using data from the detector and tracker processors. Power can be used to determine if the return signal varies differently from $1/R^4$

(where R is the target range) at the projected location of the road. If the majority of targets/tracks that originate from the location follow the road traffic pattern then their correlation is high.

Discrete's Power (Discrete ID #, Peak Power divided by average peak power over a defined range window, for CPI #). Correlations are performed by a discrete object correlator algorithm using data from the detector and tracker processors. Verify that the power varies as $1/R^4$ and the objects do not move, i.e. they do not generate a track.

Shadow/Obstacle Power (Shadow/Obstacle ID #, Peak Power divided by average peak power over a defined window, for CPI #). Correlations are performed by a shadow/obstacle object correlator algorithm using data from the detector and tracker processors. Correlating range ambiguity areas and dropped or coasted tracks help verify shadowed/obstacle locations. Shadowed regions loaded at pre-flight are computed from United States Geological Survey (USGS), or National Imagery and Mapping Agency (NIMA) databases, with an assumed flight path. If the databases are old then the terrain may have changed.

Data from IFF responses, outside sources, and other sensors are used to update jammer objects, aircraft, ground moving targets, and all unknown objects. Numerous data sources are used to register each CPI with ground "truth".

13. Intelligent Filter Processor and the Correlation, Assessment, and Learning Stage.
    Rules as to when STAP should and should not be applied are required. It is assumed that the radar is flying in a known pattern and will be looking at the same scene each time it flies the same pattern. During the first complete flight over the defined scene the AIRS could execute a standard non STAP algorithm. The KB performance processor should place targets in non-homogeneous areas e.g. near roads and clutter boundaries. The position and type of synthetic targets are not made known to the KBC. In the second complete scan the KBC should attempt to use STAP where ever it can.

    A method for determining if there is a sufficient number of training range rings for STAP is required. A method is to correlate each range ring with the terrain map to identify where there are discontinuities, major roads, etc. and label each region or sector-range with a terrain type. A classification code range ring correlator algorithm will implement this method in collaboration with the intelligent filter processor. The major or minor classification codes used in the USGS database, e.g. urban, forest, water, etc. will be used. Once range rings are chosen they can be evaluated for their homogeneity by using NHD. With a combination of the pre-flight loaded database, the use of the radar returns and the NHD, the system can "learn" which areas are homogeneous and evolve its rules as to which filter algorithms to employ.

    During this state the controller will assign a low, medium, and high performance threshold levels for beam performance. This information along with requests of where to place nulls in the beam pattern will be provided to the intelligent processor. After a number of CPIs the KBC will evaluate performance measures from all the processors. Based upon this evaluation the KBC may assign different performance threshold levels and null requests for the filter processor.

14. Intelligent Detector Processor and the Correlation, Assessment, and Learning Stage.
    This state uses the correlation data provided by the KBC to recognize terrain boundary locations. For those test cells within homogeneous regions the standard detection cell averaging algorithm and window sizes will be used. For those test cells near boundaries the CFAR processors will choose reference cells, algorithms, and window sizes as developed under the ES-CFAR program (1,5). The processor will perform detections, implement thresholds as assigned, re-compute and adjust probability of false alarm (Pfa) thresholds, evolve rules to apply the standard cell averaging rules, determine when to apply different algorithms, and when to recommend changing the detection threshold.

15. Intelligent Tracker Processor and the Correlation, Assessment, and Learning Stage.
    Discrete objects, shadow regions, roads, and federal aviation administration (FAA) data will be obtained from the KB Controller and used to help correlate with existing targets and tracks. Correlations of dropped tracks and highways will be performed with the KBC. Performance measures (number of correct tracks, number of dropped tracks, number of incorrect tracks) and sorting of tracks will be computed. It will report back to the KBC all its tracks and any discrepancies with the data obtained from the KBC. Discrepancies will be settled by the KBC and the other processors. As corrections are made the AIRS will evolve its rules and learn.

16. KB Performance Processor and the Steady State.
    The performance processor will constantly measure the performance of all processors to determine whether AIRS is performing better. The processor will continually look for changes or requests submitted by the user or changes in data from outside sources. It will monitor performance by checking the beam pattern performance data, detection data, and track data. It will insert known radar cross section (RCS) synthetic targets at locations where there are boundaries in terrain types and evaluate the detection capability of the system. By placing different targets at different locations the performance of the current rules can be computed. If performance is low then the rules being used by the KBC will be modified.

17. KB Controller and the Steady State.
    The KBC will access the same performance measures as presented in [16]. Based upon these performance values the KBC will asses its current rules and apply changes accordingly. The rules the KBC can change are based upon a processor's reported data and the user requests, such as change in the antenna's beam pattern and the A/Cs flight path.

18. Intelligent Filter Processor and the Steady State.
    This processor will monitor its beam pattern performance. It will change its rules based upon the environment and the number of nearby jammers and discretes. For example, the processor should manage the number of degrees of freedom required to notch jammers and discretes and yet maintain enough degrees of freedom to perform STAP processing. It will measure its own performance and report it to the KBC for total sensor performance evaluation.

19. Intelligent Detector Processor and the Steady State.
    During this state its processor measures performance based upon the number of detections and number of false alarms. It will increase or decrease the threshold level, change window sizes for CFAR algorithms, and change rules for choosing CFAR algorithms based upon previous flights over the same or similar clutter interfaces.

20. Intelligent Tracker Processor and the Steady State.
    This state measures performance based upon number of correct tracks, missed tracks, and number of false tracks. Based upon these numbers and the terrain, the processor will adjust its rules and thresholds to increase its performance.

KB Tracking

In the previous sections we presented an overview of AIRS and its end-to-end processing sequence. We discussed its feedback and learning structure and the sharing of information and data from outside sources. In two other papers contained herein Dr. Wicks provided information about expert system Constant False Alarm Rate (CFAR) processing and the results of a study where the choice of secondary or training data for STAP filtering was greatly enhanced by using map data. These are two examples of using external knowledge and KB processing for enhancing the performance of radar signal processing. The rules for picking the best training rings or the best CFAR processing algorithms are both based upon knowledge of the terrain obtained from map data. The rules for their choice were hypothesized by the researchers and then tested by using actual radar data. This same procedure is recommended for the development of AIRS.

To complete the end-to-end processing architecture of an AIRS we will present a KB tracking algorithm that extends our US Air Force (USAF) funded work (2). We will present an overview of this tracking algorithm and some of its AI rules e.g. maneuver or obstacle rules and shadow rules. An AI logic structure for implementing these rules is discussed next and some additional rules for our AIRS design are provided.

The logic structure is independent of any tracking algorithm and can address aircraft or ground moving targets. It is compatible with the overall AIRS design and is modifiable. The thrust of this logic structure is to utilize as much auxiliary data (e.g. maps, other sensors, target kinematics, and radar platform characteristics) as possible to maintain individual identifiable tracks. With today's tracking algorithms if a track is dropped and another track is formed there is minimum effort expended to determine if the two tracks were formed from the same target. If a track is dropped algorithms, for the most part, do not investigate why and then use this information in enhancing the overall signal processing performance. Algorithms do not learn based upon their previous performances. They are memoryless once a track is dropped. The proposed logic structure presented herein addresses these issues and investigates the potential for building an AI based tracking algorithm.

Our current tracking algorithm (2) has three separate instantiations. There is an uncoupled two state alpha beta filter with position and velocity component states, an uncoupled three state Kalman filter with position, velocity, and acceleration component states, and an extended four state Kalman filter with both x and y position and velocity component states. The tracker gathers reports, evaluates the reports and correlates them with known tracks, forms a correlation matrix and distance matrix, performs an association logic based upon nearest neighbor and oldest track, and performs track maintenance i.e. update extant track states, spawn new tentative tracks with unused reports and drops tracks with a state value of zero. A diagram illustrating the state logic is shown in figure 5. A new tentative track is given a state of 1. If its projected position is detected again on the next coherent processing interval (CPI) it is given a state of 2, and so on. Once the target is in state 4 it is considered in a firm state as long as it is still detected for each subsequent CPI. Once in the firm state, if there are four consecutive CPIs in which the target is not detected (i.e. a Miss) then the track is dropped. It is our contention that once a tentative track exists then we should maintain its history even if it receives one or more misses. This is important in order to correlate false or dropped tracks with roads, or jammers, discretes, shadow regions, etc. This information is needed to feed back to the KBC and to the other processors as discussed in the previous sections.

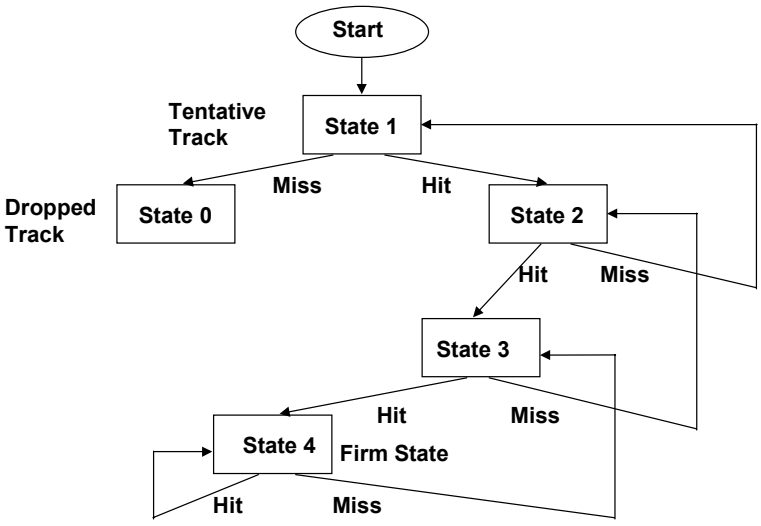

Figure 5. Integrating AI Rules

The following is a preliminary design of a logical structure to capture AI rules for the tracking portion of AIRS. It is by no means complete and does not address each of the numerous attributes for tracking any specific type of target (e.g. aircraft, ground vehicles, missiles) for all its possible scenarios embedded in all possible environments or clutter. It is constructed to work with a radar tracking filter such as alpha beta or Kalman. The logical structure is shown in figure 6. It is an abstract model and will require numerous detail level designs before it can be coded and tested. The logic is described using alpha characters to indicate where in the structure we are referring. Throughout the description the use of outside data sources is illustrated and the addition or verification of data sources is presented.

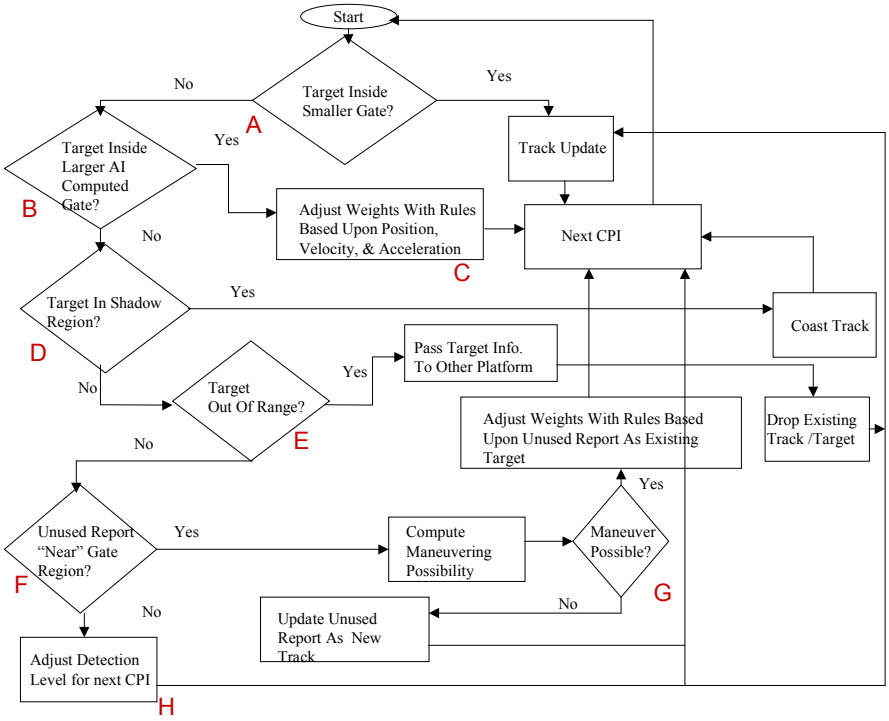

Figure 6. Logical Structure

A. Within this decision block (A) we are asking whether a detected target is within the gate of a known and therefore projected track. If the answer is yes then we simply update the track using the tracking filter of choice (e.g. Kalman). If however a target is detected and it is not within any projected track's gate (i.e. an unused report) then we need to determine whether it lies in a larger AI computed gate. The idea of using more than one size or variable size gate is discussed in the literature. Skolnik (3) suggests "The size of the small gate would be determined by the accuracy of the track. When a target does not appear in the small gate, a larger gate would be used whose search area is determined by the maximum acceleration expected of the target during turns." Brookner (4) states while discussing the g-h filter

"However, aircraft targets generally go in straight lines, rarely doing a maneuver. Hence, what one would like to do is use a Kalman filter when the target maneuvers, which is rarely, and to use a simple constant g-h filter when the target is not maneuvering. This can be done if a means is provided for detecting when a target is maneuvering. In the literature this has been done by noting the tracking-filter residual error, that is, the difference between the target predicted position and the measured position on the nth observation. The detection of the presence of a maneuver could be based either on the last residual error or some function of the last m residual errors. An alternative approach is to switch when a maneuver is detected from a steady-state g-h filter with modest or low g and h values to a g-h filter with high g and h values, similar for track initiation. This type of approach was employed by Lincoln Laboratory for its netted ground surveillance radar system. They used two prediction windows to detect a target maneuver. If the target was detected in the smaller window, then it was assumed that the target had not maneuvered and the values of g

and h used were kept ... If the target fell outside of this smaller 3 sigma window but inside the larger window called the maneuver window, the target was assumed to have maneuvered."

B. These references were provided to indicate that the radar community has tried different approaches for varying the gate sizes for tracking maneuvering targets. The Kalman filter is more suited for maneuvering targets. However, a universal method for choosing a larger gate size because of a maneuver is not well established. If the larger gate is too large then multiple targets may occur within them. The maneuverability of a target is target dependent and may be human dependent and very unpredictable. What we are proposing is that the larger gate be built using AI techniques. Let the history of the target's flight and a priori knowledge about a potential target dictate how to compute the larger AI gate.

Since we are building an intelligent surveillance system we will have data obtained from sources outside our radar system, e.g. map data, intelligence data, and other sensors. We can assume we know what type of targets we are tracking, such as helicopters, tanks, scud launchers, surveillance aircraft, fighter aircraft, and missiles. If so then we know something about their kinematics, i.e. their minimum, maximum and average velocities for different altitudes, their maximum gravitational (G) force turn they can withstand and at what radius, and their maximum acceleration. Using these data we can construct rules that will compute the larger size gate based upon a degree of belief given the type of target, e.g. helicopter or a fighter aircraft. This degree of belief can be computed using information from outside data sources, its previous kinematics data (velocity, location, etc.), radar cross section, and altitude amongst other factors such as the type of mission, its position in the scene, and sensitive locations or targets.

A simple rule is to take the maximum velocity for the target type that has the highest belief and compute the maximum distance it could have traveled from the previous position on the last CPI. This allows us to compute a semi-circle around the vector the target was heading. See figure 7. This approach may be fine for a target like a surveillance aircraft, but not for a tank or track vehicle or scud launcher. For example, a tank which can easily turn 180 degrees, a circle may have to be drawn with radius equal to the maximum distance that can be traveled within the time between CPIs. The more we know about the targets we are tracking the more intelligent we can be in designing our rules and estimate our gate sizes.

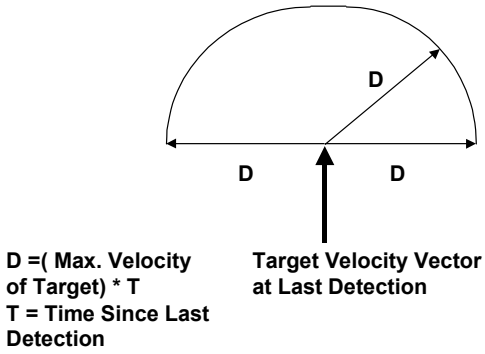

Figure 7. Example AI Computed Gate

C. If the target is detected in the larger gate then we need to adjust the weights of our tracking filter. Indicated in block C we can adjust the weights with rules based upon position, velocity and acceleration. These rules can be simple, e.g. if the target was detected in the larger gate then set the weights for the next CPI as if the target were detected the first time. This will eliminate any memory or smoothing that the filter had performed and start off with a larger gate size. More sophisticated rules can be employed and should be investigated further, dependent upon the tracking filter used.

D. If the target was not found in the smaller or the larger gate then we need to determine if it is being shadowed from our radar, possibly by terrain. Our logic is assuming that the radar system has a priori data that are available such as terrain data containing elevation attributes, roads, and bridges. With this information we can compute whether or not given the elevation of the radar and the last position of the track if there is terrain obstructing the radar's illumination of the target. If there is an obstruction then we should be able to project, given the last known velocity of the track and the changing position of the radar, how many CPIs the track will be obstructed. Based upon these computations we can then coast the track until the next CPI. For each coasted CPI we should also look for new unused reports that can occur due to our coasted track changing its projected velocity while it is being obscured. See figure 8. If this does occur and a new track is initiated we should "flag" this track that it may be the coasted track. Once we compute when or which CPI the original track should be visible and if it isn't, even after two additional CPIs, we should then revisit the new track. During this revisit we need to compute whether or not the dynamics of the target/track were capable of maneuvering to the position that the radar detected the target. (See paragraphs F and G for more details.) If it is shown possible, then the new track should be updated as being the old track with some degree of belief. If however, the original track is detected after it has moved beyond the obstruction then we should go back to the new track that was initiated and remove the "flag" indicating the possibility that this was a firm track that was coasted.

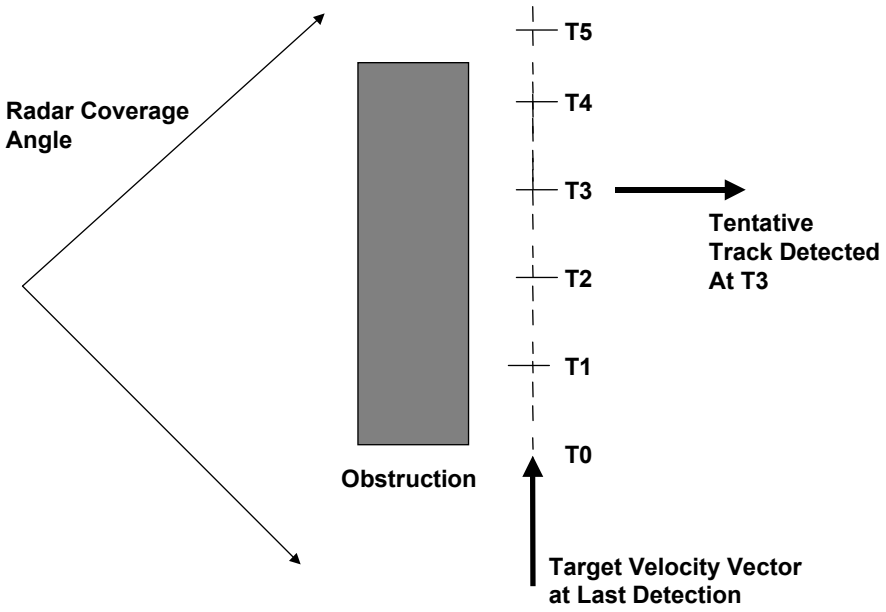

Figure 8. Track Obstruction

E. If the target is not in either gate and it is not shadowed then maybe the target is out of range. This is easy to compute given its last position relative to the radar. If it is out of range then we should pass this information to another sensor platform along with the track data we have acquired. The knowledge of when a target is going to reach this point can be predicted earlier than the last CPI. However, the point in space when a target will be out of range is a variable dependent upon the radar and the target's movements.

The information that can be passed to the other platform can contain the time of the first acquisition, its history path, velocity range, hypothesis of type of target, and any other kinematics or knowledge that has been gathered throughout its track. This data can be used by the message receiving platform in assigning degrees of belief about the target's maneuverability, type of target, and identification.

F. If the target is not in either gate, not shadowed, and not out of range then what happened to it? Maybe our knowledge about its kinematics was incorrect? Maybe our sensor and filtering model has more error variation than we thought? Maybe the target maneuvered and its radar cross section (RCS) is too low and therefore not detected. Maybe the clutter is too large and we can't detect the target?

What we can do is determine if there are any unused reports. If unused reports exist then maybe one of these are our target. First we need to perform a quick culling to determine if at maximum velocity (Vmax) our target could have traveled from where we last detected it to where the unused report was detected, a distance of D. If Vmax times T (time between the two detections) is less than D then this unused report can't possibly be due to the same track. If all unused reports result in the same finding then we conclude that there are no unused reports that may be due to our track. If however, one or more computations show that the distance to the possible reports could have been traveled by the target then we need to compute its possibility and assign a degree of belief to each report.

G. A simple algorithm for computing the possibility of an A/C maneuverability is illustrated in figure 9. D is the distance between the last detection and the position of an unused report. The different radii (R1 and R2) represent the different radius that one can construct that can pass a circle or arc through the two end points of the chord of length D. If we assume that the acceleration is a maximum then we can assume that the velocity is our last estimated velocity or its maximum velocity. Each assumption has a certain amount of error. We can compute different values of R by the following:

Rest = (Vlast)2/Accmax,

Rmax = (Vmax)2/Accmax.

For different values of R and D we can compute the distance of the arc connecting the end points of the chord D. It can be shown from figure 6 that:

Theta = 2(arcsin((D/2)/Rest)) or
Theta = 2(arcsin((D/2)/Rmax)).

The distance along the arc is 2*Pi*Rest/(Theta/360) = Darcest. Therefore if at (Vlast)*T is less than Darcest then the maneuver is not possible. Similarly if (Vmax)*T is less than Darcmax then the maneuver is not possible.

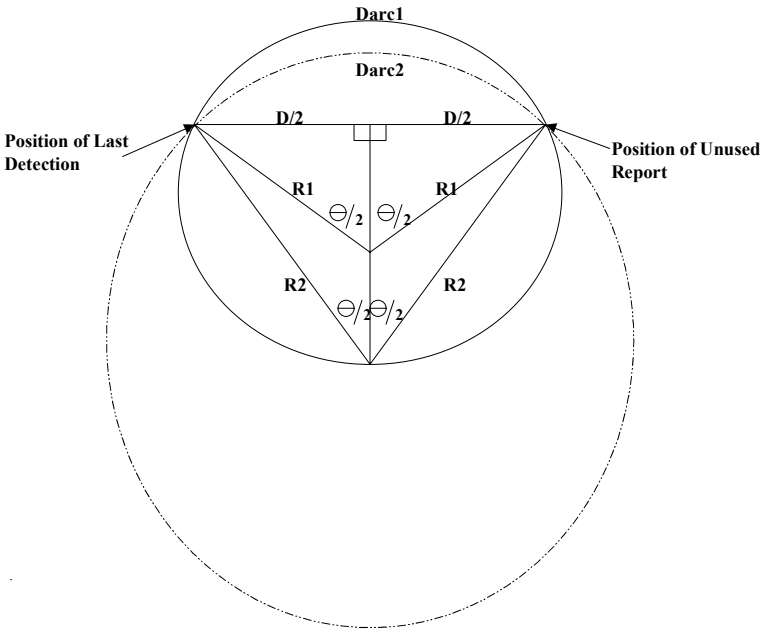

Figure 9. Maneuver Possibilities

Similar rules can be developed for different targets and their kinematics to determine the best rules for each. The developed rules can be verified and modified by consulting with experts who are aware of a target's kinematics.

H. If the target is not in either gate, not shadowed, not out of range, and our kinematics is verified then what happened to the target? It may have maneuvered such that its RCS decreased. If it's a ground slow moving target it may have stopped. It may be hidden by a tunnel. The level of detail for examining why a target track is undetectable needs to be perused dependent upon the target, the environment, the amount of detail a priori data available, and the scenario under investigation. For this iteration of our AI logic structure we have elected to halt our level of investigation and to coast the target. The algorithm would request the KBC to reduce the detection level for the location which we lost the target and the locations where we project the track to be for the next four CPIs. We should identify that the track is potentially dropped and treat the track as a coasted track. If after four CPIs it cannot be correlated with a detection then the tracking filter will drop the track.

Summary

This paper has provided an overview of a hypothesized integrated end-to-end radar signal and data processing chain. The paper has discussed how the use of ontologies can be used for sensors to communicate and share information on board the same platform and between platforms. The majority of the paper was devoted to describing an airborne intelligent radar system (AIRS). A description of the AIRS architecture was provided along with a detailed and high level description of the four states of processing and the functions performed by the KB performance processor, KB controller and the filter, detector, and tracker processors. The last section briefly described a tracking algorithm and proposed an AI logic structure for incorporating rules for different targets, environments, and scenarios. The driving force of this logic structure is to use AI to learn about each track and to analyze each track completely before it is dropped. The logic structure is independent of any tracking algorithm, environment, target type, or scenario.

The AIRS architecture is new and revolutionary. Its potential is great. It is one element in a bigger program dealing with waveform diversity and sensors as robots.

Acknowledgements

The authors would like to recognize the efforts of the following people. We would like to thank Mr. Gerard Genello, Mr. William Baldygo, and Dr. Mike Wicks for providing the resources, encouragement, guidance, and the opportunity in the pursuit of our goals. We would also like to thank Mr. John Spina for chairing this lecture series and Mr. Christopher Capraro and Mr. Gerald Berdan of Capraro Technologies, Inc. for their help throughout. Thank you all.

References

1. W. Baldygo, M. Wicks, R. Brown, P. Antonik, G. Capraro, and L. Hennington, “Artificial intelligence applications to constant false alarm rate (CFAR) processing”, Proceedings of the IEEE 1993 National Radar Conference, Boston, MA, April 1993.

2. R. Senn, “Knowledge Base Applications To Adaptive Space-Time Processing”, Unpublished Final Report, July 1999.

3. M., L., Skolnik, "Introduction to Radar Systems", McGraw Hill, New York, 1980.

4. E., Brookner, "Tracking and Kalman Filtering Made Easy", Wiley, New York, 1998.

5. M. C. Wicks, W. Baldygo, and R. D. Brown, “US Patent 5,499,030 Expert System Constant False Alarm Rate (CFAR) Processor”, filed March 18, 1994 issued March 12, 1996

Closing Remarks

John F. Spina
AFRL/SNRT
26 Electronic Parkway
Rome, NY 13341-4514
UNITED STATES

Email: John.F.Spina@rl.af.mil

Lt.-Col Fiamingo, honored attendees; this has been a very productive and enlightening two days. I am grateful to our sponsors, the NATO Research and Technology Organization and the Sensors and Electronic Technology Panel, and to its hard-working and dedicated staff, for making this possible. Thank you, Lt.-Col Guiseppe Fiamingo and local coordinators Dr. Odman, Sweden; Mr. Muranyi, Hungary; Lt. Col. Lillo, Italy for the outstanding effort to make the LS team's job easier and for the many courtesies shown over the past several days. I also want to very much offer a sincere word of appreciation to all the people who are listed as staff and technical support in the programs in the list of participants: To Jane Brooks of the Research and Technology Agency staff; to Stephanie Branch of the Sensors and Electronic Technology Panel, who did such an able job with the many administrative tasks; I also want to thank all of our speakers, all of whom have very responsible jobs; this is a very significant devotion of their time taking themselves away from their daily routine to spend these two days with us in these discussions. That is very much appreciated. You were just great and provided us with superb presentations over the last few days and some great questions and responses and I think it has been very stimulating. Thank you for informing us, inspiring us, and entertaining us. Finally, I wish to thank the audience here today for your participation, attentiveness, and your excellent contribution to the success of this LS. Let's give ourselves a round of applause.

I would also like to note the involvement and exceptional support of Lt-Col Arturo Salzano, Lt-Col Fiamingo's predecessor as SET Panel executive. Lt-Col Salzano's early support was crucial in getting approval and funding for this LS. For that, I am indebted.

I had contemplated giving you a summary of each of the lectures with what I thought were the most pertinent points, but I think that would in itself be impertinent and redundant since people have mostly absorbed what has been said. I saw this as a starting point for the engineers and scientists of the NATO alliance to think in terms of knowledged-based techniques and I think that has been very much achieved. Many of the basics have been fleshed out, a lot of the opportunities for future implementations have been discussed and it is my hope that each of you have benefited from what has been presented here.

Over the last two days we have come a long way in understanding the potential of knowledge-based technologies for improving the performance of sensor systems. We have reviewed the fundamentals of radar systems and discussed the implementation of knowledged-based techniques in a way that clearly demonstrates the usefulness of such techniques.

Radar systems are an important component of NATO military operations. In response to increasingly severe threats from military targets with reduced radar cross sections, slow moving and low flying targets, targets

Paper presented at the RTO SET Lecture Series on "Knowledge-Based Radar Signal and Data Processing", held in Stockholm, Sweden, 3-4 November 2003; Rome, Italy, 6-7 November 2003; Budapest, Hungary, 10-11 November 2003; Madrid, Spain, 28-29 October 2004; Gdansk, Poland, 4-5 November 2004, and published in RTO-EN-SET-063.

hidden in foliage and under trees, and in environments with large numbers of targets, knowledge-based (KB) signal and data processing techniques offer promise of significantly improved performance of NATO operated radar systems. In addition, radar systems under knowledge-based control can be deployed to better utilize valuable resources such as air space and runways and aid human operators in carrying out their missions. As battlefield scenarios become more complex with ever growing numbers of sensors and weapon systems, the challenge will be to effectively use already available information to enhance radar performance. Knowledge-based processing fills this need and helps meet the challenge.

The objective of this Lecture Series was to present a state-of-the-art assessment of knowledge-based radar signal and data processing techniques, and thereby increase awareness of their value to the NATO scientific community. We reviewed the current developments in the area and presented examples of improved radar performance for augmented and upgraded systems, and projected the impact of KB technology on future systems.

It is certain that many more things could be listed, but it is late in the day. The spirit of cooperation continues and we have much work to do together.

What a pleasure it has been to meet with you for the past two days and to participate in this outstanding interchange of ideas and concepts which we expect to be important to the NATO and its members. Thank you all for your participation in this Lecture Series and, for the many of you who have come long distances, I wish you a safe journey back to your homes.

Thank you for coming.

I declare the Lecture Series adjourned.

REPORT DOCUMENTATION PAGE

1. Recipient's Reference	2. Originator's References	3. Further Reference	4. Security Classification of Document
	RTO-EN-SET-063 AC/323(SET-063)TP/49	ISBN 92-837-1139-4	UNCLASSIFIED/ UNLIMITED

5. Originator

Research and Technology Organisation
North Atlantic Treaty Organisation
BP 25, F-92201 Neuilly-sur-Seine Cedex, France

6. Title

Knowledge-Based Radar Signal and Data Processing

7. Presented at/Sponsored by

The Sensors and Electronics Technology Panel (SET) to support a Lecture Series presented on 3-4 November 2003 in Stockholm, Sweden; 6-7 November 2003 in Rome, Italy; 10-11 November 2003 in Budapest, Hungary; 28-29 October 2004 in Madrid, Spain and 4-5 November 2004 in Gdansk, Poland.

8. Author(s)/Editor(s)	9. Date
Multiple	August 2005
10. Author's/Editor's Address	**11. Pages**
Multiple	222

12. Distribution Statement

There are no restrictions on the distribution of this document. Information about the availability of this and other RTO unclassified publications is given on the back cover.

13. Keywords/Descriptors

Adaptive processing
Adaptive systems
Algorithms
Data fusion
Data processing
Digital signal processing
Expert computer systems
Knowledge bases
Knowledge representation
Operational effectiveness
Radar detection
Radar signals
Signal processing
STAP (Space Time Adaptive Processing)

14. Abstract

The objective of this Lecture Series was to present a state-of-the-art assessment of knowledge-based (KB) radar signal and data processing techniques, and thereby increase awareness of their value to the NATO scientific community. The Lecture Series covered: Fundamentals of Relevant Knowledge-Based Techniques; Detailed Characterization of the General Radar Problem; Expert System Application to Constant False Alarm Rate Processor; Knowledge-Based Control for Space Time Adaptive Processing; KB Techniques Applied to Performance Improvement of Existing Radar Systems; Impact of KB Techniques for Emerging Technologies; Integrated End-to-End Radar Signal & Data Processing with Over-Arching KB Control. The Lecture Series reviewed the current developments in the area and present examples of improved radar performance for augmented and upgraded systems. In addition, the series projected the impact of KB technology on future systems.

NORTH ATLANTIC TREATY ORGANISATION

RESEARCH AND TECHNOLOGY ORGANISATION

BP 25
F-92201 NEUILLY-SUR-SEINE CEDEX • FRANCE
Télécopie 0(1)55.61.22.99 • E-mail mailbox@rta.nato.int

DIFFUSION DES PUBLICATIONS

RTO NON CLASSIFIEES

Les publications de l'AGARD et de la RTO peuvent parfois être obtenues auprès des centres nationaux de distribution indiqués ci-dessous. Si vous souhaitez recevoir toutes les publications de la RTO, ou simplement celles qui concernent certains Panels, vous pouvez demander d'être inclus soit à titre personnel, soit au nom de votre organisation, sur la liste d'envoi.

Les publications de la RTO et de l'AGARD sont également en vente auprès des agences de vente indiquées ci-dessous.

Les demandes de documents RTO ou AGARD doivent comporter la dénomination « RTO » ou « AGARD » selon le cas, suivi du numéro de série. Des informations analogues, telles que le titre est la date de publication sont souhaitables.

Si vous souhaitez recevoir une notification électronique de la disponibilité des rapports de la RTO au fur et à mesure de leur publication, vous pouvez consulter notre site Web (www.rta.nato.int) et vous abonner à ce service.

CENTRES DE DIFFUSION NATIONAUX

ALLEMAGNE
Streitkräfteamt / Abteilung III
Fachinformationszentrum der
Bundeswehr (FIZBw)
Friedrich-Ebert-Allee 34, D-53113 Bonn

BELGIQUE
Etat-Major de la Défense
Département d'Etat-Major Stratégie
ACOS-STRAT – Coord. RTO
Quartier Reine Elisabeth
Rue d'Evère, B-1140 Bruxelles

CANADA
DSIGRD2
Bibliothécaire des ressources du savoir
R et D pour la défense Canada
Ministère de la Défense nationale
305, rue Rideau, 9e étage
Ottawa, Ontario K1A 0K2

DANEMARK
Danish Defence Research Establishment
Ryvangs Allé 1, P.O. Box 2715
DK-2100 Copenhagen Ø

ESPAGNE
SDG TECEN / DGAM
C/ Arturo Soria 289
Madrid 28033

ETATS-UNIS
NASA Center for AeroSpace
Information (CASI)
Parkway Center, 7121 Standard Drive
Hanover, MD 21076-1320

FRANCE
O.N.E.R.A. (ISP)
29, Avenue de la Division Leclerc
BP 72, 92322 Châtillon Cedex

GRECE (Correspondant)
Defence Industry & Research
General Directorate, Research Directorate
Fakinos Base Camp, S.T.G. 1020
Holargos, Athens

HONGRIE
Department for Scientific Analysis
Institute of Military Technology
Ministry of Defence
H-1525 Budapest P O Box 26

ISLANDE
Director of Aviation
c/o Flugrad
Reykjavik

ITALIE
Centro di Documentazione
Tecnico-Scientifica della Difesa
Via XX Settembre 123
00187 Roma

LUXEMBOURG
Voir Belgique

NORVEGE
Norwegian Defence Research Establishment
Attn: Biblioteket
P.O. Box 25, NO-2007 Kjeller

PAYS-BAS
Royal Netherlands Military
Academy Library
P.O. Box 90.002
4800 PA Breda

POLOGNE
Armament Policy Department
218 Niepodleglosci Av.
00-911 Warsaw

PORTUGAL
Estado Maior da Força Aérea
SDFA – Centro de Documentação
Alfragide
P-2720 Amadora

REPUBLIQUE TCHEQUE
LOM PRAHA s. p.
o. z. VTÚLaPVO
Mladoboleslavská 944
PO Box 18
197 21 Praha 9

ROYAUME-UNI
Dstl Knowledge Services
Information Centre, Building 247
Dstl Porton Down
Salisbury
Wiltshire SP4 0JQ

TURQUIE
Milli Savunma Bakanlığı (MSB)
ARGE ve Teknoloji Dairesi Başkanlığı
06650 Bakanliklar – Ankara

AGENCES DE VENTE

NASA Center for AeroSpace Information (CASI)
Parkway Center, 7121 Standard Drive
Hanover, MD 21076-1320
ETATS-UNIS

The British Library Document Supply Centre
Boston Spa, Wetherby
West Yorkshire LS23 7BQ
ROYAUME-UNI

Canada Institute for Scientific and Technical Information (CISTI)
National Research Council
Acquisitions, Montreal Road, Building M-55
Ottawa K1A 0S2, CANADA

Les demandes de documents RTO ou AGARD doivent comporter la dénomination « RTO » ou « AGARD » selon le cas, suivie du numéro de série (par exemple AGARD-AG-315). Des informations analogues, telles que le titre et la date de publication sont souhaitables. Des références bibliographiques complètes ainsi que des résumés des publications RTO et AGARD figurent dans les journaux suivants :

Scientific and Technical Aerospace Reports (STAR)
STAR peut être consulté en ligne au localisateur de
ressources uniformes (URL) suivant:
http://www.sti.nasa.gov/Pubs/star/Star.html
STAR est édité par CASI dans le cadre du programme
NASA d'information scientifique et technique (STI)
STI Program Office, MS 157A
NASA Langley Research Center
Hampton, Virginia 23681-0001
ETATS-UNIS

Government Reports Announcements & Index (GRA&I)
publié par le National Technical Information Service
Springfield
Virginia 2216
ETATS-UNIS
(accessible également en mode interactif dans la base de
données bibliographiques en ligne du NTIS, et sur CD-ROM)

NORTH ATLANTIC TREATY ORGANISATION

RESEARCH AND TECHNOLOGY ORGANISATION

BP 25
F-92201 NEUILLY-SUR-SEINE CEDEX • FRANCE
Télécopie 0(1)55.61.22.99 • E-mail mailbox@rta.nato.int

DISTRIBUTION OF UNCLASSIFIED RTO PUBLICATIONS

AGARD & RTO publications are sometimes available from the National Distribution Centres listed below. If you wish to receive all RTO reports, or just those relating to one or more specific RTO Panels, they may be willing to include you (or your Organisation) in their distribution.

RTO and AGARD reports may also be purchased from the Sales Agencies listed below.

Requests for RTO or AGARD documents should include the word 'RTO' or 'AGARD', as appropriate, followed by the serial number. Collateral information such as title and publication date is desirable.

If you wish to receive electronic notification of RTO reports as they are published, please visit our website (www.rta.nato.int) from where you can register for this service.

NATIONAL DISTRIBUTION CENTRES

BELGIUM
Etat-Major de la Défense
Département d'Etat-Major Stratégie
ACOS-STRAT – Coord. RTO
Quartier Reine Elisabeth
Rue d'Evère
B-1140 Bruxelles

CANADA
DRDKIM2
Knowledge Resources Librarian
Defence R&D Canada
Department of National Defence
305 Rideau Street
9th Floor
Ottawa, Ontario K1A 0K2

CZECH REPUBLIC
LOM PRAHA s. p.
o. z. VTÚLaPVO
Mladoboleslavská 944
PO Box 18
197 21 Praha 9

DENMARK
Danish Defence Research Establishment
Ryvangs Allé 1
P.O. Box 2715
DK-2100 Copenhagen Ø

FRANCE
O.N.E.R.A. (ISP)
29, Avenue de la Division Leclerc
BP 72
92322 Châtillon Cedex

GERMANY
Streitkräfteamt / Abteilung III
Fachinformationszentrum der Bundeswehr (FIZBw)
Friedrich-Ebert-Allee 34
D-53113 Bonn

GREECE (Point of Contact)
Defence Industry & Research General Directorate, Research Directorate
Fakinos Base Camp, S.T.G. 1020
Holargos, Athens

HUNGARY
Department for Scientific Analysis
Institute of Military Technology
Ministry of Defence
H-1525 Budapest P O Box 26

ICELAND
Director of Aviation
c/o Flugrad, Reykjavik

ITALY
Centro di Documentazione Tecnico-Scientifica della Difesa
Via XX Settembre 123
00187 Roma

LUXEMBOURG
See Belgium

NETHERLANDS
Royal Netherlands Military Academy Library
P.O. Box 90.002
4800 PA Breda

NORWAY
Norwegian Defence Research Establishment
Attn: Biblioteket
P.O. Box 25, NO-2007 Kjeller

POLAND
Armament Policy Department
218 Niepodleglosci Av.
00-911 Warsaw

PORTUGAL
Estado Maior da Força Aérea
SDFA – Centro de Documentação
Alfragide, P-2720 Amadora

SPAIN
SDG TECEN / DGAM
C/ Arturo Soria 289
Madrid 28033

TURKEY
Milli Savunma Bakanlığı (MSB)
ARGE ve Teknoloji Dairesi Başkanlığı
06650 Bakanliklar – Ankara

UNITED KINGDOM
Dstl Knowledge Services
Information Centre, Building 247
Dstl Porton Down
Salisbury, Wiltshire SP4 0JQ

UNITED STATES
NASA Center for AeroSpace Information (CASI)
Parkway Center, 7121 Standard Drive
Hanover, MD 21076-1320

SALES AGENCIES

NASA Center for AeroSpace Information (CASI)
Parkway Center
7121 Standard Drive
Hanover, MD 21076-1320
UNITED STATES

The British Library Document Supply Centre
Boston Spa, Wetherby
West Yorkshire LS23 7BQ
UNITED KINGDOM

Canada Institute for Scientific and Technical Information (CISTI)
National Research Council
Acquisitions
Montreal Road, Building M-55
Ottawa K1A 0S2, CANADA

Requests for RTO or AGARD documents should include the word 'RTO' or 'AGARD', as appropriate, followed by the serial number (for example AGARD-AG-315). Collateral information such as title and publication date is desirable. Full bibliographical references and abstracts of RTO and AGARD publications are given in the following journals:

Scientific and Technical Aerospace Reports (STAR)
STAR is available on-line at the following uniform resource locator:
http://www.sti.nasa.gov/Pubs/star/Star.html
STAR is published by CASI for the NASA Scientific and Technical Information (STI) Program
STI Program Office, MS 157A
NASA Langley Research Center
Hampton, Virginia 23681-0001
UNITED STATES

Government Reports Announcements & Index (GRA&I)
published by the National Technical Information Service
Springfield
Virginia 2216
UNITED STATES
(also available online in the NTIS Bibliographic Database or on CD-ROM)

ISBN 92-837-1139-4